Water Quality Effects on the Bubble-Particle Attachment of Sulfide Minerals

Lisa Louise October

A thesis submitted to the Faculty of Engineering and the Built Environment, University of Cape Town in fulfilment of the requirements for the degree of **Doctor of Philosophy**, in Chemical Engineering

June 2020

Plagiarism Declaration

I, Lisa Louise October hereby declare that the work showcased in this thesis is based is my original work except in cases where it has been appropriately acknowledged. This thesis includes 5 papers which contains work that I have performed as part of answering the key questions set to satisfy the overall objective of this PhD; this work was done under the supervision of A/Prof Kirsten Corin, Dr Malibongwe Manono, Dr Nora Schreithofer and Mrs Jenny Wiese. I have appropriately cited all work done by others in accordance with the UCT-Harvard referencing style.

I confirm that I have been granted permission by the University of Cape Town's Doctoral Degrees Board to include the following publications in my PhD thesis, and where co-authorships are involved, my co-authors have agreed that I may include the publications:

Lisa October, Kirsten Corin, Nora Schreithofer, Malibongwe Manono and Jenny Wiese (2019) Water Quality Effects on Bubble-particle Attachment of Pyrrhotite. Minerals Engineering 131 230–236. https://doi.org/10.1016/j.mineng.2018.11.017

L.L October, K.C Corin, M.S Manono, N. Schreithofer, J.G Wiese (2020). A Fundamental Study Considering Specific Ion Effects on the Bubble-Particle Attachment of Sulfide Minerals. Minerals Engineering 151 pp: 106313. https://doi.org/10.1016/j.mineng.2020.106313

L.L October, K.C Corin, M.S Manono, N. Schreithofer, J.G Wiese (2021). Fundamental and Flotation Techniques Assessing the Effect of Water Quality on Bubble-Particle Attachment of Chalcopyrite and Galena. Minerals Engineering 167 106880. https://doi.org/10.1016/j.mineng.2021.106880

L.L October, K.C Corin, N. Schreithofer, M.S Manono, J.G Wiese (2019). Considering the Ionic Strength and pH of Process Water on Bubble-Particle Attachment of Sulfide Minerals: Implications for Froth Flotation in Saline Water. In: Khayrulina, E.; Wolkersdorfer, Ch.; Polyakova, S.; Bogush, A.: Mine Water – Technological and Ecological Challenges. ISBN Number: 978-5-91252-145-4. p. 437 – 445; Perm, Russia (Perm State University)

Signed by candidate

Signed: Lisa Louise October Date: 1 June 2020

Acknowledgements

I was tremendously privileged to be supervised by a team of world class researchers. To my primary supervisor **Associate Professor Kirsten Corin**, firstly thank you for giving me the opportunity to embark on my postgraduate studies with you, thank you for the unparalleled guidance and support that you have given with every aspect of this research. Thank you for allowing me to present my work internationally and nationally. Also thank you for encouraging this PhD when I was still doing the MSc. Thank you for allowing me the opportunity to travel to Finland twice and quite literally allowing me to experience a whole new world of opportunity. I am eternally grateful for the most positive effect you have had on my life.

To **Dr Malibongwe Manono**, I don't even know where to begin. The impact you have had on my life as a researcher has been remarkable. Thank you for all the long and insightful conversations about water and ions, you are truly the "godfather of electrolytes". On a personal level, thank you for all the pep talks and just always understanding; you have become a brother to me throughout this journey and I cannot thank you enough for the support. Thank you for encouraging me to upgrade the MSc to a PhD and believing in this project as much as you did. Thank you for being a phone call away whenever I needed advice.

To **Dr Nora Schreithofer**, thank you for making my time in Finland as comfortable as possible, I could not have asked for a better host, furthermore, thank you for all the technical help and advice regarding bubble-particle attachment.

To **Mrs Jenny Wiese**, thank you for all the advice regarding the UCT experimental component of this work and all the technical input.

To **Mr Tim Bellers**, thank you for taking some time out of your dissertation write-up period to train me on the Bubble Bee on my first trip to Finland. **Dr Robert Hartmann**, thank you for putting Bubble Bee together so nicely after the move to Otakari 3 and for always being there to offer assistance on my Finland trip 2.0.

To **Monde Bekhapi** and **Kenneth Maseko** at the CMR lab thank you for all the help with preparing my mineral samples and for the lighter moments in the lab; the laughs in the lab always brightened my day. To **Shireen Govender**, thank you for ensuring that I had everything that I needed in the CMR lab.

To **Ms Heather Sundstrom** for being amazing and efficient with all my finance and admin related issues, your kindness is much appreciated.

To the members on my PhD proposal panel, **Prof Jochen Petersen**, **Prof Dave Deglon** and **A/Prof Nico Fischer** thank you for your valuable insights and for aiding in the smooth upgrade from MSc to PhD.

To **Lucia Dzinza**, thanks for all the motivation, believing in me more than I did in myself, for always making yourself available when I just needed to talk about life or just bouncing some ideas around. Thank you, sister.

Brenda Mehlo, Thabo Mabuka, Tinashe Ndimera, Leolyn Alexander, Resoketswe Manenzhe (my twin), Simba Nyakunuhwa, Mathew Dzingai, Ngoni Mhonde my friends in Chem Eng building thank you for all the encouragement and fun times on campus.

Katlego Sejanamane and **Gerard 'Dr Dr' Letheba** thank you for always being there to listen.

To **Herbert Hill**, my "bestie" and "partner in crime" you have been there since my first year of undergraduate studies. I will never forget us motivating each other from undergrad to motivating each other to undertake a MSc Eng degree through to you motivating me to do this PhD. Thank you Mr H, you've taught 'us' some life lessons that will always be remembered.

To **Blanche Dirk**, for believing in me way more than I deserve and for being the most supportive manager.

Vedanth Baiju, you came into my life at the last and most stressful leg of this journey but your constant encouragement, belief in me, motivation and making sure that I reach my "write-up" targets were immensely appreciated. Thank you for going above and beyond to make sure that I was comfortable during the writing process and for being a phone call away whenever I needed someone to talk to.

To mom **Therisa October**, I can't even begin to express my gratitude to you, thank you for always encouraging the furthering of my education, thank you for ensuring that I always had everything I needed to excel from primary school to the point of this dissertation. None of this would have been possible without you and the sacrifices that you have made.

To my dad, **Edmund October** thank you for the support you have offered throughout my years of study, driving me to where I needed to be before I could drive and for ensuring that I always had what I needed to successfully complete my studies. Greatest thank you to my parents for your hard work and teaching me independence.

To my siblings **Grant and Gary October** thank you always being there whenever I needed assistance. My sister in law **Tina** and nieces **Robin and Kelly** thank you for always believing in me.

To my late grandmother **Ma Iris**, thank you for always keeping me in your prayers; I wish you were here to see this.

To the **Leisure Education Trust** and managing trustee **Mr Ed Chantler**, thank you for the sponsorship during my high school years and motivating me to get better grades every term; this eventually got me to University. I am eternally grateful to your kindness.

Finally, to God Almighty who gave me the strength to keep pushing on to reach heights that I never thought I could; I am absolutely humbled by all the opportunities He has given me.

Statement of Funding

Many thanks for the funding of this project by the various institutions, companies and donors.

This work is financed by the **National Research Foundation of South Africa (NRF)** [Grant number 103641] and this project has received funding from the **Academy of Finland Mineral Resources and Material Substitution MISU program** and the **European Union H2020 programme** under grant agreement No 730480. Any opinion, finding and conclusion or recommendation expressed in this material is that of the authors and the NRF does not accept any liability in this regard. Further the financial and technical contributions from the **South African Minerals to Metals Research Institute (SAMMRI)** project No S1703 is also acknowledged. Thanks to **the John Davidson Trust** for the additional funding through the **UCT Postgraduate Funding Office**.

List of Journal Publications and Conference Proceedings

L.L October, K.C Corin, M.S Manono, N. Schreithofer, J.G Wiese (2021). Fundamental and Flotation Techniques Assessing the Effect of Water Quality on Bubble-Particle Attachment of Chalcopyrite and Galena. Minerals Engineering Minerals Engineering 167 106880. https://doi.org/10.1016/j.mineng.2021.106880

L.L October, K.C Corin, N. Schreithofer, M.S Manono, J.G Wiese (2020). A Fundamental Study Considering Specific Ion Effects on the Bubble-Particle Attachment of Sulfide Minerals**.** Minerals Engineering 151 pp: 106313. https://doi.org/10.1016/j.mineng.2020.106313

L.L October, K.C Corin, M.S Manono, N. Schreithofer, J.G Wiese (2019). Fundamental and Flotation Techniques Assessing the Effect of Water Quality on Bubble-Particle Attachment of Chalcopyrite and Galena. Proceedings of MEI Flotation '19. Cape Town, South Africa

L.L October, K.C Corin, M.S Manono, N. Schreithofer, J.G Wiese (2019). Considering the Ionic Strength and pH of Process Water on Bubble-Particle Attachment of Sulfide Minerals: Implications for Froth Flotation in Saline Water. In: Khayrulina, E.; Wolkersdorfer, Ch.; Polyakova, S.; Bogush, A.: Mine Water – Technological and Ecological Challenges. ISBN Number: 978-5-91252-145-4. p. 437 – 445; Perm, Russia (Perm State University)

Lisa October, Kirsten Corin, Nora Schreithofer, Malibongwe Manono, Jenny Wiese (2019). Water Quality Effects on Bubble-Particle Attachment of Pyrrhotite. Minerals Engineering 131 230–236. https://doi.org/10.1016/j.mineng.2018.11.017

L.L October, K.C Corin, M.S Manono, N. Schreithofer, J.G Wiese (2018). Specific Ion Effects on the Bubble-Particle Attachment of Pyrrhotite. Parts of this work were presented at WISA 2018. Cape Town, South Africa

L.L October, K.C Corin, N. Schreithofer, M.S Manono, J.G Wiese (2017). Water Quality Effects on the Bubble-Particle Attachment of Pyrrhotite. Proceedings of MEI Flotation '17. Cape Town, South Africa

Synopsis

The attachment of hydrophobic particles to air bubbles is the most critical requirement for successful flotation to take place. For this reason, bubble-particle attachment has been studied in the most fundamental way from as early as 1934 by bringing a bubble into contact with a flat mineral surface. However, since then, advanced techniques measuring this interaction have emerged. This study uses a novel device to measure bubble-particle interaction, this device is housed at Aalto University in Finland and is called the Automated Contact Time Apparatus (ACTA). This device has six needles, each needle generates a bubble and is brought into contact with the particle bed, this is done across the particle bed in 66 cycles thus resulting in 396 opportunities for bubble-particle attachment. After each cycle, an image is taken which is used to detect for the attachment of particles and then the particles that successfully attached to the bubbles are deposited in a collection bin. At the end of the 66 cycles the contents of the collection bin are filtered, dried and weighed to determine the mass of particles recovered and the images are studied to determine attachment probability. Therefore, this instrument yields two outputs, the attachment probability and mass recovered; in principle these two outputs should be aligned. It was deemed necessary that the use of the ACTA as a measure of mineral floatability be validated against the classical microflotation technique; as both of these techniques consider the bubble-particle interaction in the pulp phase although the ACTA is more fundamental and static while microflotation is comparatively more dynamic.

The pulp phase consists of 80-85% water, making water an essential process and transport medium in the flotation process. With the current water scarcity in countries like South Africa, the need to recirculate process water within mining operations is becoming greater. Recycled process water is however more saline and thus of higher ionic strength. Flotation under saline water compared to fresh water will almost certainly affect the flotation process in terms of grades and recoveries as their water structures are significantly different. It is of great importance therefore to understand exactly how changes in water chemistry affect the flotation process. This study specifically considers how changes in water quality affect bubble-particle attachment.

Studies assessing the effect of inorganic electrolytes on bubble-particle attachment have been limited to single salt solutions and the increase in concentration thereof as well as studies in plant water but only with the increase of one specific ion. These studies have not assessed how increasing the concentration of all inorganic constituents within plant water affect bubble-particle attachment and whether there is a single ion that affects this bubble-particle attachment sub – process more. Further to that, the underlying reasons for these plant water/single ion effects on bubble-particle attachment are not well understood from a fundamental perspective that considers effects into reagent adsorption and zeta potential.

The main aim of this work is therefore to investigate the effect of complex process waters and the recycling thereof on the bubble-particle attachment sub-process in a sulfide mineral system; as well as to identify specific ions within process water that control the bubble-particle attachment sub-process by either enhancing, hindering or having no effect on the bubble-particle attachment of sulfide minerals. This work

also aims to corroborate the use of the ACTA as a means to assess bubble-particle attachment at a fundamental level by comparison with the classical microflotation technique.

Three sulfide minerals were used in this study, namely, pyrrhotite, galena and chalcopyrite. Synthetic plant waters of 0.0241 M, 0.1205 M and 0.241 M were used to simulate the recycle of plant water while single salt solutions of $CaSO_4$, $Ca(NO_3)_2$ and $NaNO_3$ at 0.1205 M were used in the specific ion studies. Tests under these water qualities were conducted with each of the sulfide minerals from a fundamental bubble-particle attachment perspective and microflotation perspective by means of the ACTA and microflotation respectively. In this way microflotation tests were also used as a way to validate the ACTA as a method to measure floatability. Furthermore, adsorption studies and zeta potential determination tests were conducted under the various water qualities for each mineral to assess the effect of inorganic electrolytes on collector adsorption and zeta potential respectively; this in turn was to be related back to the outcome of the bubble-particle attachment tests.

Phase one of this work was done with pyrrhotite with the synthetic plant water and single salt solutions. The effect of water quality on the bubble-particle attachment of pyrrhotite was evaluated first. This was the first time the ACTA was used to determine the effect of a process parameter on bubble-particle attachment. Therefore, it was necessary to fully understand the operational parameters and how the ACTA responds to changes in water quality before including additional minerals. Generally, as the ionic strength of the synthetic plant water increased the attachment probability decreased. However, due to the fine particle size (-75+38 μm) used, no particles were collected in the collection bin, although attachment was observed by the images taken. Subsequently, phase two of this work used a larger particle size (-125+106 μm) for the ACTA experiments.

Phase two work showed a clear trend in attachment probability, mass of particles recovered in the ACTA and further validation with microflotation recovery that bubble-particle interaction increases as the ionic strength of the plant water increases. This was the case with both chalcopyrite and galena particles. Literature would suggest that this result of an increase in particle recovery and bubble-particle attachment may be due to the increase in concentration of inorganic electrolytes; which leads to the compression of the electrical double layer and the subsequent faster rupturing of the film at the air – water and solid – water interfaces resulting in faster bubble-particle attachment.

Zeta potential determination tests showed that the zeta potential of the particles became less negative as the ionic strength of the water increased; this indicates the adsorption of cations on the particle surface. Furthermore, at the pH these tests were conducted (pH 6.5 to 7), the zeta potential was closer to 0 mV as the ionic strength increases. A zeta potential of 0 mV is known to result in particle agglomeration; therefore, in addition to faster rupturing of the film between the bubble and particle, particle agglomeration may also be responsible for the increase in bubble-particle attachment with increasing ionic strength of the plant water.

Adsorption studies across all minerals showed that less xanthate adsorbs on the mineral surface as the ionic strength of the plant water increases; this indicates that the increase of inorganic electrolytes hindered xanthate adsorption on the mineral surface. Intuitively it is expected that this decrease in xanthate adsorption with water of higher ionic strength will translate to lower recoveries and bubble-particle attachment; the opposite was shown to be the case.

The effect of the synthetic plant waters at pH 11 on bubble-particle attachment was also studied in this work. Zeta potential determination tests showed a distinct increase in zeta potential of all minerals with the three waters at pH 11; it was thus thought to be of interest to investigate this effect on bubble-particle attachment. Speciation diagrams of these waters show oxyhydoxyl constituents present at pH 11. Therefore, the presence of these species on the mineral surface is the reason for the increase in mineral zeta potential. At pH 11, poor mineral recoveries regardless of the water type were observed as compared to the recovery with these waters at the natural pH (pH 6.5 to 7). It can thus be concluded that these oxyhydroxyl species hinder the flotation of the pyrrhotite particles as well as processes such as collector adsorption and the action of the electrical double layer.

Another objective of this study was to ascertain whether certain ions within the plant water existed that either have a negative or positive effect on the bubble-particle interactions. If it is the case that one specific ion has a negative effect on bubble-particle attachment, then the removal of this ion would be a more cost effective and environmentally friendly exercise compared to treating the water or bringing in fresh water. Microflotation and ACTA studies with chalcopyrite, galena and pyrrhotite showed that Ca^{2+} containing solutions resulted in lower recoveries and attachment probabilities respectively. While the $NaNO_3$ solution resulted in the highest recoveries and attachment probabilities across the three sulfide minerals. These results were observed both in the presence and absence of SIBX.

Studies in literature have shown that the stability of the hydration layer in monovalent solutions of high ionic strength result in shorter induction times and thus improved bubble-particle attachment. This study also showed that the monovalent Na^{+} showed higher attachment probability and mineral recovery. Less xanthate was adsorbed on the sulfide mineral surfaces in Ca^{2+} containing solutions, hence the poorer bubble-particle attachment with the fundamental attachment timer and microflotation systems. The increased zeta potential and therefore high zeta potential on the mineral surface in Ca^{2+} containing solutions may hinder the adsorption of xanthate as other authors have proposed that the collector adsorption reaction is driven by the electrical double layer and high zeta potentials may hinder this reaction. Therefore, it may be that the passivation of Ca^{2+} on the mineral surface may hinder the action of collector; as Ca^{2+} may compete with collector ions for sites on the mineral or that the high zeta potential may be hindering the collector – mineral reaction.

This work produced a number of outcomes. The validation of the use of the ACTA as a means of measuring mineral floatability through comparison with classical microflotation tests was displayed. The importance of showcasing both the attachment probability and mass of particles collected when taking measurements

with the ACTA was evident in this work. This work also showed that the performance of bubble-particle attachment under ionic solutions was attributed to underlying factors such as the zeta potential and collector – mineral adsorption. The adsorption of xanthate decreased in waters of high ionic strength and Ca^{2+} containing solutions. Waters of higher ionic strength further resulted in more positive zeta potential and possible particle agglomeration resulting in higher recoveries. Bubble-particle attachment was also seen to reduce dramatically at pH 11 under the various synthetic plant waters; this was attributed to the presence of oxyhydroxyl species depositing on the mineral surface inducing surface hydrophilicity. Ca^{2+} was identified as resulting in lower mineral recoveries and attachment probabilities; Ca^{2+} passivated the sulfide minerals' surface more than Na^{+} and less collector adsorbed on the mineral surface in the presence of this ion. The latter result alludes to the fact that higher attachment probabilities and recoveries may be achieved by the removal of Ca^{2+} in recirculated plant water.

The ACTA was constructed with the intent of it being a quick diagnostic tool on flotation plants to assess the bubble-particle efficiency under varying conditions; the outcome of this work showed that this instrument is a viable option as a measure for particle floatability. It is further believed that the findings of this work will provide flotation operations with an understanding of how specific ions within plant water affect bubble-particle attachment; which will allow for the water quality to be tailored towards achieving high mineral recoveries.

Statement of Originality

This study considers the effect of water quality on bubble-particle attachment of sulfide minerals. The effect of increasing ionic strength of plant water and the effect of specific ions within plant water was therefore studied so as to answer the questions, "*How do changes in water quality affect the bubble-particle attachment of sulfide minerals?*" and "*Are there any specific ions within plant water that affect bubble-particle attachment more greatly?*". It is acknowledged that work which considers the effect of ions on bubble-particle attachment has been previously published. However, these publications have used single salt solutions and increased the concentration of the single salt, furthermore these studies were conducted with induction/attachment timers that did not provide a large enough data set. This study made use of the Automated Contact Time Apparatus (ACTA) housed at Aalto University and aimed to validate that this instrument can be used as a quick measure for the floatability of mineral particle.

The original contributions of this thesis are outlined briefly below:

- ✓ This study validated the use of the ACTA as a measurement for floatability. This was done by complementing ACTA testwork with classical microflotation testwork. This study found that the outputs of the ACTA coincided well with that of the microflotation testwork. This study also showed the importance of showcasing both the attachment probability and mass of particles collected when taking measurements with the ACTA. This instrument was initially developed as a quick diagnostic tool on flotation plants, the output of this work shows that under the conditions described in this thesis, this instrument can be used as a measure for floatability.

- ✓ The effect of ions on the zeta potential of the minerals and the resulting impact on the electrical double layer was demonstrated in this work (Mechanism I). This work showed a relationship between the ionic strength of the plant water and bubble-particle attachment, this is due to the underlying relationship between the ionic strength of the plant water and the zeta potential of sulfide minerals.

- ✓ The effect of ions on the collector and the resulting impact on mineral-collector interactions affecting bubble-particle attachment was demonstrated in this work (Mechanism II). A relationship between the valency of cations and the degree to which these ions (at high concentrations) passivated the sulfide mineral surface was shown. Further, relationships were shown between the degree to which the mineral was passivated with the metal ion and the adsorption of collector on the sulfide mineral surface. The bubble-particle attachment was thus affected by these two related and underlying factors, namely zeta potential and collector adsorption.

Nomenclature and Abbreviations

1SPW	Synthetic plant water with a TDS of 1023 mg/L
5SPW	Synthetic plant water with a TDS of 5115 mg/L
10SPW	Synthetic plant water with a TDS of 10230 mg/L
ACTA	Automated Contact Time Apparatus
Ca^{2+}	Calcium cation
$[Ca^{2+}]$	Calcium cation concentration
$Ca(NO_3)_2$	Calcium nitrate
$CaSO_4$	Calcium sulphate
$CuFeS_2$	Chalcopyrite
°C	Degrees centigrade
DI	De-Ionised water
DLVO	Derjaguin, Landau, Verwey and Overbeek
$Fe_{(1-x)}S$	Pyrrhotite
g/t	Grams per ton
I	Ionic strength measured in $mol.dm^{-3}$
i.e.p.	Iso-electric point
L/min	Litres per minute
Mg^{2+}	Magnesium cation
$Mg(OH)_2$	Magnesium hydroxide
Na^+	Sodium cation
NaCl	Sodium chloride
$NaNO_3$	Sodium nitrate
PbS	Galena
PGM	Platinum Group Mineral
P.Z.C.	Point of zero charge

SIBX	Sodium isobutyl xanthate
SO_4^{2-}	Sulphate anion
TDS	Total dissolved solids usually measure in mg/L
ULP	Ultra-purified water
XRD	X-Ray Powder Diffraction
XRF	X-Ray Fluorescence

Table of Contents

List of Figures

List of Tables

Chapter 1 **Introduction**

1.1 Background

Froth flotation is a mineral beneficiation process which takes advantage of a mineral's natural and induced surface properties, resulting in physico-chemical separation between the valuable and non-valuable minerals (Smith and Warren, 1989). The overall froth flotation process is affected by a number of factors, operational, hydrodynamic as well as chemical (Klimpel, 1984). Additionally, these factors may affect each other; therefore, as a result of the interactive nature of these factors the process becomes more complex. Careful consideration is therefore required when attempting to understand the effect of certain parameters on the overall flotation performance.

The overall flotation process consists of a number of sub-processes, this includes the creation of the hydrophobic mineral surface, the formation of air bubbles, the attachment of hydrophobic minerals to air bubbles, the transfer of the bubble-particle aggregates to the froth phase and the collection of these bubble-particle aggregates (Bradshaw, 1997). The most important requirement for successful flotation is the attachment of hydrophobic minerals to air bubbles in the pulp phase (Albijanic *et al.,* 2010).

Considering the importance of bubbles and bubble-particle attachment, it is evident that the pulp phase facilitates the events most vital for successful flotation.

1.2 Problem Definition

The pulp phase consists of 80-85% water (Muzenda, 2010) by volume, making water an essential process and transport medium in the froth flotation process. With current water restrictions in water scarce countries like South Africa, the use of fresh water in mining operations is becoming more and more impractical. Although the mining industry's water consumption is not as high as other industries like agriculture; mining operations are largely situated in arid regions which makes the need for the use of alternative water sources more urgent. Alternative water sources such as grey water, semi-treated and recycled water thus need to be considered in mining operations. Recycled and recirculated water consists of increased dissolved solids and therefore have a higher ionic strength compared to fresh water. This increase in ionic strength of process water may affect the flotation process (Slatter *et al.,* 2009). Therefore, understanding how changes in water chemistry affect the overall flotation efficacy is of vital importance. More importantly, understanding how changes in water quality affect bubble-particle attachment is critical.

The equipment used to determine attachment or induction time generally comprises of a single needle which generates a single bubble which is brought into contact with a particle bed on a set number of areas on the bed; the contact time at which particles first attach at all the areas tested is defined as the attachment time (Yoon and Yordan, 1991; Gu *et al.*, 2003; Albijanic *et al.,* 2012). The problem that arises with using this method is that these areas on the bed may not be representative of the entire particle bed.

Limited studies have focussed on how ions affect bubble-particle attachment. Yoon and Yordan (1991) studied how increasing the KCl concentration affected bubble-particle attachment in a quartz system. Gu *et al.* (2003) studied process water and how increasing the Ca^{2+} concentration affected bubble-particle attachment in a bitumen system. The need to study the effect of process water of increasing ionic strength as well as the effect of specific ions present in process water on the bubble-particle attachment efficiency in a sulfide mineral system is therefore evident. Understanding the effect of specific ions within plant water on the bubble-particle attachment is equally as important as gaining an understanding of how this sub-process responds to increasing the concentration of all the ions present in the water; as it may be that a specific ion is responsible for hindering or improving bubble-particle attachment. If it is that a specific ion does have a hindering effect, the removal of this ion may be a more cost effective and environmentally friendly exercise compared to treating the water or bringing in fresh water. It is also important to note that the effect of inorganic electrolytes on the bubble-particle attachment sub-process may be due to underlying factors such as changes in particle zeta potential and collector adsorption; this too needs to be understood and how these factors contribute to the eventual bubble-particle attachment in the presence of inorganic electrolytes.

1.3 Value of Work

The bubble-particle attachment sub-process is the most vital for an effective separation of value from non-value in froth flotation and given the current water crisis worldwide, the effect of using recycled process water on the bubble-particle attachment process must be understood. Previous studies have looked at the effect of increasing the concentration of single electrolytes in quartz, bitumen and coal systems (Yoon and Yordan, 1991; Gu *et al.*, 2003). No research has been done regarding the effect of using process water of increasing ionic strength on the bubble-particle attachment process in a sulfide mineral system. This work thus aims to close the gap in understanding the effect of recycled water and specific ions on bubble-particle attachment. Further this work aims to investigate underlying mechanisms by which recycled water and specific ions affect the bubble-particle attachment sub-process by examining water quality and specific ion effects on the mineral zeta potential and collector adsorption.

The novel attachment timer named the Automated Contact Time Apparatus (ACTA) (Aspiala *et al.,* 2018) used in this work further allows for a more robust bubble-particle attachment probability measurement. Unlike common attachment timers the one used in this work generates six bubbles and tests the entire length of the particle bed, furthermore the particles that have successfully attached to the bubbles are recovered and can be further analysed (recovery, shape, size and composition). This work also aims to corroborate the use of the ACTA as a means to assess bubble-particle attachment at a fundamental level by comparison with the classical microflotation technique.

1.4 Scope of the Study

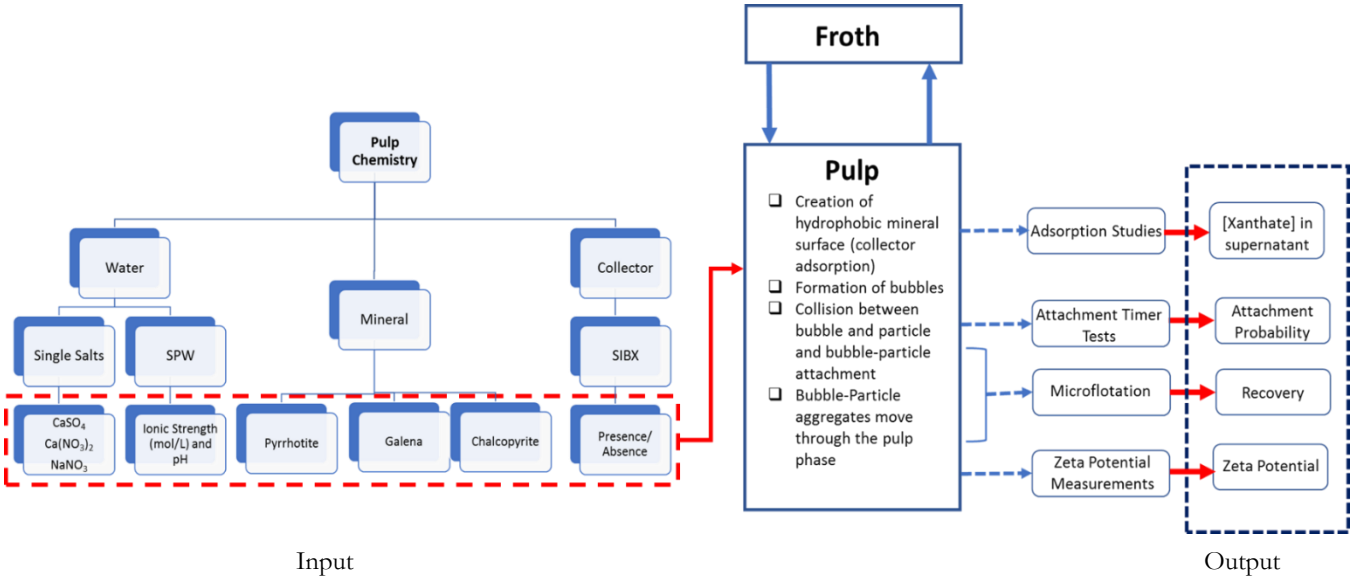

Figure 1-1: Scope of the thesis

1.5 Thesis Layout

This thesis comprises of published and submitted papers. A synopsis of each paper appearing in this thesis and where it has been published or presented is provided in this section.

Chapter 2: Literature Review

This review begins with froth flotation fundamentals and the factors that affect the overall flotation process; emphasis is placed on mineral type, collectors and how collectors adsorb on the mineral surface. Then bubble-particle attachment fundamentals, techniques used to measure bubble-particle attachment, factors influencing the attachment of particles to air bubbles and differences between floatability and hydrophobicity of particles are considered. The review concludes with a section reviewing water quality within froth flotation. The final section focusses on the structure of water, mineral – water interactions, mineral – electrolyte interactions, mineral – electrolyte – collector interactions, the effect of ionic solutions on the froth phase and the effect of ionic solutions on the potential of air bubbles. The literature review chapter is then concluded by positioning the research of this thesis and reinforces the need for this work based on the gaps identified in literature.

Chapter 3: Research Approach

This chapter details the research questions, hypotheses, aims and objectives. These objectives attempt to address some of the research gaps identified in the literature review**.** This chapter further provides how each of the key questions will be addressed from an experimental methodology perspective.

Chapter 4: The Automated Contact Time Apparatus (ACTA)

This chapter details the setting up of this Automated Contact Time Apparatus, its operation as well as the process of taking measurements on the ACTA.

Chapter 5: Detailed Methodology

Chapter 5 describes the experimental techniques and materials that were used in this study. Considering that this study investigates the effect of water quality on bubble-particle attachment, various water qualities were used. Two techniques assessed the bubble-particle attachment under varying water quality. Details of the sample preparation and water qualities, namely three synthetic plant waters, three single salts and the synthetic plant waters at elevated pH are included in this chapter. The Automated Contact Time Apparatus (ACTA) and microflotation set-up were used to assess the bubble-particle interactions from a fundamental and flotation perspective respectively. The microflotation procedure is described in this chapter while a detailed description of the ACTA has been documented in Chapter 4. Furthermore, in order to better understand the bubble-particle interactions under various water qualities, collector adsorption tests and zeta potential determination tests were performed. This chapter also provides the details of these two experimental techniques.

Chapter 6: Lisa October, Kirsten Corin, Nora Schreithofer, Malibongwe Manono and Jenny Wiese (2019) Water Quality Effects on Bubble-particle Attachment of Pyrrhotite. Minerals Engineering 131 230–236. https://doi.org/10.1016/j.mineng.2018.11.017

Abstract

In froth flotation, separation between the valuable and the gangue minerals comes as a result of the attachment of hydrophobic particles to air bubbles. Considering the importance of bubble formation and bubble-particle attachment, it is evident that the pulp phase facilitates the events for the most crucial requirements of successful flotation. Water forms the bulk of the pulp phase; and as a result of water scarcities in countries like South Africa, the need to recycle process water within mining operations is increasing. Hence it is of great importance to understand the effects of water quality on the vital sub-processes within the flotation process, particularly bubble-particle attachment. A novel attachment timer which allows for 396 opportunities for bubble-particle attachment was used for the bubble-particle attachments tests in this work. Three water qualities of increasing ionic strength were tested both in the presence and absence of a xanthate collector to see the effect of increasing ionic strength of synthetic plant water on the bubble-particle attachment probability. The attachment time measurements showed a general decrease in attachment probability as the ionic strength of the synthetic plant water increased both in the absence and presence of a collector. This result indicated that increasing the concentration of the ions present in synthetic plant water lowered the probability of pyrrhotite particles attaching to air bubbles. Further, adsorption studies showed that less xanthate adsorbs on the mineral surface at the highest ionic strength of synthetic plant water under study. This indicates that increases in the ionic strength of synthetic

plant water hindered the xanthate adsorption on the pyrrhotite surface. Furthermore, an increase in the zeta potential of pyrrhotite with increasing ionic strength was reported, indicating cation adsorption on the mineral surface. The study presented shows a direct relationship between the zeta potential and attachment probability.

Chapter 7: L.L October, K.C Corin, M.S Manono, N. Schreithofer, J.G Wiese (2020). Specific Ion Effects on the Bubble-Particle Attachment of Pyrrhotite. Parts of this work were presented at WISA 2018. Cape Town, South Africa

Abstract

Froth flotation takes advantage of the natural and induced surface properties of minerals, resulting in a separation between the valuable and non-valuable minerals. Process water used to facilitate the froth flotation process comprises of many different ions. Previous studies have looked at both the effect of using recycled process water and whether certain ions are responsible for what is observed in the final concentrate in terms of mineral grades and recoveries. However, the attachment of mineral particles to air bubbles is a fundamental sub-process without which separation of value from non-value cannot occur. It is therefore of interest to assess the effect of specific ions on the probability of mineral particles attaching to an air bubble. The attachment probability of pyrrhotite to air bubbles in the presence of three different electrolytes namely, $NaNO_3$, $Ca(NO_3)_2$ and $CaSO_4$ at 0.1205 M was investigated. A synthetic plant water of the same ionic strength was also tested for comparison. This experimental approach allowed for an anionic and cationic effect to be established with regards to attachment probability, microflotation recovery and zeta potential. The attachment probability measurements were carried out using an Automated Contact Time Apparatus (ACTA) housed at Aalto University. The presence of Na^+ resulted in a more superior performance compared to Ca^{2+} in terms of the attachment probability and recovery of pyrrhotite particles. Furthermore, upon studying the anion effect, SO_4^{2-} performed better than NO_3^- when paired with Ca^{2+}; thus, indicating a negative effect on flotation response when Ca^{2+} and NO_3^- ions are used together. The implications of this work are thus of great significance for the effective management of ions in recycled process water in the froth flotation process.

Chapter 8: L.L October, K.C Corin, M.S Manono, N. Schreithofer, J.G Wiese (2021). Fundamental and Flotation Techniques Assessing the Effect of Water Quality on Bubble-Particle Attachment of Chalcopyrite and Galena. Minerals Engineering Minerals Engineering 167 106880. https://doi.org/10.1016/j.mineng.2021.106880

Abstract

Bubble-particle attachment has been studied in the most fundamental way from as early as 1934 by bringing a bubble into contact with a flat mineral surface and since then, techniques measuring this interaction have advanced. Water quality within flotation will impact the bubble particle attachment and as more operations recycle their water on site, an understanding of this process becomes vital. This study uses an Automated

Contact Time Apparatus (ACTA) to assess the effect of water quality on bubble-particle attachment of selected sulfide minerals; galena and chalcopyrite, from a fundamental perspective. Classical microflotation tests are complemented with collector adsorption and mineral potential under degrading water quality to validate the ACTA and gain an understanding of the effect of water quality on bubble-particle attachment as well as subsequent flotation. This investigation showed that the results from the ACTA qualitatively showed similar trends as that of the classical microflotation technique for measuring floatability, however the quantitively these methods showed very different results. Due to the dynamic nature of the microflotation technique it may be assumed that plant recovery will resemble the results from this technique closer than that of the ACTA. Furthermore, this investigation showed an increase in zeta potential of both minerals as the concentration of inorganic electrolytes in the water increased. It can thus be speculated that the increase in bubble-particle attachment with increasing ionic strength of synthetic plant water may be attributed to electrical double layer compression and particle agglomeration.

Chapter 9: L.L October, K.C Corin, M.S Manono, N. Schreithofer, J.G Wiese (2019). Considering the Ionic Strength and pH of Process Water on Bubble-Particle Attachment of Sulfide Minerals: Implications for Froth Flotation in Saline Water. In: Khayrulina, E.; Wolkersdorfer, Ch.; Polyakova, S.; Bogush, A.: Mine Water – Technological and Ecological Challenges. ISBN Number: 978-5-91252-145-4. p. 437 – 445; Perm, Russia (Perm State University)

Abstract

Due to the current climate of water scarcity in mining areas and the fact that water treatment is costly; the recirculation of process water seems to be a viable option in mineral processing. A consequence of the recirculation of water is the build-up of ions such as Ca^{2+}, Mg^{2+}, Na^{+}, SO_4^{2-} and NO_3^{-} as well as increases in pH. This study thus considers the combined effect of increasing ionic strength and pH of process water on the froth flotation process. These parameters are important to study simultaneously because complex water systems at high pH values, may result in the formation of various hydroxo complexes compromising the flotation efficiency.

Both fundamental bubble-particle attachment tests and microflotation show decreases in attachment and sulfide recovery as the pH is increased to 11. However, at the elevated pH the recovery increases as the ionic strength (water recycles) is increased. This could be due to the compression of the electrical double layer by the indifferent ions as seen by the zeta potential determination tests. The zeta potential also shows steep increases with sulfide minerals at pH 11.

Although this work suggests that process water with a pH as high as 11 will result in decreased mineral recoveries, it has been shown that at increased levels of ionic strength (increased recirculation of process water) higher recoveries can be obtained. Thus, it can be concluded that if the pH of process water was to reach a pH of 11, the combined effect of recirculation of process water would not necessarily have detrimental effects on sulfides flotation performance.

Chapter 10: L.L October, K.C Corin, M.S Manono, N. Schreithofer, J.G Wiese **(**2020). A Fundamental Study Considering Specific Ion Effects on the Bubble-Particle Attachment of Sulfide Minerals. Minerals Engineering 151 pp: 106313. https://doi.org/10.1016/j.mineng.2020.106313

Abstract

Bubble-particle attachment is one of the most fundamental sub-processes in froth flotation. It is of critical importance in achieving the separation of value from non-value. This sub-process is affected by many factors such as the chemistry of the pulp, action of the reagents, hydrodynamics and operational factors. Understanding the effects of these factors on bubble-particle attachment is thus crucial as they may in turn affect the mineral recoveries attained. With the current drive towards zero effluent discharge on mineral concentrators water quality is an important factor to understand as it can change the pulp chemistry and subsequently affect mineral recoveries. This study thus considers the effect of specific ions found in process water on the bubble-particle attachment of chalcopyrite and galena. Adsorption studies and zeta potential determination tests were conducted to interpret the outcomes of the bubble-particle attachment tests. Pulps containing Ca^{2+} resulted in lower bubble-particle attachment probability and recovery of galena and chalcopyrite. Adsorption studies complemented the bubble-particle attachment findings well and showed that in Ca^{2+} containing waters, less xanthate was adsorbed on both the chalcopyrite and galena surfaces. The zeta potential increased with Ca^{2+} containing salts compared to the very negative zeta potential in $NaNO_3$. This work provides evidence of the passivation of the mineral surface with Ca^{2+}; which hindered the adsorption of xanthate on the mineral surface in Ca^{2+} containing solutions and subsequently resulted in poor bubble-particle attachment.

Chapter 11: Discussion

This chapter presents a consolidated discussion of the various publications and conference proceedings included in this dissertation. This chapter also aims to bring together and provide answers to the key questions as well as interrogate the results compared to what was hypothesised in Chapter 3. Four main themes are discussed in this chapter, namely the use of the ACTA as a means to measure floatability, the effect of synthetic plant water of increasing ionic strength on bubble-particle interactions, the effect of specific ions on bubble-particle interactions and the combined effect of ionic strength and pH of synthetic plant water on bubble-particle interactions.

Chapter 12: Conclusions and Recommendations

This short chapter concludes the findings of the work of this study and the implications thereof. Furthermore, based on the findings and unanswered questions of this work recommendations for future work is proposed at the end of this chapter.

1.6 References

Albijanic, B., Ozdemir, O., Nguyen, A. and Bradshaw, D. (2010). A review of induction and attachment times of wetting thin films between air bubbles and particles and its relevance in the separation of particles by flotation. Advances in Colloid and Interface Science. 159: 1-21.

Albijanic, B., Bradshaw, D. and Nguyen, A. (2012). The relationships between the bubble–particle attachment time, collector dosage and the mineralogy of a copper sulfide ore. Minerals Engineering. 36-38: 309-313.

Aspiala, M., Schreithofer, N., Serna-Guerrero, R. (2018). Automated contact time apparatus and measurement procedure for bubble-particle interaction analysis. Minerals Engineering. 121, 77–82.

Bradshaw, D. (1997). Synergistic effects between thiol collectors used in the flotation of pyrite. PhD Thesis, University of Cape Town, Faculty of Engineering and the Built Environment, Chemical Engineering Department, Cape Town, South Africa

Gu, G., Xu, Z., Nandakumar, K. and Masliyah, J. (2003). Effects of physical environment on induction time of air-bitumen attachment. International Journal of Mineral Processing. 69: 235-250.

Klimpel, R. D. (1984). Froth flotation: The kinetic approach. Mintek 5. Johannesburg, South Africa.

Muzenda, E. (2010). An Investigation into the Effect of Water Quality on Flotation Performance. World academy of Science, Engineering and Technology.

Slatter, K.A., Plint, N.D., Cole, M., Dilsook, V., De Vaux, D., Palm, N., Oostendorp, B. (2009). Water Management in Anglo Platinum Process Operations: Effects of Water Quality on Process Operations. In: Abstracts of the International Mine Water Conference, Pretoria, South Africa, 19th – 23rd October 2009 Proceedings ISBN Number: 978-0-9802623-5-3. pp. 46–55.

Smith, P. G. and Warren, L. J. (1989). Entrainment of particles in flotation. Mineral Processing and Extractive Metallurgy Review, 5 (1-4), 123-145.

Yoon, R. and Yordan, J.L. (1991). Induction-time measurements for the quartz-amine flotation system. Journal of Colloid and Interface Science. 141 (2): 374-383.

.

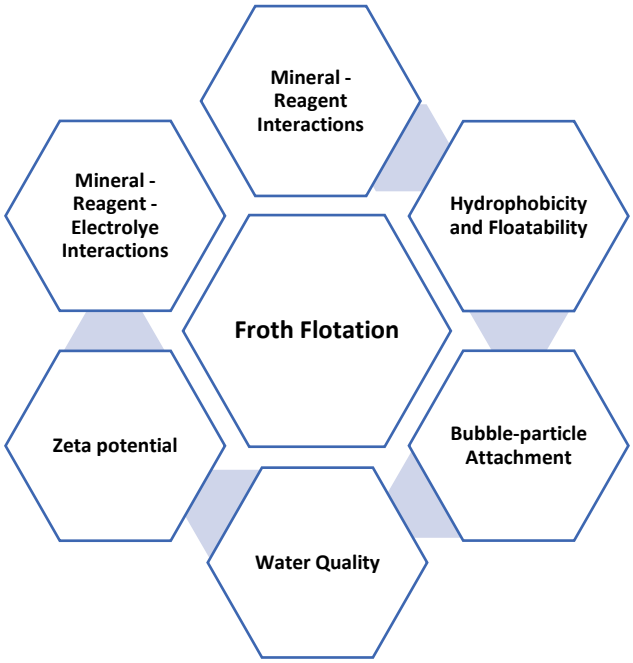

2.1 Introduction

Extensive research has been done in the area of bubble-particle attachment as one of the sub-processes of froth flotation. This includes experimental techniques and equipment, factors affecting bubble-particle attachment and the modelling of bubble-particle attachment probability within flotation systems. Studies investigating the effect of water quality on bubble-particle attachment are limited and those that do exist show conflicting effects. This review aims to fully outline the effect that an electrolyte solution has on the charge on the mineral surface and mechanism of interaction between collectors and the mineral surface.

This review begins with froth flotation fundamentals and the factors that affect the overall flotation process; emphasis is placed on mineral type, collectors and how collectors adsorb on the mineral surface. Then bubble-particle attachment fundamentals, techniques used to measure bubble-particle attachment, factors influencing the attachment of particles to air bubbles and differences between floatability and hydrophobicity of particles are considered. The review concludes with a section reviewing water quality within froth flotation. The final section focusses on the structure of water, mineral – water interactions, mineral – electrolyte interactions, mineral – electrolyte – collector interactions, the effect of ionic solutions on the froth phase and the effect of ionic solutions on the potential of air bubbles.

2.2 Froth Flotation Fundamentals

Froth flotation is a mineral beneficiation process which takes advantage of a mineral's natural and induced surface properties, resulting in physico-chemical separation between the valuable and gangue minerals (Smith and Warren, 1989). Flotation systems consist of the pulp phase and the froth phase. Air bubbles are generated and passed through the mineral pulp and hydrophobic mineral particles then attach to the air bubble resulting in bubble-particle aggregates. The bubble-particle aggregates then rise through the pulp phase to the froth phase where the particles are eventually collected; this is termed true flotation.

Hydrophobicity refers to the tendency of a surface to repel water while hydrophilicity refers to the tendency of molecules being attracted to water molecules. Hydrophobicity in froth flotation is discussed in Section 2.7.1. A particle's true flotation is largely due to the hydrophobicity of the particle and occurs when a particle contacts with and adsorbs onto an air bubble. For true flotation to occur the air bubble with attached particles must rise to the water surface; furthermore, the agitator in the flotation cell provides enough turbulence promoting particle-bubble collisions (Wills and Napier-Munn, 2016).The hydrophilic particles are thus not transported to the surface as they cannot be recovered by true flotation and remain suspended in the slurry (Bradshaw *et al.*, 2005). This process is illustrated in Figure 2-1. Chemical reagents are often added to enhance the differences in surfaces properties; i.e. make valuable particles hydrophobic and gangue particles hydrophilic.

Entrainment is a flotation mechanism whereby fine particles suspended in water are transferred to the froth phase and are recovered along with particles that were recovered through true flotation. According to Wang *et al.* (2016) entrainment is a two-step process, first the particles ascend upwards to the froth phase and in the second step, these particles in the froth are transferred to the concentrate launder together with water. Therefore, the recovery of particles by entrainment is correlated with the state of the solid's suspension in the pulp phase, drainage in the froth (as described in Section 2.3.2.3) and water recovered. This mechanism is thus largely dependent on particle size and density. Entrainment is not a selective mechanism and therefore allows gangue material to enter the concentrate (Smith and Warren, 1989).

True flotation is therefore more desirable than entrainment in order to increase mineral grades and recovery. It is also worth noting that naturally floatable gangue like talc, which is naturally hydrophobic, can be transported to the froth by either true flotation or entrainment, thus lowering mineral grades (Becker *et al.*, 2009).

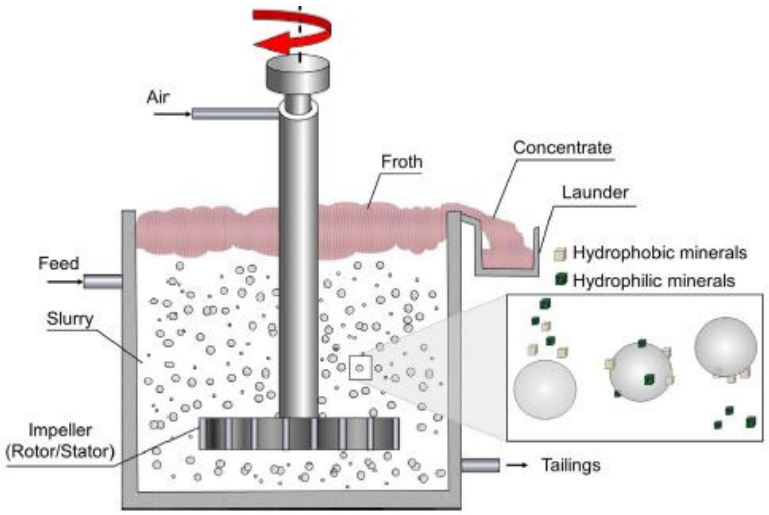

Figure 2-1: Illustration of a froth flotation cell and its components (Wills and Finch, 2016)

The overall flotation process therefore comprises six sub-processes (Bradshaw, 1997); 1: The creation of the hydrophobic mineral surface, this includes the adsorption of collector molecules on the mineral surface and changing the pulp conditions, 2: The formation of bubbles with a fixed size and distribution, 3: The collision between the mineral and bubble and potential attachment, this sub-process involves the thinning and rupture of the wetting film between the mineral and bubble, however detachment can also occur, 4: The transport of the bubble-particle aggregate through the pulp phase, 5: The transfer of the bubble-particle aggregate to the froth phase, here particles can fall back into the pulp phase, 6: The collection of the bubble-particle aggregate from the froth phase (Bradshaw, 1997).

2.3 Factors Affecting Froth Flotation

The froth flotation process is very complex and is affected by many parameters, Klimpel (1984) categorised these factors into three groups; pulp chemistry, hydrodynamic components and operational constituents. Figure 2-2 provides a summary of these parameters.

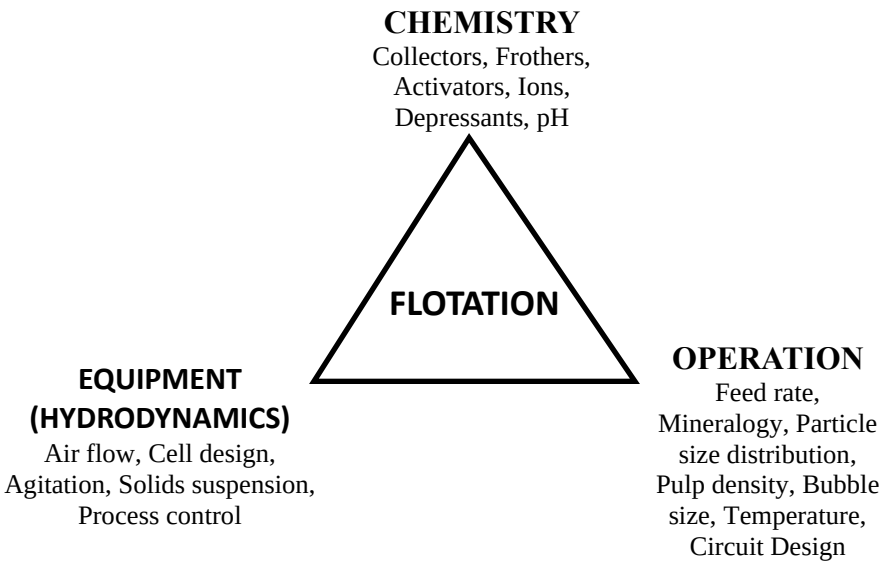

Figure 2-2: Factors that affect the flotation process (adapted from Klimpel, 1984)

2.3.1 Operational Factors

Figure 2-2 shows the various operational factors that affect the flotation process, which comprises of mineral, bubble and pulp characteristics. However, owing to the focus of this investigation being on bubble particle attachment, the following section will only provide a detailed description of the impact of mineral type on the flotation process. This work considers three sulfide minerals namely, pyrrhotite, chalcopyrite and galena due to their varying floatability and due to the fact that their recoveries are of importance in a number of industries.

2.3.1.1 Minerals

2.3.1.1.1 Galena

Galena (PbS) is a lead sulfide mineral and is the primary mineral of lead. Galena is often associated with other sulfide minerals such as sphalerite (ZnS). The crystal structure of galena is cubic and when broken in pieces, it shows perfect cleavage in three directions which intersect at 90° (Figure 2-3). Galena has a high specific gravity of 7.4 to 7.6 as lead is its primary element. According to Wills and Napier-Munn (2016), galena feed grades are between 1% to 5% Pb; the flotation of galena and subsequent separation from sphalerite is a well-established industrial process. Naturally, galena is more floatable compared to sphalerite thus galena is floated first while sphalerite is depressed by means of zinc sulfate. For an optimal recovery of galena, a combination of dithiophosphate and xanthate collectors are used while a weaker frother such as MIBC is usually used in lead flotation. Unlike copper, lead does not readily change oxidation states and thus extensive fundamental studies have been done using galena (Fuerstenau, 1982). The natural flotation of galena, without the use of a collector has been attributed to the formation of elemental sulfur or the formation of a lead deficient, sulfur rich species on its surface (Leja, 2004).

.

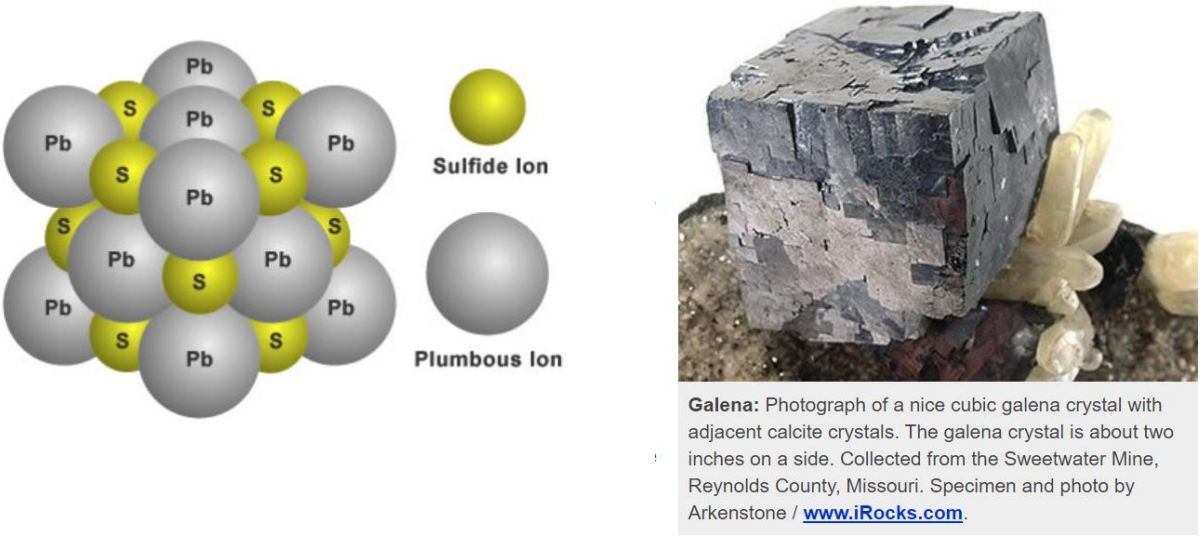

Figure 2-3: Structure of galena (left) and photograph of a cubic galena crystal with adjacent calcite crystals (right) (http://geology.com/minerals/galena.shtml)

2.3.1.1.2 Pyrrhotite

Pyrrhotite (Fe1-xS) as depicted in Figure 2-4 is an abundantly found iron sulfide mineral. Pyrrhotite is non-stoichiometric with varying density between 4.58 and 4.65. The x value can vary between 0 and 0.2, thus the amount of sulfur atoms can be between 50 and 55 per 50 atoms of iron. When x is 0, FeS, the pyrrhotite mineral is known as troilite. The crystal structure of pyrrhotite may have one of two symmetries, hexagonal or prismatic, when it is relatively low in sulfur or it may be monoclinic when the pyrrhotite is high in sulfur. Furthermore, the magnetism of pyrrhotite also varies, with a low magnetism in hexagonal pyrrhotite (x is 0) and a high magnetism when x is closer to 0.2.

Figure 2-4: Photograph of pyrrhotite (https://www.minerals.net/mineral/pyrrhotite.aspx)

Pyrrhotite is usually associated with pentlandite, ankerite, chalcopyrite and quartz. In the case of Copper – Nickel ores, pyrrhotite is rejected to the flotation tailings as waste.

Pyrrhotite flotation is however important in processing Platinum Group Minerals (PGM) ores of the South African Bushveld Complex as the PGMs are associated with base metal sulfides such as pyrrhotite, chalcopyrite and pentlandite. Therefore, the depression or flotation of pyrrhotite is an important operational driver based on the ore that is being processed. The sulfides in the treatment of PGM's are usually recovered with sodium iso-butyl (SIBX) as the primary collector, and often a secondary collector such as dithiophosphate may be used. Pyrrhotite has been described as "notoriously slow floating" by Hochreiter *et al.* (1985). Thus, the residence time in PGM operation flotation circuits are often increased to allow for the flotation of pyrrhotite (Alison and O'Çonnor, 2011). The recovery of pyrrhotite is sometimes still unsatisfactory in conditions where the adsorption of the xanthate collector is expected to occur; this has been attributed to the substantial oxidation that occurs during milling (Bushwell *et al.,* 2002). Further, it has been shown that pyrrhotite is a poor catalyst for oxygen reduction; this is necessary for the electrochemical adsorption of xanthate on the mineral surface (Bushwell and Nicol, 2002).

A number of studies have further shown that at low pH and under mild oxidation potential, iron deficient/sulfur rich metastable intermediates form at the pyrrhotite surface resulting in a hydrophobic surface and thus collectorless flotation (Hayes and Trahar,1984; Buckley and Woods, 1985; Hodgson and Agar, 1984). These authors described this action by the reactions shown in Equation 2-1 to 2-3.

$$Fe_{1-x}S + 3yOH^- = yFe_{1-(x+y)}S + yFe(OH)_3 + 3ye^- \quad \text{Equation 2-1}$$

and

$$Fe_{1-x}S + 3(1-x)H_2O = (1-x)Fe(OH)_3 + S + 3(1-x)H^+ + 3(1-x)e^- \quad \text{Equation 2-2}$$

As mentioned previously pyrrhotite surfaces do oxidise rapidly upon air exposure and the longer the surface is exposed, the more it becomes covered with an overlay of iron (III) hydroxide. This is described by the reaction below:

$$Fe_{1-x}S + (7-3x)H_2O = (1-x)Fe(OH)_3 + {SO_4}^{2-} + (11-3x)H^+ + (9+3x)e^- \quad \text{Equation 2-3}$$

Under these conditions, no natural flotation can occur due to the hydrophilic iron hydroxide at the pyrrhotite surface (Smart *et al.,* 2003; Hayes and Trahar, 1984; Buckley and Woods, 1985).

2.3.1.1.2 Chalcopyrite

Chalcopyrite (CuFeS2) has a brassy to golden colour and was first discovered in 1847 in Polk Country. Chalcopyrite is the most abundant copper bearing mineral occurring on Earth (Nesse, 2000) and is the most stable copper sulfide due its face-centred lattice. Chalcopyrite crystallises in a tetragonal structure; half

the cations are replaced by copper and the other half by iron. The ions are arranged such that each Fe(III) and Cu(I) is tetrahedrally bound by four sulfide ions and that the sulfide ions are bound by two Fe(III) and two Cu(I) ions (Persson, 1994).

Chalcopyrite is one of the three primary base metal sulfides in Merensky and UG2 reefs; comprising of about 16% of the base metal sulfides in Merensky ores (Alison and O'Connor, 2011).

2.3.2 Chemistry Factors

2.3.2.1 Collectors

Collectors are hetero-polar reagents which are added to form a hydrophobic layer on a specific minerals' surface. The collector molecule comprises of a non-polar hydrocarbon radical and a polar reactive group. Due to chemi- and physi-sorption between the polar reactive head and the mineral surface, the collector adsorbs onto the mineral particle with the non-polar hydrocarbon part orientated to the solution as illustrated in Figure 2-5. The stability of the hydrated layer which separates the mineral from the air bubble is then reduced to such an extent that the attachment of the particle to the bubble is made upon contact. Investigations have shown that a stronger induced hydrophobicity is achieved with collectors that have a longer alkyl chain length (Rao, 1982; Fuerstenau, 2005; Taguta *et al.,* 2017).

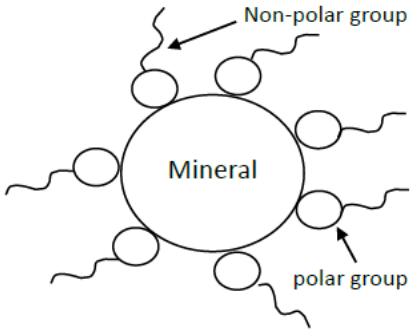

Figure 2-5: Collector molecules adsorbing on a mineral surface

In the flotation of base metal sulfides and PGMs thiol collectors are widely used; common thiol collectors include xanthates, dithiophosphates and dithiocarbonates. The mechanism of mineral – collector adsorption depends on the type of mineral surface (and its charge) and collector type; and may result in either the collector being chemisorbed or physisorbed (Bradshaw, 1997). The mechanism of adsorption of thiol collectors onto sulfide minerals is said to follow a mixed potential model (Alison *et al.* 1972; Finkelstein and Goold 1972; Rao 1982). As described in Section 2.4 the mixed potential model is when the adsorption of thiol collectors onto the surface of sulfide minerals comprises of the cathodic reduction of oxygen and the anodic oxidation of the collector (Woods, 1984).

2.3.2.2 Depressants

Depressants prevent the flotation of gangue minerals by averting the adsorption of collectors onto an existing hydrophilic mineral or by adsorbing onto a hydrophobic gangue mineral, rendering its surface hydrophilic (Bradshaw *et al.,* 2005). Depressants therefore increase the selectivity of the valuable mineral floatability by preventing the flotation of gangue minerals. Depressants can be either organic or inorganic. Organic depressants are less toxic, cheaper and more resistant to oxidation compared to inorganic depressants (King, 1982). For the depression of talcaceous gangue minerals, polysaccharide depressants such as carboxymethyl cellulose (CMC) and guar are most commonly used in South Africa when recovering PGMs (Wills and Napier-Munn, 2016).

2.3.2.3 Frothers

Frothers adsorb at the air – water interface; the orientation by which this adsorption occurs interrupts the interaction between the water molecules, thus decreasing the water surface tension which results in stable air bubbles (Figure 2-6). These surface-active heteropolar organic compounds therefore encourage smaller bubble generation and prevent the coalescence of bubbles such that a stable froth is created which allows for the selective drainage of unwanted gangue from the froth phase (Wills and Napier-Munn, 2016).

As shown in Figure 2-6, frothers adsorb with the hydrophilic part on the water side and hydrophobic part on the air side.

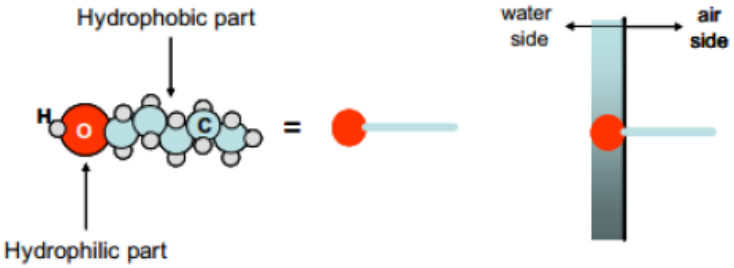

Figure 2-6: Schematic illustrating frother adsorption (Finch et al., 2008)

2.3.2.4 pH modifiers

pH is a measure of the H^+ concentration in solutions and has been shown to affect the selectivity of flotation due to it being able to either aid or hinder the adsorption of surfactants at the ionised mineral-solution interface (Rao, 2004). pH modifiers also affect the potential at the bubble surface; flotation is therefore dependant on a careful balance between collector concentration and pH (Wills, 1998).

2.3.2.5 Water Quality

In flotation systems water is an important process and transport medium and its properties are important to facilitate the execution of each of the sub-processes making up the overall flotation process. The presence of dissolved salts in water can alter the zeta potential of the mineral, the adsorption of reagents on the surface, the pH of the solution and can result in the formation of metal complexes. A detailed description of water quality and its effects on froth flotation is presented in Section 2.8.

2.4 Mineral – Reagent Interactions

The adsorption of thiol collectors onto the surface of sulfide minerals comprises of the cathodic reduction of oxygen together with the anodic oxidation of the collector (Woods, 1984). This is termed the mixed potential mechanism. The occurrence of these electrochemical reactions are facilitated by the sulfide mineral surface due to its semiconductor nature.

Both the electrochemical potential of the system and the term thermodynamics of the reactions occurring determine which surface products are formed (Finkelstein and Goold, 1972; Woods, 1984). The surface products of the anodic oxidation have been recognised to be metal thiol compounds, chemisorbed collector and collector dithiolates; these three mechanisms of reaction for the oxidation of collectors are further described in the following section.

2.4.1 Chemisorption

Adsorption of the thiol collector on the mineral surface via chemisorption occurs through covalent bonds forming between the collector molecules and the metal atoms on the surface of the mineral as depicted in Figure 2-7. Electrochemically, this occurs with the collector adsorption as the anodic reaction (Equation 2-4) and a concurrent cathodic oxygen reduction reaction; with the mineral surface facilitating the electron transfer. The overall reaction is given in Equation 2-5.

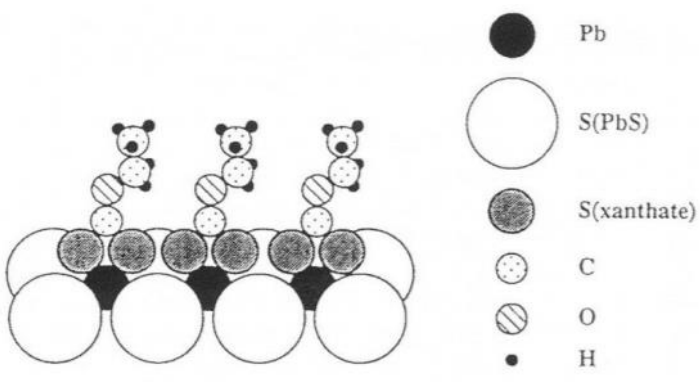

Figure 2-7: Schematic of chemisorbed Xanthate on Galena surface (Woods, 2010)

$X^- \leftrightarrow X_{adsorbed} + e^-$ ……..…….…*Equation 2-4*

$4X^- + 2H_2O + 4e^- \leftrightarrow 4X_{adsorbed} + 4OH^-$ ……..……..*Equation 2-5*

XPS studies by Buckley and Woods (1994) showed chemisorbed xanthate at the surface of galena while Leppinen *et al.* (1989) confirmed this mechanism by voltammetry and spectroscopy techniques on chalcocite, galena and silver.

2.4.2 Metal – Thiol Formation

When minerals are readily oxidised or metal thiol formation is favoured, an electrochemical reaction occurs followed by a chemical reaction (Nicholson and Shain, 1964). The electrochemical potential of the pulp controls the mineral oxidation (Equation 2-6) as it is the electrochemical potential that determines the

availability of metal ions on the mineral surface. The stability constant (pKsp) of the metal thiolate controls the chemical reaction (Equation 2-7) due to the stability constant aiding in determining if the compound will be formed at the specific condition.

$MS \rightarrow M^{2+} + S^0 + 2e^-$ ……..……..…Equation 2-6

$M^{2+} + 2X^- \rightarrow MX_2$ ……Equation 2-7

Overall reaction:

$MS + 2X^- \rightarrow MX_2 + S^0 + 2e^-$ ……..Equation 2-8

Furthermore, authors have shown that the concentration of metal thiol complexes do affect the flotation of sulfide minerals.

2.4.3 Catalytic Oxidation

The adsorption of thiol collectors onto sulfide minerals via catalytic oxidation of the collector results in the formation of dimers, termed dithiolates. Dithiolates have been reported to be that most hydrophobic species that can form on a sulfide mineral surface (Woods, 2010). The formation of dithiolates is strongly reliant on the pH and pulp potential of the solution.

The oxidation of thiol collectors to dithiolates can occur as an anodic process $(2X^- \leftrightarrow X_2 + 2e^-)$ to the cathodic reduction of oxygen or other reducing agents coupled with the oxygen reduction reaction (Equation 2-9 presents the overall reaction). This transfer of electrons from where the collector is oxidised to where the oxygen is reduced is facilitated by the mineral surface; the mineral surface however is unaltered as it does not partake in the reaction. The resultant dithiolate is then physisorbed and weakly held to the mineral surface.

$4X^- + O_2 + 2H_2O \leftrightarrow 2X_{2adsorbed} + 4OH^-$ ……..Equation 2-9

2.4.4 Galena – Collector

By means of thermochemical measurements, Mellgren and Rao (1968) reported the formation of lead xanthate upon a reaction between ethyl xanthate and galena. Poling (1976) showed the same result as the aforementioned authors by electrochemical techniques; they found the formation of lead xanthate more favourable than that of dixanthogen. These findings were then further supported by the work of Fuerstenau (1982), and Yoon and Basilio (1993).

2.4.5 Pyrrhotite – Collector

According to Hodgson and Agar (1989) no chemisorption of xanthate on the pyrrhotite surface was detected. These authors however postulated the adsorption of xanthate by Coulombic interaction by the scheme of reactions shown in Equation 2-10 to 2-12.

$Po + H_2O \leftrightarrow Po(OH)\,[S]^+ + H^+ + e^-$ ……..……..….Equation 2-10

$Po(OH)[S]^+ + X^- \leftrightarrow Po(OH)[S][X]$ ……..……..Equation 2-11

Xanthate is then oxidized to dixanthogen at the pyrrhotite surface.

$$Po(OH)[S][X] + X^- \leftrightarrow Po(OH)[S][X_2] + e^- \quad \text{Equation 2-12}$$

The oxidation reaction is further accompanied by the (cathodic) oxygen reduction reaction to form the hydroxide ion.

2.4.6 Chalcopyrite – Collector

In 1977, Finkelstein and Poling provided evidence of only dixanthogen species forming on the chalcopyrite surface. Studies by Ackerman et al. (1987) reported the formation of dixanthogen on the chalcopyrite surface, while other copper sulfide minerals such as chalcocite, bornite and covellite showed metal xanthate formation. This difference in the oxidation species formed was said to be due to the differences in the semi-conductor type of the minerals (Ackerman et al., 1987).

2.5 Froth Flotation Mathematical Description

The collection efficiency was first proposed by Derjaguin and Dukhin (1960) and it focusses on three components where hydrodynamic interactions, interfacial forces and bubble-particle aggregate stability are dominant. The model for this collection efficiency was described by Finch and Dobby (1990) to be

$$E_{collection} = E_{collision} \cdot E_{attachment} \cdot E_{detachment} \quad \text{Equation 2-13}$$

The collision efficiency is controlled by the hydrodynamics of the system such as the superficial gas rate, energy input and bubble size. It is further defined by the ratio between the number of particles that encounter bubble and the number of particles that approach the bubble in a flow tube of equivalent diameter.

When a bubble and particle collide, the particle may attach to the bubble or bounce off the surface of the bubble. The attachment efficiency is therefore defined as the number of particles that attach to the bubble over the number of particles that collide with that bubble (Finch and Dobby, 1990). The attachment efficiency is strongly dependant on the mineral surface hydrophobicity and the hydrodynamics of the system.

The detachment efficiency is described as the fraction of attached particles that detach from the bubble surface; the detachment efficiency is strongly affected by the hydrodynamics in the flotation cell and the stability of the bubble-particle aggregates.

2.6 Bubble-Particle Attachment

In froth flotation the attachment of particles to air bubbles determines the selective separation between hydrophobic and hydrophilic particles; making bubble-particle attachment the most crucial requirement to successfully separate the valuable particles from the gangue particles.

When a bubble and a particle approach each other, a film between the air-water and solid-water interfaces begin to form. Figure 2-8 illustrates the bubble-particle attachment process in three steps.

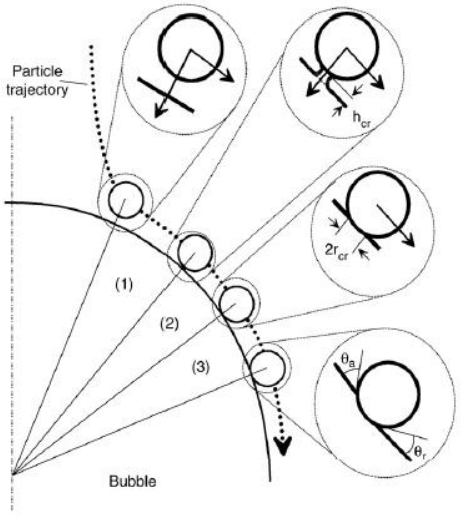

Figure 2-8: Schematic illustrating bubble-particle attachment (Albijanic et al., 2010)

The first step shows the thinning of the film at the air-water and solid-water interfaces to critical thickness. In the second step of the bubble-particle attachment sub-process the bubble and particle are in even closer contact; the film then becomes unstable and ruptures leading to the establishment of a three-phase contact line and bubble-particle attachment occurs. The final step consists of the bubble-particle contact line spreading across the surface, forming a stable wetting perimeter with equilibrium contact angles (Albijanic *et al.,* 2010).

The attachment time is defined as the time it takes for all three steps to occur (Albijanic *et al.,* 2010). The induction time is the time it takes for only step one to occur and is used to predict the susceptibility of a particle to float; the faster the wetting film thins to critical thickness the greater the chances of the mineral floating.

For the attachment of particles to air bubbles to occur, the attachment time must be shorter than the time the bubble is brought in contact with the particle, ie.

$t_{attachment} \leq t_{contact}$ ……..*Equation 2-14*

The collision contact time and sliding contact time theories were both formulated to measure the bubble-particle attachment in flotation cells. The collision contact time theory caters for high momentum bubble particle interactions; this generally occurs with particles of large diameter and high density and at high radial particle velocity in the agitator region of the cell. The collision contact time is the time at which a bubble and particle move towards each other in a straight line such that the bubble surface becomes deformed. The sliding contact time theory however can be applied to particles with low inertia and density or fine particles. The sliding contact time is the time it takes for a particle to slide along a bubble surface such that there is no deformation of the bubble (Albijanic *et al.,* 2010). Ralston *et al.* (1999) further stated that during collision interactions particles usually rebound from the surface of the bubble which results in multiple collisions and subsequently the collision interaction becomes a sliding interaction. The sliding contact time

is overall longer than that of the collision contact time; and as a result, the sliding contact time is used as $t_{contact}$ in Equation 2-14 for modelling purposes. The contact time available for attachment increases proportionally with bubble size. Good induction times are usually around the order of 10 ms.

Ye *et al.* (1989) used the attachment time measurements to describe the hydrophobicity of mineral particles, both natural and induced with surfactant. Albijanic *et al.* (2010) described attachment time measurements to be "*of paramount importance for the mineral processing industry*" because they are a more sensitive indicator for mineral floatability compared to that of equilibrium contact angle and dynamic surface tension measurements. Attachment time measurements use a particle bed which resembles the flotation system more closely as opposed to the polished mineral surface used for contact angle measurements. Furthermore, attachment time takes both hydrodynamics and surface chemistry of flotation into consideration while equilibrium contact angle only takes into account the thermodynamics.

2.6.2 Experimental Systems for Determining Attachment Time

Sven-Nilsson (1934) first presented the concept of induction time and described it as the minimum time that a bubble and particle are in contact, resulting in the thinning of the hydration film to critical thickness where film rupture happens. This author first measured the induction time between a bubble and particle by bringing a captive bubble towards a flat mineral surface for a set contact time and then moving it away from the mineral surface. The set contact time (t) used and the number of times the bubble was brought in contact with the surface (n) before attachment occurred was noted and plot of 1/n vs t was used by Sven-Nilsson (1934) to determine the attachment time. He determined the attachment time to be the contact time at 50% of 1/n (Figure 2-9).

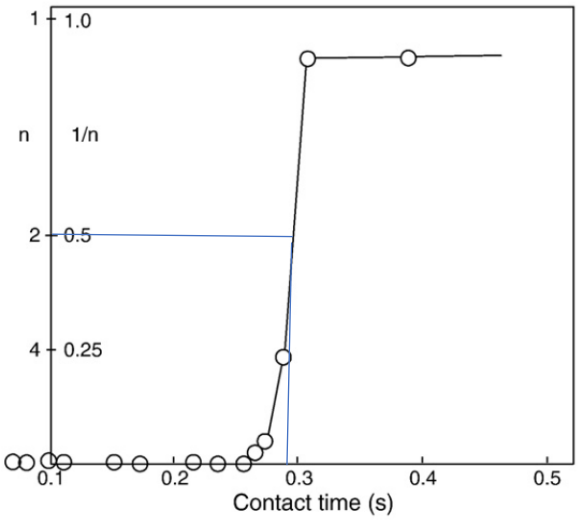

Figure 2-9: Graph of how attachment time was first determined by Sven-Nillson in 1934 (Sven-Nilson, 1934)

Glembotsky (1953) used a similar technique to determine the induction time however instead of a flat mineral surface, the single bubble was brought into contact with a bed of particles. The use of a bed of particles resembles an actual flotation system more than a flat mineral surface. This technique developed

by Glembotsky is still currently the most widely used method of measuring attachment time and has proven to be a successful one in flotation research; with this technique authors have shown the effects that parameters such as pH, ionic strength, particle size and particle shape have on the bubble-particle attachment sub-process (Ye *et al.,* 1989; Yoon and Yordan, 1991; Gu *et al.,* 2004) (Section 2.6.3.1).

In 1960 however, Eigeles and Volova carried out an induction time investigation by bringing the particle bed into contact with a stationary captive bubble. The findings of this work showed trends in induction time with changes in parameters such as collector dosage, particle size and temperature. Krasowska and Malysa (2007) and Nakamura *et al.* (1988) determined the attachment time by blowing a bubble onto a flat mineral surface that was immersed in solution and determining the attachment by means of a high-speed video microscope.

2.6.3 Measuring Devices for Bubble-Particle Attachment

2.6.3.1 The Induction/Attachment Timer

Modern induction timers operate on the principle that a captive bubble is brought into contact with a particle bed for a set contact time; the bubble size is controlled and the bubble it held on a glass capillary. After contact with the particle bed, the bubble and capillary return to the starting position. The bubble is then studied for attachment at the specific contact time via a video camera or microscope. The aforementioned steps are then repeated at various areas on the particle bed and the fraction of observations that resulted in attachment is determined for that specific contact time. These steps are then repeated at different contact times such that a distribution of attachment percentage versus contact time is attained. The contact time where 50% of the observations result in attachment is subsequently termed the attachment time. Figure 2-10 provides a schematic of the attachment between a moving captive bubble and a particle bed.

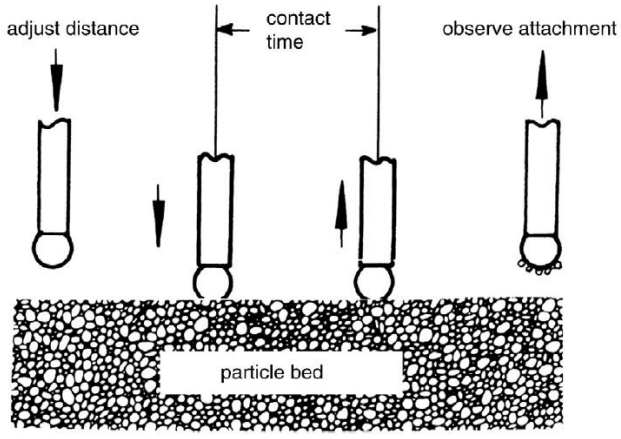

Figure 2-10: Measurement of attachment time using attachment timer apparatus (Ye et al., 1989)

2.6.3.2 Microflotation/Bubble-Loading

Particles enter the froth phase either by the bubble-particle attachment or they enter the froth phase directly via entrainment, unselective upwards flow. Bubble loading is a technique that evaluates purely the bubble-particle attachment as it occurs in the pulp phase; this includes the collision between a stream of rising bubbles and hydrophobic particles, their attachment and possible detachment. The bubble loading technique thus takes the thermodynamic and kinetic properties of the mineral floatability into consideration. Air is introduced at the base of the cell at a set flowrate (bubble size and bubble size distribution previously determined by the UCT Bubble Sizer (Randall, 2005), the loaded bubble rises through the cell and deflects off the cone, eventually reporting to the launder. The recovered particles are then tapped out of the launder and filtered to determine recovery (Bradshaw and O'Connor, 1996); a schematic of the flow through a microflotation cell is shown in Figure 2-11.

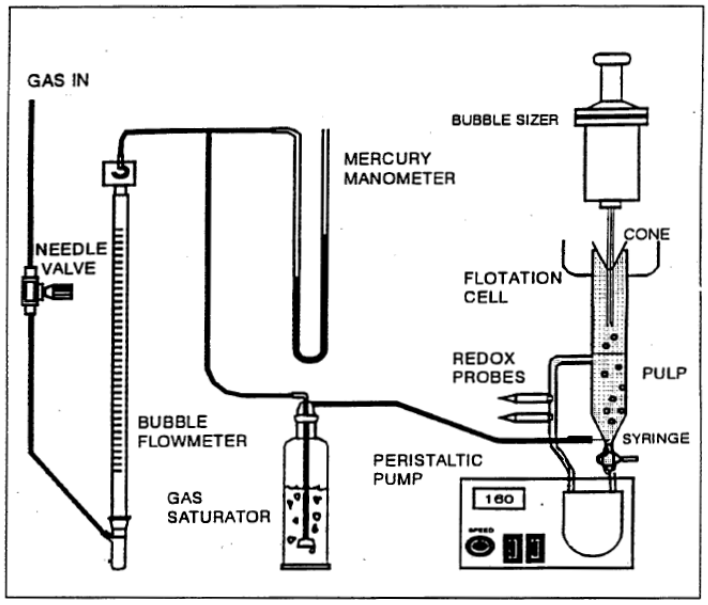

Figure 2-11: Schematic of a microflotation set-up (Bradshaw and O'Connor, 1996)

2.6.3.3 Atomic Force Microscopy (AFM)

When force measurements between colloidal particles and deformable surfaces are conducted the AFM gives the force acting on the particle versus the piezo displacement between the bubble and the particle. Normally the output would give the force acting on the particle against the gap between bubble and particle (Butt, 1994; Ducker et al., 1994) but given the bubbles ability to deform, this gap cannot be measured accurately. Many authors have investigated the force measurements between colloidal particles and deformable surfaces and the importance of the hydrodynamic force in certain cases (Butt, 1994; Webber et al., 2008; Ozdemir et al., 2009; Krasowska et al., 2011). Force details on this subject the work of the aforementioned authors can be viewed. For the purpose of this investigation, it is important to note that AFM can be used in bubble-particle attachment studies.

Figure 2-12 shows a schematic of an AFM set-up where the interaction between a coal particle (which is glued on a microfabricated cantilever) and an air bubble.

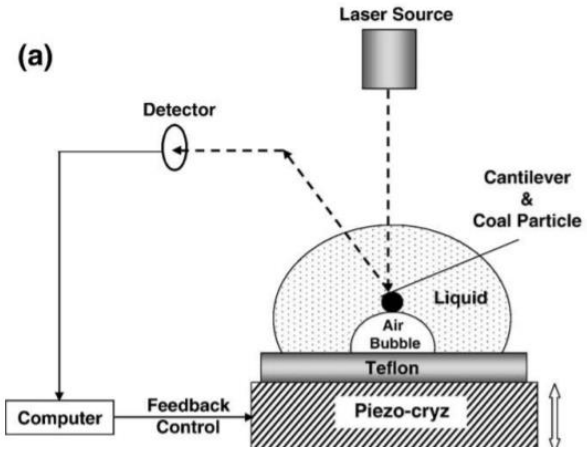

Figure 2-12: Schematic of Atomic Force Microscopy apparatus (Ozdemir et al., 2009)

2.6.3.4 Integrated Thin Film Drainage Apparatus

The operating principle of the ITFDA is based on a combination of the induction timer and the Atomic Force Microscope (AFM). As with the induction timer a single motion-controlled bubble is used, however it is brought in contact with a single particle as opposed to a bed of particles. This single particle is attached to a force sensor as with AFM tests. The motion-controlled bubble and single particle are carefully aligned to achieve direct interactions. The time between the detection of a slight repulsion force to the moment of attachment is defined as the film drainage time (Wang *et al.,* 2013). Figure 2-13 shows the integrated film drainage apparatus set-up used by Wang *et al.* (2013).

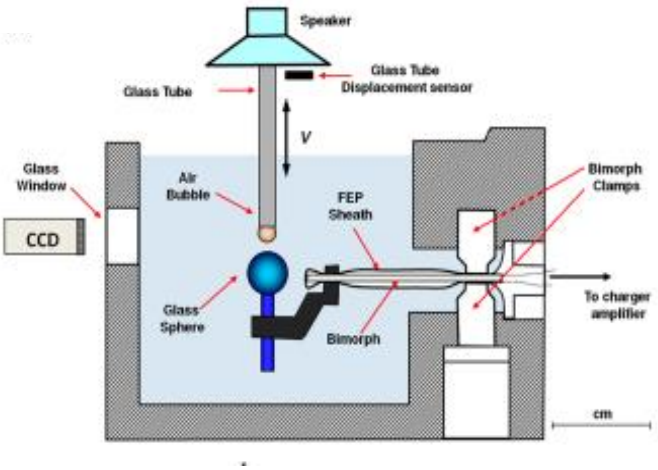

Figure 2-13: Schematic of the integrated film drainage apparatus (Wang et al., 2013)

2.6.3.5 Comparing Bubble-Particle Interaction Equipment

The main difference between microflotation tests and induction time/AFM studies is that in the latter the motion of the bubbles is rather constrained whereas microflotation follows the natural motion of the

particles/bubbles; making it particularly suitable for site and applied laboratory research (Verrelli and Albijanic, 2015). The induction time method of evaluating bubble-particle interactions from a fundamental level as described in Section 2.6.3.1 is more time efficient and resembles flotation more compared to AFM studies. This method does however raise questions of whether the limited areas on the particle bed tested are representative of the entire particle bed.

2.6.4 Attachment Time of Naturally Hydrophobic Minerals

The flotation of naturally hydrophobic particles such as coals, hydrocarbons, bitumen, fluorite, waxes and molybdenite rarely require the addition of reagents to induce hydrophobicity however atmospheric oxidation can reduce the hydrophobicity of the naturally hydrophobic particles. Figure 2-14 shows work by Yoon (2000) who reported an increase in the induction time of coal particles from 3 ms to 6 ms after its oxidation in water for 28 days.

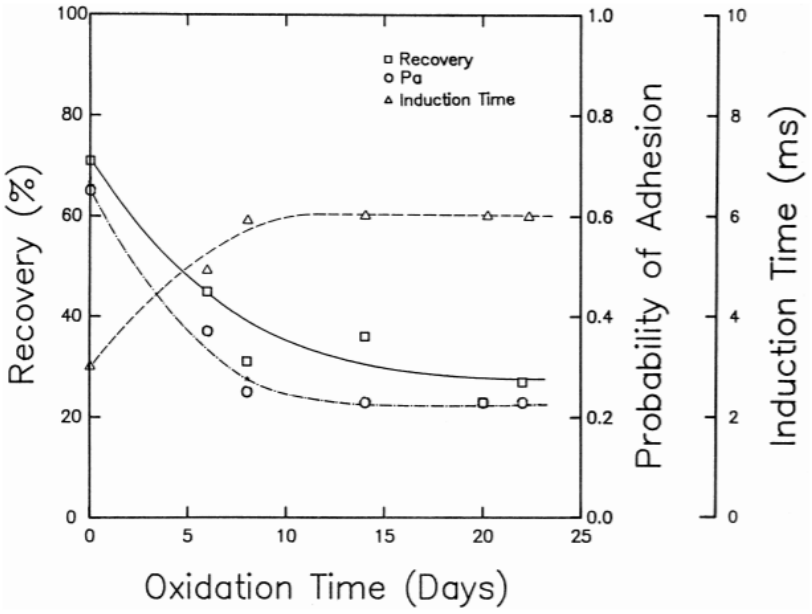

Figure 2-14: Induction time of hydrophobic coal particles that was exposed to the atmosphere over a period of time (Yoon, 2000)

2.6.5 Factors affecting Bubble-Particle Attachment

The factors that affect bubble-particle attachment include the particle and particle surface characteristics, bubble characteristics, pulp chemistry as well as hydrodynamic factors. These factors and their effects on bubble-particle attachment are hereafter discussed in detail.

2.6.5.1 Particle and Particle Surface Characteristics

2.6.5.1.1 Particle Size

A study by Bradshaw and O'Connor (1996) investigated the effect of particle size class on bubble-particle attachment by means of bubble loading experiments. The results from this study showed that the number of particles per bubble decreased as the size fraction increased and the mass per bubble increased at

increased size fractions. Yoon and Yordan (1991) used induction time equipment to investigate the effect of particle size on induction time. This study showed that induction time increased with increasing particle size. Thus bubble-particle attachment occurred faster with smaller particles. The authors of this study attributed this to the fact that it takes longer to displace the water film on larger particles. This justification can be extended to why less particles attached to the bubble for particles of larger size fractions as shown by Bradshaw and O'Connor (1996).

2.6.5.1.2 Surface Liberation of Value

Albijanic *et al.* (2011) investigated the relationship between bubble-particle attachment time and the mineralogy of a copper sulfide ore. As a result of this being a real ore the attachment of the particles to the air bubbles will be governed by particle composition and liberation and hence the need for the study. The results from this study showed that the attachment time was the lowest for concentrate one (25 ms) and increased as the concentrate number increased. The attachment time for the tails sample was 17 000 ms. These results were attributed to the low amount of valuable liberated particles in higher concentrate numbers/tails; shown by the mineral liberation analyser (MLA) in this investigation. The MLA additionally showed that liberated particles in all products had a higher recovery compared to middlings and poorly liberated particles.

2.6.5.1.3 Particle Shape

Particle shape can vary greatly and largely depends on the comminution process employed prior to flotation. Koh *et al.* (2009) found that ground ballotini balls generally resulted in a better flotation performance compared to spherical ballotini balls. Vizcarra *et al.* (2011) also found that angular (ground) chalcopyrite particles with no collector reported to the concentrate at a faster rate compared to round particles. Furthermore, Verrelli *et al.* (2012) showed that shortened induction times were achieved with angular particles. This was attributed to the fact that the thinning and rupturing of the film at the air-water and solid-water interface occurs faster as a result of the roughened edges characteristic of angular particles. The study by Vizcarra *et al.* (2011) however showed that there is no relation between particle shape and flotation performance when particles are highly floatable (naturally or induced).

2.6.5.1.4 Surface Roughness

Surface roughness is one of the parameters characterizing surface morphology. The various grinding media/devices have an effect on the structural changes of the solid particles. Rahimi *et al.* (2012) found that particles ground in a rod mill yielded an increase in particle surface roughness and elongation ratio but produced a lower roundness compared to particles ground in a ball mill. In 1977 Anfruns and Kitchener proposed that roughness on the surface of the particle stimulated the rupture of the liquid film in bubble-particle attachment; increasing the efficiency of bubble-particle attachment. In a later investigation by Kraskowski and Malysa (2007) it was validated that an increase in roughness results in a shorter induction time and also reduces the bubble bounce on the surface before attachment. According to Feng and Aldrich when dry grinding samples a proportion of the energy is consumed for crystal defects with rougher surfaces,

which increases the concentration of microstructural defects. These active points are said to accelerate the adsorption of reagents on the mineral surface. Furthermore, Hassas *et al.* (2016) showed that smooth spherical particles resulted in a longer induction time than roughened spherical particles. This same trend was seen in a study by Zawala *et al.* (2008) where roughened fluorite particles yielded a much shorter induction time compared to smooth fluorite particles. These authors attributed this to pillars on hydrophobic rough surfaces, which lead to a greater probability of film rupture as the critical thickness of the wetting film is locally thinner on rough surfaces.

2.6.5.2 Bubble Characteristics

2.6.5.2.1 Bubble Size

Gu *et al.* (2003) studied the effect of bubble diameter on bubble-particle attachment. The bubble diameter was varied, and attachment time equipment was used with a bed of silica particles. The results revealed that the time for particles to attach to the bubble increases with increasing bubble diameter. In a study by Wang *et al. (*2005), methylated beads were used to determine the effect of bubble size on induction time; here it was also shown that induction time increased with bubble size. Yoon and Yordan (1991) explained the effect of bubble size on induction time and consequently rate of film thinning by the Reynolds lubrication theory. This theory states that the drainage velocity of the thin film between the sphere (bubble) and an infinitely large plate (particle bed) is directly proportional to the force at which the sphere is approaching. The film thickness is inversely proportional to both the viscosity of the film and the squared radius. Thus, larger bubbles will have a lesser rate of film thinning; resulting in an increase in induction time. Additionally, as with larger particles it will take longer to displace the film between the bubble and particle with larger bubbles time (Yoon and Yordan, 1991; Ye *et al.*, 1989).

2.6.5.2.2 Gas Type

Gu *et al.* (2004) studied the effect of the type of gas used to form bubbles on the attachment time. These authors found that hydrogen bubbles resulted in shorter attachment times compared to oxygen bubbles; they attributed this to the fact that oxygen molecules are more polar and will result in strong hydrogen bonding when it encounters water which in turn stabilises the liquid film, resulting in longer attachment times.

2.6.5.3 Pulp Chemistry

2.6.5.3.1 Pulp Temperature

The effect of temperature on induction time is said to be explained by the Arrhenius equation shown in Equation 2-15 (Albijanic *et al.,* 2010).

$$t_{at} = t_0 . exp\left(\frac{E}{kT}\right) \quad \text{.....Equation 2-15}$$

Where t_0 is a time constant, E denotes the activation energy to achieve bubble-particle attachment, k represents the Boltzmann constant and T is the temperature (absolute). From Equation 2-15, time is inversely proportional to temperature; this was reinforced by studies by Yoon and Yordan (1991) and Gu

et al. (2003). Yoon and Yordan (1991) showed that the induction time decreases as the temperature increases for all collector concentrations tested in a quartz system while Gu *et al.* (2003) showed the same result in a bitumen system.

2.6.5.3.2 pH

The pH of the system has been responsible for significant changes in the flotation performance; the use of a cationic collector at a low pH results in competition between the cations and H^+ on the adsorption of the mineral surface. Whereas the use of anionic collectors at high levels of pH results in competition between the anions and OH^- for the adsorption on the mineral surface. Both cases described have a detrimental effect on flotation performance (Albijanic *et al.,* 2010). The effect of pH on bubble-particle attachment is dependent on the particular system in terms of whether an anionic or cationic collector is used. The collector used in the system has a critical pH where there is a high adsorption of collector ions on the mineral surface; leading to increased hydrophobicity and hence faster bubble-particle attachment (Albijanic *et al.,* 2010). Yoon and Yordan (1991) showed that in a quartz-dodecylammonium hydrochloride (DAH collector) system the shortest induction time is achieved at a critical pH of 10.5. This study showed that the attachment time decreases up to the critical pH, where the adsorption of NH_3^+ on the mineral surface is the greatest. After the critical pH is reached the attachment time decreases as the collector ions begin to precipitate on the mineral surface. A collector concentration versus pH thermodynamic diagram can be used to see the regions of concentration and solution pH where the collector ions undergo precipitation or micellization.

2.6.5.3.3 Electrolytes / Dissolved Ions

Yoon and Yordan (1991) also looked at the effect of electrolytes on induction time. The same method as when particle size was investigated was employed except at a fixed quartz particle size and the concentration of KCl was varied. The results showed that at a lower collector concentration, the induction time shortened with increasing KCl concentration. This follows what was found by Laskowski and Iskra (1970) also in a quartz system; they attributed this result to the compression of the electrical double layer. The compression of the electrical double layer consequently results in the acceleration of the rupturing of the wetting film, leading to faster bubble-particle attachment. At high collector concentrations Yoon and Yordan (1991) found that the induction time was longer with increasing electrolyte (KCl) concentrations. The authors attributed this to the association of the collector ions and its subsequent adsorption on the surface of the mineral in bimolecular layers; increasing bubble-particle attachment time. The results obtained from this study can be seen in Figure 2-15.

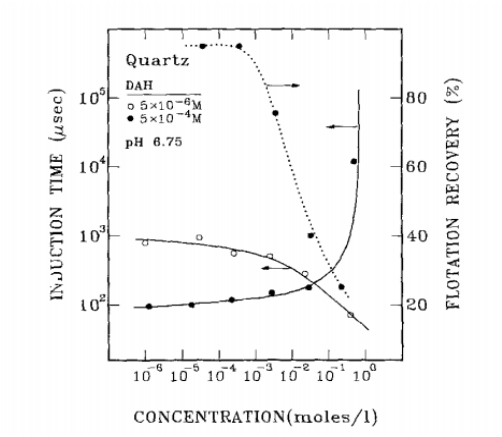

Figure 2-15: Effect of KCl concentration on induction time (Yoon and Yordan, 1991)

Gu *et al.* (2003) studied the effect of water quality on induction time in a bitumen system. The investigation was carried out using induction time equipment, generating a bubble of fixed diameter and moving it towards and away from a bed of bitumen particles. This procedure was performed with de-ionised water, process water, process water with 50 ppm calcium ions, process water with 0.5% solids and the addition of 50 ppm calcium ions to the process water with 0.5% solids. The results obtained from this study can be seen in Figure 2-16.

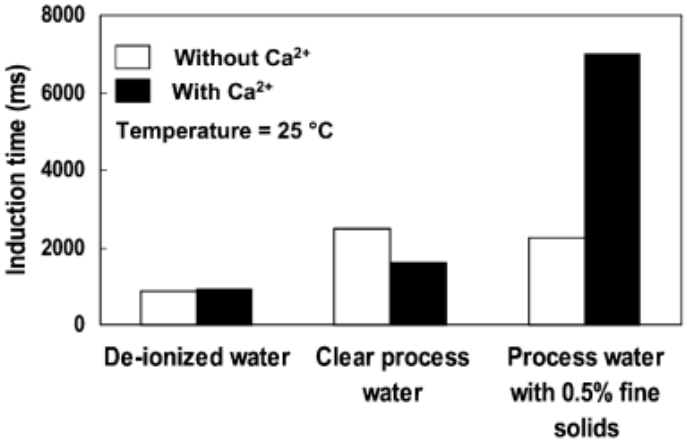

Figure 2-16: Effect of water quality on induction time in a bitumen system (Gu et al., 2003)

The study revealed that the induction time shortened upon the addition of calcium ions to clear process water compared to without calcium ions. This result could also be explained by the conclusions drawn from Laskowski and Iskra (1970); whereby the electrical double layer is compressed in the presence of ions, leading to the acceleration of the rupturing of the wetting film and ultimately decreasing the bubble-particle attachment time.

This trend was however not observed when process water containing solids was tested; upon the addition of calcium ions to this water type, the induction time increased significantly compared to without the calcium ions. This result therefore indicates a synergy between the solid particles and calcium ions. The

authors of this study explained this to be as a result of the negative surface of bitumen; thus, upon the introduction of solids and calcium ions, the calcium ions act as a binder between the solids and the bitumen surface. With a coating of solids on the bitumen, resulting in a more hydrophilic bitumen surface and hence increasing the time for bubble-particle attachment to occur.

2.7 Hydrophobicity and Floatability

2.7.1.1 Surface Forces Acting Before Bubble-Particle Adhesion

According to the DLVO (Derjaguin, Landau, Verwey and Overbeek) theory (Derjaguin and Landau, 1941; Verwey and Overbeek, 1948) the surface forces between particles immersed in liquid are the sum of the van der Waals and electric double layer forces. Two similar colloidal particles have an attractive van der Waals force while the electric double layer force is repulsive. Bostom et al. (2001) showed that the DLVO theory has a number of limitations, for this reason the theory has been extended to include steric forces and solvation forces. The latter depends on the physico-chemical properties of the surface of the particle and the properties of the intervening medium; these can be broken down as attractive hydrophobic force and repulsive hydration forces in an aqueous solution. While steric forces exist in systems with macromolecular reagents (Israelachvili and Pashley 1982; Leneveu et al. 1977).

2.7.1.2 Hydrophobic Force in Flotation

In froth flotation the electric double layer, van der Waal and hydrophobic forces are the most important in the adhesion of particles to air bubbles.

Commonly in flotation systems both the bubble and the particle are negatively charged meaning that the bubble and particle should repel each other if only the electric double layer forces at play. In such a system the electric double layer force cannot be responsible for the rupturing of the liquid between the bubble and particle resulting in its adhesion. In 1969 Laskowski and Kitchener (1969) showed that van der Waals forces too are repulsive at the liquid film between the bubble and particle. Many researchers have thus attributed the attachment of a negatively charged bubble and negatively charged particle to be as a result of the attractive hydrophobic force (Laskowski and Kitchener 1969; Israelachvili and Pashley 1982; Rabinovich and Yoon, 1994; Ralston et al., 2001).

The presence of nano-bubbles is one explanation provided by many researchers for the origin of long-range hydrophobic forces as these nano-bubbles may have a bridging effect between hydrophobic surfaces due to nano-bubbles which are adhered to the particle surfaces (Ralston et al., 2001; Krasowska et al., 2009; Peng et al., 2013). However, since Laskowski and Kitchener (1969) first discussed this (hydrophobic) force which does not fit the DLVO theory, many authors have studied the hydrophobic force, its origin and hydrophobic interactions (Laskowski and Kitchener 1969; Israelachvili and Pashley 1982; Rabinovich and Yoon, 1994; Ralston et al., 2001). The hydrophobic force still is one of the least understood surface forces. As it is not the focus of this investigation the origins of the hydrophobic force will not be detailed but Meyer et al. (2006) provides a good review of the hydrophobic force. As a summary these authors detail

seven possible mechanisms for the attraction of hydrophobic forces, this includes nano-bubbles at the solid surface.

At a high-level hydrophobicity refers to the propensity of a mineral surface to repel water and thus make it possible for mineral particles to attach to air bubbles.

Young's equation (Equation 2-16) represents this thermodynamic property.

$\Delta G^{XS} = \gamma_{LV}(1 - cos\theta)$ ……*Equation 2-16*

Here ΔG^{XS} refers to the changes in Gibbs free energy, the surface tension between the solution and gas is given by γ_{LV} and θ is the contact angle between the bubble and mineral surface.

A large contact angle signifies a hydrophobic surface and will result in a negative ΔG^{XS}. Bubble-particle attachment occurs when ΔG^{XS} is negative. Young's equation therefore represents the thermodynamic criterion for flotation to occur. The extent of collector surface coverage and contact angle has classically been indicative of hydrophobicity. The effect of hydrophobicity on flotation has been widely studied; Blake and Ralston (1985) showed that for flotation to occur a for a particular particle size, a critical surface coverage must be achieved with a hydrophobising agent.

2.7.2.1 Contact Angle Measurements

Contact angle measurements are often performed to indicate the hydrophobicity of particles; this method involves a bubble being attached to a solid surface and the angle between the solid – liquid and liquid – air interfaces is measured via the liquid phase. A schematic representation of contact angle measurement is shown in Figure 2-17.

The surface chemistry of the system dictates the contact angle; this measurement provides information of the particles hydrophobic ability and is a thermodynamic measurement at equilibrium (Yoon and Yordan, 1991)

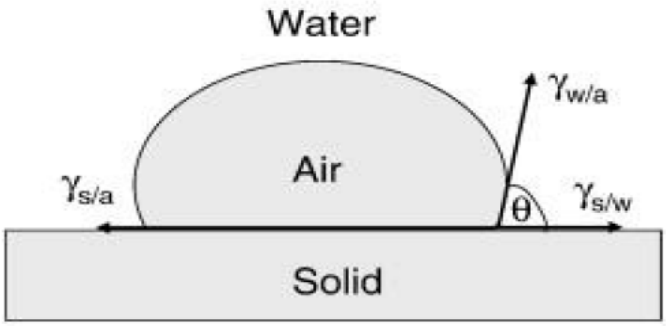

Figure 2-17: Schematic representation of contact angle measurement (Chau et al., 2009)

2.7.2.2 Limitations of Measuring Surface Hydrophobicity

Froth flotation is highly affected by the kinetics and hydrodynamics of the system (Ye *et al*, 1989). Contact angle measurements provide a thermodynamic indication and may also be used to provide information regarding collector adsorption it however does not take kinetic into account.

Contact angle measurements do not provide a sensitive measurement when studying the effects of various parameters and can vary between 0° and 120° (Yoon and Yordan, 1991).

Furthermore, contact angle measurements are performed on a polished mineral surface, these surfaces do not resemble flotation conditions well as the surface forces on the polished mineral surface are very different to actual particle used in flotation (Ye *et al.,* 1989). Additionally, the creation of polished mineral surfaces requires large amounts of mineral particles.

2.7.3 Particle Floatability

In froth flotation the ability of a mineral particle to attach to an air bubble and rise through the pulp is known as the particle's floatability. The floatability of particles is dependent on their surface properties and hydrodynamic conditions in the cell. Floatability measurements therefore take into account kinetics and thermodynamics.

Methods of measuring floatability include, attachment time, The Microfloat Floatability index (MFI) (Chudacek and Fichera, 1991) and bubble loading (Bradshaw and O'Connor, 1996). Attachment time (as described in Section 2.6) is generally a more sensitive indicator compared to contact angle measurements and the particle bed the measurements are performed on resembles the particles in the pulp phase more closely (Bradshaw, 1997).

2.8 Water Quality

2.8.1 Introduction

Water scarcity has become a reality in many countries around the world and as a result, various industries have had to reconsider their water management processes and even develop new strategies to use water more sustainably (Levay *et al.,* 2001; Manono *et al.,* 2018; Slatter *et al.,* 2009). Although the mining industry's water usage is not as high as other industries like agriculture; mining operations are largely situated in arid regions. Many in the mining industry are required to re-evaluate their fresh water consumption as a result of strict water restrictions and water release policies.

In flotation systems water is an important process and transport medium and represents 80-85% of the mineral pulp in flotation cells by volume (Muzenda, 2010). The properties of water are important as water facilitates the execution of each of the sub-processes making up the overall flotation process. However, water restrictions are usually imposed and mining operations are being encouraged to reduce fresh water consumption, and explore alternatives such as recycled process water, wastewater and sea water.

The chemistry of these alternative water sources is however very different to that of fresh water (Rao and Finch, 1989). Process water from mineral processing operations contains dissolved solids and as the process water is recycled, a build-up of solids occurs increasing its ionic strength and may result in abnormal concentrations of certain electrolytes (Slatter *et al.*, 2009). Furthermore, recycled process water is usually sourced from a combination of varying water streams such as thickener overflows, tailings dams, filtrate and water obtained from milling, leaching and roasting sections of a mineral processing plant; this may additionally result in pH variations of the water (Levay *et al.,* 2001). Common ions in the process water include SO_4^{2-} and H^+ which are added during leaching; Fe^{3+} and Fe^{2+} attained from the milling and roasting processes as well as those ions common in water systems such as Ca^{2+}, Mg^{2+}, Cl^-, Na^+ and CO_3^- (Barker, 1986).

The use of recycled water in mineral processing operations is advantageous due to the fact that no new water is required to be brought into the system and decreasing the volume of discharge. However, the efficacy of reagents may be compromised as a result of contaminants in the water (Slatter *et al.,* 2009)

Due to the surface-active nature of inorganic electrolytes on negatively charged surfaces, the collector adsorption sub-process may be affected (Yoon and Basilio, 1993). The difference in water chemistry between fresh water and recycled water could potentially negatively affect the separation efficiency of the overall flotation process. It is thus deemed necessary to fully understand the effects of recycling water on flotation systems.

In flotation the interaction of the water molecules with both the mineral surface and the electrical double layer at the mineral water interface is an important factor when mineral particles are in water (Fuerstenau, 1982) the following section thus focusses on water structure, how the structure is altered in the presence of inorganic electrolytes and what happens at the solid – liquid interface.

2.8.2 Water Structure

The characteristic functioning of water has been attributed to its molecular structure as it plays a key role in interactions of hydrogen bonding and hydrophobic forces (Isrealachvili, 1992). Water molecules become associated with each other as a result of hydrogen bonding; and each molecule forms four connections with other molecules which consequently forms a tetrahedral coordination of water molecules; this further results in three dimensional networks of water molecules.

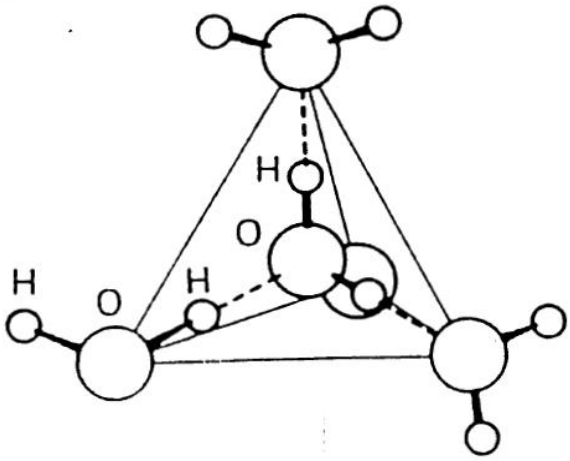

Figure 2-18: Tetrahedral structure of water molecules (Israekachvili, 1992)

In the presence of cations and anions, the structure of water may still be very strongly hydrogen bonded, these ions are termed "structure making" because they retain the strong hydrogen bonds. Structure making ions are small inorganic ions such as Na^+, Li^+, Mg^{2+}, F^- and Cl^- and are of high charge density. They are therefore strongly hydrated and result in an increase in the viscosity of the solution. Conversely ions that tend to destroy the strongly hydrogen bonded structure of water are termed "structure breakers". Structure breakers are large ions such as Cs^+ and I^- that are weakly hydrated; these ions also tend to increase the fluidity of the solution (Wang and Peng, 2014; Burdukova, 2007; Ma and Pawlik, 2005).

Hencer *et al.* (2001) studied the interfacial structure of water at KCl, NaCl and KI surfaces by means of contact angle measurements. The results as depicted in Figure 2-19 illustrate that Na^+ led to the most stable hydration state (with a contact angle of 0°) at the surface of NaCl compared to its potassium counterpart, KCl (contact angle of 8°); making Na^+ a stronger structure maker than K^+. The KI surface led to the largest contact angle (25°) and thus the least stable interfacial water structure.

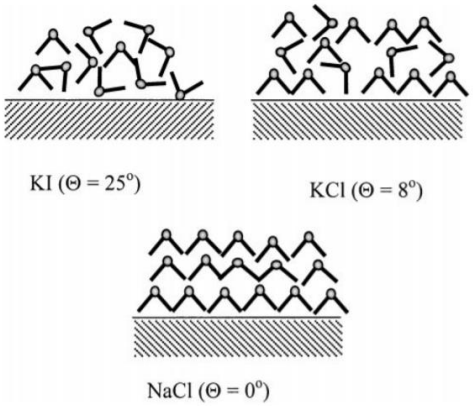

Figure 2-19: Arrangement of water molecules at the surface of KI, KCl and NaCl salts (Hencer et al., 2001)

The water structure is thus influenced by the type and concentration of the inorganic ions in the solution which in turn affects the viscosity of the solution (Desnoyers and Perron, 1972). Figure 2-20 illustrates

work by the aforementioned authors and how ion type and concentration change the viscosity of solutions. In a flotation context, changes in the viscosity of the pulp affects the hydrodynamics of the process (Abrahamson, 1975) and thus the rate at which particles collide with air bubbles. The rate of bubble-particle collision is said to be a function of the bubble size, densities of the bubble and particle, energy dissipated and viscosity of the solution; the latter is inversely proportional to bubble-particle collision rate. Thus, with increases in solution viscosity, the rate of bubble-particle collision decreases.

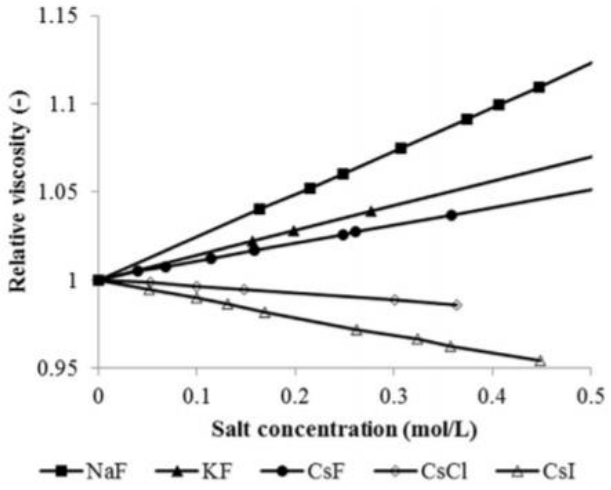

Figure 2-20: Effect of structure breaking and structure making salts on the viscosity of the solution (Desnoyers and Perron, 1972 adapted by Michaux et al., 2018)

2.8.3 Mineral – Water Interaction

The water layers orientated at the surface of the mineral influence the adsorption at the mineral – water interface. At the mineral – water interface, the first water molecule layer may consist of water dipoles in an "up" or "down" position; water dipoles oriented in a down position will have the hydrogen atoms oriented to the mineral solution and the oxygen atom oriented towards the solution. This water layer is oriented by dipole-dipole interactions whereas the second layer contains less oriented water molecules (Martinovic, 2005). Inorganic ions can adsorb within the first or second water layers. A change in the charge on the mineral surface can therefore arise from either the adsorption of ions from solution or by the dissociation of surface groups to the solution (Martinovic, 2005).

Ions of opposite charge to that of the mineral surface are known as counter ions and these ions are attracted to the surface of the mineral in order to maintain overall neutrality. Ions of the same charge as the mineral surface however are repelled by the mineral. As a result, an electrical double layer is formed; this ultimately controls the adsorption of ions at the mineral solution interface. The electrical double layer at the mineral water interface is illustrated in Figure 2-21.

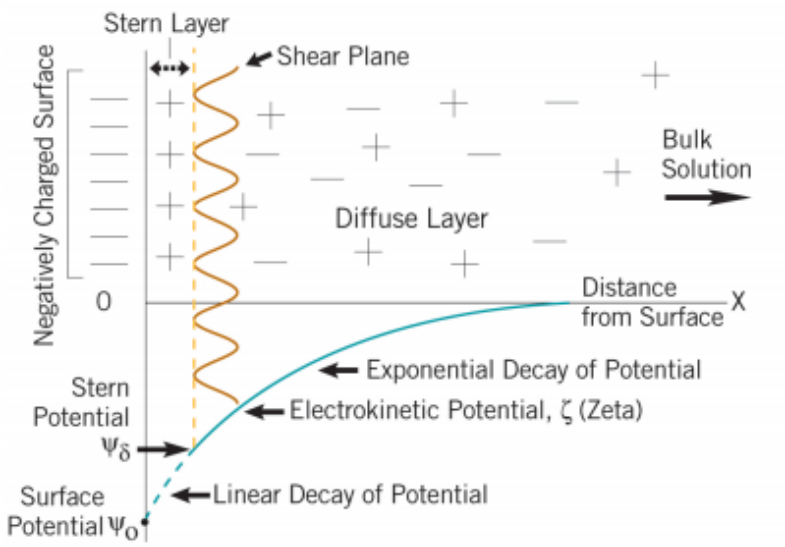

Figure 2-21: Illustration of the electrical double layer at the mineral surface water interface (http://www.particlesciences.com/news/technical-briefs/2012/overview-of-zeta-potential.html)

In Figure 2-21, the mineral surface bears a negative charge, thus the first layer of counter ions has a positive charge aiming to maintain electrical neutrality; these two layers form the electrical double layer at the mineral water interface. The first layer of counter ions is known as the Stern layer and the potential at the boundary of the Stern layer is called the Stern potential. The layer of more loosely bound ions (both negative and positive) following the Stern layer is known as the diffuse layer and the boundary of this layer is known as the Shear/Slipping plane. The potential at the Shear/Slipping plane is known as the Zeta potential.

The zeta potential is used to conclude the behaviour of the mineral surface in an aqueous solution (Martinovic, 2005). The adsorption on the mineral surface can be recognised by the sign of the Zeta coefficient. Positive Zeta coefficients indicates cationic adsorption on the mineral surface while a negative Zeta coefficient shows anionic adsorption.

2.8.4 Zeta Potential

Changes in pH, pulp temperature, conditioning time, reagent type and concentration may alter the surface speciation on the mineral particle and this affects the zeta potential of the mineral (Chandra and Gerson, 2009). Zeta potential determination tests are also often used to regulate the amount of collector adsorption on the mineral surface. Zeta potential determination tests are often performed as a function of pH due to it being strongly affected by the pH of the solution. The pH at which the zeta potential of a particle (pH_{iep}) is zero is known as the isoelectric point (as shown in Figure 2-22); at this pH the particle has a neutral net electrical charge meaning that positive and negative charges are present in equal quantities on the particles' surface. At this pH the colloid system is least stable and indicates strong agglomeration and precipitation of particles in solution.

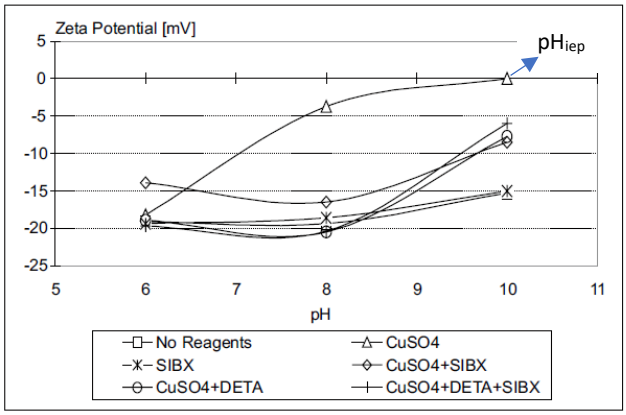

Figure 2-22: Zeta potential of pyroxene versus pH graph showing the isoelectric point (O'Çonnor et al., 2005)

The point of zero charge (PZC) however, is the pH at which the particle in solution carries no net electrical charge (as shown in Figure 2-23); that is there are no positive or negative charges at the particles' surface (Adamson and Gast, 1967). The point of zero charge is established by titration in different concentration of electrolyte solutions; the zeta potential is then plotted as a function of pH and where the curves intersect at zero is the PZC charge (Adamson and Gast, 1967).

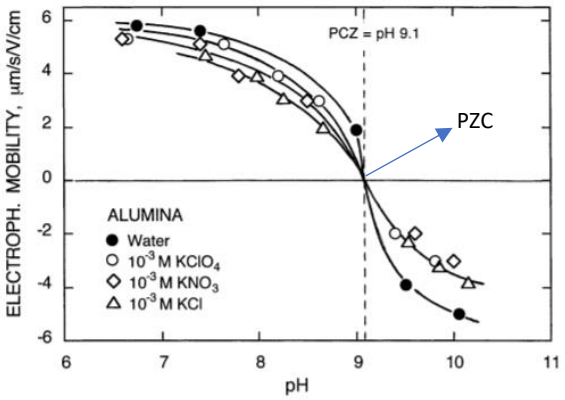

Figure 2-23: Zeta potential of α-alumina versus pH graph showing the point of zero charge (Fuerstenau and Pradip, 2005)

2.8.5 Effects of Electrolytes on the Pulp Phase

2.8.5.1 Mineral – Electrolyte Interactions

The ionic strength of the solution directly affects the thickness of the electrical double layer at the mineral – solution interface. The Debye length (K^{-1}), a term used for the thickness of the electrical double layer can be related to the ionic strength of the solution through Equation 2-17.

$$K^{-1} \propto \frac{1}{\sqrt{Ionic\ Strength}} \quad \text{.....Equation 2-17}$$

When the electrical double layer is compressed, the magnitude of the mineral surfaces' zeta potential decreases. Figure 2-24 illustrates this phenomenon by showing the effect on the zeta potential in fresh water versus that in saline water of high ionic strength.

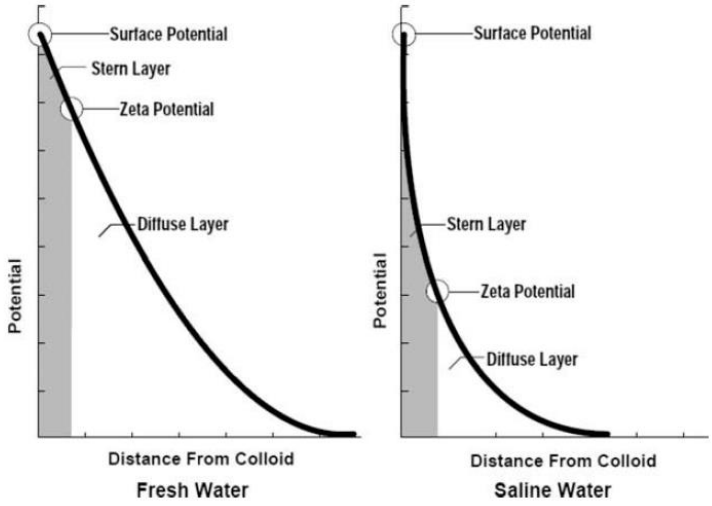

Figure 2-24: Schematic of the effect of ionic strength on the electrical double layer thickness (Jeldres et al., 2016)

As with particles, when a bubble exists in an electrolyte solution an electrical double layer also forms at the bubble surface. Therefore, when a bubble and particle come close to one another in an electrolyte solution both the double layers interact resulting in double layer repulsions; (long range repulsion in low ionic strength solutions) For bubble-particle attachment to occur the repulsion must be overcome with kinetic energy and attractive forces; the double layer repulsions thus behave as an energy barrier.

High electrolyte solutions, as mentioned, do have the ability to compress the electrical double layers, ultimately leading to the attachment between the two surfaces (Laskowski *et al.,* 1991). A study by Laskowski *et al.* (1991) showed that hydrophobicity is not the only factor that affects flotation rate but also on the energy barrier that opposes the bubble-particle attachment. With methylated quartz of a contact angle of 53°; as the KCl solution concentration increased, the energy barrier decreased and consequently resulted in high flotation rates as shown in Figure 2-25.

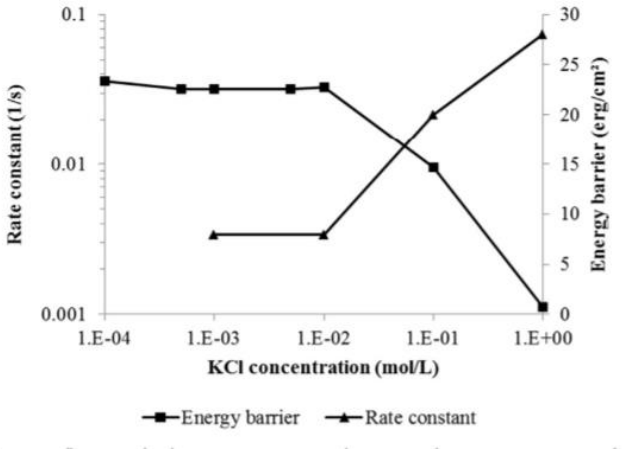

Figure 2-25: Effect of KCl concentration on the energy barrier and flotation kinetics of methylated quartz particles (Laskowski et al., 1991 adapted by Michaux et al., 2018)

Coal flotation in electrolyte solutions has been studied extensively and a number of mechanisms have been proposed with regards to the enhanced flotation in saline solutions. Work by Paulson and Pugh (1996), and Yoon and Sabey (1989) attribute the enhancement to be as a result of the reduced electrostatic force between the particles and bubbles; which is resultant of the compression of the electrical double layer and the subsequent reduction in the zeta potential of the particles and bubbles in saline water. Blake and Kitchener (1972) attributed this enhancement to be due to the inorganic ions destabilising the hydrated layers around the coal particles, thus reducing the surface hydration of the particles and making it more hydrophobic. While other studies by Marrucci and Nicodemo (1967) and Craig *et al.* (1993) ascribed this phenomenon to events in the froth phase; and proposed a decrease in bubble coalescence and increases in froth stability.

2.8.5.2 Mineral – Electrolyte – Collector Interactions

In a study by Hancer *et al.* (2001), it was proposed that if collectors adsorb at the salt interface (saline water – particle interface) it will penetrate through the water and displace the interfacial water. These authors then concluded that if the water structure is strongly hydrogen bonded due to structure making ions; collectors will have difficulty adsorbing on the mineral. Figure 2-26 shows how the adsorption of collector is inhibited as a result of the strong interfacial water structure. Conversely structure breakers like KCl have the tendency to break the structure of water, resulting in a weaker interfacial water structure; making it easier for the collector to adsorb at the mineral surface.

Research by many authors has illustrated the negative impact of Ca^{2+} on xanthate adsorption (Ikumapayi *et al.,* 2012; Wang *et al.,* 2015; Elizondon-Alvarez *et al.,* 2017; Fuerstenau, 1982). In studies with galena, Ikumapayi *et al.* (2012) presented evidence of Ca^{2+} forming soluble complexes of calcium carbonate and sulfoxy species which in turn reduced the amount of xanthate adsorbed on the galena surface. Similarly, by means of contact angle measurements, zeta potential and Cryo-XPS, Wang *et al.* (2015) reported the inhibition of xanthate adsorption on sphalerite surfaces due to high ion concentration.

Elizondo-Alvarez *et al.* (2017), found the hindering action of the xanthate collectors' adsorption to be due to the chemisorption of Ca^{2+} on active sites; resulting in competition between the collector and Ca^{2+}. While work by Fuerstenau (1982) reported that above pH 6, Ca^{2+} adsorbs onto negatively charged pyrite via an electrostatic attraction; therefore, hindering the oxidation of xanthate and consequently its adsorption on the mineral surface. Studies by Li *et al.* (2017) described the increase in xanthate adsorption on chalcopyrite surfaces in monovalent electrolyte solutions but the opposite effect was observed with divalent salts.

Conversely, Kirjavainen *et al.* (2002) reported increased adsorption of xanthate on the surface of sulfide minerals after grinding in steel mill at its natural pH, these authors also showed that thiosulfate decreased adsorption of xanthate on the mineral surface but reduced the effect of hydrophilic species on the surface of sulfide minerals.

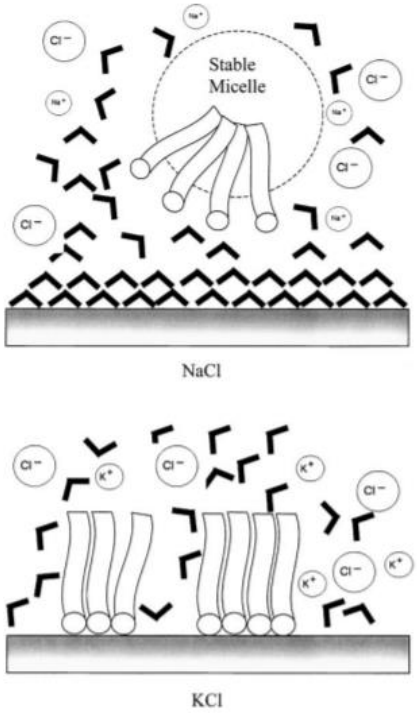

Figure 2-26: Effect of collector adsorption in the presence of structure making and breaking ions (top) NaCl as structure making electrolyte and (bottom) KCl as structure breaking electrolyte (Hencer et al., 2001)

2.8.5.3 Effects of Water Quality on Sulfide Mineral Flotation

Ikumapayi *et al.* (2012) studied the effect of calcium and sulphate ions on the flotation of galena. This study showed that process water generally yielded lower recoveries of galena compared to de-ionised water. In this study zeta potential was determined, and showed that the zeta potential of galena increased when calcium ions were added; which indicates the adsorption of calcium ions on the surface of galena. Further, the FTIR studies conducted in this study showed that the xanthate bands were lower upon the addition of Ca^{2+}, consequently indicating the inhibition of xanthate adsorption in the presence of Ca^{2+}.

Investigating the effect of water quality on the flotation performance of complex sulfide ores, Boujounoui *et al.* (2015) found that high concentrations of Mg^{2+} in process water depressed galena, chalcopyrite and sphalerite while increased concentrations of Ca^{2+} depressed sphalerite. This was attributed to the formation of hydrophilic layers on the mineral surface in the presence of these ions; preventing the adsorption of the collector (Boujounoui *et al.*, 2015).

Manono *et al.* (2016) investigated the effects of ion type on the floatability of a Merensky ore. It was found that sodium salts resulted in a higher amount of solids recovered to the concentrate, whereas nitrates resulted in a slightly lower solids recovery. There was no apparent effect on the recovery of copper and nickel with changes in ion type. However, a cation effect was evident in terms of copper and nickel grade as sodium salts yielded lower grades. An anion effect was also observed in this investigation as nitrate salts yielded higher copper and nickel grades. This increase in grade and decrease in solids recovery for nitrate salts is due to nitrates' ability to deactivate gangue minerals of copper and nickel ores (Slatter *et al.*, 2009).

Hirajima *et al.* (2016) reported significant decreases in the floatability of molybdenite and chalcopyrite in $CaCl_2$ and $MgCl_2$ solutions at pH values greater than 9; they ascribed this to the formation of $Mg(OH)_2$ and $CaCO_3$ precipitates and its adsorption on the mineral surface, thus reducing the surface hydrophobicity. These authors also reported the $MgCl_2$ solution to be more depressing compared to $CaCl_2$. Similar studies by Li *et el.* (2017) assessing the effect of divalent and monovalent ions on chalcopyrite flotation at pH 10 showed the monovalent solutions improve the chalcopyrite flotation. These authors attributed this to the lower energy barrier and decrease in the hydration layer stability on the chalcopyrite surface in monovalent solutions. Li *et al.* (2017) then further reported the depression of chalcopyrite in $MgCl_2$ at high concentrations and like Hirajima *et al.* (2016) these authors ascribed this to the precipitation and adsorption of $Mg(OH)_2$ on the surface thus reducing the hydrophobicity.

2.8.6 Effects of Electrolytes on the Froth Phase

Frothers are added to create a froth, stable enough to allow selective drainage of entrained gangue from the froth and to increase flotation kinetics (Wills and Napier-Munn, 2016). The action of the frother comes as a result of inhibiting or retarding bubble coalescence (Harris, 1982). Two – phase flotation column work by Quinn *et al.* (2007) reported that plant water of high inorganic electrolyte content decreased the amount of frother required; this is due to the bubble size reducing ability of salt solutions.

Marruci and Nicodem (1967) showed that inorganic ions in solution reduced bubble coalescence and ascribed this to inorganic ions in water slowing the inter-bubble drainage. Thus, when inorganic ions are present in high ionic strengths bubble coalescence is inhibited effectively. Studies by Manono *et al.* (2013) showed that increases in the ionic strength of synthetic plant water lead to increased water recovery and decreased bubble size. In line with the findings by Manono *et al.* (2013) and Zieminski and Whittemore (1971) further proposed the reduction in bubble size in electrolyte solutions to be due to the effects of water – ion interactions such as ionic entropy of hydration.

A comparative study of ionic strength and frother dosage by Corin and Wiese (2014) showed that either the ionic strength or frother can be changed to meet the operational solid and water recoveries. These authors also showed that an increase in ionic strength resulted in a greater mass pull and higher solids recoveries compared to that with increased frother dosages.

2.8.7 Effect of Electrolytes on the Potential of Air Bubbles

As with particles, when bubbles are suspended in ionic solutions the zeta potential on the bubble will change. Bubbles can acquire a charge in many ways; through the asymmetry of the water molecules that sit at the air – liquid interface, via the adsorption of ions, the dissociation of ionic groups and through charge separation. An electrical double layer is formed as a result of the special distribution of ions in solution when a charge exists in the bubble liquid surface. The electrical double layer of the bubble can therefore affect bubble-particle and bubble – oil droplet attachment as well in bubble coalescence. Yang *et al.* (2001) described the zeta potential to be dependent on the solution pH, type and concentration of ions present in solution. These authors also showed that NaCl resulted in the most negative bubble potentials. Takahashi (2005) showed a strong reduction in the negative potential of the bubble with the addition of $MgCl_2$; i.e. the bubble zeta potential became less negative compared to the potential of the bubble with the addition of monovalent salts and it is clear that the ionic valency plays an import role in the bubble zeta potential.

Takahashi (2005) explained the effect of valency on the bubble potential in the following way: "*Increases in counterions reduces the zeta potential by the amount of counterions that occur between the slipping plane and solution – bubble interface. Due to the force of attraction being subject to the valency of the counterions, multivalent ions are more strongly attracted to the interface owing to static electricity. This in turn results in a dense concentration inside the slipping plane thus decreasing the zeta potential.*"

2.9 The Existing Gap in Literature on the Effect of Water Quality on Bubble-particle Attachment

Section 2.6.5 detailed the factors affecting bubble-particle attachment; various authors showed that shorter induction times were achieved with smaller particles, smaller bubbles, high temperatures, full liberation of the value in ores, hydrogen bubbles and angular particles. However, in terms of dissolved ions, the effect on bubble-particle attachment was not as clear as compared to the aforementioned operating conditions. In quartz, bitumen and coal systems studies have shown the effect of Ca^{2+} and K^{+} on the induction time to be largely dependent on the collector dosage or whether there were solid particles in the process water (Gu *et al.,* 2003; Yoon and Yordan, 1991).

The effect of using process water of increasing ionic strength (i.e. the concentration of all the ions present in process water increases as a result of the process water recirculation) on the bubble-particle attachment sub-process is however not clear. Studies using batch flotation tests have however shown that mineral particle recovery increases as the ionic strength of the synthetic plant water increases; this result has been attributed to increases in froth stability, decreases in bubble size and the compression of the electrical double layer at the air-water and solid-water interfaces (Manono *et al.,* 2013; Zieminski and Whittemore,

1971). It is however also important to understand the effect of plant water of increasing ionic strength at the bubble-particle level without the effect of the froth so as to enable the understanding of the effect of inorganic electrolytes on each of the sub-processes of froth flotation.

Moreover, limited studies have been done regarding whether there are single ions present in process water that control or have no effect on the bubble-particle attachment of sulfide minerals. As a result of understanding this level of detail; it could provide operations with the alternative of removing specific ions as opposed to treating the recycled water.

Underlying factors such as the zeta potential of the mineral and the ability of the collector to adsorb on the mineral surface may be altered due to the presence of inorganic electrolytes. Studies have shown that the adsorption of xanthate on galena decreases in the presence of Ca^{2+} this is said to be due to chemisorption of Ca^{2+} on active sites, deterring the action of the collector. (Ikumapayi *et al.,* 2012; Elizondo-Alvarez *et al.,* 2017). The effects of Ca^{2+} and SO_4^{2-} on collector adsorption has been studied by a number of authors; effects of other inorganic electrolytes making up plant water such as Na^{+} and NO_3^{-} on collector adsorption is not well understood. How these underlying factors are affected by inorganic electrolytes individually, on each other and its potential resulting effect on bubble-particle attachment is also not well understood.

2.10 References

Abrahamson, J. (1975). Collision rates of small particles in a vigorously turbulent fluid. Chemical Enineering Science. 30, 1371–1379.

Ackerman, P.K., Harris, G.H., Klimpel, R.R. and Aplan, F.F. (1987). Evaluation of flotation collectors for copper sulphides and pyrite, I. Common sulphydryl collectors. International Journal of Mineral Processing vol. 21, pp 105-127.

Adamson, A. and Gast, A. (1967). Physical chemistry of surfaces 6th edition., Wiley - Interscience.

Albijanic, B., Amini, E., Wightman, E., Ozdemir, O., Nguyen, A. and Bradshaw, D. (2011) A relationship between bubble-particle attachment time and the mineralogy of a copper-sulphide ore. Minerals Engineering. 24: 1335-1339.

Albijanic, B., Ozdemir, O., Nguyen, A. and Bradshaw, D. (2010) A review of induction and attachment times of wetting thin films between air bubbles and particles and its relevance in the separation of particles by flotation. Advances in Colloid and Interface Science. 159: 1-21.

Allison, S.A., Goold, L., Nicol, M. and Granville, A. (1972). A determination of the products of reaction between various sulfide minerals and aqueous xanthate solution, and a correlation of the products with electrode rest potentials. Metallurgical and materials transactions. A, Physical metallurgy and materials science, 3(10), pp. 2613-2618.

Allison, S.A., and O'Connor, C.T. (2011). An investigation into the flotation behaviour of pyrrhotite. Minerals Engineering, 98 (3-4), 202–207.

Anfruns, J.F., Kitchener, J.A. (1977) Rate of capture of small particles in flotation. Transactions of the Instutition Mining Metallurgy. 86: C9-C15.

Barker, L. M. (1983). The Effect of Electrolytes on the Flotation of Pyrite. MSc.Eng Thesis, University of Cape Town, Chemical Engineering.

Becker, M., Harris, P. J., Wiese, J. G., and Bradshaw, D. J. (2009). Mineralogical characterisation of naturally floatable gangue in Merensky reef ore flotation. International Journal of Mineral Processing (93), 246-255.

Blake, T.D.andKitchener, J.A. (1972). Stability of aqueous films on hydrophobic methylated silica. Journal of the Chemical Society 68, 1435–1442.

Blake, P. and Ralston, J. (1985): Particle size, surface coverage and flotation response. Colloids and Surfaces, 16: 41-53.

Bradshaw, D. and O'Connor, C. (1996). Measurement of the sub-process of bubble loading in flotation. Minerals Engineering. 9: 443-448.

Bradshaw, D. (1997). Synergistic effects between thiol collectors used in the flotation of pyrite. PhD Thesis, University of Cape Town, Faculty of Engineering and the Built Environment, Chemical Engineering Department, Cape Town, South Africa.

Bradshaw, D. J., Harris, P. J., and O'Connor, C. T. (2005). The effect of collectors and their interactions wih depressants on the behaviour of the froth phase in flotation. Proceedings of Centenary of Flotation Symposium. Brisbane.

Bostrom, M., Williams, D. R. M., Ninham, B. W. (2001)Specific Ion Effects: Why DLVO Theory Fails for Biology and Colloid Systems. Physical Review Letters. 87, 168103. DOI: 10.1103/PhysRevLett.87.168103

Boujounoui, K., Abidi, A, Bacaoui, A., Amari, K.E.I. and Yaacoubi, A. (2015). The influence of water quality on the flotation performance of complex sulphide ores: case study at Hajar Mine, Morocco. Journal of the South African Institute of Mining and Metallurgy, 1243-1251.

Buckley, A.N., Woods, R. (1985). X-ray photoelectron spectroscopy oxidized pyrrhotite surfaces II. Exposure to aqueous solutions. Applied Surface Science. 20, 280.

BuckleY, A. N. and Woods, R. (1994). Xanthate chemisorption on lead sulfide. Colloids and Surfaces, 89, pp 71-76.

Burdukova, E. (2007). Surface properties of New York Talc as a function of pH, polymer adsorption and electrolyte concentration. PhD Thesis. University of Cape Town, Faculty of Engineering and the Built Environment, Department of Chemical Engineering, Cape Town, South Africa.

Buswell, A.M., Bradshaw, D.J., Harris, P.J., Ekmekci, Z. (2002). The use of electrochemical measurements in the flotation of a platinum group minerals (PGM) bearing ore. Minerals Engineering. 15 (March), 395– 404.

Buswell, A.M., Nicol, M.J. (2002). Some aspects of the electrochemistry of the flotation of pyrrhotite. Journal of Applied. Sciences. 32, 1321– 1329.

Butt, H.-J. (1994). A technique for measuring the force between a colloidal particle in water and a bubble. Journal of Colloid and Interface Science.. 166 (1), 109–117.

Chandra, A.P. and Gerson, A.R. (2009). A review of the fundamental studies of the copper activation mechanisms for selective flotation of the sulfide minerals, sphalerite and pyrite. Advances in Colloid and Interface Science, 145(1), pp.97– 110.

Chudacek, M.W. and Fichera, M.A. (1991). The relationship between the testtube flotability test and batch cell flotation. Minerals Engineering., vol. 4, no.1, pp 25-35.

Corin, K.C., Wiese, J.G. (2014). Investigating froth stability: A comparative study of ionic strength and frother dosage. Minerals Engineering, 66-68, pp.130–134.

Craig, V. S., Ninham, B. W., and Pashley, R. M. (1993). The effect of electrolytes on bubble coalescence in water. The Journal of Physical Chemistry. 97 (39), 10192-10197.

Derjaguin, B.V. and Landau, L. (1941). Theory of the Stability of Strongly Charged Lyophobic Sols and of the Adhesion of Strongly Charged Particles in Solutions of Electrolytes, Acta physicochimica U.S.S.R., 14, (6), 633-662.

Derjaguin, B.V. and Dukhin, S.S. (1960). Theory of flotation of small and medium-size particles. Transactions of the Institution of Mining and Metallurgy. pp221-245.

Desnoyers, J. E., Perron, G. (1972). The viscosity of aqueous solutions of alkali and tetraalkylammonium halides at 25°C. Journal of Solution Chemistry 1972, 1, 199.

Ducker, W.A., Xu, Z., Israelachvili, J.N. (1994). Measurements of hydrophobic and DLVO forces in bubble–surface interactions in aqueous solutions. Langmuir 10 (9), 3279–3289.

Eigeles, Volova. (1960). Kinetic investigation of effect of contact time, temperature and surface condition on the adhesion of bubbles to mineral surfaces. Proceedings, 5th International Mineal. Processing Congress Institution of Mining and Metallurgy. London 271–284.

Elizondo-Alvarez, M.A., Flores-Alvarez, J.M., Davila-Pulido, G.I., Uribe-Salas, A. (2017). Interaction mechanism between galena and calcium and sulfate ions. Minerals Engineering. 111, 116–123.

Finch, J.A. and Dobby, G.S. (1991). Column flotation: A selected review, part 1, International Journal of Mineral Processing. 33, 343-354.

Finkelstein, N. and Goold, L. (1972). The reaction of sulphide minerals with thiol compounds. National Institute of Metallurgy, South Africa.Report, (1439).

Finkelstein, N.P. and Poling, G.W. (1977). The Role of Dithiolates in the Flotation of Sulphide Minerals. Minerals Science Engineering, 9(4), pp. 177-197.

Fuerstenau, D.W. (1982). Mineral-water interfaces and the electrical double layer. In: King, R.P. (Ed.), Principles of Flotation. South African Institution of Mining and Metallurgy, Johannesburg, pp. 17–30.

Fuerstenau, D.W. (2005): A Century of Developments in the Chemistry of Flotation. Centenary of Flotation Symposium, (June) p.13.

Fuerstenau, D.W. and Pradip (2005). Zeta potentials in the flotation of oxide and silicate minerals. Advances in Colloid and Interface Science, 114, pp.9–26.

Glembotsky, V.A. (1953). The time of attachment of bubbles to solid particles in flotation and its measurement. Lzv. Akad. Nauk SSSR, Otd. Tckhn. Nauk. 11, 1524–1531.

Gu, G., Sanders, R.S., Nandakumar, K., Xu, Z., Masliyah, J.H. (2004). Hydrogen and Oxygen Bubble Attachment to a Bitumen Drop. Canadian Journal of Chemical Engineering. 82, 846–849. doi:10.1002/cjce.5450820426.

Harris, P. J. (1982). Frothing phenomena and frothers. In R. P. King (Ed.), Principles of flotation. Johannesburg: South African Institute of Mining and Metallurgy.

Hassas, B.V., Caliskan, H., Guven, O., Karakas, F., Cinar, M., Celik, M.S. (2016). Effect of roughness and shape factor on flotation characteristics of glass beads, Colloids and Surfaces A: Physicochemical and Engineering Aspects, 492 (2016) 88-99.

Hencer, M., Celik, M. S., and Miller, J. D. (2001). The significance of interfacial water structure in soluble salt flotation systems. Journal of Colloid and Interface Science, 235. pp. 150–161.

Heyes, G.W., Trahar, W.J. (1984). The flotation of pyrite and pyrrhotite in the absence of conventional collectors. In: Richardson, P.R., Srinivasan, S.S., Woods, R. (Eds.), Proceedings of the International Symposium of Electrochemistry in Mineral and Metal Processing. Electrochem. Soc., Pennington, NJ, 84–10, p. 189.

Hirajima, T., Pandhe, G., Suyantara, W., Ichikawa, O., Mohamed, A., Miki, H. and Sasaki, K. (2016). Effect of Mg^{2+} and Ca^{2+} as Divalent Seawater Cations on the Floatability of Molybdenite and Chalcopyrite. Minerals Engineering 96–97. Elsevier Ltd: 83–93. https://doi.org/10.1016/j.mineng.2016.06.023.

Hochreiter, R.C., Kennedy, D.C., Muir, W., Woods, A.I. (1985). Platinum in South Africa (metal review no. 3). Journal of the South African Institute of Mining and Metallurgy . 85 (6), 165–18.

Hodgson, M., Agar, G.E. (1984). An electrochemical investigation into the natural flotability of pyrrhotite. In: Richardson, P.R., Srinivasan, S.S., Woods, R. (Eds.), Electrochemistry in Mineral and Metal Processing. ECS, Pennington, NJ, USA, pp. 185–201.

Ikumapayi, F., Makitalo, M., Johansson, B. and Hanumantha, K. (2012). Recycling of Process Water in Sulfide Flotation : Effect of Calcium and Sulphate Ions on Flotation of Galena. Minerals Engineering 39. Elsevier Ltd: 77–88. https://doi.org/10.1016/j.mineng.2012.07.016.

Israelachvili, J.N. and Pashley, R.M. (1982). The hydrophobic interaction is long range, decaying exponentially with distance, Nature, 300, (5890), 341-342.

lsraelachvili, J.N. (1992). Intermolecular and surface forces. 2nd ed. Academic Press. London. pp 122-141.

Jeldres, R.I., Forbes, L., Cisternas, L.A. (2016). Effect of seawater on sulfide ore flotation: a review. Mineral Processing and Extractive Metallurgy Review:37 (6), 369– 384. http://dx.doi.org/10.1080/08827508.2016.1218871.

King, R. P. (1982). Principles of Flotation. Johannesburg: Southern African Institute of Mining and Metallurgy.

Kirjavainen, V., Schreithofer, N. and Heiskanen, K. (2002). Effect of calcium and thiosulfate ions on flotation selectivity of nickel-copper ores. Minerals Engineering , 59 (1-2), 1-5.

Klimpel, R. D. (1984). Froth flotation: The kinetic approach. Mintek 5. Johannesburg, South Africa

Koh, P.T.L., Hao, F.P., Smith, L.K., Chau, T.T., Bruckard, W.J. (2009). The effect of particle shape and hydrophobicity in flotation. International Journal of Mineral Processing. 93, 128–134. doi:10.1016/j.minpro.2009.07.007.

Krasowska, M.; Malysa, K. (2007) Kinetics of bubble collision and attachment to hydrophobic solids: I. Effect of surface roughness. International Journal of Mineral Processing. 81, 205–216.

Krasowska, M., Zawala, J. and Malysa, K. (2009): Air at hydrophobic surfaces and kinetics of three phase contact formation. Advances in Colloid and Interface Science, 147-148: 155-169.

Krasowska, M., Carnie, S.L., Fornasiero, D., Ralston, J. (2011). Ultrathin wetting films on hydrophilic titania surfaces: equilibrium and dynamic behavior. Journal of Physical Chemistry C 115 (22), 11065–11076.

Laskowski, J. and Kitchener, J. A. (1969): The hydrophilic-hydrophobic transition on silica. Journal of Colloid and Interface Science, 29(4): 670–679.

Laskowski, J. and Iskra, J. (1970). Role of capillary effects in bubble-particle collision in flotation. Transactions of the Institution of Mining and Metallurgy. 79, C6.

Laskowski, J.S., Xu, Z., Yoon, R.H. (1991). Energy barrier in particle to bubble attachment and its effect on flotation kinetics. In: 17th International Mineral Processing Congress, Dresden. pp. 237–249.

Leja, Jan (2004): Surface Chemistry of Froth Flotation, vol. 2. Academic/Plenum Publishers, 2nd edition.

Leneveu, D. M., Rand, R. P., Parsegian, V. A., Gingell, D. (1977) Measurement and Modification of Forces between Lecithin Bilayers. Biophysical Journal 18, 209– 230, DOI: 10.1016/S0006-3495(77)85608-7

Leppinen, J.O., Basilio, C.l. and Yoon, R.H. (1989). In situ FTIR study of ethyl xanthate adsorption on sulphide minerals under conditions of controlled potential. International Journal Mineral Processing. vol. 26, pp 259-274.

Levay, G., Smart, RStC, and Skinner, W. M. (2001). The impact of water quality on flotation performance. Journal of the South African Institute of Mining and Metallurgy, 101, 69-75.

Li, Wanqing, Xiao, Qing, He, Nan, Ren, Zijie, Lartey, Clement, Gerson, Andrea (2017). The influence of common monovalent and divalent chlorides on chalcopyrite flotation. Minerals 7, 111. https://doi.org/10.3390/min7070111.

Manono, M.S., Corin, K.C., and Wiese, J.G. (2013). The effect of ionic strength of plant water on foam stability: A 2-phase flotation study. Minerals Engineering, 40, 42-47.

Manono, M.S., Corin, K.C. and Wiese, J.G. (2016). The influence of electrolytes present in process water on the flotation behaviour of Cu-Ni containing ore. Minerals Engineering. 96-97, 99-107.

Manono, M.S, Corin, K.C. and Wiese, J.G. (2018). Perspectives from Literature on the Influence of Inorganic Electrolytes Present in Plant Water on Flotation Performance. Physicochemical Problems of Mineral Processing 54 (4): 1191–1214. https://doi.org/10.5277/ppmp18157.

Marruci, G., and Nicodemo, L. (1967). Coalescence of gas bubbles in aqueous solutions of inorganic electrolytes. Chemical Engineering Science , 60,1257-1265.

Martinovic, J. (2004). Investigation of the Surface Properties of Gangue Minerals in PGM bearing ores. MSc.Eng Thesis, University of Cape Town, Faculty of Engineering and the Built Environment, Chemical Engineering Department, Cape Town, South Africa.

Mellgren, O. and Ramachandra Rao, S. (1968). Heat of adsorption and surface reactions of potassium diethyl dithiocarbamate on galena. Transactions of the Institution of Mining and Metallurgy. C65.

Meyer, E.E., Rosenberg, K.J., Israelachvili, J. (2006) Recent progress in understanding hydrophobic interactions. Proceedings of the National Academy of Sciences, 103 15739-15746.

Michaux, B., Rudolph, M., Reuter, M.A. (2018). Challenges in predicting the role of water chemistry in flotation through simulation with an emphasis on the influence of electrolytes. Minerals Engineering. 125, 252–264.

Muzenda, E. (2010). An Investigation into the Effect of Water Quality on Flotation Performance. World academy of Science, Engineering and Technology.

Nakamura, M., Hara, M., and Uchida, K. (1988). Effects of surfactants on the rate of thinning of the dimple between a horizontal glass plate and an air bubble in water. Journal of Colloid and Interface Science. 123, 317.

Nesse, W. D. (2000). Introduction to mineralogy. Oxford University Press, Oxford, 1 - 10.

Nicholson, R.S. and Shain, 1. (1964). Theory of stationary electrode polargraphy. Analytical Chemistry. vol. 36, no 4, pp 706-723.

O'Connor, C.T., Malysiak, V., Shackelton, N.J. (2006). The interaction of xanthates and amines with pyroxene activated by copper and nickel. Minerals Engineering 19, 799–806.

Ozdemir, O., Taran, E., Hampton, M.A., Karakashev, S.I., Nguyen, A.V. (2009). Surface chemistry aspects of coal flotation in bore water. International Journal of Mineral Processing 92 (3–4), 177–183.

Peng, H., Hampton, M.A. and Nguyen, A.V. (2013): Nanobubbles do not sit alone at the solid-liquid interface. Langmuir, 20:6123-6130.

Poling, G. (1976). Reactions between thiol reagents and sulphide minerals. Flotation--A.M.Gaudin Memorial.

Rabinovich, Y.I. and Yoon, R.H. (1994): Use of atomic force microscope for the measurements of hydrophobic forces. Colloids and Surfaces A: Physicochemical and Engineering Aspects, 93: 263–273.

Rahimi, M., Dehghani, F., Rezai, B., Aslani, M.R. (2012). Influence of the roughness and shape of quartz particles on their flotation kinetics, International Journal of Minerals Metallurgy and Materials. 19 284-289.

Ralston, J., Fornasiero, D., Hayes, R. (1999). Bubble–particle attachment and detachment in flotation. International Journal of Mineral Processing 56, 133–164. https://doi.org/10.1016/S0301-7516(98)00046-5.

Ralston, J., Fornasiero, D. and Mishchuk, N. (2001): The hydrophobic force in flotation - a critique. Colloids and Surfaces A, 192 (1-3): 39-51.

Randall, E. (2005). The UCT Bubble Size Analyser. University of Cape Town, Chemical Engineering Department, Cape Town, South Africa.

Rao, S.R. (1982): Surface Chemistry of Froth Flotation Volume 1: Fundamentals, 1st edition. Kluwer Academic / Plenum Publishers, New York.

Rao, S.R. (2004). Surface Chemistry of Froth Flotation, 2nd edition, Kluwer Academic/Plenum Publishers, New York.

Slatter, K.A., Plint, N.D., Cole, M., Dilsook, V., De Vaux, D., Palm, N., Oostendorp, B. (2009). Water Management in Anglo Platinum Process Operations: Effects of Water Quality on Process Operations. In: Abstracts of the International Mine Water Conference, Pretoria, South Africa, 19th – 23rd October 2009 Proceedings ISBN Number: 978-0-9802623-5-3. pp. 46–55.

Smith, P. G. and Warren, L. J. (1989). Entrainment of particles in flotation. Mineral Processing and Extractive Metallurgy Review , 5 (1-4), 123-145.

Smart, R.S.C., Amarantidis, J., Skinner, W.W., Prestidge, C.A., Vanier, L.L., Grano, S.R. (2003). Surface analytical studies of oxidation and collector adsorption in sulfide mineral flotation. In: Wandelt, K., Thurgate, S. (Eds.), Solid–Liquid Interfaces. Topics in Applied Physics. 85, pp. 3–60.

Snyder, B.A., Aston, D.E., Berg, J.C. (1997). Particle drop interactions examined with an atomic force microscope. Langmuir 13 (3), 590–593.

Sven-Nilsson, I. (1934). Einfluß der Berührungszeit zwischen Mineral und Luftblase bei der Flotation. Kolloid-Zeitschrift 69, 230–232. doi:10.1007/BF01433238.

Taguta, J., O'Connor, C.T., McFadzean, B. (2017). The effect of the alkyl chain length and ligand type of thiol collectors on the heat of adsorption and floatability of sulphide minerals. Minerals Engineering. 110, 145–152.

Takahashi, M. (2005). ζ Potential of microbubbles in aqueous solutions: electrical properties of the gas−water interface. The Journal of Physical Chemistry. B 109, 21858–21864. https://doi.org/10.1021/jp0445270.

Verrelli, D.I., Albijanic, B. (2015). A comparison of methods for measuring the induction time for bubble–particle attachment. Minerals Engineering. 80, 8–13. doi:10.1016/j.mineng.2015.06.011.

Verrelli, D.I., Bruckard, W.J., Koh, P.T.L., Schwarz, M.P., Follink, B. (2012). Influence of particle shape and roughness on the induction period for particle–bubble attachment, XXVI International Mineral Processing Congress (IMPC 2012), Indian Institute of Mineral Engineers (IIME) and Indian Institute of Metals (IIM), New Delhi, India.

Verwey, E.J.W. and Overbeek, J.T.G. (1948). Theory of the Stability of Lyophobic Colloids, Elsevier, Amsterdam

Vizcarra, T.G., Harmer, S.L., Wightman, E.M., Johnson, N.W., Manlapig, E.V. (2011). The influence of particle shape properties and associated surface chemistry on the flotation kinetics of chalcopyrite. Minerals Engineering. 24, 807–816. doi:10.1016/j.mineng.2011.02.019

Wills, B.A. and Finch, J.A. (2016). WILLS' Mineral Processing Technology, An introduction to the practical aspects of ore treatment and mineral recovery. Eighth Edition. Butterworth-Heinemann Elsevier.

Wang, B., Peng, Y. (2014). The effect of saline water on mineral flotation – a critical review. Minerals Engineering. 66–68, 13–24. https://doi.org/10.1016/j.mineng.2014.04.017.

Wang, J.Y., Xie, L., Liu, Q.X., Zeng, H.B. (2015). Effects of salinity on xanthate adsorption on sphalerite and bubble-sphalerite interactions. Minerals Engineering. 77, 34–41.

Wang, L., Peng, Y., Runge, K. (2016). Entrainment in froth flotation: the degree of entrainment and its contributing factors. Powder Technology. 288, 202–211.

Wang, L., Sharp, D., Masliyah, J., Xu, Z. (2013). Measurement of Interactions between Solid Particles, Liquid Droplets, and/or Gas Bubbles in a Liquid using an Integrated Thin Film Drainage Apparatus. Langmuir 29, 3594–3603. doi:10.1021/la304490e

Wang, W., Zhou, Z., Nandakumar, K., Masliyah, J and Xu, Z. (2005). An induction time model for the attachment of an air bubble to a hydrophobic sphere in aqueous solutions. International Journal of Mineral Processing. 75: 69-82.

Webber, G. B., Manica, R.., Edwards, S. A.., Carnie, S. L.., Stevens, G. W., Grieser, F., Dagastine, R.R., Chan, D. Y. C. (2008). Dynamic forces between a moving particle and a deformable drop. Journal of Physical Chemistry C 112, 567

Woods, R.. (1984). Electrochemistry of sulphide flotation. in Principles of the Minerals Industry. eds M.H. Jones and J.T. Woodcock. Australasian Institute of Mining and Metallurgy, Melbourne, pp 91-115.

Woods, R. (2010). Electrochemical Aspects of Sulfide Mineral Flotation. In: C.J. GREET, ed, Flotation Plant Optimisation: A Metallurgical Guide to Identifying and Solving Problems in Flotation Plants. Spectrum Series 16 edn. AuSIMM, pp. 123-134.

Yoon, R. H., and Sabey, J. B. (1989). Coal flotation in inorganic salt solutions. In Botsaris, G. D., Glazman, Y. M. (Eds.), Interfacial Phenomena in Coal Technology, In Surfactant Science Series, 32, 87-114.

Yang, C., Dabros, T., Li, D., Czarnecki, J., Masliyah, J.H. (2001). Measurement of the zeta potential of gas bubbles in aqueous solutions by microelectrophoresis method. Journal of Colloid and Interface Science. 243, 128–135. https://doi.org/10.1006/jcis.2001.7842.

Ye, Y. and Miller, J.D. (1989). Induction-time measurements at a particle bed. International Journal of Mineral Processing. 25 (3-4): 221-240.

Yoon, R.H. (2000). The role of hydrodynamic and surface forces in bubble–particle interaction. International Journal of Mineral Processing 58 (1–4), 129–143.

Yoon, R.H. and Basilio C. (1993). Adsorption of thiol collectors on sulphide minerals and precious metals - a new perspective. Proceedings of XVIII Int. Miner. Process. Cong., Sydney, pp 611-617.

Yoon, R. and Yordan, J.L. (1991). Induction-time measurements for the quartz-amine flotation system. Journal of Colloid and Interface Science. 141 (2): 374-383.

Zawala, J., Drzymala, J., Malysa, K. (2008). An investigation into the mechanism of the three-phase contact formation at fluorite surface by colliding bubble, International Journal of Mineral Processing. 88 72–79.

Zieminski, S.A. and Whittemore, R.C. (1971). Behavior of gas bubbles in aqueous electrolyte solutions. Chemical Engineering Science, 26, 509-520.

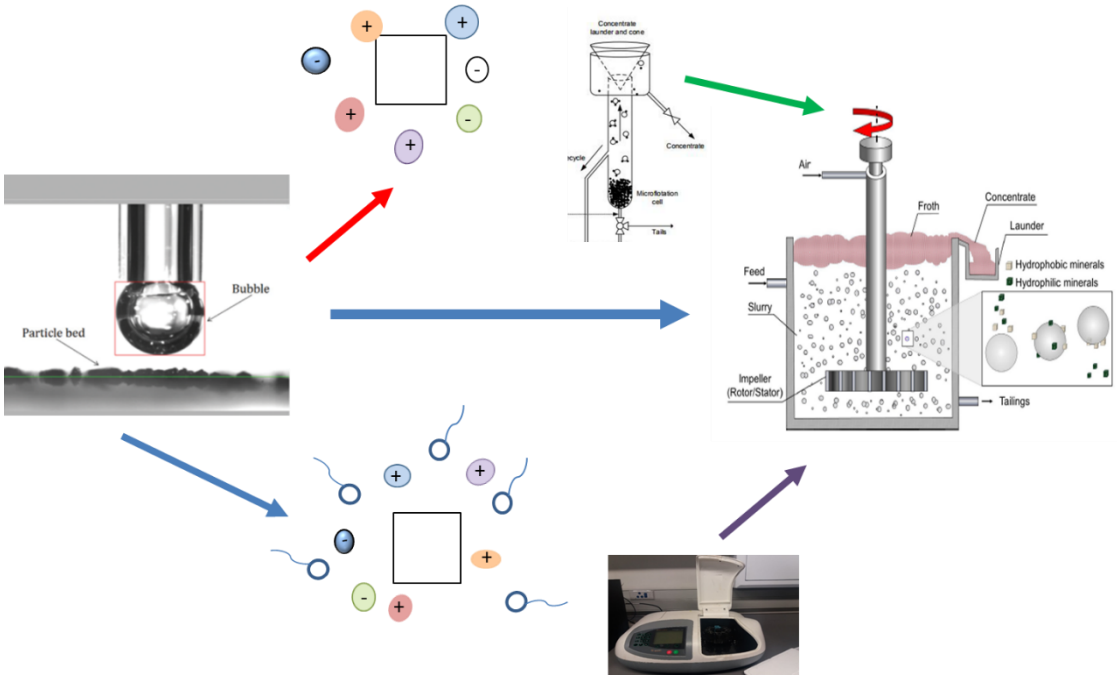

3.1 Aims and Objectives

The main aim of this work is to investigate the effect of complex process waters and the recycling thereof on the bubble-particle attachment sub-process in a sulfide mineral system; as well as to identify specific ions within process water that control the bubble-particle attachment sub-process by either enhancing, hindering or having no effect on the bubble-particle attachment of sulfide minerals. This work also aims to corroborate the use of the ACTA as a means to assess bubble-particle attachment at a fundamental level by comparison with the classical microflotation technique.

Specific objectives within the study is to understand:

- The effect of increasing ionic strength of plant water on the attachment of pyrrhotite, chalcopyrite and galena particles to air bubbles in terms of fundamental bubble-particle attachment and microflotation experimental methods.
- The effect of synthetic plant water of increasing ionic strength on the zeta potential of pyrrhotite, chalcopyrite and galena.
- The effect of synthetic plant water of increasing ionic strength on SIBX adsorption on pyrrhotite, chalcopyrite and galena
- The effect of process water of increasing ionic strength at pH 11 on the attachment of sulfide minerals (pyrrhotite, chalcopyrite, galena) to air bubbles (in the presence of SIBX collector) in terms of fundamental bubble-particle attachment and microflotation experimental methods.

- Whether there is a single ion that controls attachment of pyrrhotite, chalcopyrite and galena particles to air bubbles in terms of fundamental bubble-particle and microflotation experimental methods.
- Whether there is a single ion in the process water that hinders xanthate adsorption or if it is the combined effect of the various ions present in process water that hinder xanthate adsorption on pyrrhotite, chalcopyrite and galena.
- The drivers responsible for changes in bubble-particle interactions under changes in water quality in terms of collector adsorption and sulfide mineral potential.

3.2 Key Questions

The main question which drives this work can be stated as "How do changes in water quality affect the bubble-particle attachment of sulfide minerals and subsequently collector adsorption and mineral potential?"

Table 3-1 provides an account of the key questions that were formulated to satisfy the objectives of this investigation. The experimental technique and operating conditions are also briefly provided on how each of these key questions will be answered.

Table 3-1: Research approach which will address the key questions and satisfy the aim of this investigation

Key Question	**Experiment**	**Conditions**
How does an increase in ionic strength of plant water affect the bubble-particle interactions for selected sulfide minerals?	Attachment Time Tests (Bubble-Particle Attachment Probability) Microflotation (Mineral Recovery)	Synthetic Plant Water (Wiese *et al.,* 2005) of 0.0213 M, 0.0977 M and 0.1860 M. Pyrrhotite, Chalcopyrite and Galena.
How does an increase in the ionic strength of plant water affect the adsorption of xanthate on the mineral surface of selected sulfide minerals?	Adsorption Studies	Synthetic Plant Water of 0.0213 M, 0.0977 M and 0.1860 M. Pyrrhotite, Chalcopyrite and Galena.
Are there specific ions in plant water that either deter/improve the adsorption of xanthate on the mineral surface of selected sulfide minerals?	Adsorption Studies	$CaSO_4$, $Ca(NO_3)_2$ and $NaNO_3$ single salts solutions at fixed ionic strength. Pyrrhotite, Chalcopyrite and Galena.
How does an increase in ionic strength of plant water affect the zeta zeta potential of selected sulfide minerals?	Zeta Potential Determination Tests	Synthetic Plant Water of 0.0213 M, 0.1205 M and 0.213 M. Pyrrhotite, Chalcopyrite and Galena.
Are there specific ions in plant water that control bubble-particle interactions on selected sulfide minerals?	Attachment Time Tests (Bubble-Particle Attachment Probability) Microflotation (Mineral Recovery)	Synthetic Plant Water of 0.0213 M, 0.0977 M and 0.1860 M. Pyrrhotite, Chalcopyrite and Galena.
How do specific ions present in plant water affect the zeta potential on selected sulfide minerals?	Zeta Potential Determination Tests	Synthetic Plant Water of 0.0213 M, 0.0977 M and 0.1860 M. Pyrrhotite, Chalcopyrite and Galena
How does an increase in ionic strength of plant water at high pH affect the bubble-particle interactions for selected sulfide minerals?	Attachment Time Tests (Bubble-Particle Attachment Probability) Microflotation (Mineral Recovery)	Synthetic Plant Water of 0.0213 M, 0.0977 M and 0.1860 M. pH modifier: NaOH. Pyrrhotite, Chalcopyrite and Galena

3.3 Hypotheses

- In a sulfide mineral system, the attachment of mineral particles to air bubbles will be improved in solutions of higher ionic strength. Upon the addition of ions to a three-phase system, the electrical double layer is compressed. When the electrical double layer is compressed the energy barrier for bubble-particle attachment to occur decreases leading to the faster rupturing of the film at the air-water and solid-water interface.
- Divalent ions such as Ca^{2+} and SO_4^{2-} will result in a greater attachment probability compared to monovalent ions. Divalent ions result in increased adsorption onto the mineral surface compared to monovalent ions; reducing the magnitude of the negative mineral charge and thus decreasing the energy barrier for bubble-particle attachment.
- The amount of SIBX adsorbed onto the mineral surface will decrease as the ionic strength of the process water is increased. The addition of ionic collector to an electrolyte solution could result in competition between the ions and collector for adsorption on the mineral surface. This in turn could result in less adsorption of xanthate on the mineral surface at high ionic strengths.

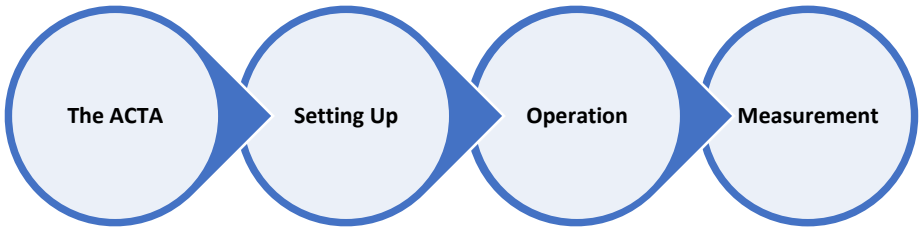

4.1 Introduction to the ACTA

The Automated Contact Time Apparatus (ACTA) was developed at Aalto University's Department of Chemical and Metallurgical Engineering (Aspiala *et al.,* 2018). The ACTA, shown in Figure 4-1 is in principle an advanced version of an induction timer.

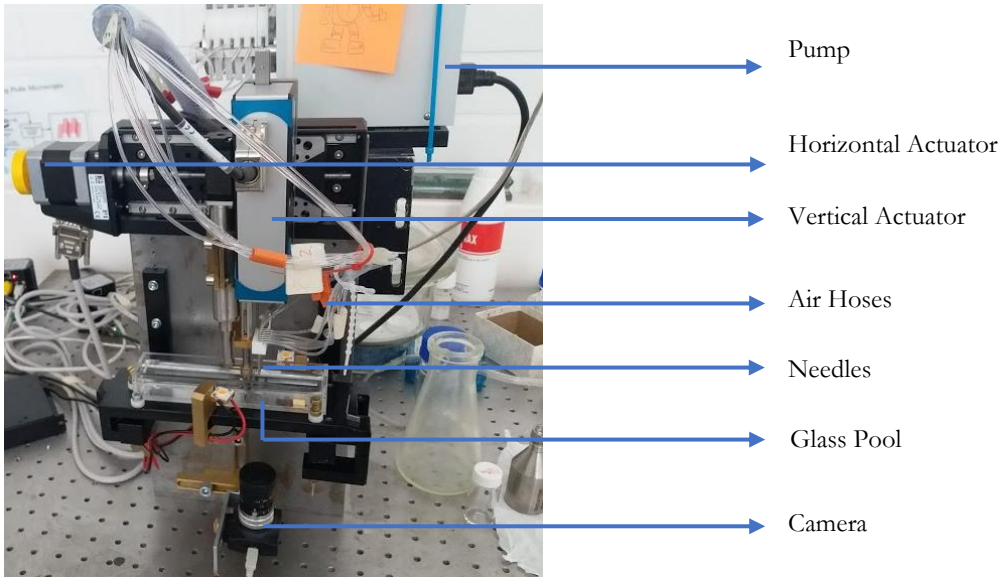

Figure 4-1: Picture of the ACTA

As discussed in Chapter 2, traditional induction timers have one needle and create a single bubble; this bubble is usually brought into contact with a particle bed and the induction time is typically measured at about ten different areas on the particle bed (Yoon and Yordin, 1990; Gu *et al.,* 2003; Albijanic *et al.,* 2011). This method raises some concerns, firstly whether these chosen areas are representative of the entire particle bed, secondly whether enough opportunities for bubble-particle attachment are provided to predict the induction time. The ACTA provides a solution to such concerns. The ACTA has six needles, thus

creating an array of six bubbles at the same time; the entire length of the particle bed is then given the opportunity for bubble-particle attachment by the movement of the horizontal actuator.

4.2 Operation of the ACTA

The principle intention of this instrument is described as follows;

Six bubbles are generated at the ends of the array of needles, the bubbles are brought into contact with the particle bed for a set contact time, the bubble-particle aggregates are automatically transported to the camera zone where two pictures are taken, the first image with white light illumination (LED) is taken to determine bubble size, the bubble size is then automatically saved (shown in Figure 4-11). The second image allows for manual detection of whether particles have or have not attached to the bubbles (shown in Figure 4-12). The detection of particles is made easier through the contrast between the green light and black particles; this green light is as a result of green LED attached to optical fibres inside each of the needles thus lighting the generated bubbles up from the inside.

After the images are taken the bubble-particle aggregates are automatically transported to a collection bin where air is blown through the needles such that they detach and the particles remain in the collection bin. Figure 4-10 shows the deposition of the particles in the collection bin.

The array of needles then moves to the next 1 mm of the particle bed and the process is repeated until the entire length of the particle bed has been tested. The length of the particle bed is measured in 66 cycles and having generated six bubbles per cycle, 396 opportunities of bubble-particle attachment are provided in one measurement run.

The particles collected in the collection bin may then be weighed, analysed for composition, shape and size provided that enough particles are collected. This is an advantage of the ACTA since standard induction timers only generate one bubble and the particles attached are not collected. The collection process of particles collected from one bubble may prove to be very difficult, as it may be that only a few particles (possibly only one or two) attach to the bubble; collecting this, filtering and even weighing these particles could be problematic. The ACTA collects particles attached to 396 bubbles, due to more particles this makes the collection process (depositing into bin, filtering, drying, weighing) much simpler.

The instrument is operated by National Instruments™ LabVIEW code which allows for parameters such as the particle bed height, approach distance, bubble size, compression, contact time and approach velocity to be set. All the movements performed by the instrument are achieved with 3 actuators (vertical and horizontal movements of the array of needles as well as the shovel).

Figure 4-2 shows part of the ACTA prior to particle bed preparation, here the needles are situated at the farthest end of the bed i.e this is usually where the last measurement is taken.

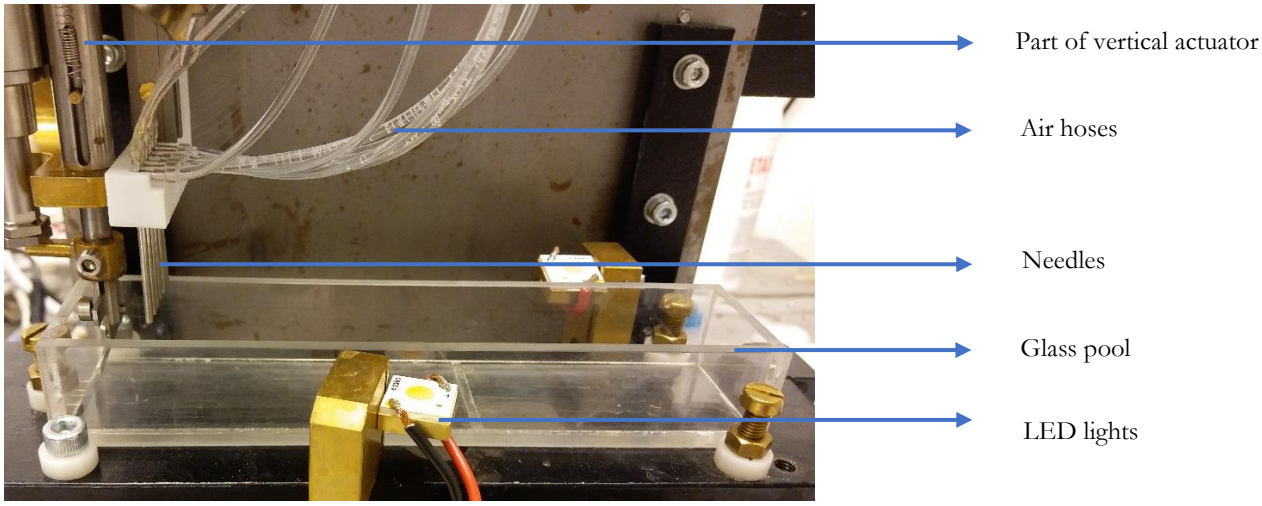

Figure 4-2: Components of the ACTA prior to measurements

The plastic collection bin as depicted in Figure 4-3 (A) is placed inside the glass pool at the end to the right of the LED lights (area shown in Figure 4-2). A metal cover plate is slid onto the plastic collection bin to keep the collection bin closed and thus prevent any collected particles from escaping the collection bin. The needles enter the six slits on the metal cover plate after each cycle, thus depositing the attached particles into the collection bin. The particles settle to the bottom of the collection bin; the needles then move up and return to the particle bed for another cycle.

A B

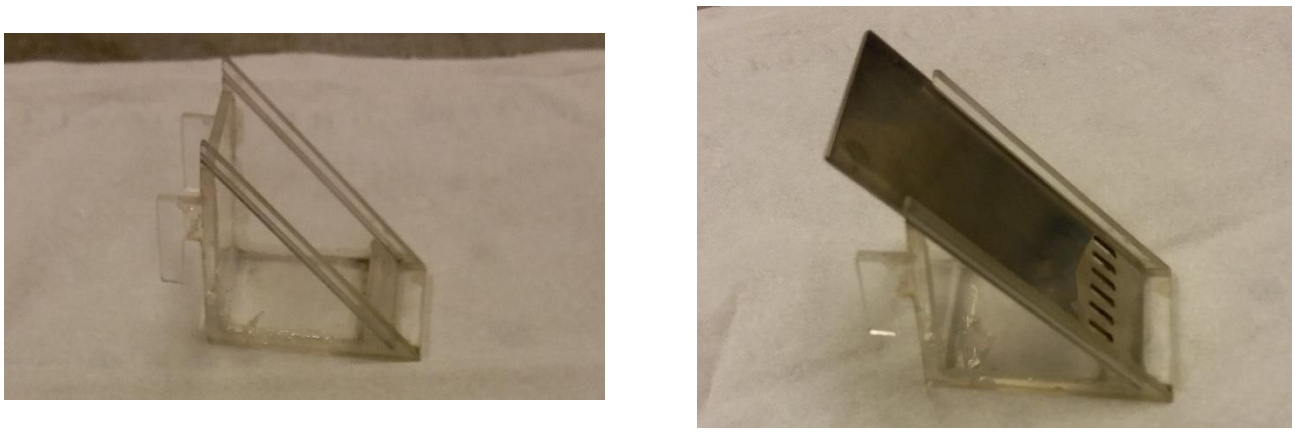

Figure 4-3: (A) Plastic collection bin and (B) collection bin with metal cover plate which contains slits for the particle deposition

Images for bubble size measurements and particle detection are taken with an IDS UI-1580LE camera with resolution of 4.92 MP, fitted with a 23FM25SP Tamron lens; the camera may be operated with LabVIEW code. As shown in Figure 4-4 the camera is placed on a mount; in order to get the widest parts of the bubbles in focus, the height of the mount and focus is adjusted as needed.

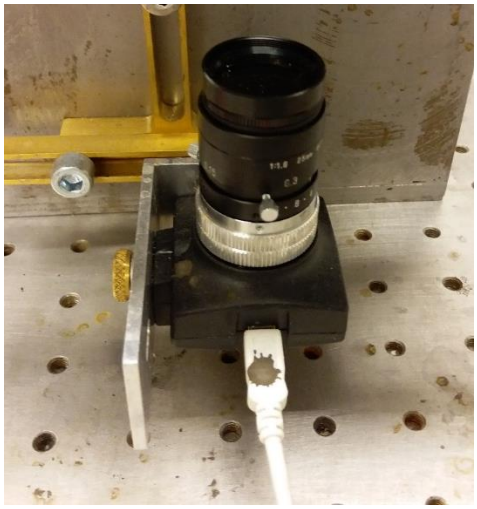

Figure 4-4: Digital camera attached to ACTA

4.2.1 Moving Components

The shovel height is controlled by the MP-15 actuator, the array of needles' up and down movements are controlled by the V-273 actuator and the horizontal movement of the shovel as well as array of needles is controlled by the PLS-85 actuator. Figure 4-5 shows where these actuators are situated on the ACTA.

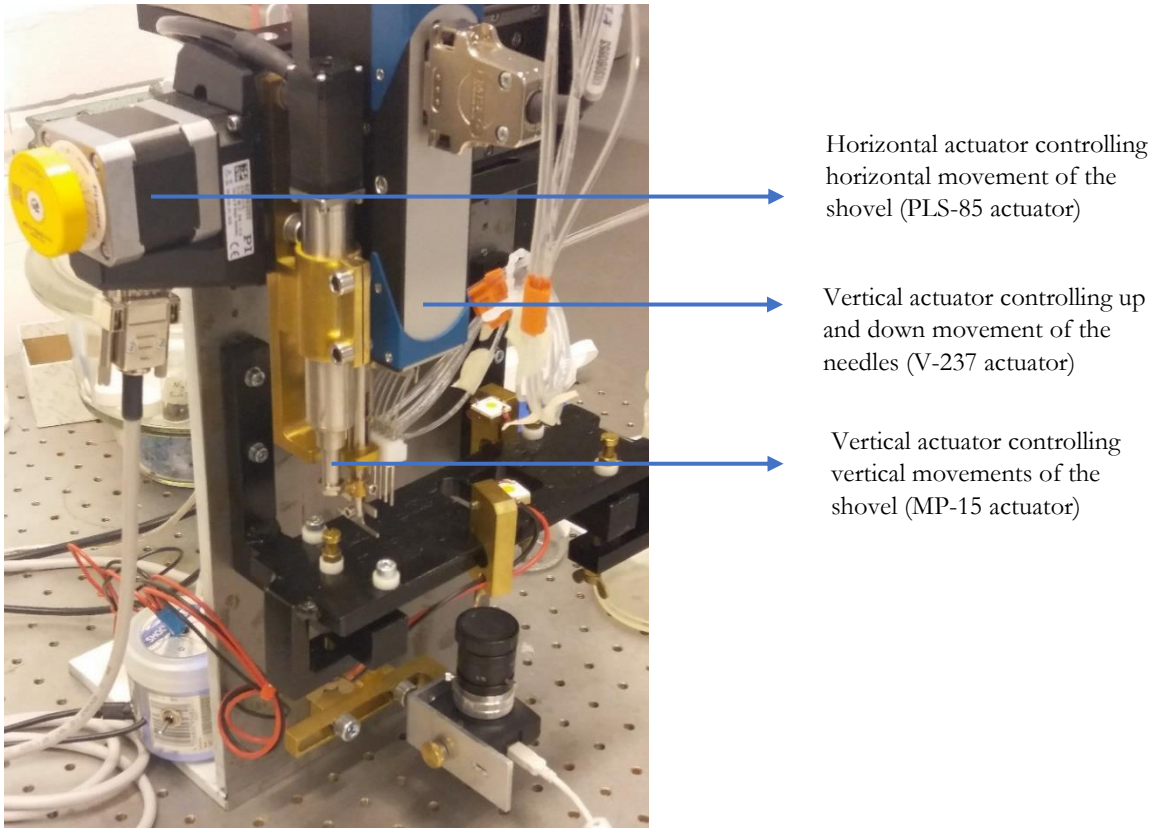

Figure 4-5: Location of actuators on the ACTA

The process of bringing the needles into contact with the particle bed must be controlled such that the needles are just the right distance from the particle bed and that this distance is consistent throughout the measurements. Furthermore, the particle bed must be created at the correct height. For these reasons the shovel was calibrated manually at the start of each day that measurements were taken. The actuator controlling the vertical movements of the needles is set to a position of -10 mm and a calibration piece is attached to the shovel. This calibration piece thus ensures that the shovel and its position with the array of needles are aligned. The screw on the shovel is then tightened at this point; thus, the zero position of the actuator controlling the shovels vertical movements is aligned with the calibrated position of the shovel with the needle array. Figure 4-6 shows a picture of this calibration process.

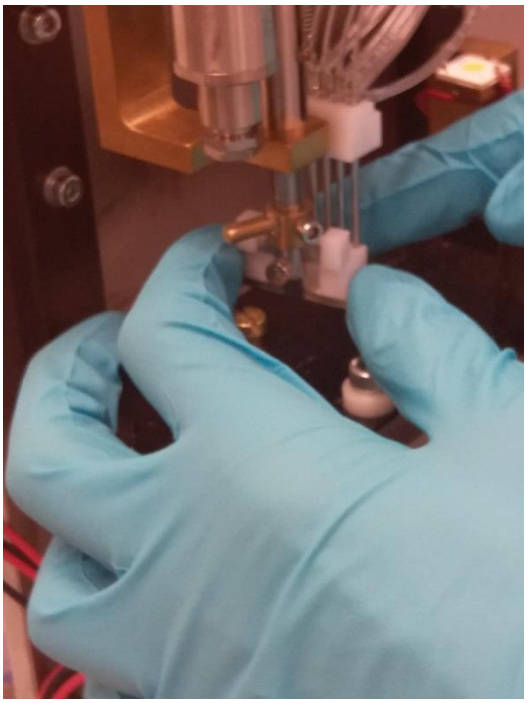

Figure 4-6: Shovel calibration

4.2.2 Particle Bed Making

A slurry consisting of 20 g of mineral sample and 100 mL of the particular water type under investigation was made up in a glass bottle. 100 g/t of SIBX was added to the slurry and it was conditioned for 2 minutes for the tests that were performed in the presence of a collector. The mineral particles in the slurry were then allowed to settle for 3 to 5 minutes as shown in Figure 4-7.

Figure 4-7: Particles settling in glass bottle

The clear liquid above the settled particles was removed with a pipette and filtered with a glass funnel and filter paper such that a clear water was obtained and only about 2 cm of liquid above the settled particles remained in the flask. The filtered liquid was transferred to the glass pool filling ¾ of the pool.

Using a pipette, a heap of the settled particles was added to the glass pool containing the water. The automated shovel attached to the linear actuator was used to flatten the particle bed. Particles were gradually pipetted into the pool and shovelled until a flat particle bed of 2 mm across the length of the pool was attained. The particle collection bin was then carefully inserted in place within the glass pool. Furthermore, a metal stopper was used to prevent finer particles from entering the collection zone.

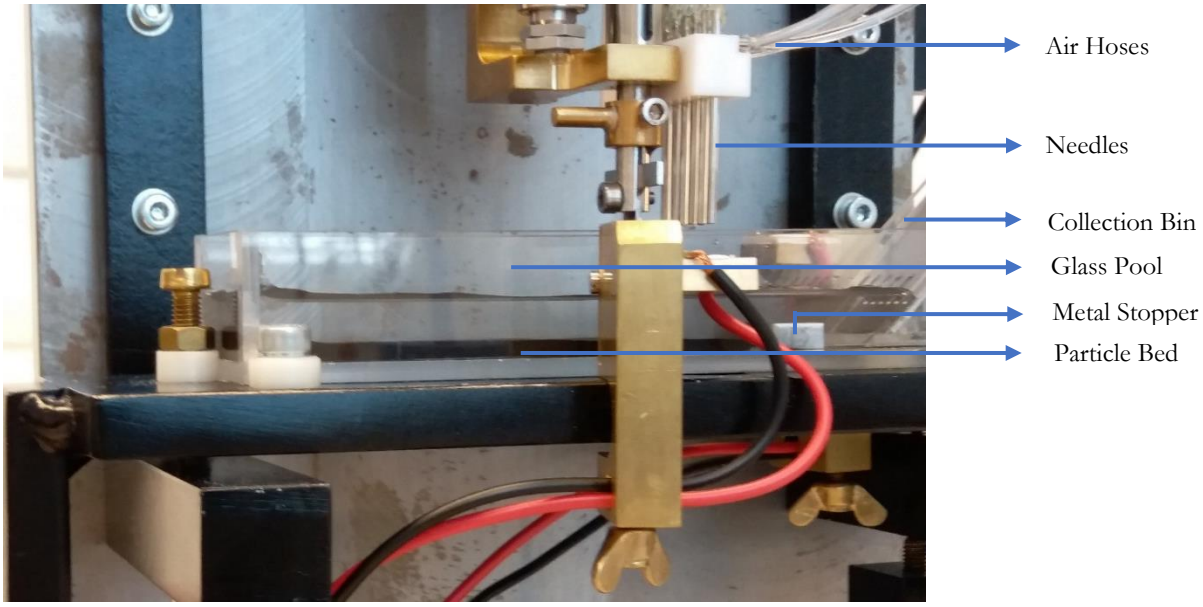

Figure 4-8: ACTA after particle bed preparation

At this point the set up should look as illustrated in Figure 4-8, more water should be added dropwise at the collection bin end of the pool until the holes of the metal cover plate on the collection bin are fully immersed in water.

4.2.3 ACTA Operational Parameters

The approach velocity, retract velocity, approach distance, pumping time, bubble size and bubble compression were kept constant throughout this test work. The actual values chosen for the experiments were chosen based on the initial exploratory work done by Bellers (2017). The approach velocity and retract velocity were set to 50 mm/s, while the approach distance and bubble compression were set to 0.5 mm and 0.1 mm respectively. For the first phase of the experimental work on pyrrhotite contact times of 100 and 200 ms were used. The second phase of the work with galena and chalcopyrite used a contact time of 50 ms as these experiments were done only in the presence of a collector, thus the contact time was reduced such that a difference in attachment probability could still be observed.

Figure 4-9 illustrates the operating interface for the ACTA on LabVIEW the various operating parameters can be set using this interface. The waveform graph is also displayed in a window on this view, here the actual contact time can be monitored. The file path of the folder where the images must be saved is also specified on this console; furthermore, this view provides a preview of the image taken for each cycle in the window below the waveform graph allowing the user to keep track of the cycles.

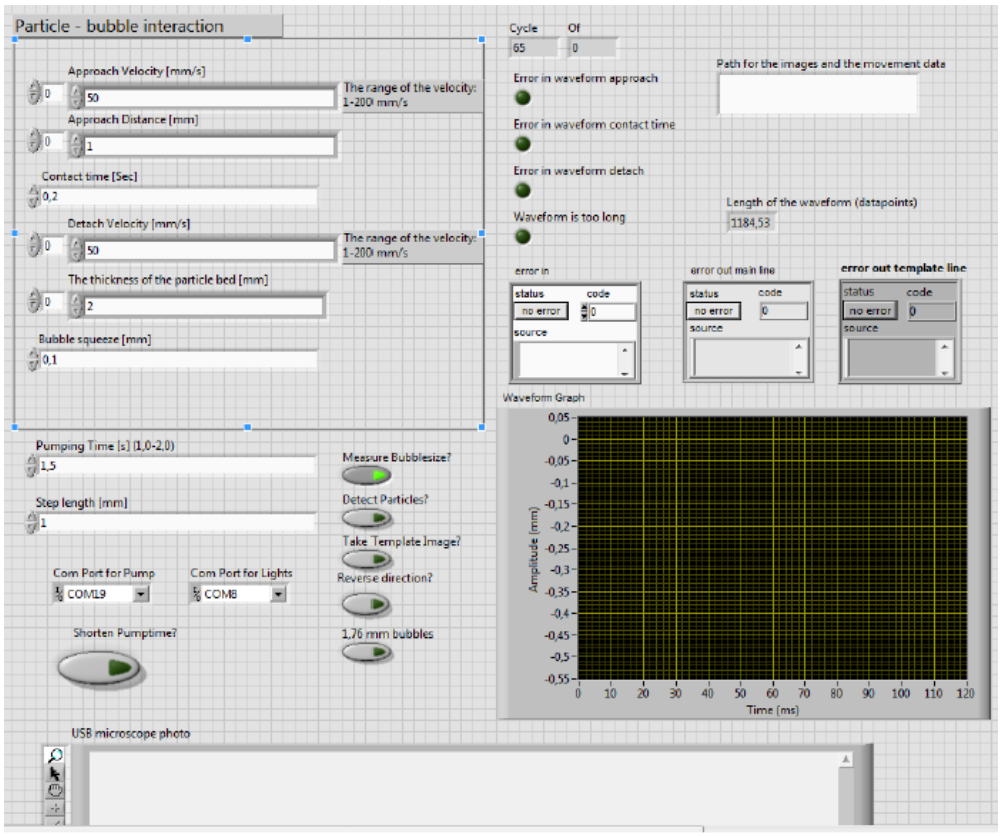

Figure 4-9: Operating interface for the ACTA in LabVIEW

After the preparation of the particle bed and having set the operating parameters, the process of taking measurements can start. Upon initialising the programme, the needles will move to the first 1 cm of the particle bed (left end to the camera); when the tips are fully immersed in the water bit still above the particle bed, the pump will start up which leads to the generation of a bubble at the end of each of the needles. The needles with bubbles approach the particle bed at the specified velocity and the bubbles make contact with the particle bed for the pre-set contact time. The needles with contacted bubbles then retreat and move to the camera area while still fully immersed in the water (preventing the bubbles from bursting). LED lights located at both sides of the pool light up and an image is taken from the bottom of the pool; it is then saved in the specified folder. The needles with contacted bubbles move to the collection bin, through the grooves on the metal cover plate as shown in Figure 4-10. Additional air is pumped through the needles so as to burst the bubbles and release the particles that have attached to the bubbles into the collection bin. The needles then rise up and move horizontally to the left to the next 1 cm of the particle bed and the process is repeated until 66 cycles are completed.

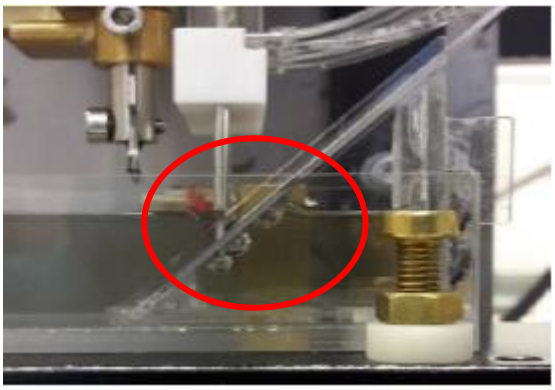

Figure 4-10: Particle deposition in collection bin

4.2.5 Measurement outputs

The digital camera below the glass pool (Figure 4-4) takes two images of the bubble at the tip of the needle for each cycle. The first image with white light illumination (LED at sides of pool) is used to determine the bubble size and is shown in Figure 4-11. Figure 4-12 is used to determine whether particles are attached to the bubbles, the green colour is as a result of a green LED which is attached to optical fibres inside each of the needles which lights the bubbles from the inside. The contrast between the green light and black particles makes the detection of particle attachment relatively straightforward.

Figure 4-11: Image for bubble size determination

Figure 4-12: Image used for particle detection

Upon the completion of the 66th cycle, the collection bin is removed from the pool and the contents of the collection bin are filtered. For the phase one measurements with pyrrhotite of 38 to 75 microns it was observed that the particles were too fine and sufficient mass was not recovered across all the experimental conditions. Therefore, when phase two of the measurements commenced particles of 106 to 125 microns were used. With this size fraction it was clearly observed that particles were present in the collection bin. The particles were filtered with 13 mm Nitrocellulose MFTM 0.45 µm Membrane Filters and Millipore filter as shown in Figure 4-13.

A

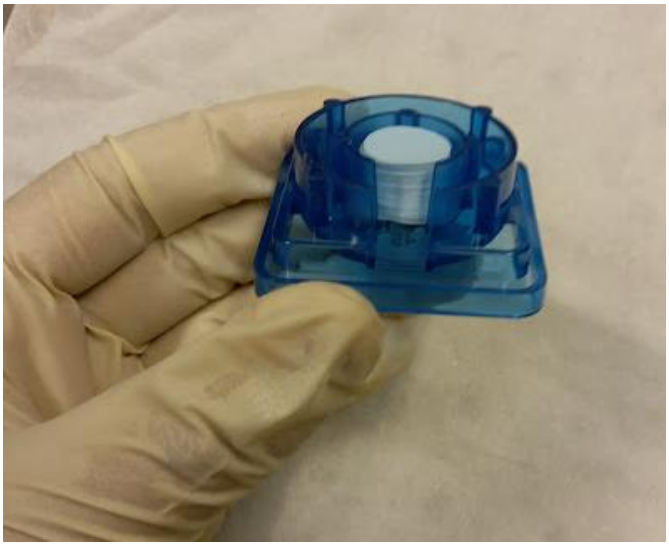

B

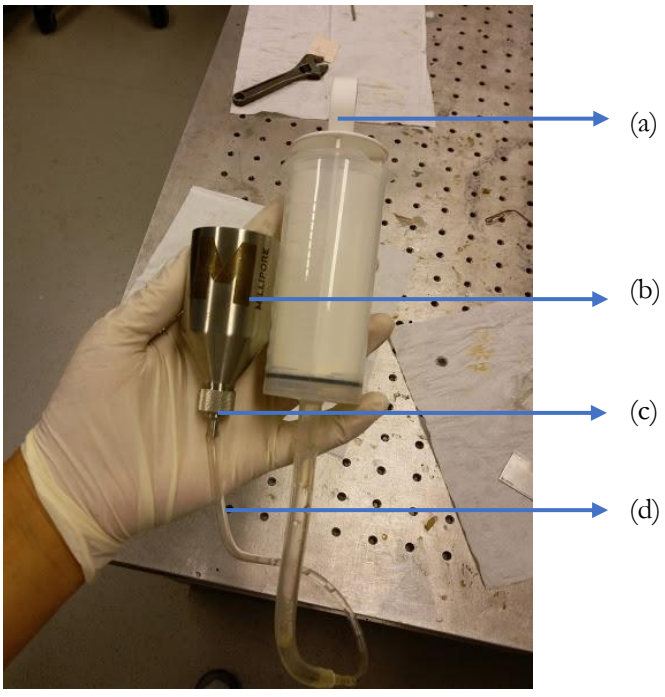

Figure 4-13: (A) Nitrocellulose Membrane Filters and (B) Millipore filter and suction set-up for filtration (The membrane filter is placed inside (c) and screwed on to (b), the contents of the collection bin is poured in (b). (a) is pulled upward creating suction in (b). The particles collected will sit on the microfiber on (c) and the filtrate is collected in (b). The collected particles on the microfiber are collected by unscrewing (c).

The filter paper with the particles is placed on caps and kept in a desiccator overnight. Figure 4-14 shows galena particles collected from one cycle after it had been in the desiccator. Having weighed each filter

paper prior to filtration and weighing the dried particles and filter paper, the mass of particles recovered can be calculated and a recovery determined.

Figure 4-14: Galena particles collected in collection bin

4.3 Studies with the ACTA

The work in this study conducted testwork with the ACTA in two phases. Phase one included work on pyrrhotite where the particle bed consisted of -75+38 μm particles. Water Quality Effects on Bubble-Particle Attachment of Pyrrhotite was subsequently published from phase one work in Minerals Engineering 131 230–236. https://doi.org/10.1016/j.mineng.2018.11.017. This was the first time work was done of this apparatus determining the effect of a process parameter on bubble-particle attachment. Initial work by Aspiala *et al. (*2018) was related to the commissioning of the instrument. This study then continued with phase two work with galena and chalcopyrite with a particle size of -125+106 μm. Phase two work also included the use of microflotation work in order to validate the use of the instrument as a measure for floatability which is detailed in Fundamental and Flotation Techniques Assessing the Effect of Water Quality on Bubble-Particle Attachment of Chalcopyrite and Galena in the Proceedings of MEI Flotation '19. Cape Town, South Africa presented as Chapter 8 in this study.

Subsequently after the completion of these two phases, authors such as Pienaar *et al.* (2019) and Hartmann and Serna-Guerrero (2020) validated these findings as well under the specified conditions for the use of the ACTA as a measure for particle floatability. The study by Pienaar *et al.* (2019) was also done using a sulfide mineral, galena; the galena particles were of the same size as the galena particle in this investigation and a contact time of 20 ms was used. These authors showed a good correlation between microflotation test and the attachment probability from the ACTA; the mixture containing hexanol and SDEDTP showed the highest recovery and attachment probability while in the absence of reagents, low recoveries and attachment probabilities were achieved. The study by Hartmann and Serna-Guerrero (2020) used quartz particles of particle size -180+75 μm under various contact times; these authors also showed that the attachment probability coincided well with the flotation recovery.

4.4 References

Albijanic, B., Amini, E., Wightman, E., Ozdemir, O., Nguyen, A. and Bradshaw, D. (2011) A relationship between bubble-particle attachment time and the mineralogy of a copper-sulphide ore. Minerals Engineering. 24: 1335-1339.

Aspiala, M., Schreithofer, N., Serna-Guerrero, R. (2018). Automated contact time apparatus and measurement procedure for bubble-particle interaction analysis. Minerals Engineering. 121, 77–82. doi:10.1016/j.mineng.2018.02.018.

Gu, G., Sanders, R.S., Nandakumar, K., Xu, Z., Masliyah, J.H. (2004). Hydrogen and Oxygen Bubble Attachment to a Bitumen Drop. Canadian Journal of Chemical. Engineering. 82, 846–849. doi:10.1002/cjce.5450820426.

Hartmann, R., and Serna-Guerrero, R. (2020). Towards a quantitative analysis of the wettability of microparticles using an automated contact timer apparatus. Minerals Engineering. 149:106240. doi: 10.1016/j.mineng.2020.106240.

Pienaar, D., Jordaan, T., McFadzean, B., O'Connor, C.T. (2019) The synergistic interaction between dithiophosphate collectors and frothers at the air-water and sulphide mineral interface. Minerals Engineering 138, 125–132.

Yoon, R. and Yordan, J.L. (1991). Induction-time measurements for the quartz-amine flotation system. Journal of Colloid and Interface Science. 141 (2): 374-383.

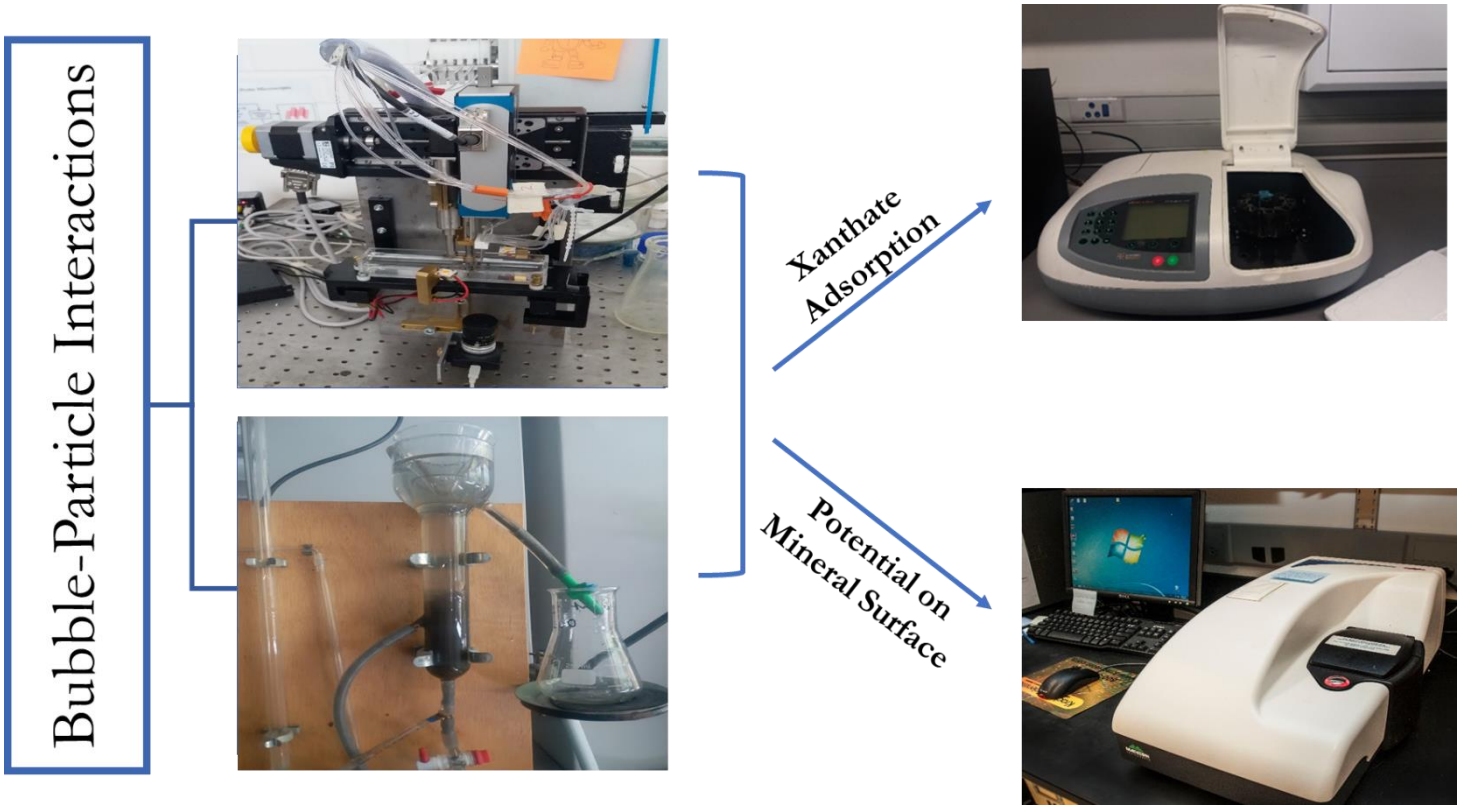

Chapter 5 describes the experimental techniques and materials that were used in this study. Considering that this study investigates the effect of water quality on bubble-particle attachment, various water qualities were used. Two techniques assessed the bubble-particle attachment under varying water quality. Details of the sample preparation and water qualities, namely three synthetic plant waters, three single salts and the synthetic plant waters at elevated pH are included in this chapter. The Automated Contact Time Apparatus (ACTA) and microflotation set-up were used to assess the bubble-particle interactions from a fundamental and flotation perspective respectively. The microflotation procedure is described in this chapter while a detailed description of the ACTA has been documented in Chapter 4. Furthermore, in order to better understand the bubble-particle interactions under various water qualities, collector adsorption tests and zeta potential determination tests were performed. This chapter also provides the details of these two experimental techniques.

5.1 Materials

5.1.1 Sample Preparation

The sulfide minerals (Pyrrhotite, Galena and Chalcopyrite) used in this study were obtained from Ward's Science in 1 kg batches. Table 5-1 provides an account of the mineralogical compositions of the sulfide minerals under study. Powder XRD spectra were obtained using a Bruker D8 Advance powder diffractometer with Vantec detector and fixed divergence and receiving slits with Co-Ka radiation. The

phases were identified using Bruker Topas 4.1 software (Coelho, 2007) and the relative phase amounts (weight %) were estimated using the Rietveld method.

As discussed in Chapter 4, it was found that a particle size of 106-125 μm worked well for the attachment time tests in terms of recovering particles large enough such that the collected mass of particles could be weighed. Microflotation tests are generally done with particle size of 38-75 μm (Lange *et al.,* 1997; Castelyn, 2012). While studies looking at the zeta potential of pure minerals tend to use particle sizes as fine as -25 μm (Nyabeze, 2015).

Figure 5-1 presents a summary of the pulverisation and screening process. The respective mineral samples were manually hammered to -1000 μm and then pulverised by means of a Sieb mill and screened. Each of the samples in the various size fractions was split by means of a rotary splitter into 10 further samples, bottled, purged with nitrogen and stored below -5 °C in the laboratory. This method of sample preparation was performed on all 3 sulfide minerals.

Table 5-1: Compositions of the XRD of the sulfide minerals under study

SULFIDE MINERAL	XRD RESULTS	
	Mineral	**Composition (%)**
PYRRHOTITE	Quartz	4.20
	Sphalerite	2.56
	Chalcopyrite	1.62
	Pyrrhotite 5C	91.62
GALENA	Galena	100.00
CHALCOPYRITE	Quartz	13.21
	Sphalerite	3.15
	Chalcopyrite	78.67

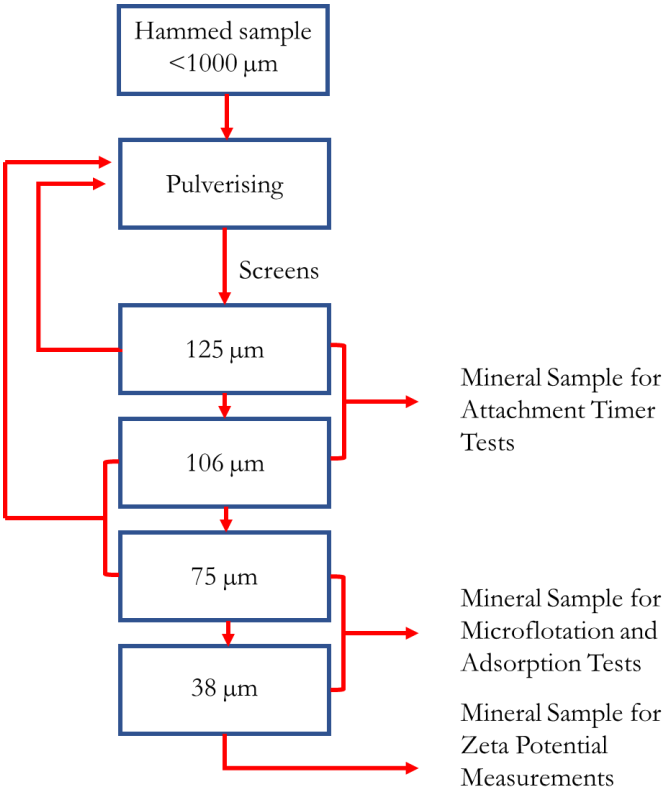

Figure 5-1: Mineral Sample Preparation: Division of Size Fractions

5.1.2 Synthetic Plant Water

Ultra-purified water was used as a baseline (with the physicochemical properties shown in Table 5-2. Standard synthetic plant water (1 SPW) as described by Wiese et al. (2005) was used to mimic actual plant water and to simulate the recycle (recirculation) of plant water, 1SPW equivalent to 1023 total dissolved solids (TDS) was increased by 5 and 10 times, referred to as 5 SPW and 10 SPW respectively. All the salts used to make up the synthetic plant water were of analytical grade and supplied by Merck. The concentrations of the various ions making up 1, 5 and 10 SPW are presented in Table 5-3.

Table 5-2: Properties of Ultra-Purified Water

Ultra-Pure Water	**Resistivity at 25 °C (MΩ·cm)**	**Conductivity (µs/cm)**	**Total Organic Carbon (µg/L)**	**Na^+ (µg/L)**	**Cl^- (µg/L)**
	18.2	<0.055	<5	<1	<1

Table 5-3: Ionic Concentrations of the Various Synthetic Plant Water

Plant Water Type	Ca^{2+} (mg/L)	Mg^{2+} (mg/L)	Na^{+} (mg/L)	Cl^{-} (mg/L)	SO_4^{2-} (mg/L)	NO_3^{-} (mg/L)	CO_3^{2-} (mg/L)	TDS (mg/L)	Ionic Strength (IS) (mol/L)
1 SPW	80	70	153	287	240	176	17	1023	0.0241
5 SPW	400	350	765	1435	1200	880	85	5115	0.1205
10 SPW	800	700	1530	2870	2400	1760	170	10230	0.241

In order to gain an understanding of whether there are specific ions within the plant water recipe that control bubble-particle attachment and either aid or hinder the adsorption of xanthate; single salt solutions were also used in this study. Single salt solutions were used at the ionic strength of 5 SPW. $NaNO_3$, $CaSO_4$ and $Ca(NO_3)_2$ were the three single salts used in this work and their compositions are provided in Table 5-4. These salts were carefully selected such that a cation effect could be established (Ca^{2+} versus Na^{+} with both having a NO_3^{-} anion) and an anion effect (SO_4^{2-} versus NO_3^{-} with both having a Ca^{2+} cation). These salts were specifically chosen as Manono *et al.* (2016) showed that Ca^{2+}, NO_3^{-}, Na^{+} and SO_4^{2-} ions are the ions of interest in the plant water recipe.

Table 5-4: Ionic Concentrations of Single Salt Solutions at an ionic strength equivalent to 5SPW

Water Type	Ca^{2+} (mg/L)	Mg^{2+} (mg/L)	Na^{+} (mg/L)	Cl^{-} (mg/L)	SO_4^{2-} (mg/L)	NO_3^{-} (mg/L)	CO_3^{2-} (mg/L)	TDS (mg/L)	IS (mol/L)
$Ca(NO_3)_2$	**1305**	**-**	**-**	**-**	**-**	**4039**	**-**	**5344**	**0.1205**
$CaSO_4$	**979**	**-**	**-**	**-**	**2346**	**-**	**-**	**3325**	**0.1205**
$NaNO_3$	**-**	**-**	**2246**	**-**	**-**	**6058**	**-**	**8304**	**0.1205**

5.1.3 Reagents

Sodium Iso-Butyl Xanthate (SIBX) was the only flotation reagent used in this test programme. The SIBX of 97% purity was sourced from Senmin. Due to the decomposing nature of xanthates, 1% (w/v) solutions were made fresh daily by dissolving 1 g of SIBX powder in 100 mL of ultra-purified water in a volumetric flask. Since the effect of pH is also investigated in this work NaOH and HCl (1% w/v), as supplied by Merck, were used to modify the pH of the synthetic plant water to 11.

5.2 Experimental Methods

5.2.1 Attachment Timer Tests

This machine was used to determine the attachment probability and mass recovered in the collection bin with the various water qualities (Table 5-2 to Table 5-4). The minerals used to build the particle bed were pyrrhotite, galena and chalcopyrite, each of these minerals was tested under ultra-purified water, the 3 synthetic plant waters and 3 single salt solutions. Specific settings used on the attachment timer as well as experimental details are described in Chapter 4. Figure 5-2 gives an account of the experimental programme for the attachment timer tests.

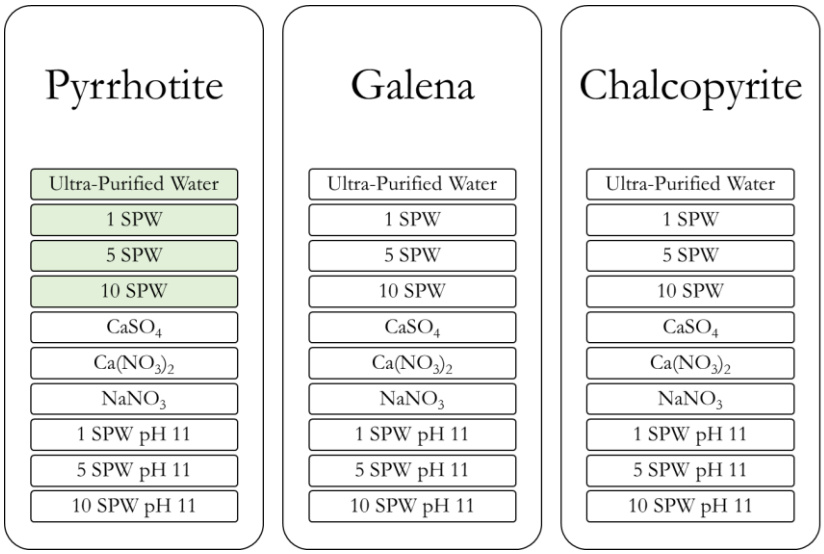

Figure 5-2: Experimental Conditions for the Attachment Contact Time Apparatus

The tests highlighted in green in Figure 5-2 were done both in the presence and absence of SIBX. As a result of low attachment probability with no collector in the system, the subsequent tests with galena and chalcopyrite were done with 50 g/t of SIBX. The initial tests with pyrrhotite used a collector concentration of 100 g/t as this is an acceptable industry standard. The preliminary test work with galena and chalcopyrite however resulted in almost 100% attachment across the water qualities. It was thus decided to use a collector dosage of 50 g/t such that a difference in attachment could be seen as a result of the water quality.

5.2.2 Microflotation

Although the attachment timer considers bubble-particle attachment from a fundamental level, it does not take into account the hydrodynamics of a flotation system. Microflotation tests were thus performed under the same conditions as the attachment timer tests as this technique resembles real flotation better than the fundamental bubble-particle technique. The same experimental programme as in Figure 5-2 was used however each condition was done with and without SIBX.

The microflotation cell, developed by Bradshaw and O'Connor (1996), is shown in Figure 5-3. Two grams of the pure mineral sample (38-75 μm) was weighed and mixed with 50 mL of the water quality under study. The mineral mixture was then ultra-sonicated for 5 minutes to ensure the removal of oxidation products from the surface of the mineral as well as to ensure good dispersion of the suspension. The slurry was transferred to the microflotation cell from the top with the use of a funnel. Mineral particles stuck on the glass beaker and funnel were washed into the cell with that particular water quality under study until the cell had slurry up to just above the recycle point. The peristaltic pump was turned on and the pulp was circulated at a speed of 90 rpm for 5 minutes. A microsyringe was used to add a volume (10 μL) equivalent to 50 g/t of 1% SIBX solution and conditioned for 1 minute. Air was introduced at the base of the microflotation cell at 7 mL/min by means of a microsyringe connected to an air supply. Concentrates were collected at 2, 6, 12 and 20 minutes of flotation. The tails were collected and the cell was washed by means of a wash bottle to ensure that all the tails were collected. The four concentrates and tails were filtered, dried in the oven at 80 °C and weighed. The microflotation tests were performed in duplicate to minimise error.

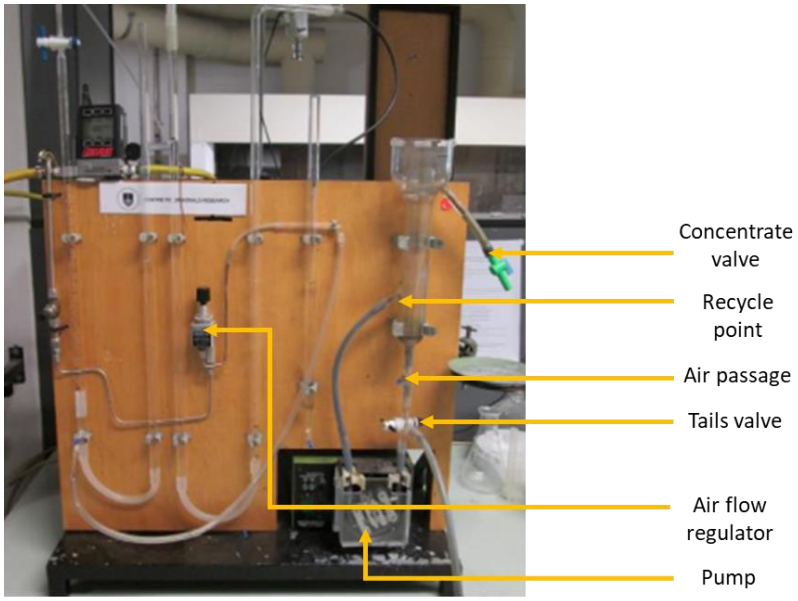

Figure 5-3:Microflotation Cell developed by Bradshaw and O'Connor (1996)

5.2.3 Adsorption Tests

These tests were done to better understand the xanthate adsorption at the mineral surface under degrading water qualities. The aim of this method was to determine the concentration of xanthate left in solution and by mass balance, calculate the concentration that adsorbed on the mineral surface under changing water quality. This procedure thus aids in elucidating the results obtained in both the microflotation and attachment timer tests.

Three grams of pure mineral sample was mixed with 30 mL of the particular water quality under study. A volume equivalent to 50 g/t of 1% SIBX solution (15 μL) was added to the flask containing the suspension.

The maximum amount of xanthate in the slurry was thus 5 mg/L The top of the flask was covered with tin foil and placed in the Ecobath shaker at a controlled temperature of 20 °C and speed of 141 rpm for 15 minutes. After 15 minutes in the water bath, a plastic syringe was used to draw out 15 mL of the suspension. A 0.45 μm filter was then attached at the end of the syringe and the filtrate was collected in a sample container. The filtrate was transferred to a quartz cuvette and inserted in the UV-Vis spectrophotometer shown in Figure 5-4 B. The absorbance of the solution was measured at 301 nm. All the conditions shown in Figure 5-2 were tested in this way and done in triplicate to minimise experimental error. Figure 5-4 shows the equipment used for the adsorption test work.

A B

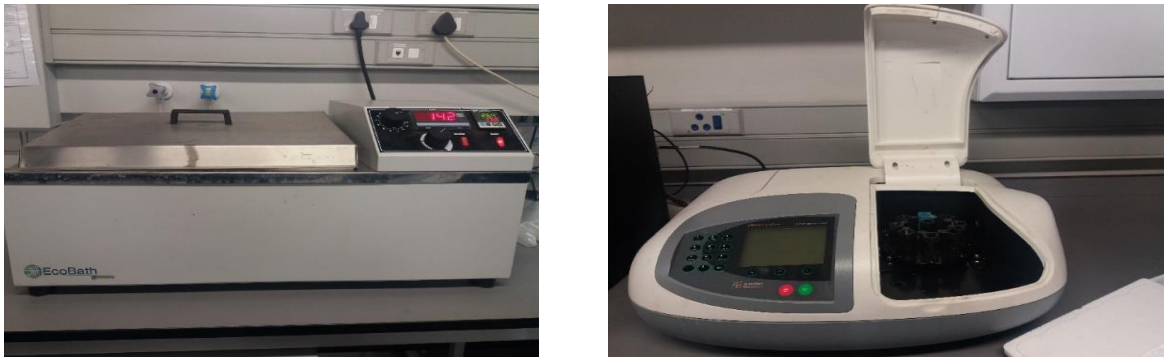

Figure 5-4: Equipment used for adsorption studies (A) Ecobath shaker and (B) Spectrophotometer

To determine the concentration of xanthate left in solution and subsequently the amount adsorbed on the mineral surface, Beer-Lambert's Law was employed. This law, which is used in spectrophotometry, states that the absorbance of a species (A) changes linearly with the concentration of the solution (c) and the coefficient of extinction (ε) when light passes through the path length (l). The relationship between these parameters is expressed in Equation 5-1 (Yates, 2009)

$$A = \varepsilon c l \quad \text{Equation 5-1}$$

Considering that ε and *l* will be constant in a particular solution in a cell or cuvette with a fixed path length (usually 1 cm), these constants can be grouped together and zero can be added without altering the value such that Equation 5-2 is obtained.

$$A = (\varepsilon l)c + 0 \quad \text{Equation 5-2}$$

Thus, if A (absorbance) obtained from the spectrophotometer is plotted against c (concentration of solution) with the intercept set to 0 a straight line is obtained with a gradient of εl. This straight line is known as the calibration curve. In this way, unknown concentrations can be determined from the gradient of the straight line and absorbance measured on the spectrophotometer.

In order to determine the concentration of xanthate left in solution (unknown concentration) and generate a calibration curve, the wavelength at which xanthate has a peak absorbance had to be established. This was done by adding a known concentration of xanthate to the various water solutions tested and measuring the absorbance over a range of wavelengths. Figure 5-5 shows the absorbance of xanthate at 5 concentrations in ultra-purified water over a range of wavelengths from 200 nm to 400 nm.

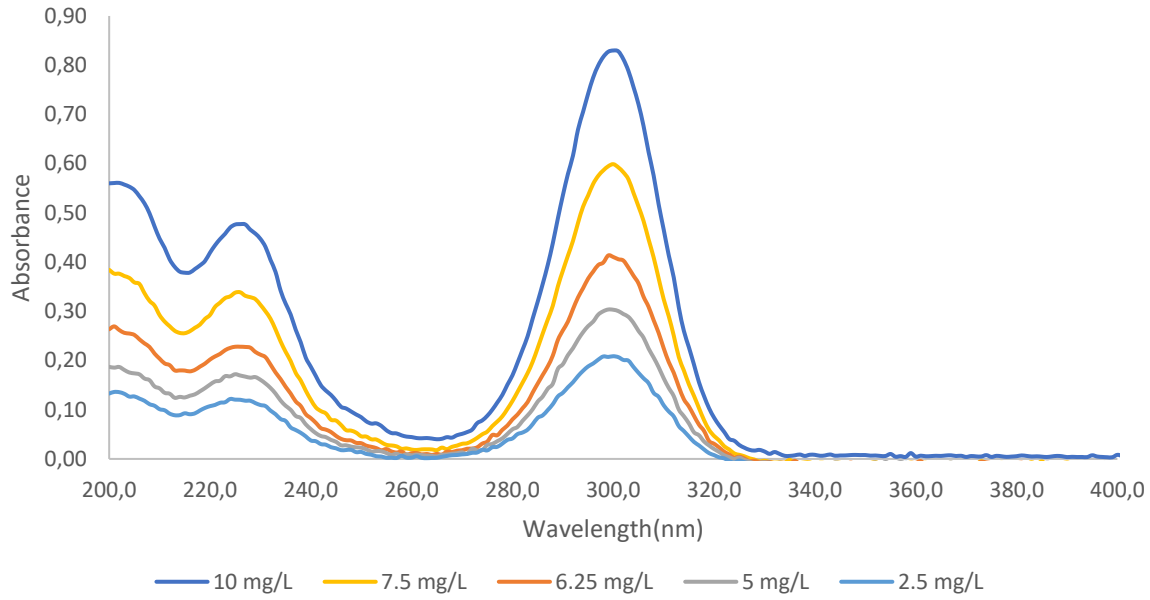

Figure 5-5: Absorbance of SIBX Over a Range of Wavelengths at Different SIBX Concentrations

Similar curves were obtained for all the water solutions under study. Figure 5-5 indicates that the maximum xanthate absorbance occurs at 301 nm. The maximum absorbance of xanthate at 301 nm has been confirmed by other authors (Montalti *et al.,* 1991; Alison and O'Connor, 2011; Dávila-Pulido *et al.,* 2015) Calibration curves for the various water solutions were generated. It is important to note that new calibration curves were determined whenever a fresh 1% xanthate solution was made up. Figure 5-6 shows the calibration curve obtained with 1 SPW.

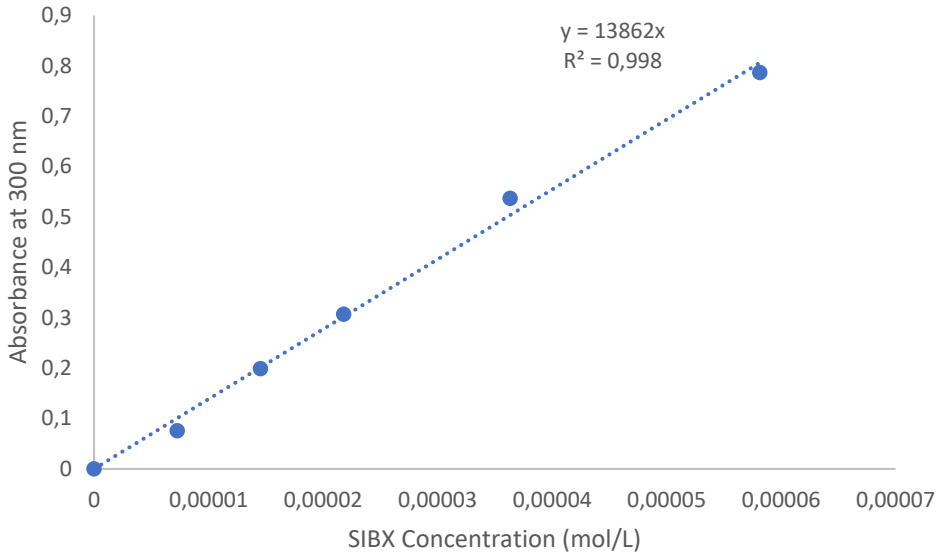

Figure 5-6: Calibration curve for 1 SPW

The concentration of SIBX left in solution with 1 SPW could then be determined by dividing the measured absorbance of the solution with unknown concentration by the gradient of the calibration curve. Calibration curves for 5 and 10 SPW were plotted using a similar procedure. The procedure was then also repeated for the three synthetic plant waters at pH 11 and for the three single salt solutions.

5.2.4 Zeta Potential Determination

Zeta potential determination tests were performed on dilute pure mineral suspensions by means of the Malvern ZetaSizer 4, shown in Figure 5-7. The instrument gives the zeta potential by directly measuring the electrophoretic mobility and calculating the zeta potential from Henry's equation shown in Equation 5-3 (Hunter, 1993).

$$U_E = \frac{2\,\varepsilon\,\zeta\,f(\kappa a)}{3\eta} \quad \text{Equation 5-3}$$

U_E refers to the electrophoretic mobility, ε the dielectric constant, ζ is the zeta potential, η the viscosity and $f(\kappa a)$ is Henry's constant which comprises of the particle radius (a) and Debye-Huckel parameter (κ). Zeta Potential determination through electrophoretic calculations are usually made in aqueous solutions of low electrolyte concentrations; in which case Henry's function is 1.5. Thus, transforming Henry's equation into what is known as the Smoluchowski equation yields Equation 5-4.

$$U_E = \frac{\varepsilon\zeta}{\eta} \quad \text{Equation 5-4}$$

At 25 °C this equation is reduced to Equation 5.5.

$$\zeta = 12.85\,U_E \quad \text{Equation 5-5}$$

A B

Figure 5-7: (A) Malvern ZetaSizer 4 and (B) Malvern Dip Cell

To investigate the effect of increasing the ionic strength of synthetic plant water on the zeta potential of the mineral surface, zeta potential determination tests were done with ultra-purified water (as a baseline) and the three synthetic plant waters of increasing ionic strength as shown in Table 5-3. Furthermore, to establish how specific ions affect the potential of the mineral surface, single salt solutions were used to measure the zeta potential of the three respective sulfide minerals.

0.075 g of pure mineral sample was added to 100 mL of the particular water quality to be tested; the suspension was placed on a magnetic stirrer. Six pH values were tested per water quality, namely, 2, 4, 6, 8, 10 and 12. The pH of the suspension was adjusted with either NaOH or HCl as needed and placed on the magnetic stirrer again for about 10 minutes. The pH was measured for a second time and adjusted again to the exact value as required. The suspension was allowed to settle for 2 minutes. A plastic pipette was used to draw the very fine particles suspended in the liquid from the top (left after settling) and transferred to the Malvern Dip Cell shown in Figure 5-7 B. The zeta potential was measured using the Malvern ZetaSizer. Fresh solutions were made for each pH value and the process was repeated until the zeta potential of all the pH values for that particular water quality were measured. This was then further repeated for the seven water qualities. To validate this method, the zeta potential of chalcopyrite in purified water was measured and compared against the results of Ikumapayi *et al.* (2012) who measured the potential of chalcopyrite in purified water, across a similar pH range. Figure 5-8 shows an acceptable correlation between the two data sets.

It should be noted that all experiments were conducted in an air-conditioned laboratory of a constant temperature of 21°C.

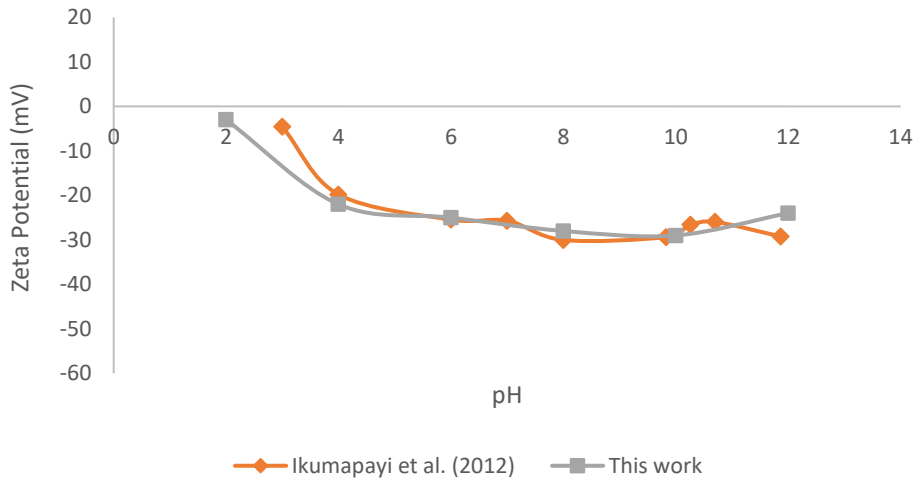

Figure 5-8: Zeta potential of chalcopyrite with purified water: comparison between this work and Ikumapayi et al. (2012)

5.2.5 Speciation of the Water Solutions

Visual MINTEQ version 3.1 was used to calculate the species distribution of the various synthetic plant water qualities. This software is a free/open source chemical equilibrium model for the calculation of metal speciation of various water types based on thermodynamic equilibrium (Wang *et al.,* 2016).

5.3 References

Allison, S.A., and O'Connor, C.T. (2011). An investigation into the flotation behaviour of pyrrhotite. Minerals Engineering, 98 (3-4), 202–207.

Bradshaw, D., O'Connor, C. (1996). Measurement of the sub-process of bubble loading in flotation. Minerals Engineering. 9, 443–448.

Castelyn, D. (2012). The effect of mixing thiol collectors in the flotation of pure sulphide ores. MSc Thesis. University of Cape Town, Faculty of Engineering and the Built Environment, Department of Chemical Engineering, Cape Town, South Africa.

Cohelo, A. (2007) TOPAS-Academic, Coelho Software, Brisbane, Australia.

Davila-Pulido, G.I., Uribe-Salas, A., Alvarez-Silva, M., Lopez-Saucedo, F. (2015). The role of calcium in xanthate adsorption onto sphalerite. Minerals Engineering. 71, 113–119.

Hunter, R.J. (1993). Introduction to modern colloid science, Oxford University.

Ikumapayi, F., Makitalo, M., Johansson, B. and Hanumantha, K. (2012). Recycling of Process Water in Sulfide Flotation : Effect of Calcium and Sulphate Ions on Flotation of Galena. Minerals Engineering 39. Elsevier Ltd: 77–88. https://doi.org/10.1016/j.mineng.2012.07.016.

Lange, A.G., Skinner, W.M. and Smart, R. St. C. (1997) Fine, coarse particle interactions and agglomeration in sphalerite flotation, Minerals Engineering. 10(7), 681-692.

Manono, M.S., Corin, K.C. and Wiese, J.G. (2016). The influence of electrolytes present in process water on the flotation behaviour of Cu-Ni containing ore. Minerals Engineering. 96-97, 99-107.

Montalti, M., Fornasiero, D. and Ralston, J. (1991). UV-Visible Spectroscopic Study of the kinetics of adsorption of ethyl xanthate on pyrite. Journal of Colloid and Interface Science. 143, pp 440 450.

Nyabeze, W. (2015). The effect of copper sulphate on froth stability. MSc Thesis. University of Cape Town, Faculty of Engineering and the Built Environment, Department of Chemical Engineering, Cape Town, South Africa.

Wang, X., Liu, R., Ma, L., Qin, W., and Jiao, F. (2016). Depression mechanism of the zinc sulfate and sodium carbonate combined inhibitor on talc. Colloids and Surfaces A: Physicochemical Engineering Aspects. 501, 92–97.

Wiese, J.G., Harris, P.J., Bradshaw, D.J. (2005). The influence of the reagent suite on the flotation of ores from the Merensky reef. Minerals Engineering. 18 (2), 189–198.

Yates, P. (2012, November 1). Using the Equation of a Straight Line. Retrieved from The Royal Society of Chemistry: https://eic.rsc.org/maths/using-the-equation-of-a-straight-line/2000169.article.

Published in Minerals Engineering 131 230–236. https://doi.org/10.1016/j.mineng.2018.11.017

The effect of water quality on the bubble-particle attachment of sulfide minerals was evaluated with pyrrhotite first. This was the first time the ACTA was used to determine the effect of a process parameter on bubble-particle attachment. Hence it was deemed necessary to fully understand the operational parameters and how the ACTA responds to changes in water quality before including additional minerals.

The publication **"Water Quality Effects on Bubble-Particle Attachment of Pyrrhotite"** published in Minerals Engineering assesses the attachment probability of pyrrhotite under synthetic plant water of increasing water quality, both in the presence and absence of a collector. This study further aims to unravel the bubble-particle attachment results at from an understanding of the impact of water quality on the zeta potential of the mineral and the adsorption of a collector.

This part of the investigation was also deemed to be used as a learning curve in terms of the operational parameters of the machine and understanding what works and does not work for future studies.

Water Quality Effects on Bubble-Particle Attachment of Pyrrhotite

Lisa October[1], Kirsten Corin[1], Nora Schreithofer[2], Malibongwe Manono[1] and Jenny Wiese[1]

[1]Centre for Minerals Research, Department of Chemical Engineering, University of Cape Town

[2] Department of Bioproducts and Biosystems, Clean Technologies Research Group, School of Chemical Engineering, Aalto University, Finland

Abstract

In froth flotation, separation between the valuable and the gangue minerals comes as a result of the attachment of hydrophobic particles to air bubbles. Considering the importance of bubble formation and bubble-particle attachment, it is evident that the pulp phase facilitates the events for the most crucial requirements of successful flotation. Water forms the bulk of the pulp phase; and as a result of water scarcities in countries like South Africa, the need to recycle process water within mining operations is increasing. Hence it is of great importance to understand the effects of water quality on the vital sub-processes within the flotation process, particularly bubble-particle attachment. A novel attachment timer which allows for 396 opportunities for bubble-particle attachment was used for the bubble-particle attachments tests in this work. Three water qualities of increasing ionic strength were tested both in the presence and absence of a xanthate collector to see the effect of increasing ionic strength of synthetic plant water on the bubble-particle attachment probability. The attachment time measurements showed a general decrease in attachment probability as the ionic strength of the synthetic plant water increased both in the absence and presence of a collector. This result indicated that increasing the concentration of the ions present in synthetic plant water lowered the probability of pyrrhotite particles attaching to air bubbles. Further, adsorption studies showed that less xanthate adsorbs on the mineral surface at the highest ionic strength of synthetic plant water under study. This indicates that increases in the ionic strength of synthetic plant water hindered the xanthate adsorption on the pyrrhotite surface. Furthermore, an increase in the zeta potential of pyrrhotite with increasing ionic strength was reported, indicating cation adsorption on the mineral surface. The study presented shows a direct relationship between the zeta potential and attachment probability.

Keywords: Bubble-particle Attachment, Froth Flotation, Pyrrhotite

Graphical Abstract

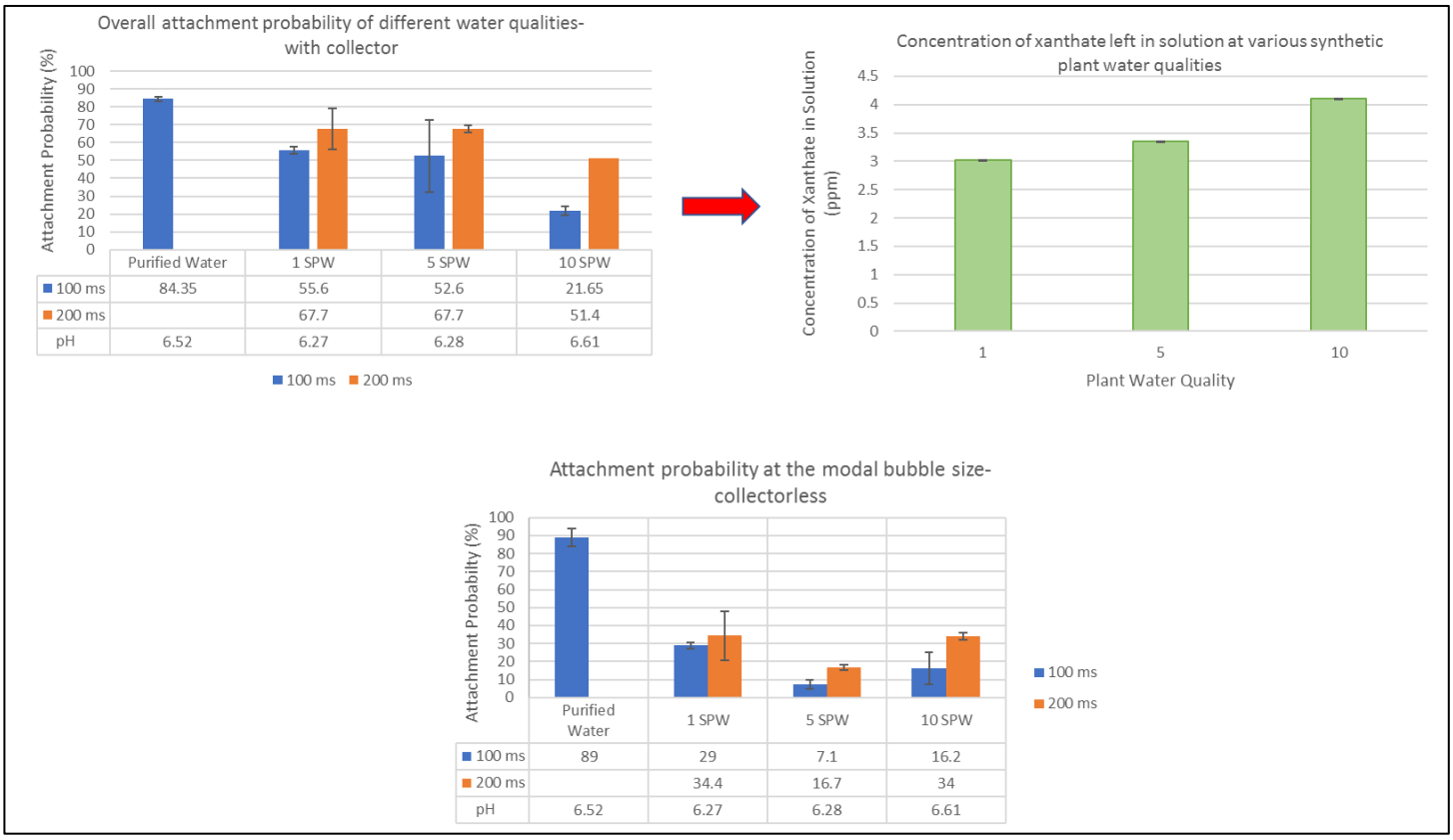

6.1 Introduction

With the current water scarcity in countries like South Africa, the need to recirculate process water within mining operations is becoming greater. The ionic strength of the process water however increases with each recirculation and this may affect the flotation process (Slatter *et al.*, 2009). Considering that the most basic requirement for an effective separation is the attachment of hydrophobic particles to air bubbles, it is essential to understand how changes in water chemistry affect the bubble-particle attachment sub-process.

When a bubble and a particle approach one another and come into close contact, the liquid film between the air-water and solid-water interfaces becomes thinner. The bubble-particle attachment process begins with the thinning of the liquid film at the air-water and solid-water interfaces to critical thickness; followed by the rupturing of the liquid film as it becomes unstable, leading to the establishment of a three-phase contact line and the occurrence of bubble-particle attachment. This process is concluded when the bubble-particle contact line spreads across the surface, forming a stable wetting perimeter with equilibrium contact angles (Albijanic *et al.*, 2010).

The attachment timers, traditionally referred to in literature as "Induction timer" instruments are commonly used to measure and predict the susceptibility of particles to float. The technique consists of a particle bed and a bubble generated at the tip of a single needle. The bubble is then brought in contact with the particle

bed for a set contact time at several locations on the particle bed and this process is repeated for a range of contact times. Commonly 10 different locations are used on the particle bed and the attachment time is defined as the contact time at which the attachment probability is a certain percentage determined prior to the experiment (Albijanic *et al.*, 2012; Glembotsky, 1953; Gu *et al.,* 2003; Yoon and Yordan, 1991).

Within literature the terms *induction time* and *attachment time* are often used synonymously (Gu *et al.,* 2003; Ralston *et al.,* 1999). However, in current terminology, the attachment time is a larger concept encompassing the induction time. To avoid confusion, in this paper the authors have followed the terminology used by Albijanic *et al.,* (2010), where the particle-bubble attachment occurs as a result of three sub-processes: 1.) drainage and thinning of the liquid film to the critical thickness, referred to as the induction time (t_i), 2.) rupture of the film and formation of a three-phase contact nucleus, referred to as rupture time (t_r), 3.) expansion of the three-phase contact line from the critical nucleus radius to a stable wetting perimeter, referred to as three-phase contact time (t_{tpc}). The attachment time is expressed as follows:

$$t_{att} = t_i + t_r + t_{tpc} \quad \text{Equation 6-1}$$

All three of these steps need to take place for the particle to be attached to the bubble and therefore attachment will not occur if the contact time is lower than t_{att} *(Albijanic et al., 2010; Evans, 1954; Verrelli et al.,* 2011).

The effect of water quality on induction time with a bitumen system was studied by Gu *et al.* (2003) and it was shown that the attachment time decreased upon the addition of Ca^{2+} to clear process water compared to without Ca^{2+}. Yoon and Yordan (1991) showed a decrease in attachment time (and hence increase in floatability) with increasing KCl concentration in a quartz-dodecylammonium hydrochloride (DAH collector) system at low DAH dosage. This was attributed to the compression of the electrical double layer in the presence of ions leading to the acceleration of the rupturing of the liquid film between the bubble and particle; ultimately decreasing the bubble-particle attachment time. An opposite trend in floatability was observed by these authors with an increase in collector dosage under constant water conditions; this was said to be resulting from the collector ions associating with one another and their subsequent adsorption on the mineral surface in bimolecular layers. Thus, from previous studies conducted in this area, it is clear that there is little knowledge regarding the effect of plant water of increasing ionic strength on the bubble-particle attachment process in sulfide minerals.

Platinum bearing ores from the Merensky reef consist of approximately 1% sulfides and about 45% of the sulfide is pyrrhotite (Liddel *et al.,* 1986); making pyrrhotite the main sulfide mineral in the Merensky reef. Pyrrhotite however readily oxidizes to ferric hydroxide under conventional flotation conditions, pH 9 and open to the atmosphere (Miller *et al.,* 2005). Both the natural and induced hydrophobicity of pyrrhotite have been widely studied and factors such as oxidation potential, pH and activation have been shown to have significant effects on pyrrhotite flotation (Hodgson and Agar, 1984; Miller *et al.,* 2005; Montalti, 1994; Peters, 1977). The effect of ionic strength on pyrrhotite flotation is however unclear.

Thus, the aim of this study was to assess the bubble-particle attachment probability of pyrrhotite under synthetic plant water of increasing ionic strength both in the presence and absence of a collector. It should be noted that the ions could also affect the bubble surface. A study by Takahashi (2005) showed that with increasing concentration of NaCl the zeta potential of the bubble decreased while the zeta potential decreased even more so with increasing concentration of $MgCl_2$. This work is however focussed on the effect of ions in solution on the particle surface.

The experiments were done by the means of the Automated Contact Time Apparatus described by Jávor *et al.* (2016); Aspiala *et al.* (2018) elsewhere and a brief description of its operation will be given in the next section.

6.2 Materials and Experimental Procedures

The pyrrhotite used in this investigation was obtained from Ward's Science. 1 kg of pyrrhotite sample was hammered manually to 100% passing 1000 microns. The crushed sample was then pulverized and subsequently sieved through 75 and 38 microns sieves. The fraction of particles greater than 75 microns was then re-pulverized such that the size fraction of the entire sample was less than 75 microns. This sample was purged with nitrogen and refrigerated. Upon arrival at Aalto University the pyrrhotite particles of -75+38 microns were split into 10 samples using a rotary splitter. The samples were purged with argon and stored in bottles in a refrigerator.

Both purified water and synthetic plant waters were used for the attachment timer measurements. Synthetic plant water (1 SPW) as described by Wiese et al. (2005) was used as the water quality with low ionic strength and to simulate a recirculation of this synthetic plant water, the content of dissolved solids was increased 5 and 10 times, and are referred to as 5 SPW and 10 SPW respectively. Table 6-1 gives an account of the concentrations of the various ions in the synthetic plant waters tested. This is without any collector in the system, noting that both the TDS and ionic strength would be practically the same in both cases with and without collector. The properties of the purified water used are shown in Table 6-2.

Table 6-1: Concentrations of ions for the various water qualities

Plant Water Type	Ca^{2+} (mg/L)	Mg^{2+} (mg/L)	Na^{+} (mg/L)	Cl^{-} (mg/L)	SO_4^{2-} (mg/L)	NO_3^{-} (mg/L)	CO_3^{2-} (mg/L)	Total Dissolved Solids (mg/L)	Ionic Strength (mol/L)
1 SPW	80	70	153	287	240	176	17	1023	0.0241
5 SPW	400	350	765	1435	1200	880	85	5115	0.1205
10 SPW	800	700	1530	2870	2400	1760	170	10230	0.241

Table 6-2: Properties of purified water

Ultra-Pure Water	Resistivity at 25 °C (MΩ·cm)	Conductivity (µs/cm)	Total Organic Carbon (µg/L)	Na^{+}(µg/L)	Cl^{-} (µg/L)
	18.2	<0.055	<5	<1	<1

The salts used for preparation of the synthetic plant waters were of analytical grade, while the SIBX was 97% purity.

6.2.2 Attachment Time Measurements

6.2.2.1 Experimental setup

The Automated Contact Time Apparatus used in this investigation was described by Jávor *et al.* (2016) and Aspiala *et al.* (2018) elsewhere, therefore only a brief description of its operation will be given below. The main advantage of the instrument is, that it allows the collection of a large amount of data for statistical analysis within a relatively short time period. Previously authors have chosen to measure 10 particle-bubble contacts per condition with commonly used attachment timers (Albijanic *et al.,* 2011; Gu *et al.,* 2003; Yoon and Yordan, 1991), while the Automated Contact Time Apparatus allows for 396 contacts within the particle bed hence providing 396 opportunities for bubble-particle attachment. Furthermore, the particles that successfully attach to the bubbles are collected in a collection bin and can be analysed further in terms of shape, composition, size and mass recovered.

The Automated Contact Time Apparatus housed at Aalto University shown on Figure 6-1.

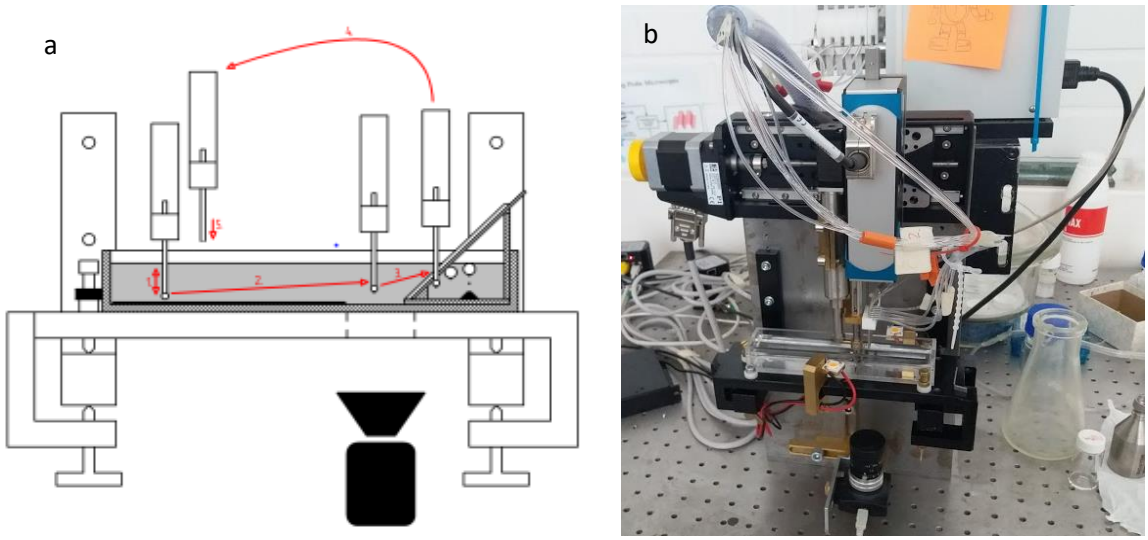

Figure 6-1: (a) Schematic of the attachment timer (Aspiala et al. 2018), (b) photograph of the Automated Contact Time Apparatus.

The instrument consists of six needles with each needle generating a bubble with set diameter; once the bubbles are generated they are brought into contact with the particle bed for a set contact time. The needles are then automatically lifted and moved to the area where an image of the bubble-particle aggregates is taken; LED lights located at both sides of the pool light up as the picture is taken in order to obtain clear images suitable for analysis. After the image is taken the needles with the bubble-particle aggregates are automatically transferred to the particle collection bin, where additional air is pumped through the needles to release the bubble-particle aggregates. After this deposition the needles then automatically move to the next 1 mm of the particle bed. This process is repeated such that the complete length of the particle bed is given an opportunity for bubble-particle attachment; resulting in a total of 66 cycles with 396 bubble-particle contacts per experiment.

Prior to the start of the 66 measurement cycles certain parameters are set on the experimental controller programme. These parameters included the contact time, approach distance, approach velocity, detachment velocity, retreat distance, bubble size, compression and pumping time. Although the volume of air used to generate the bubbles is set on the experimental controller programme, the reported bubble size in this device is largely dependent on the chemical environment within the cell such as the ionic strength of the water investigated. Consequently, parameters such as the compression with the particle bed, approach and retreat distance which are dependent on bubble size may also differ slightly from what was set. However, the actual measured values of these parameters for each cycle are given upon the completion of the 66 cycles.

The digital camera situated below the cell takes two images of the bubble-particle aggregate at the tip of the needle for each cycle. The first image with white light illumination is used to determine the bubble

size, Figure 6-3. An optical fibre is located inside each of the six needles attached to a green LED which lights the bubbles from the inside, Figure 6-2. This creates a good contrast that facilitates the automatic detection of attached particles to the bubbles. All the images of the 66 cycles are saved.

All measurements were done in duplicate in a random order to minimise experimental error.

6.2.2.2 Sample and particle bed preparation

A slurry was made with 9 g pyrrhotite and 100 ml of the particular water type under investigation. Experiments were performed both in the presence and absence of a collector. When a collector was utilised, the slurry was conditioned for 2 minutes with 100 g/t (standard industry dosage) sodium isobutyl xanthate collector (SIBX), thereafter it was allowed to settle for approximately 3 minutes. The liquid at the top was removed with a pipette and filtered with a glass funnel and filter paper such that a clear water was obtained and only a thin layer of liquid above the settled particles was left in the flask. The clear liquid was transferred to the cell of the attachment timer and the settled particles were used to make the particle bed.

Once the liquid pool was ¾ full, a heap of particles was introduced. An automated shovel attached to the linear actuator was then used to obtain a flat particle bed of a pre-set bed height. More particles were added to fill the length of the pool; and between each addition of particles the shovel controller was employed until a flat particle bed of 2 mm was obtained. The bed height is arbitrary, but the approach distance and bubble size were chosen based on the bed height, such that sufficient compression of the bubbles with the particle bed was achieved. The particle collection bin was then inserted into the cell.

6.2.3 Adsorption Studies

A slurry of 9 g pyrrhotite and 100 ml of the particular synthetic plant water was made. 90 µL of 1% SIBX solution was added to the slurry which is equivalent to the addition 100 g of xanthate per tonne of pyrrhotite; resulting in a slurry with 10 ppm xanthate. The slurry was then placed in a temperature-controlled water bath (25 °C) for 20 minutes; stirred at 450 rpm. A 0.45 micron filter was attached to a syringe to draw 3 ml of solution. The absorbance of the clear solution was measured with UV-VIS spectrophotometer at 301 nm. A calibration curve was constructed using the absorbance of xanthate at known concentrations; therefore, the concentration of xanthate in the clear solution could be calculated. All measurements were done in triplicate to minimise experimental error.

6.2.4 Zeta Potential Measurements

Very dilute mixtures of the particular water type and pyrrhotite particles were made up; the dilute mixtures were then equally divided in six containers and the pH was adjusted to 2, 4, 6, 8, 10 and 12 with dilute HCl or dilute NaOH. After 15 minutes on the magnetic stirrer the pH was measured again and adjusted where needed. 1 mL of the suspension was then transferred to the Malvern Dip Cell and inserted in the Malvern ZetaSizer where measurements were taken. All zeta potential measurements were performed in triplicate to reduce experimental error.

6.3. Results and Discussion

The images generated were studied to establish the bubble-particle attachment probability for the different water qualities tested. Figure 6-2 shows an example of an image before attachment and after a measurement cycle.

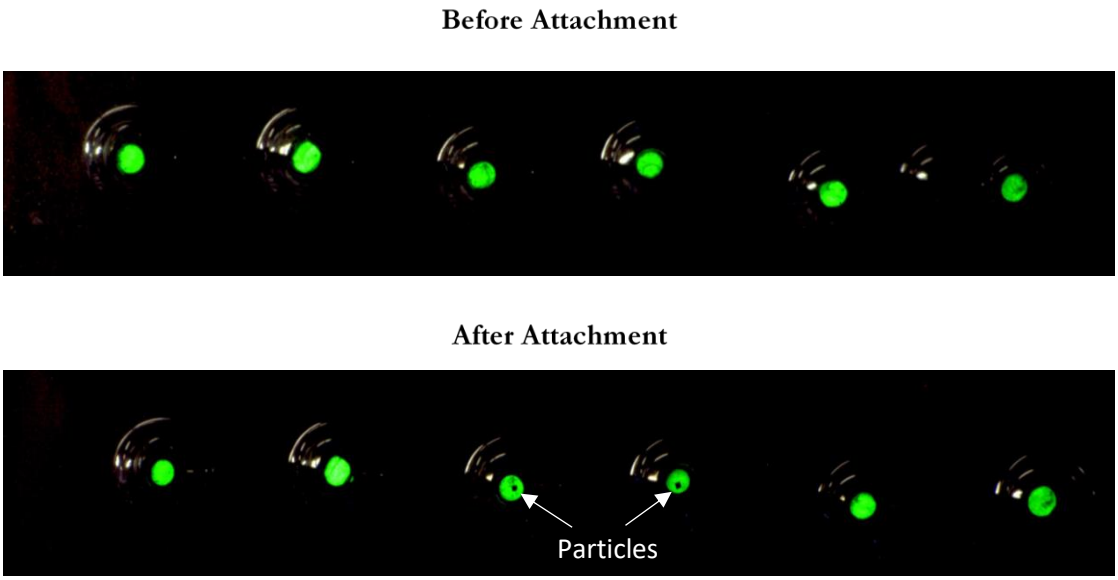

Figure 6-2: Image of the array generated for bubble-particle attachment detection

Figure 6-2 shows that there was attachment of particles occurring at two of the six bubbles (indicated by the black dots at the surface of the bubbles generated by needles three and four, from left to right). Therefore, for this cycle the probability of attachment was 2/6 (i.e. 33.33%) The 66 images obtained per condition investigated were studied in this way to quantify the probability of bubble-particle attachment under water of increasing ionic strength.

Figure 6-3: Image used to determine bubble size

Figure 6-3 shows the first image taken, which is used to determine the bubble size. The bubble size is determined by applying a pre-calibrated circle finding programme; details in Aspiala *et al.* (2018) Figure 6-4 shows the identification lines added by the programme used to determine the bubble size.

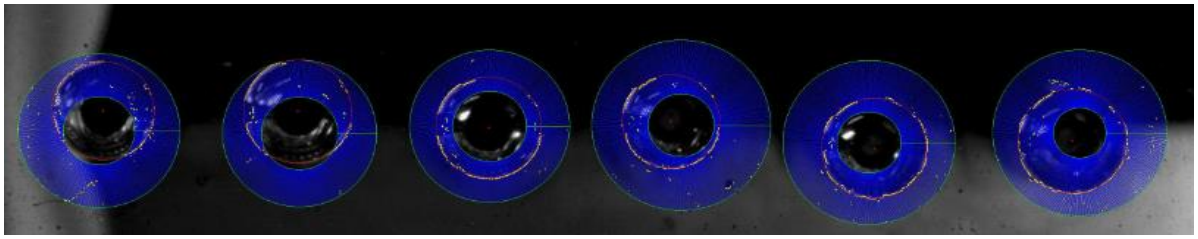

Figure 6-4: Identification lines added by programme to determine bubble size

6.3.1 The Effect of Water Quality on Attachment Probability in the Presence of a Collector

The actual bubble sizes generated by each needle for the 66 cycles was returned by the experimental programme. Figure 6-5 depicts the bubble size distribution averaged across the two contact times (100 ms and 200 ms) for every water quality tested. This could be done as the contact time chosen is not expected to change the size of the bubble generated by the Automated Contact Time Apparatus used in this work.

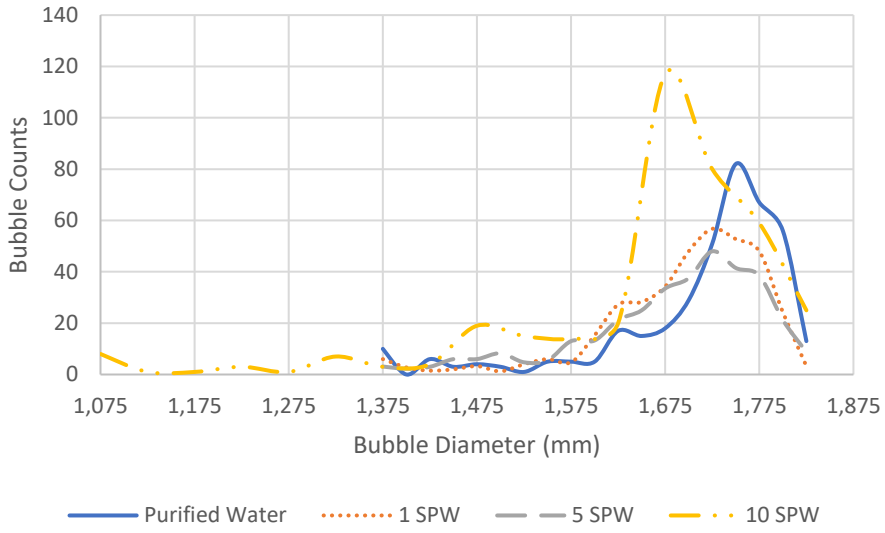

Figure 6-5: Bubble size distribution for the various water qualities with SIBX collector

The bubble size distribution in Figure 6-5 shows that the largest modal bubble size was generated with purified water (1.75 mm), while the smallest modal bubble size was generated with 10 SPW (1.65 mm).

The overall attachment probability is presented in Figure 6-6 and is essentially the percentage attachment achieved over the 396 bubble-particle contacts.

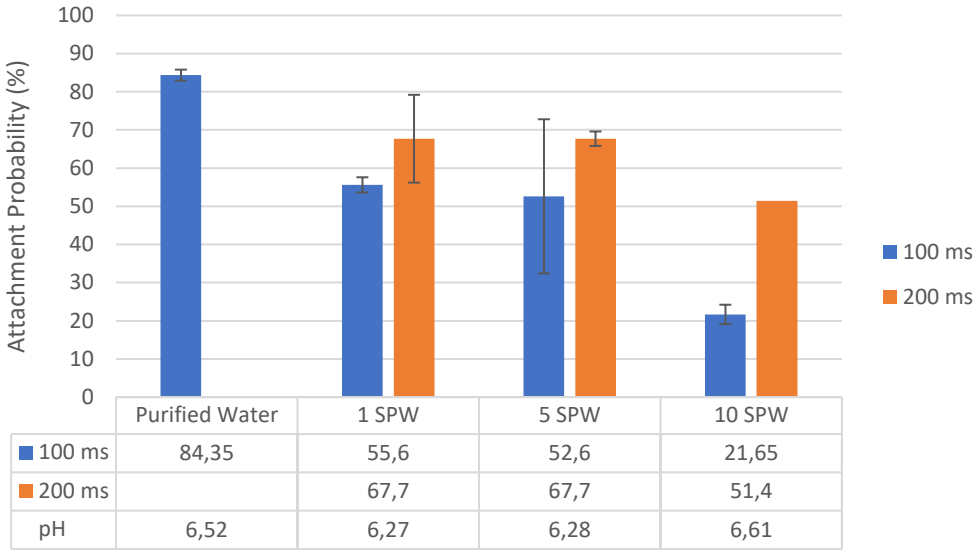

	Purified Water	1 SPW	5 SPW	10 SPW
100 ms	84,35	55,6	52,6	21,65
200 ms		67,7	67,7	51,4
pH	6,52	6,27	6,28	6,61

Figure 6-6: Overall attachment probability of different water qualities with collector (SIBX)

Figure 6-6 shows the attachment probability using purified water and the three synthetic plant waters of increasing ionic strength at contact times 100 ms and 200 ms. The attachment probability was greater at a contact time of 200 ms across all the water qualities investigated, this result was expected as the longer the bubble is in contact with the particle bed the greater the opportunity for particles to attach to the bubbles. The results shown in Figure 6-6 show that the overall average attachment probability decreases with deteriorating water quality. The attachment probability of purified water at 200 ms was not tested, it was clear that the highest attachment probability is achieved with a higher contact time as the bubble is in contact with the particle bed for longer. The ultra-purified water was thus merely used as a baseline to see the effect with no ions in solution.

It was expected that with an increase in ionic strength of plant water the floatability of the mineral would increase as explained by the electrical double layer theory (Laskowski and Iskra, 1970; Yoon and Yordan, 1991). Hodgson and Agar (1989) indicated that Ca^{2+} increased the amount of xanthate necessary to create a hydrophobic pyrrhotite surface; suggesting that the presence of Ca^{2+} induces hydrophilicity. Moreover, Ikumapayi *et al.* (2012) described the decrease in galena recovery with increasing Ca^{2+} to be as a result of Ca^{2+} inhibiting the adsorption of xanthate on the mineral surface. Additionally, Kirjavainen *et al.* (2002) found that calcium and thiosulfate ions had a negative effect on the floatability of sulfides in the absence of iron ions that are leached into solution during milling. It was thus speculated that the reduction in attachment probability as the ionic strength of water was increased as observed in Figure 6 was as a result of the increasing concentration of ions such as Ca^{2+}, which inhibited the adsorption of xanthate on the mineral surface. This could further be supported by the fact that the attachment probability was highest in purified water.

6.3.2 Adsorption of Xanthate

Figure 6-7 shows the concentration of xanthate left in solution and adsorbed on the mineral surface at the different synthetic plant water qualities. An increase in xanthate concentration in solution is observed with an increase in ionic strength of the synthetic plant water. This indicates that less xanthate adsorbs on the mineral surface as the ionic strength increases. However, considering that xanthate concentration in the pyrrhotite slurry was 10 ppm, the amount of xanthate that adsorbed is not significantly different across the three synthetic plant waters. Previous studies have shown that the addition of ionic collector to an electrolyte solution results in a further increase in the ionic strength which will lower the concentration of collector required to form hydrophilic micelles at the mineral surface (Laskowski, 2013; Evans and Wennerström, 1994). Studies have also shown that insoluble complexes form between the collector and ions, reducing the amount of xanthate available for adsorption on the mineral surface (Fuerstenau and Somasundaran, 2003). 10.8% more xanthate is adsorbed with 1 SPW compared to with 10 SPW which does indicate the deterring of xanthate adsorption on pyrrhotite at synthetic plant water of high ionic strength.

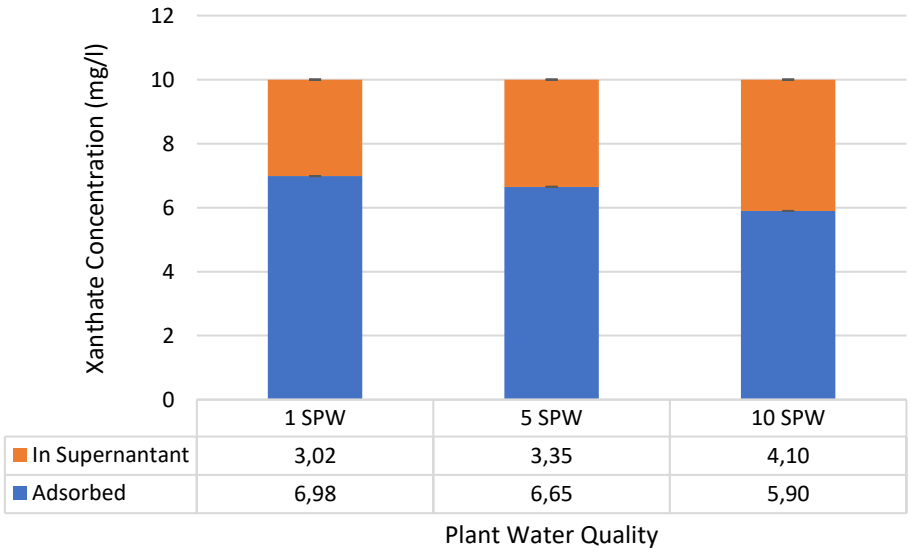

Figure 6-7: Concentration of xanthate adsorbed on mineral and left in solution at various synthetic plant water qualities

6.3.3 The Effect of Water Quality on Attachment Probability in the Absence of a Collector

Figure 6-8 gives an account of the bubble size distribution averaged across the two contact times (100 ms and 200 ms) for every water quality tested with no collector in the system.

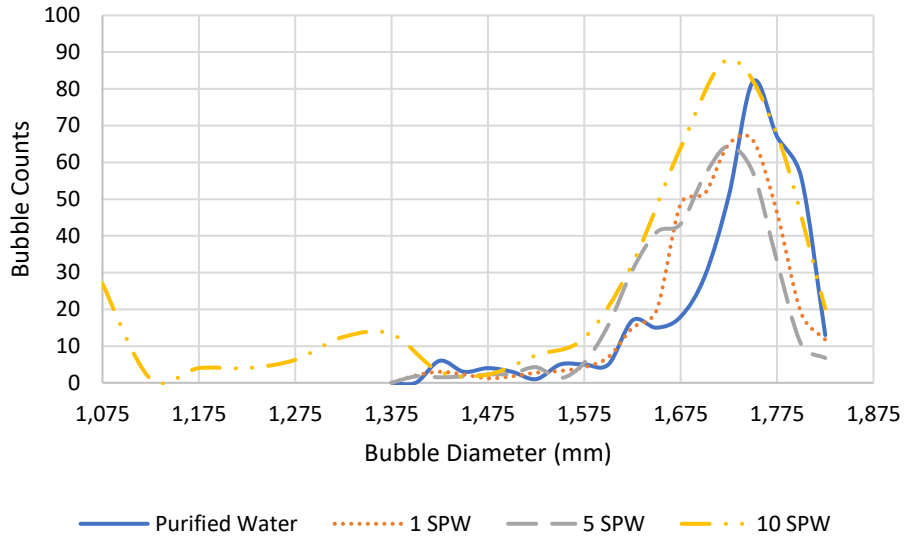

Figure 6-8: Bubble size distribution for the various water qualities with no collector

Similarly, as in Figure 6-5 the modal bubble size tends to decrease as the ionic strength of plant water increased. Furthermore, multimodal profiles were observed for 10 SPW either indicating an insufficient number of measurements taken or that different competing mechanisms were simultaneously at play.

Figure 6-9 summarises the attachment probability at the modal bubble size for each of the water qualities investigated.

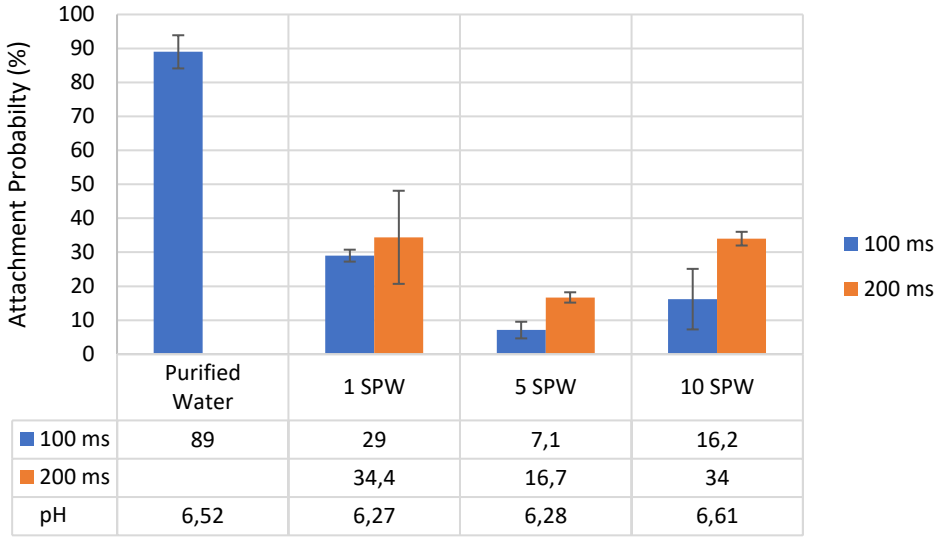

	Purified Water	1 SPW	5 SPW	10 SPW
100 ms	89	29	7,1	16,2
200 ms		34,4	16,7	34
pH	6,52	6,27	6,28	6,61

Figure 6-9: Attachment probability at the modal bubble size in the absence of a collector

The natural pH of this system was measured to be between 6.27 and 6.61 and it is evident that attachment does indeed occur in this pH range. This result was contrary to the findings of Miller *et al.* (2005) where contact angle measurements showed that the hydrophilic state of pyrrhotite stabilized (contact angle of zero) at pH values above 4.5 in the absence of collector. However, it has been reported that elemental sulfur is a product of pyrrhotite oxidation (Steger and Desjardins, 1978; Steger, 1982; Belzile *et al.,* 2004) which is

hydrophobic and can remain stable for long periods (Miller *et al.,* 2005). The sulfur at the pyrrhotite surface could thus be the reason for the observed floatability of pyrrhotite in this pH range.

According to the electrical double layer theory as previously stated, an increase in ionic strength of the solution should increase the floatability of the mineral but Figure 6-9 shows a general decrease in the probability of attachment of pyrrhotite particles to air bubbles with an increase in the concentration of dissolved solids. The surface of pyrrhotite is known to oxidize rapidly when exposed to air and results in the surface of the mineral being covered with ferric hydroxide (Miller *et al.,* 2005); rendering the mineral hydrophilic. This phenomenon will undoubtedly hinder any activation reaction from occurring on the surface of the mineral and could possibly obstruct the expected effect of the electrical double layer.

The flotation of pyrrhotite is recognised to be very complicated and is influenced mainly by oxidation potential and pH. The plant water with an intermediate level of ionic strength tends to show a lower probability for the attachment of pyrrhotite particles to the bubbles. This result could potentially be explained by a combined effect of pH, oxidation potential and electrolytes in the system yielding a minima in attachment probability.

Upon comparison between Figures 6-6 and 6-9 it is clear that the attachment probability is higher in the presence of a collector as opposed to without a collector for all the synthetic plant water tested. This result was expected as the primary role of a collector is to induce hydrophobicity on the valuable mineral particles. The result of SIBX collector enhancing the hydrophobicity of pyrrhotite was thus strengthened even in this static bubble-particle attachment system.

6.3.4 Zeta Potential Measurements

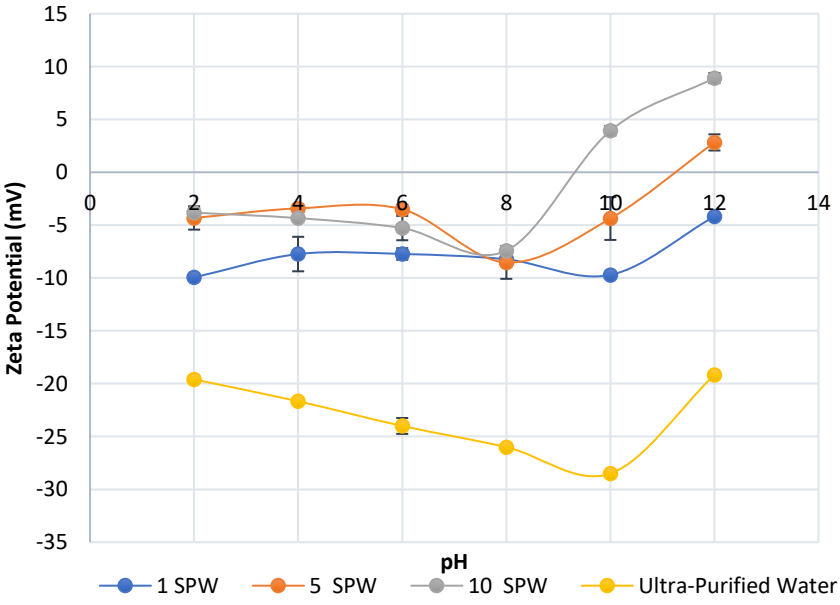

Figure 6-10: Zeta Potential of Pyrrhotite in the Various Water Qualities

Figure 6-10 gives an account of the zeta potential of pyrrhotite in the 4 water qualities tested over a pH range of 2 to 12. It is evident that the pyrrhotite particles in purified water resulted in the most negative zeta potential, while generally the zeta potential of pyrrhotite tends to increase with increasing ionic strength; indicating possible adsorption of the specific metal cations on the mineral surface (Moignard *et al.,* 1977). The effect of the indifferent ions is evident in Figure 6-10 in terms of modifying the magnitude of the zeta potential by compression of the electrical double layer. The compression of the electrical double is evident as the magnitude of the zeta potential of pyrrhotite decreases (becomes more positive) with increasing ionic strength. The results obtained in Figure 6-10 also demonstrates that at higher ionic concentrations, the ions cover the mineral surface to a greater extent and hence increase its potential. It is expected that as the zeta potential of the mineral surface is increased the repulsion between the particles and air bubbles will be reduced; which should result in an increased bubble-particle attachment.

The results obtained from this study however shows that pyrrhotite particles with a more negative zeta potential result in a higher attachment probability. This could be due to the zeta potential of the bubble also changing in the presence of the various ionic solutions. A study by Yang *et al.* (2001) showed that the zeta potential is dependent not only on the solution pH, but also on the concentration of electrolytes and type of metal ions present in the system. NaCl was found to decrease the zeta potential towards more negative values, while multivalent metal ions Ca^{2+} and Al^{3+} had a greater impact on the magnitude of the zeta potential and can even reverse the charge polarity. Similar findings were reported by Takahashi (2005) with regard to NaCl, showing that the zeta potential increased even more so with increasing concentration of $MgCl_2$. Furthermore, the passivation of the mineral surface by the ions could possibly have a depressing effect, resulting in the low attachment probability achieved by the pyrrhotite particles in solutions of high ionic strength. Zeta potential values close to 0 mV tend to indicate strong agglomeration and precipitation in the suspension (Salopek *et al.,* 1992) and hence could explain the lower attachment observed with plant water of high ionic strength.

As previously stated the tests were carried out at pH values of 6.27 to 6.61 (the natural pH of the system); the zeta potential measurements at this pH range show that the zeta potential of the pyrrhotite in 5 SPW is slightly higher than it is at 10 SPW. This result could possibly explain the low attachment probability achieved with 5 SPW as seen in Figure 6-7.

6.4. Conclusions

The results presented in this study generally show a decrease in the attachment probability of pyrrhotite to air bubbles as the ionic strength of synthetic plant water is increased both in the presence and absence of a collector. Further, the attachment probability across all water qualities was higher in the presence of SIBX compared to without the collector. Previous studies have shown that Ca^{2+} increases the amount of xanthate required to create a hydrophobic pyrrhotite surface and adsorption studies in this work indicated that more xanthate is left in solution at the highest ionic strength tested. This indicates that less xanthate adsorbs on the pyrrhotite surface with synthetic plant water of higher ionic strength.

Furthermore, it is well known that pyrrhotite readily oxidises when exposed to the atmosphere, resulting in ferric hydroxide formation on the mineral surface. In the absence of a collector this trend may possibly be due to the joint effects of oxidation, pH and ionic strength; individually these factors are known to affect the natural flotation of pyrrhotite. Zeta potential measurements have shown a general increase in zeta potential of pyrrhotite as the ionic strength of the water is increased. This indicates an increase in the adsorption of cations on the mineral surface at high ionic strengths; and this may cause the lower attachment probability as the ionic strength of plant water increases.

6.5 Acknowledgements

Funding for this research was provided by the National Research Foundation of South Africa (NRF) [Grant number 103641] and Academy of Finland Mineral Resources and Material Substitution MISU program - Protocol development for evaluation of water-saving alternatives in minerals processing - "Bridging North to South" project. Any opinion, finding and conclusion or recommendation expressed in this material is that of the authors and the NRF does not accept any liability in this regard. Further the financial and technical contributions from the South African Minerals to Metals Research Institute (SAMMRI) is also acknowledged.

6.6 References

Albijanic, B., Bradshaw, D.J., Nguyen, A. V. (2012). The relationships between the bubble–particle attachment time, collector dosage and the mineralogy of a copper sulfide ore. Minerals Engineering. 36, 309–313. doi:10.1016/j.mineng.2012.06.007.

Albijanic, B., Ozdemir, O., Nguyen, A. V., Bradshaw, D. (2010). A review of induction and attachment times of wetting thin films between air bubbles and particles and its relevance in the separation of particles by flotation. Advances in Colloid and Interface Science. 159, 1–21. doi:10.1016/j.cis.2010.04.003.

Aspiala, M., Schreithofer, N., Serna-Guerrero, R. (2018). Automated contact time apparatus and measurement procedure for bubble-particle interaction analysis. Minerals Engineering. 121, 77–82. doi:10.1016/j.mineng.2018.02.018.

Belzile, N., Chen, Y., Cai, M., Li, Y. (2004). A review on pyrrhotite oxidation. Journal of Geochemical Exploration. 84: 65-76.

Evans, L.F. (1954). Bubble-mineral attachment in flotation. Industrial and Engineering Chemistry Research. 46, 2420–2424.

Evans, D.F., Wennerström, H. (1994). Structure and Properties of Micelles, The Colloidal Domain - where Physics, Chemistry, Biology, and Technology Meet. VCH Publishers, New York.

Fuerstenau, M.C., Somasundaran, P. (2003). Flotation. In: Fuerstenau, M.C., Han, K. (Eds.), Principles of Mineral Processing. Society for Mining, Metallurgy, and Exploration (SME), Littleton, Colorado, pp. 245–306.

Glembotsky, V.A., 1953. The time of attachment of bubbles to solid particles in flotation and its measurement. Lzv. Akad. Nauk SSSR, 11, 1524–1531.

Gu, G., Xu, Z., Nandakumar, K., Masliyah, J., 2003. Effects of physical environment on induction time of air–bitumen attachment. International Journal of Mineral Processing. 69, 235–250. doi:10.1016/S0301-7516(02)00128-X

Hodgson, M., Agar, G.E., 1989. Eilectrochemical Investigations into the Flotation Chemistry of Pentlandite and Pyrrhotite: Process Water and Xanthate Interactions. Canadian Metallurgy Quarterly. 28, 189–198. doi:10.1179/cmq.1989.28.3.189.

Ikumapayi, F., Makitalo, M., Johansson, B., Rao, K.H., 2012. Recycling of process water in sulfide flotation: Effect of calcium and sulphate ions on flotation of galena. Minerals Engineering. 39, 77–88. doi:10.1016/j.mineng.2012.07.016.

Jávor, Z., Schreithofer, N., Heiskanen, K., Serna, R., 2016. Technical Note on the Development of a New Attachment Timer for Predicting the Change in Ore Floatability, in: Proceedings of the XXVIII International Mineral Processing Congress (IMPC 2016), September 11-15, 2016. Canadian Institute of Mining, Metallurgy and Petroleum, Québec City.

Kirjavainen, V., Schreithofer, N., Heiskanen, K., 2002. Effect of some process variables on flotability of sulfide nickel ores. International Journal of Mineral Processing. 65, 59–72.

Miller, J.D., 2005. A review of pyrrhotite flotation chemistry in the processing of PGM ores. Minerals Engineering. 18 18, 855–865. doi:10.1016/j.mineng.2005.02.011.

Montalti, M., 1994. Interaction of Ethyl Xanthate with Pyrite and Pyrrhotite Minerals. University of South Australia.

Laskowski, J. and Iskra, J. (1970). Role of capillary effects in bubble-particle collision in flotation. Transactions of the Institution of Mining and Metallurgy. 79, C6.

Laskowski, J.S., 2013. From amine molecules adsorption to amine precipitate transport by bubbles: a potash ore flotation mechanism. Minerals Engineering. 45, 170–179.

Liddell, K. S., McRae, L. B., and Dunne, R. C. (1986). Process routes for beneficiation of noble metals from Merensky and UG-2 ores. Mintek Review No.4, Randburg.

Peters, E. (1977). In: Rand, D.A.J., Welsh, B.J. (Eds.), Trends in Electrochemistry. Plenum Press, NY, 267.

Ralston, J., Fornasiero, D., Hayes, R., 1999. Bubble–particle attachment and detachment in flotation. International Journal of Mineral Processing. 56, 133–164. doi:10.1016/S0301-7516(98)00046-5.

Salopek, B., Krasic, D., Filipovic, S. 1992. "Measurement and Application of Zeta-Potential." Rudarsko-Geolosko-Naftni Zbornik 4: 147–51.

Slatter, K.A., Plint, N.D., Cole, M., Dilsook, V., De Vaux, D., Palm, N., Oostendorp, B., 2009. Water Management in Anglo Platinum Process Operations : Effects of Water Quality on Process Operations, in: Abstracts of the International Mine Water Conference, Pretoria, South Africa, 19th – 23rd October 2009 Proceedings ISBN Number: 978-0-9802623-5-3. pp. 46–55.

Steger, H.F., Desjardins, L.E., (1978). Oxidation of sulfide minerals: 4. Pyrite, chalcopyrite and pyrrhotite. Chemical Geology. 23, 225 – 237.

Steger, H.F. (1982). Oxidation of sulfide minerals: VII. Effect of temperature and relative humidity on the oxidation of pyrrhotite. Chemical Geology. 35, 281 – 295.

Takahashi, M., 2005. ζ Potential of Microbubbles in Aqueous Solutions: Electrical Properties of the Gas−Water Interface.Journal of Physical Chemistry B 109, 21858–21864. doi:10.1021/jp0445270.

Verrelli, D.I., Koh, P.T.L., Nguyen, A. V., 2011. Particle–bubble interaction and attachment in flotation. Chemical Engineering Science. 66, 5910–5921. doi:10.1016/j.ces.2011.08.016.

Wiese, J., Harris, P., Bradshaw, D., 2005. The influence of the reagent suite on the flotation of ores from the Merensky reef. Minerals Engineering. 18, 189–198. doi:10.1016/j.mineng.2004.09.013.

Yang, C., Dabros, T., Li, D., Czarnecki, J., Masliyah, J.H., 2001. Measurement of the zeta potential of gas bubbles in aqueous solutions by microelectrophoresis method. Journal of Colloid and Interface Science. 243, 128–135. doi:10.1006/jcis.2001.7842.

Yoon, R.-H., Yordan, J.L., 1991. Induction time measurements for the quartz-amine flotation system. Journal of Colloid and Interface Science. 141, 374–383. doi:10.1016/0021-9797(91)90333-4.

Chapter 7 **The Influence of Specific Ions and Oxyhydroxyl Species in Plant Water on the Bubble-particle Attachment of Pyrrhotite**

Parts of this work were presented at WISA 2018. Cape Town, South Africa

Chapter 6 studied the effect of water quality on the bubble-particle attachment of pyrrhotite and was also used to understand the operational parameters and how the ACTA responds to changes in water quality. Chapter 7 uses the same operational parameters and methodology for the ACTA as Chapter 6, however it focusses on the effect of specific ions on bubble-particle attachment of pyrrhotite. The study aims to determine if there are specific ions that either hinder or aid bubble-particle interactions from both a fundamental and microflotation perspective.

Chapter 6 also showed that the potential of pyrrhotite tends to increase with increasing ionic strength; indicating possible adsorption of the specific metal cations on the mineral. The zeta potential results showed that across all water types a distinct increase in potential occurred between pH 10 and 12; this may be indicative of the formation of species in the water at alkaline conditions.

Furthermore, a study into ion-reagent-mineral interactions in flotation by Manono *et al.* (2019) showed that synthetic plant waters of increasing ionic strength at pH greater than 10 had increased concentrations of oxyhydroxyl species. The presence of these oxyhydroxyl species in plant water may affect bubble-particle attachment; thus, it may be of interest to assess the impact that these oxyhydroxyl species would have on the bubble-particle attachment of pyrrhotite.

Due to the fact that this part of the study incorporates microflotation tests, it can be used to see if the current operational parameters used for the ACTA do provide results that resemble the trend of the microflotation tests under the same conditions. Hence this chapter is the first of its kind to explore the use of the ACTA as a technique that is comparable to the more classical microflotation technique for measuring bubble-particle interactions.

Once the bubble-particle interactions have been studied under various single salt solutions both fundamentally and through microflotation tests the next steps were to do deeper analyses so as to understand why the various single salts result in different bubble-particle interactions. This was investigated from both a zeta potential and ion speciation perspective.

The Influence of Specific Ions and Oxyhydroxo Species in Plant Water on the Bubble-particle Attachment of Pyrrhotite

L.L. October[1], K.C. Corin[1], M.S. Manono[1], N. Schreithofer[2] and J.G. Wiese[1]

[1]Centre for Minerals Research, Department of Chemical Engineering, University of Cape Town, Private Bag X3, Rondebosch 7701, South Africa

[2] Department of Bioproducts and Biosystems, Clean Technologies Research Group, Aalto University, Vuorimiehentie 1, 02150 Espoo, Finland

Abstract

Previous studies have considered the effect of using recycled process water in froth flotation and whether certain ions are responsible for what is observed in the final concentrate in terms of mineral grades and recoveries. The attachment of mineral particles to air bubbles is a fundamental sub-process of flotation without which separation of valuable minerals from non-valuables cannot occur, it is therefore of interest to assess the effect of specific ionic species on bubble-particle attachment. The effects of oxyhydroxo species on bubble–particle interactions were studied with three synthetic plant waters of increasing ionic strength at pH 11. The presence of these oxyhydroxo species such as magnesium and calcium hydroxides in alkaline pulps were confirmed by many authors and proven to affect bubble and particle zeta potential. Further, to ascertain whether there were certain ions within the plant water that impacted the bubble-particle attachment, tests were carried out with single salt solutions. The synthetic plant waters at pH 11 resulted in very poor pyrrhotite attachment probabilities and recoveries regardless of the water type as compared to the recovery with these waters at the pH 6.5. It can thus be concluded that these $CaOH^+$, $(MgOH)_2$ and $MgOH^+$ species that has been reported by authors in single salt studies hinder the flotation of the pyrrhotite particles as well as processes such as collector adsorption and the action of the electrical double layer. The presence of Na^+ resulted in superior performance compared to Ca^{2+} in terms of the attachment probability and recovery of pyrrhotite particles. Furthermore, upon studying the anion effect, SO_4^{2-} performed better than NO_3^- when paired with Ca^{2+}; thus, indicating a negative effect on flotation response when Ca^{2+} and NO_3^- ions are used together. The implications of this work are thus of great significance for the effective management of ions in recycled process water in the froth flotation process.

Keywords: Air – Water Interface, Bubble-Particle Attachment, Electrolytes, Floatability, Ionic Strength, Oxyhydroxo Species, Solid – Water Interface

Graphical Abstract

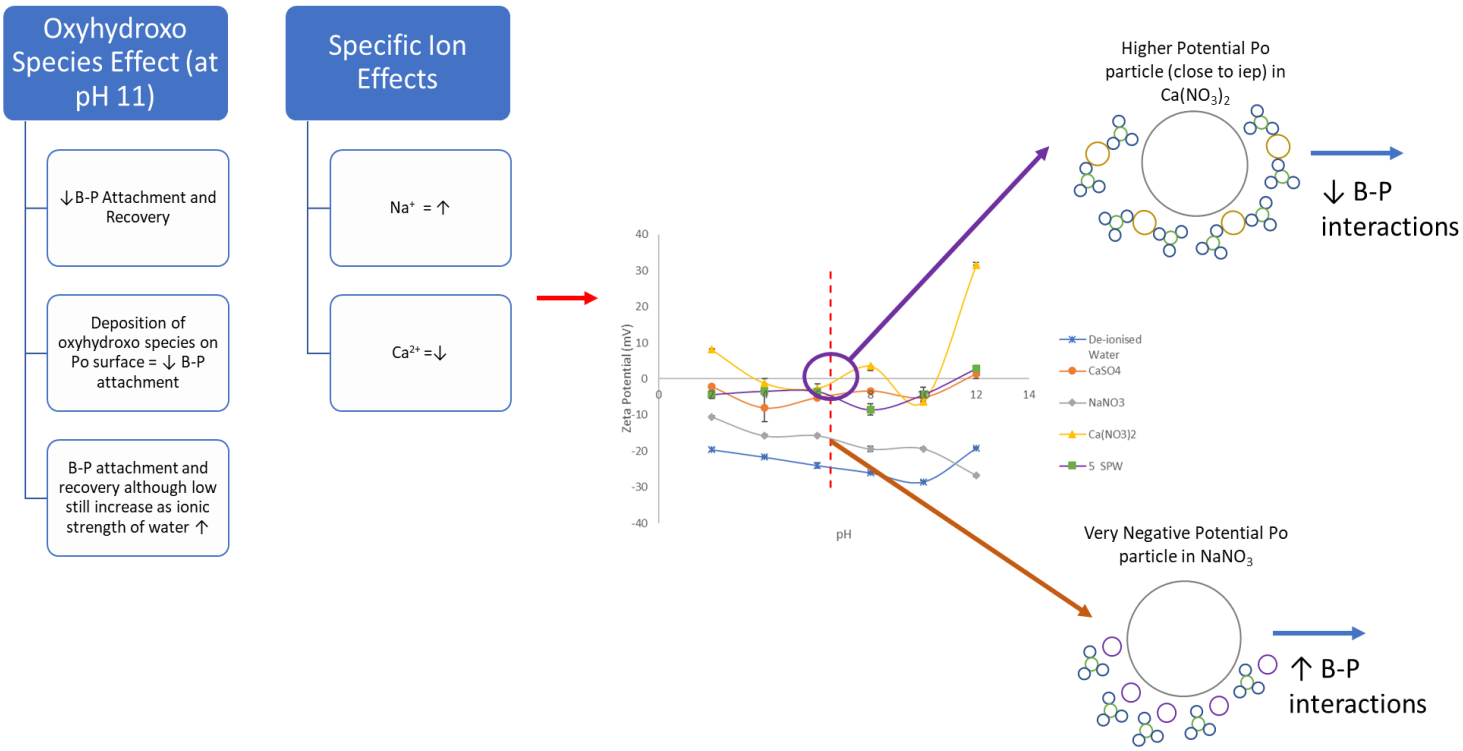

7.1 Introduction

In froth flotation the selective separation between hydrophilic and hydrophobic particles is determined by the bubble-particle attachment sub-process; which in turn is facilitated by interactions at the air – water and solid – water interfaces. This fundamental bubble-particle sub-process thus ultimately plays an important part in the recovery of valuable particles.

The bubble-particle attachment sub-process has been described in three steps by Albijanic *et al.* (2010); the first step consists of the bubble approaching the particle, a film forming at the solid-water and air-water interfaces. This film thins to critical thickness as the bubble and particle approach each other more closely. In the second step, when the bubble and particle are even closer in contact the film then becomes unstable and ruptures resulting in the formation of a three-phase contact line and bubble-particle attachment occurs. The third step consists of the bubble-particle contact line spreading across the surface, forming a stable wetting perimeter with equilibrium contact angles (Albijanic *et al.,* 2010).

Although the flotation process is central in mineral processing operations for the recovery of valuable mineral particles; it can be quite water intensive as the pulp in flotation cells consists of 80-85% water by volume (Muzenda, 2009). Current fresh water scarcities have however resulted in stringent environmental restrictions; resulting in many flotation plants seeking alternatives such as recycled and saline water. These water types do however contain high concentrations of electrolytes; and the difference in water chemistry between fresh water and recycled water may negatively affect the separation efficiency of the overall flotation process; for example, the collector adsorption sub-process may be affected due to the surface-

active nature of inorganic electrolytes on negatively charged surfaces (Yoon and Basilio, 1993). The interactions between the water molecules and the mineral surface, and the water molecules and the electrical double layer at the mineral – water interface are thus important to consider, particularly in the presence of inorganic electrolytes (Fuerstenau, 1982).

In electrolyte solutions containing bubbles and particles, both the double layers interact resulting in long-range double layer repulsions. For successful bubble-particle attachment the repulsion must be overcome with attractive forces and kinetic energy; the double layer repulsions thus behave as an energy barrier.

It has been proposed that upon the addition of electrolytes, the electrical double layer compresses, reducing the energy barrier for bubble-particle attachment to occur (Laskowski *at al.* 1991; Paulson and Pugh, 1996; Harvey *et al.,* 2002; Laskowski, 2012). The compression of the electrical double layer has been said to accelerate the rupturing of the film at the air-water and solid-water interface which in turn aids bubble-particle attachment (Laskowski and Iskra, 1970; Li and Somasundaran, 1993; Harvey *et al.,* 2002; Laskowski and Castro, 2015).

In the presence of inorganic electrolytes, the water structure may still be very strongly hydrogen bonded, in this case the ions are "structure making" because they retain the strong hydrogen bonds. These ions are small ions such as Na^+, Li^+, Mg^{2+}, F^- and Cl^- and are of high zeta potential density; therefore, structure makers are strongly hydrated and increase the viscosity of the solution. Contrary to structure making ions, ions that tend to destroy the strongly hydrogen bonded structure of water are known as "structure breakers". These are large ions such as Cs^+ and I^- and are weakly hydrated; these ions also tend to decrease the viscosity of the solution (Wang and Peng, 2014; Burdukova, 2007; Ma and Pawlik, 2005).

Manono *et al.* (2016) studied the effect of various single salts on copper and nickel recoveries. Results from this study showed no significant anion effect in terms of copper and nickel recoveries but did observe slightly higher recoveries with Na^+ from a cation perspective. This study by Manono *et al.* (2016) kept the ionic strength of the various single salt solutions constant at 0.0213 M. This ionic strength could possibly be too low to see the effect of specific ions on mineral recoveries; as the ionic strength of plant water used on a concentrator was shown to be closer to 0.0723 M and 0.1205 M (Manenzhe, 2018).

A previous study by October *et al.* (2019) studied the effect of increasing ionic strength of synthetic plant water on the bubble-particle attachment of pyrrhotite. This study showed decreased xanthate adsorption on the pyrrhotite surface as the ionic strength of the plant water increased and this resulted in decreases in attachment probability as the water quality deteriorated. It may be that it is a specific ion that is responsible for this result and if this is the case, the removal of this ion will be a more cost effective and environmentally friendly exercise compared to treating the water or bringing in fresh water. October *et al.* (2019) further showed that the potential of pyrrhotite tends to increase with increasing ionic strength; indicating possible adsorption of the specific metal cations on the mineral. The zeta potential results by the same study showed that across all water types a distinct increase in potential occurred between pH 10 and 12. Studies by Rao

and Finch (1989) and Zanin *et al.* (2019) showed that hydrophilic $CaOH^+$ species as with other polyvalent metal cations adsorb onto the surfaces of sulfide minerals resulting in a reversal in the zeta potential of the sulfide mineral surface. Furthermore, Li *et al.* (2017) confirmed via XPS studies the adsorption of $(MgOH)_2$ on the chalcopyrite surface in $MgCl_2$ solution at pH 10. These authors also showed how the pH at which $(MgOH)_2$ precipitation occurred becomes lower that pH 10 as the concentration of $MgCl_2$ is increased, in line with the work of Li and Somasundaran (1992). Ramos *et al.* (2013) reported that the charge of the bubble should be assessed when cationic hydroxyl complexes are formed in flotation pulps due to high pH of the pulp. Li and Somasundaran (1992) also reported that magnesium hydroxyl and other hydroxide complexes were approaching the liquid-air interface which resulted in a positive charge on the bubble surface. It is thus evident that magnesium hydroxyl and other hydroxide complexes coat the mineral surface at alkaline pulp conditions resulting in both a more positive bubble and particle. This effect on the charge of the bubble and particle is expected to affect the bubble-particle attachment efficiency. A more recent study by October *et al.* (2019) showed increases in the zeta potential of pyrrhotite between pH 10 and pH 12, such increases were therefore attributed to the formation of oxyhydroxo species in the synthetic plant water at alkaline conditions.

Furthermore, a study into ion-reagent-mineral interactions in flotation by Manono *et al.* (2019) showed that synthetic plant waters of increasing ionic strength at pH greater than 10 had increased concentrations of oxyhydroxo species. The presence of these oxyhydroxo species in plant water may affect bubble-particle attachment; thus it is of interest to assess the impact that these oxyhydroxo species would have on the bubble-particle attachment of pyrrhotite. Further to this it is therefore of interest to determine if there are specific ions in plant water that are either beneficial, detrimental or have no effect on the bubble-particle attachment sub-process and subsequently the overall flotation process. Pyrrhotite particles are of specific interest in this investigation as both the flotation and depression of this specific sulfide mineral is a key operational driver in many flotation plants around the world depending on the ore being processed.

7.2 Materials and Methods

7.2.1 Mineral Sample

1 kg of pyrrhotite obtained from Ward's Science was crushed to 100% passing 1000 μm with a hammer; the crushed particles were pulverized and screened to 38 – 75 μm and -25 μm fractions. A rotary splitter was used to split the sample in smaller representative samples; each of these samples were purged with nitrogen and refrigerated below -30 °C. The particle size fraction 38 – 75 μm was used for the attachment time and microflotation tests while the -25 fraction was used for the zeta potential measurements.

7.2.2 Water Quality

Synthetic plant water (SPW), of ionic strength 0.0241 M, as described by Wiese *et al.* (2005) was used in this study, further to simulate the recirculation of synthetic plant water, the amount of dissolved solids was increased by five and ten times. These plant water solutions are referred to as 5 SPW (0.1205 M) and 10 SPW (0.241 M) respectively. Also, $NaNO_3$, $Ca(NO_3)_2$ and $CaSO_4$ single salt solutions with ionic strength

of 0.1205 M were prepared along with synthetic plant water (Wiese *et al.,* 2005) of the same ionic strength. Table 7-1 shows the ionic concentration of these prepared synthetic plant waters and single salt solutions. Where necessary, the pH of the synthetic plant water solutions was adjusted with NaOH and HCl. The investigation studying the effect of an increase in pH of the synthetic plant water was conducted in the presence of sodium isobutyl xanthate (SIBX) as a collector as the study by October *et al.* (2019) showed that the adsorption of the collector on pyrrhotite was affected by the water quality and subsequently affected bubble-particle interactions. In this way the tests assessing bubble-particle interactions at the natural pH (pH 6.5) in the aforementioned study are directly compared to the work in this investigation at the adjusted pH (pH 11).

In considering specific ion effects on the bubble-particle attachment of pyrrhotite, tests on single salt solutions were carried out in the absence of a collector. Single salt studies assessing bubble-particle interactions by Yoon and Yordan (1991) showed that collector dosage may actually impact attachment time and over-power the effect of the ionic concentration. Therefore, as a starting point the single salt work in this study is in the absence of a collector.

The salts used for preparation of the synthetic plant waters were of analytical grade, while the SIBX was 97.0% purity. All salts were supplied by Merck while the powdered form of SIBX was supplied by Senmin.

Table 7-1: Concentrations of ions for the various synthetic plant water and single salt solutions

Plant Water Type	Ca^{2+} (mg/L)	Mg^{2+} (mg/L)	Na^{+} (mg/L)	Cl^{-} (mg/L)	SO_4^{2-} (mg/L)	NO_3^{-} (mg/L)	CO_3^{2-} (mg/L)	TDS (mg/L)	Ionic Strength (IS) (mol/L)
1 SPW	80	70	153	287	240	176	17	1023	0.0241
5 SPW	400	350	765	1435	1200	880	85	5115	0.1205
10 SPW	800	700	1530	2870	2400	1760	170	10230	0.241
$Ca(NO_3)_2$	1610	-	-	-	-	4981	-	6591	0.1205
$CaSO_4$	1207	-	-	-	2894	-	-	4101	0.1205
$NaNO_3$	-	-	2770	-	-	7472	-	10242	0.1205

7.2.3 Attachment Time Tests

This investigation used the automated contact time apparatus (ACTA) to measure bubble-particle interactions from a fundamental perspective. This instrument was developed at Aalto University and has been described in publications by Jávor *et al.* (2016), Aspiala *et al.* (2018) and October *et al.* (2019).

The particle bed was made by firstly mixing 9 g of pyrrhotite with 100 mL of the particular water quality under study. When a collector was utilised, the slurry was conditioned for 1 minute with 100 g/t (standard industry dosage) SIBX; the slurry was allowed to settle, and the clear liquid was pipetted out and filtered

until about 2 cm of liquid remained above the settled particles. The filtrate was placed in the glass pool after which the settled particles were pipetted into the pool for building the particle bed. Furthermore, to attain a flat particle bed of 2 mm, an automated shovel was employed. Measurements were taken for each of the water qualities in Table 7-1 and were performed in duplicate for each condition. The slurry was adjusted to pH 11 in the investigation assessing the effect of an increase in pH; this was done by means of NaOH. The tests on single salts were conducted at the natural pH which was around 6.5. The temperature was recorded to be an average of 20 °C.

7.2.4 Microflotation Tests

The microflotation cell developed by Bradshaw and O'Connor (1996) was used to perform the microflotation tests in this investigation. 3 g of pyrrhotite was mixed with 50 mL of the water quality under study. The mixture was then ultra-sonicated for 5 minutes to remove oxidation products from the mineral surface and prevent particle agglomeration. The pyrrhotite-salt solution slurry was then dispersed into the microflotation. A constant air flow of 7 mL/min was introduced to the microflotation cell and the peristaltic pump circulating the pulp was set to 90 rpm. For the tests with collector (SPW solutions) a volume (20 µL) equivalent to 100 g/t of 1% SIBX solution was added to the cell and conditioned for 1 minute. Four concentrates were collected, after 2, 6, 12 and 20 minutes. The concentrates and tails were filtered and dried. The microflotation tests were performed in duplicate for each synthetic plant water and single salt solution. Similar to the tests with the ACTA the slurry was adjusted to pH 11 with NaOH when pH 11 was considered. The single salts tests were conducted at the natural pH (6.5) and the temperature was recorded to be an average of 20 °C.

7.2.5 Zeta Potential Measurements

In a beaker, 60 mL of the single salt solution was mixed with 0.075 g of pyrrhotite particles. This dilute mixture was divided in six containers of equal volume. The pH of each container was adjusted using weak HCl and NaOH solutions to pH values of 2, 4, 6, 8, 10 and 12. Each container was labelled with the pH of its solution. Each solution was stirred for 15 minutes on a magnetic stirrer, after which the pH was measured again and if necessary re-adjusted. 1 mL of the suspension was inserted in the Malvern Dip Cell and placed in the Malvern ZetaSizer ZEN 3600 where measurements were taken. All measurements were performed in triplicate to reduce experimental error. It is important to note that zeta potential measurements of pyrrhotite in synthetic plant waters of increasing ionic strength over the pH range 2 to 12 were previously published in October *et al.* (2019). The temperature at which these measurements were conducted was recorded to be an average of 20 °C.

7.2.6 Speciation of Single Salt Solutions

The concentration of the dominant species present in the single salt solutions over the pH range 2 to 12 were calculated using Visual MINTEQ version 3.1. This tool uses thermodynamic equilibrium data to calculate the ion speciation in water (Wang *et al.,* 2016). These calculations were considered at a fixed temperature of 20 °C.

7.3 Results and Discussion

7.3.1 Oxyhydroxo Species in Synthetic Plant Water on the Bubble-Particle Attachment of Pyrrhotite

Bubble-particle interactions were studied both from a fundamental and microflotation perspective to assess the effect of presence of oxyhydroxo species in synthetic plant water. Studies by Manono *et al.* (2019) observed the existence of these species in synthetic plant water with pH greater than 10.

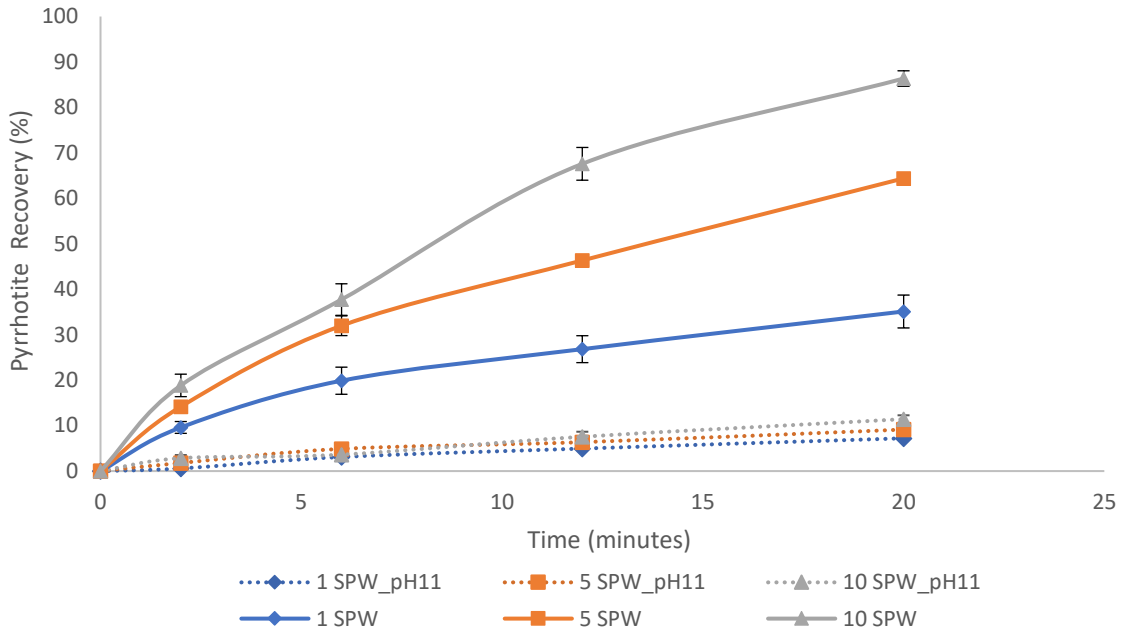

Figure 7-1: Microflotation of pyrrhotite under varying water quality at the natural pH and pH 11

Figure 7-1 shows microflotation results of synthetic plant water at pH 6.5 and pH 11. Figure 7-1 clearly shows that much more pyrrhotite is recovered at the natural pH and that recoveries at pH 11 are extremely low across all three water qualities. The recovery of pyrrhotite is shown to increase significantly as the ionic strength of the plant water increases at the natural pH. While the recovery of pyrrhotite at pH 11 does not show a discernable difference across the varying water qualities; it should however be noted that the recovery at pH 11 with 1 SPW is slightly less than that with 10 SPW. It is evident from Figure 7-1 that despite the presence of a xanthate collector, which should render the sulfide mineral sufficient hydrophobicity, the increase in pH from natural pH to pH 11 hinders the recovery of the mineral. Speciation diagrams of the synthetic plant waters published by Manono *et al.* (2019) showed that at pH 11 there existed oxyhydroxo species which were not present at pH 6.5. The decrease in pyrrhotite recovery at pH 11 is attributed to the presence of these oxyhydroxo species as these are known to have a depressive effect on pyrrhotite (Allison and O'Connor, 2011). The effect of these oxyhydroxo species is further reinforced by the zeta potential of pyrrhotite. October *et al.* (2019) showed that for a fixed ionic strength of synthetic plant water, the zeta potential of pyrrhotite increases distinctly at around pH 11 to a more positive potential. Therefore, the trend in potential of pyrrhotite at more alkaline pH values is attributed to

the formation and deposition of these oxyhydroxo species on the pyrrhotite surface, not only preventing its flotation but also in turn preventing processes such as collector adsorption and the compression of the electrical double layer from taking place.

Under the same conditions as the microflotation tests, the Automated Contact Time Apparatus (ACTA) was used to study the effect of the presence of oxyhydroxo species in synthetic plant water on bubble-particle attachment from a fundamental level. Figure 7-2 presents the attachment probability of pyrrhotite at increasing ionic strength at the natural pH (as per October *et al.* (2019)) as well as the attachment probability with these synthetic plant water types at pH 11.

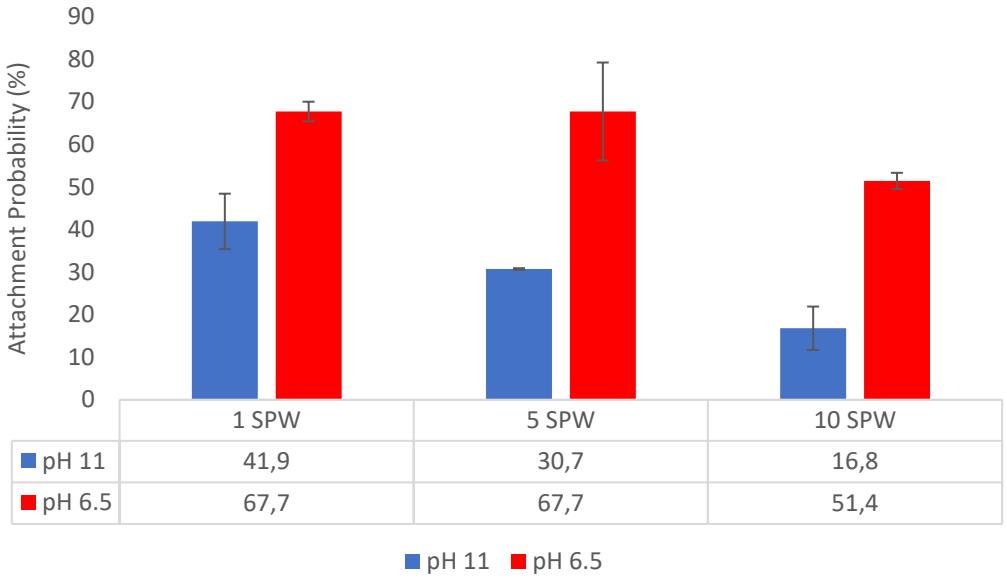

Figure 7-2: Attachment probability of pyrrhotite under varying water quality at the natural pH (adapted from October et al. (2019)) and pH 11

The attachment probability at the natural pH as reported by October *et al.* (2019) showed a decrease in attachment probability with an increase in the ionic strength of the plant water. It needs to be noted that this trend, is directly opposite of what is seen in the microflotation recoveries of pyrrhotite. This behaviour may be due to the varying operating conditions in the two machines (ACTA and Microflotation Cell). Although this is the case, it is evident that even from a fundamental level, substantially less particles attach to air bubbles at pH 11 as seen with the drop in the attachment probability at pH 11 compared to the natural pH results. Thus, a possible deposition of the oxyhydroxo species on the pyrrhotite surface may have induced the hydrophilicty of pyrrhotite particles.

Studies have shown that the adsorption of cations on the minerals surface not only changes the zeta potential of the minerals but also results in the formation of hydrophilic agglomerates (Dishon *et al.,* 2009; Manono *et al.,* 2019). The zeta potential measurements under the condition of Figure 7-1 and Figure 7-2 as shown in October *et al.* (2019) show that between pH 9 and 12 either the iso-electric point is reached or the potential of the pyrrhotite is close to 0 mV. It has been shown that at 0 mV the particles tend to

agglomerate (Salopek *et al.,* 1992; Wang and Peng, 2014); given that oxyhydroxo species exist at this pH range (Manono *et al.,* 2019), the agglomeration of pyrrhotite particles with oxyhydroxo species at its surface may result in substantial pyrrhotite depression as seen in Figure 7-1 and Figure 7-2.

7.3.2 Specific Ions on the Bubble-Particle Attachment of Pyrrhotite

In order to further understand the effects of specific ionic species within plant water, it was deemed necessary to determine if there are single ions in plant water that are either beneficial, detrimental or have no effect on the bubble-particle attachment sub-process.

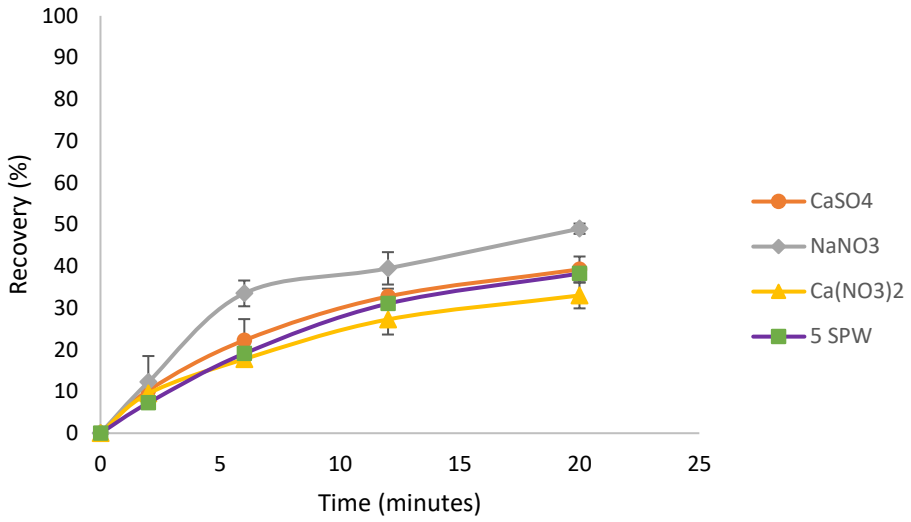

Figure 7-3: Microflotation recovery of pyrrhotite in the various solutions at the natural pH

The microflotation test results in single salt solutions are presented in Figure 7-3. Figure 7-3 shows that the $NaNO_3$ solution resulted in the highest recovery of pyrrhotite at 49.0%, followed by the $CaSO_4$ solution at 39.0% recovery; while the lowest recovery was obtained with the $Ca(NO_3)_2$ solution with 33.0% of pyrrhotite recovered. The final recovery of pyrrhotite using synthetic plant water at the same ionic strength of these single salt solutions was found to be 36.5%.

The microflotation results show that the calcium salts resulted in lower recoveries of pyrrhotite compared to that of the sodium. Studies have shown that in single salt solutions at higher ionic strengths, the hydration layer stability decreases (Blake and Kitchener, 1972; Wang and Peng, 2014; Li *et al.,* 2017). Hirajima *et al.* (2016) noted longer induction times and subsequent decreases in recovery to be due to increases in the stability of the hydration layer. Therefore, it can be inferred that in the Na^+ solution, the hydration layer stability decreases; making the time for the bubble and particle to attach shorter. In contrast other studies by Craig *et al.* (1993) and Paulson and Pugh (1996) propose that floatability is increased with electrolytes of higher valency. Although this is not the case with the Ca^{2+} cation; the SO_4^{2-} anion does outperform its NO_3^- counterpart when paired with the Ca^{2+} cation in the microflotation tests.

The attachment timer results presented in Figure 7-3 give an account of the effect of $CaSO_4$, $NaNO_3$, $Ca(NO_3)_2$ and synthetic plant water (5SPW) on the bubble-particle attachment probability of pyrrhotite particles to air bubbles from a fundamental bubble-particle attachment perspective.

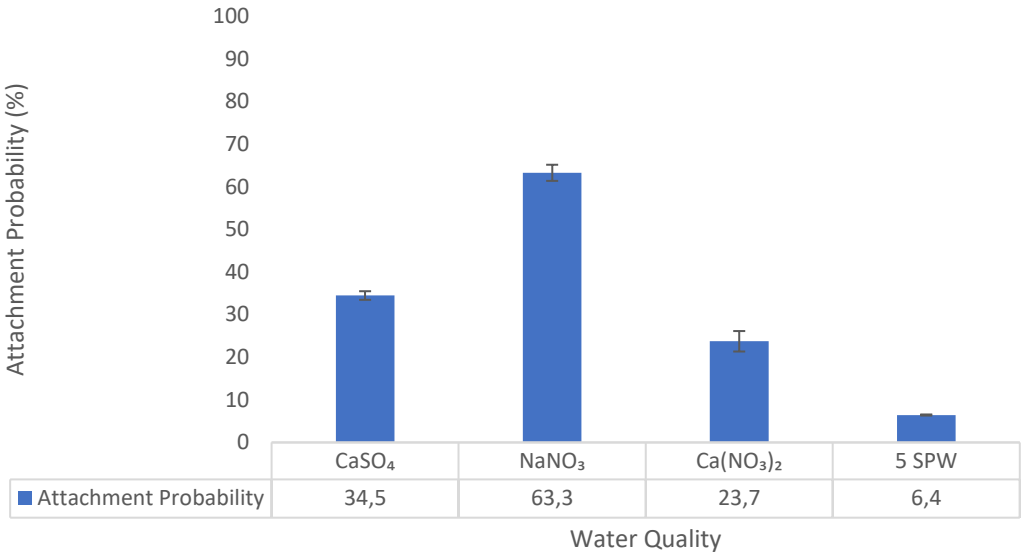

Figure 7-4: Attachment probability of pyrrhotite in various solutions at the natural pH

The highest probability of attachment in the single salt solutions was achieved in the $NaNO_3$ solution, followed by $CaSO_4$ while the lowest attachment probability was achieved with the $Ca(NO_3)_2$ single salt solution. The synthetic plant water of the same ionic strength as the three single salt solutions yielded a considerably lower attachment probability compared to the single salt solutions, this could be due to a combined effect of the various ions present in the synthetic plant water. This may also be due to the fact that the concentration of the anions and cations in the single salt solutions are higher than the concentration of the particular cation and anion of interest in the synthetic plant water matrix, although the total ionic strength is the same as seen in Table 7-1. The trend observed with the single salt solutions indicates that the Na^+ cation generally results in a higher attachment probability compared to that of the Ca^{2+} cation. This may be due to a monovalent versus divalent effect in how these types of ions passivate the mineral surface. It is expected that this effect should become clearer upon studying the effect of these ions on the mineral zeta potential.

7.3.3 Specific Ions on the Zeta Potential of Pyrrhotite

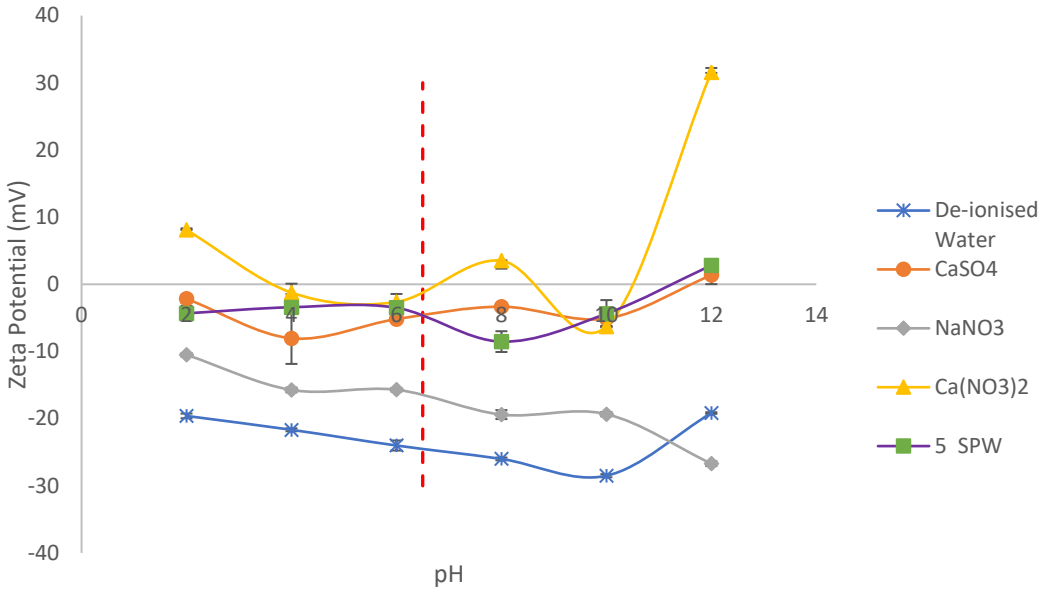

Figure 7-5: Zeta potential measurements of pyrrhotite as a function of pH in various solutions

Figure 7-5 shows the zeta potential measurements of the three salt solutions and synthetic plant water over the pH range 2 to 12, all at the same ionic strength of 0.1205 M. The dashed line in Figure 7-5 indicates the pH at which the microflotation and attachment time tests for these solutions were conducted. The speciation diagrams of the three salts under investigation are indicated in Figure 7-6 also over the pH range 2 to 12. Figure 7-5 illustrates that the zeta potentials of pyrrhotite in the salt solutions are generally less negative than in de-ioninsed water over the pH range studied; indicating the adsorption of the metal cations on the mineral surface (Moignard *et al.,* 1977). The $Ca(NO_3)_2$, $CaSO_4$ and synthetic plant water result in a much more positive potential on the pyrrhotite surface compared to the de-ioninsed water and $NaNO_3$ solution which lead to a more negative pyrrhotite surface. Due to the small, strongly hydrated nature of Na^+, it is expected that it will result in the preservation of the strongly hydrogen bonded water structure and increase the viscosity of the solution (Ma and Pawlik, 2005). It has also been shown that with an increase in the magnitude of particle potential, the viscosity increases (Tao *et al.,* 2012). This work therefore confirms that pyrrhotite potential is strongly negative in the Na^+ than the other salt solutions and this may be owing to the higher viscosity of the Na^+ solution compared to the Ca^{2+} solutions.

Evidently, the Ca^{2+} containing solutions result in a stronger passivation of the pyrrhotite surface. This result is similar to that achieved by Harvey *et al.* (2002) in coal flotation studies. These authors showed that the magnitude of the zeta potential depended on the valency of the cation; with the divalent Mg^{2+} providing a greater increase of the zeta potential compared to the monovalent Na^+. This result is in line with the results in this work whereby Ca^{2+} passivated the pyrrhotite surface more than Na^+ as seen by the more positive potential in the Ca^{2+} solution.

Furthermore, upon studying the anion effect, the $CaSO_4$ solution resulted in a lower (more negative) zeta potential than the $Ca(NO_3)_2$ solution. Evidently, the cation type played a large role in the charge of the pyrrhotite surface; when the nitrate anion is paired with the monovalent cation the pyrrhotite potential is approximately 19 mV lower than with the divalent calcium cation. On average the $Ca(NO_3)_2$ solution resulted in higher pyrrhotite potential compared to the other Ca^{2+} containing solutions; thus the combination of Ca^{2+} and NO_3^- ions results in higher pyrrhotite potentials.

a

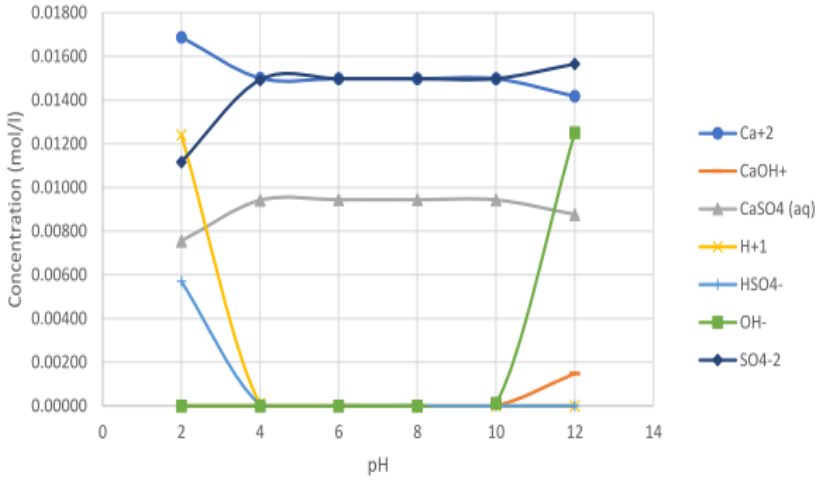

b

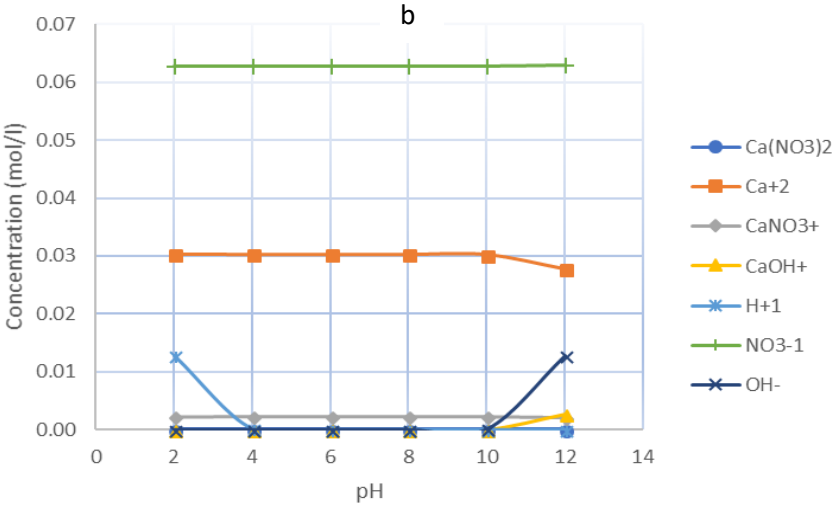

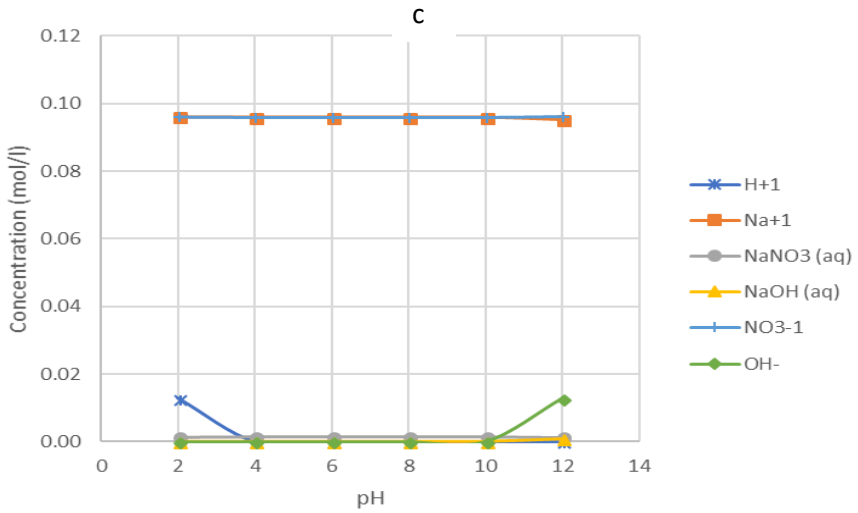

Figure 7-6: Speciation Diagrams of a) CaSO4, b) Ca(NO3)2 and c) NaNO3

Figure 7-6 illustrates the speciation of the solutions under study as generated by Visual MINTEQ. Figure 7-6 (a) shows the speciation of $CaSO_4$ solution at an ionic strength of 0.1205 M. Below pH 4, the dominant species in the solution include HSO_4^-, H^+, $CaSO_4$ (aq), SO_4^{2-} and Ca^{2+}. Between pH 4 and 10, the concentration of H^+ drops to close to 0 M. Beyond pH 10 a dramatic increase in OH^- is observed and further increases in $Ca(OH)^+$.

Figure 7-6 (b) shows the speciation of $Ca(NO_3)_2$ solution at an ionic strength of 0.1205 M. Below pH 4, dominant species in the solution include NO_3^-, Ca^{2+}, H^+ and $CaNO_3^+$. Between pH 4 and 10, HSO_4^- and H^+ drop to close to 0 M. Beyond pH 10 an increase in OH^- and $Ca(OH)^+$ concentration is evident while a decrease in Ca^{2+} is observed.

Figure 7-6 (c) shows the speciation of $NaNO_3$ solution at an ionic strength of 0.1205 M. Below pH 4, dominant species in the solution include NO_3^-, Na^+ and H^+. Between pH 4 and 10, the concentration of H^+ drops to close to 0 M; beyond pH 10 an increase in OH^- concentration is observed however, NO_3^- and Na^+ concentrations remain high.

Figure 7-6 therefore clearly shows an increase in the metal hydroxide complexes between pH 10 and 12. Hydroxide precipitation or oxidation at the mineral surface may be a reason for the increase in potential in the various salt solutions at pH 10 to 12 as observed in Figure 7-5 (Harvey *et al.,* 2002; Ikumapayi *et al.,* 2012; Hirajama *et al.,* 2016).

Relating both the attachment time and microflotation tests to the zeta potential measurements, a clear cation and anion effect is observed. The pyrrhotite recovery and bubble-particle attachment are greater with the $NaNO_3$ solution than with the $Ca(NO_3)_2$ solution while the zeta potential measurements confirm an increase in zeta potential with $Ca(NO_3)_2$. From an anion ion perspective, SO_4^{2-} performs better than NO_3^- when paired with Ca^{2+}.

Although the mechanism is not completely clear, previous studies have also shown that divalent anions such as SO_4^{2-} and $S_2O_3^{2-}$ improve flotation efficiency (Yoon, 1982; Kirjavainen *et al.,* 2002; Manono *et al.,* 2016). Furthermore it should be noted that although conducted at the same ionic strength, the Ca^{2+} concentration is higher in $Ca(NO_3)_2$ compared to $CaSO_4$; as a result this may possibly show the dominant effect of Ca^{2+}, over-powering the anion effect.

The zeta potential measurements also verify a much more negative charge with the $NaNO_3$ solution. As previously stated, increases in ionic strength compress the electrical double layer, reducing the energy barrier for bubble-particle attachment to occur (Laskowski *at al.* 1991; Paulson and Pugh, 1996; Harvey *et al.,* 2002; Laskowski, 2012). Thus, with a highly negative zeta potential as in the $NaNO_3$ solution it is expected that the high repulsion between the particle and bubble would result in a higher energy barrier, leading to decreased recoveries. This evidently was not observed indicating that another mechanism may be resulting in the higher recoveries and attachment probabilities with monovalent salt solutions. As previously described the monovalent solution may result in decreased hydration layer stability resulting in more rapid bubble-particle attachment. Another possibility could be the effect of the changes in the zeta potential of the bubble with the $NaNO_3$ solution, this may result in optimal bubble-particle attachment if the charge of the bubble becomes positive enough such that the energy barrier for attachment is decreased. Work has been done by Takahashi (2005) focusing on the charge of the bubble, and as with the particle, higher valency cations do make the zeta potential of the bubble less negative. This study was however done with the bubble in isolation and did not consider the particle.

7.4 Conclusions

Poor recoveries and attachment probabilities of pyrrhotite in various plant waters at pH 11 are attributed to the deposition of oxyhydroxo species such as $CaOH^+$ and $MgOH^+$ on the pyrrhotite surface which were shown to exist at pH>10 in a study by Manono *et al.* (2019). The formation of these oxyhydroxo were confirmed by authors such as by Rao and Finch (1989), Zanin *et al.* (2019), Li *et al.* (2017), Li and Somasundaran (1992) and Ramos *et al.* (2013). The outcomes of this work suggest that not only do these species prevent the flotation of the mineral particles, they also in turn prevent processes such as collector adsorption and compression of the electrical double layer from taking place.

A clear anion and cation effect was observed in the attachment time and microflotation tests and these were supported by zeta potential measurements. The attachment time and microflotation tests showed that $NaNO_3$ gave the highest bubble-particle attachment probability and pyrrhotite recovery respectively; while the $Ca(NO_3)_2$ solution resulted in the poorest performance. The sulfate anion was shown to be more beneficial to the floatability of pyrrhotite compared to the nitrate anion when paired with divalent cations.

The $NaNO_3$ solution led to increased performance compared to $Ca(NO_3)_2$ as confirmed by the attachment time and microflotation tests. Upon studying the potential of pyrrhotite with these two nitrate salts; a considerably lower charge with $NaNO_3$ was observed compared to pyrrhotite in $Ca(NO_3)_2$ solution indicating the effect that the calcium cation has in increasing the potential of pyrrhotite.

Thus, the findings of this study indicate that:

- plant water at pH 11 results in low bubble-particle interactions across various water qualities even in the presence of a collector due to the deposition of oxyhydroxo species on the pyrrhotite surface as suggested by increased pyrrhotite potentials (October *et al.* (2019).
- monovalent cations and divalent anions result in greater bubble-particle attachment. The fact that monovalent cations outperformed divalent cations calls for the investigation of properties such as viscosity in monovalent solutions and how these mechanistically affect the hydration layer stability. Furthermore, the zeta potential of the bubbles generated in the various solutions could add more value to this area of research if studied alongside the zeta potential of the mineral.

Acknowledgements

This work is financed by the National Research Foundation of South Africa (NRF) [Grant number 103641] and Academy of Finland (AF) as part of the joint project 'Bridging North to South' in MISU program. Any opinion, finding and conclusion or recommendation expressed in this material is that of the authors and the NRF does not accept any liability in this regard. Further the financial and technical contributions from the South African Minerals to Metals Research Institute (SAMMRI) is also acknowledged.

7.6 References

Albijanic, B., Ozdemir, O., Nguyen, A. and Bradshaw, D. (2010). A Review of Induction and Attachment Times of Wetting Thin Films between Air Bubbles and Particles and Its Relevance in the Separation of Particles by Flotation. Advances in Colloid and Interface Science 159 (1). Elsevier B.V.: 1–21. https://doi.org/10.1016/j.cis.2010.04.003.

Allison, S.A. and O'Connor, C.T. (2011). An investigation into the flotation behaviour of pyrrhotite. International Journal of Mineral Processing, 98 (3-4), 202-207. https://doi.org/10.1016/j.minpro.2010.12.003.

Aspiala, M., Schreithofer, N., Serna-Guerrero, R. (2018). Automated contact time apparatus and measurement procedure for bubble-particle interaction analysis, Minerals Engineering, 121(1):77-82.

Blake, T.D., Kitchener, J.A. (1972) "Stability of aqueous films on hydrophobic methylated silica". Journal of the Chemical Society. 68, 1435–1442.

Bradshaw, D. and O'Connor, C. (1996) Measurement of the sub-process of bubble loading in flotation. Minerals Engineering. 9: 443-448.

Burdukova, E. (2007) Surface properties of New York Talc as a function of pH, polymer adsorption and electrolyte concentration. PhD Thesis, University of Cape Town, Faculty of Engineering and the Built Environment, Department of Chemical Engineering, Cape Town, South Africa.

Corin, K.C., Reddy, A., Miyen, L., Wiese, J.G. and Harris, P.J. (2011). The Effect of Ionic Strength of Plant Water on Valuable Mineral and Gangue Recovery in a Platinum Bearing Ore from the Merensky Reef. Minerals Engineering 24 (2): 131–37. https://doi.org/10.1016/j.mineng.2010.10.015.

Corin, K.C. and Wiese, J.G. (2014). Investigating Froth Stability : A Comparative Study of Ionic Strength and Frother Dosage. Minerals Engineering. 66–68. Elsevier Ltd: 130–34. https://doi.org/10.1016/j.mineng.2014.03.001.

Craig, V.S.J., Ninham, B.W. and Pashley, R.M. (1993). The Effect of Electrolytes on Bubble Coalescence in Water. The Journal of Physical Chemistry. 97 (39). American Chemical Society: 10192–97. https://doi.org/10.1021/j100141a047.

Dishon, M., Zohar, O., and Sivan, U. (2009). From repulsion to attraction and back to repulsion: the effect of NaCl, KCl and CsCl on the force between silica surfaces in aqueous solution. Langmuir 25, 2831–2836. doi: 10.1021/la8 03022b.

Fuerstenau, D. W. (1982). Adsorption at Mineral-Water Interfaces. In R. P. King, Principles of Flotation (pp. 53-71). Johannesburg: The South African Institute of Mining and Metallurgy.

Harvey, P.A., Nguyen, A.V. and Evans, G.M. (2002). Influence of Electrical Double-Layer Interaction on Coal Flotation. Journal of Colloid and Interface Science. 250 (2): 337–43. https://doi.org/10.1006/jcis.2002.8367.

Hirajima, T., Pandhe, G., Suyantara, W., Ichikawa, O., Mohamed, A., Miki, H. and Sasaki, K. (2016). Effect of Mg^{2+} and Ca^{2+} as Divalent Seawater Cations on the Floatability of Molybdenite and Chalcopyrite. Minerals Engineering. 96–97. Elsevier Ltd: 83–93. https://doi.org/10.1016/j.mineng.2016.06.023.

Javor.Z., Aspiala, M., Schreithofer, N., Heiskanen, K., Serna, R. (2016). Development of a new attachment timer for predicting the change in ore floatability. Proceedings of the XXVIII International Mineral Processing Congress (IMPC 2016), September 11-15, 2016, Québec City, Canadian Institute of Mining, Metallurgy and Petroleum.

Kirjavainen, V., Schreithofer, N. and Heiskanen, K. (2002). Effect of some process variables on flotability of sulfide nickel ores. International Journal of Mineral Processing. 65: 59-72.

Ikumapayi, F., Makitalo, M., Johansson, B. and Hanumantha, K. (2012). Recycling of Process Water in Sulphide Flotation : Effect of Calcium and Sulphate Ions on Flotation of Galena. Minerals Engineering 39. Elsevier Ltd: 77–88. https://doi.org/10.1016/j.mineng.2012.07.016.

Laskowski, J., and Castro, S. (2015). Flotation in Concentrated Electrolyte Solutions. International Journal of Mineral Processing. 144, 50-55.

Laskowski, J. and Iskra, J. (1970). Role of capillary effects in bubble-particle collision in flotation. Transactions of the Institution of Mining and Metallurgy. 79, C6.

Laskowski, J.S. (2012). Role of model systems in fundamental studies on particle-bubble interaction, Separation Technologies (C.A. Young and G.H. Luttrell, eds.), SME, pp. 7-18.

Laskowski, J.S., Xu, Z. and Yoon, R.H. (1991). Energy barrier in particle-to-bubble attachment and its effect of flotation kinetics, Proc. 17th Int. Mineral Processing Congress, Dresden, Vol. 2, pp. 237-249.

Li, C., Somasundaran, P. (1992) Reversal of bubble charge in multivalent inorganic salt solutions—Effect of aluminum. Journal of Colloid and Interface Science.148, 587–591.

Li, C. and Somasundaran, P. (1993). Role of Electrical Double Layer Forces and Hydrophobicity in Coal Flotation in NaCl Solutions. Energy and Fuels 7 (2): 244–48. https://doi.org/10.1021/ef00038a014.

Li, Y., Li, W., Xiao, Q., He, N., Ren, Z., Lartey, C., Gerson, A. (2017). The Influence of Common Monovalent and Divalent Chlorides on Chalcopyrite Flotation. Minerals 2017, 7, 111. https://doi:10.3390/min7070111.

Ma, X. and Pawlik, M. (2005). "Effect of alkali metal cations on adsorption of guar gum onto quartz." Journal of Colloid and Interface Science 289: 48 - 55.

Manenzhe, R. (2018). Investigating the Effect of Water Quality on the Adsorption of a Xanthate Collector in the Flotation of a Sulphide Ore. MSc Thesis, University of Cape Town, Faculty of Engineering and the Built Environment, Department of Chemical Engineering, Cape Town, South Africa.

Manono, M.S., Corin K.C. and Wiese, J.G. (2012). An Investigation into the Effect of Various Ions and Their Ionic Strength on the Flotation Performance of a Platinum Bearing Ore from the Merensky Reef. Minerals Engineering 36–38. Elsevier Ltd: 231–36. https://doi.org/10.1016/j.mineng.2012.03.035.

Manono, M.S., Corin, K.C. and Wiese, J.G. (2016). The influence of electrolytes present in process water on the flotation behaviour of Cu-Ni containing ore. Minerals Engineering. 96-97, 99-107.

Manono, M.S., Corin, K.C. and Wiese, J.G. (2019). The Effect of the Ionic Strength of Process Water on the Interaction of Talc and CMC: Implications of Recirculated Water on Floatable Gangue Depression. Minerals. 9(4), 231. https://doi.org/10.3390/min9040231.

Moignard, M.S., James, R.O., Healy, T.W. (1977). Adsorption of calcium at the zinc sulphide–water interface. Australian Journal of Chemistry 30, 733–740.

Muzenda, E. (2010). An investigation into the effect of water quality on flotation performance. World Academy of Science, Engineering and Technology 69, 237–241.

October, L.L., Corin K.C., Schreithofer, N., Manono, M.S., Wiese, J.G. (2019). Water Quality Effects on Bubble -Particle Attachment of Pyrrhotite Minerals Engineering 131. Elsevier Ltd: 230–236. https://doi.org/10.1016/j.mineng.2018.11.017.

Paulson, O. and Pugh, R.J. (1996). Flotation of Inherently Hydrophobic Particles in Aqueous Solutions of Inorganic Electrolytes. Langmuir 12 (20): 4808–13. https://doi.org/10.1021/la960128n.

Ramos, O., Castro, S., Laskowski, J.S. (2013)Copper–molybdenum ores flotation in sea water: Floatability and frothability. Minerals Engineering 53, 108–112.

Rao, S.R., Finch, J.A. (1989). A review of water re-use in flotation. Minerals Engineering 2 (1), 65–85.

Takahashi, M. (2005). ζ Potential of Microbubbles in Aqueous Solutions: Electrical Properties of the Gas−Water Interface. The Journal of Physical Chemistry *B* 109 (46): 21858–64. https://doi.org/10.1021/jp0445270.

Wang, T., Ni, M., Luo, Z. Y., Shou, C.H., Cen, K. (2012). Viscosity and aggregation structure of nanocolloidal dispersions. Chinese Science Bulletin. 57: 3644−3651. https://doi.org/10.1007/s11434-012-5150-y.

Wang, B. and Peng, Y. (2014). The effect of saline water on mineral flotation- A critical review. Minerals Engineering. 66–68. Elsevier Ltd: 13–24. http://dx.doi.org/10.1016/j.mineng.2014.04.017.

Wiese, J.G., Harris, P.J. and Bradshaw, D.J. (2005). The influence of the reagent suite on the flotation of ores from the Merensky reef. Minerals Engineering 18 (2), 189–198.

Yoon, R. H. (1982). Coal Flotation. Mining Congress Journal. 68 (12), 76.

Yoon, R. H., and Basilio, C. I. (1993). Adsorption of Thiol Collectors on Sulphide Minerals and Precious Metals: A New Perspective. XVIII International Mineral Processing Congress, 611-618.

Zanin, M.; Lambert, H.; du Plessis, C.A. (2019). Lime use and functionality in sulphide mineral flotation: A review. Minerals Engineering 143, 105922.

Chapter 8 **Fundamental and Flotation Techniques Assessing the Effect of Water Quality on Bubble-Particle Attachment of Chalcopyrite and Galena**

Published in Minerals Engineering 167 106880. https://doi.org/10.1016/j.mineng.2021.106880

As noted in Chapter 6, the testwork performed in the "Water Quality Effects on Bubble-Particle Attachment of Pyrrhotite" publication was the first time the ACTA was used to determine the effect of a process parameter on bubble-particle attachment. Upon the conclusion of the testwork in the aforementioned publication, a number of operations improvements for testwork going forward are proposed.

As a result of the fine particle size used very fine and sometimes no particles were collected in the collection bin, although attachment was observed by the images. Furthermore, particles would sometimes move across to the camera area. Therefore, going forward, a particle size of 106 – 125 μm is to be used; this particle size was used in the initial work on the machine by Bellers (2017).

The testwork in "Water Quality Effects on Bubble-Particle Attachment of Pyrrhotite" also showed that in the absence of a collector, very low bubble–particle attachment is observed. Subsequent testwork studying the effect of water quality with the ACTA will thus be done only in a system with collector present.

Contact times in the same study of 100 ms and 200 ms were used, in retrospect these contact times may be too long particularly when studying highly floatable minerals, as it may be difficult to see a difference in attachment probability across varying water qualities.

The publication "Water Quality Effects on Bubble-Particle Attachment of Pyrrhotite" published in Minerals Engineering reported a decrease in attachment probability of pyrrhotite as the ionic strength of the plant water was increased. As the water quality deteriorated, increases in cation adsorption on the mineral surface was inferred from the zeta potential measurements. This may have caused the lower attachment probability as the ionic strength of plant water increased.

It is thus of interest to understand how other sulfide minerals respond to changes in water quality in terms of their propensity to attach to air bubbles.

"**Fundamental and Flotation Techniques Assessing the Effect of Water Quality on Bubble-Particle Attachment of Chalcopyrite and Galena**" published in Minerals Engineering, takes into account the operational improvements proposed and assesses the effect of water quality on two additional sulfide minerals, namely chalcopyrite and galena. This paper further uses classical microflotation techniques as a method to corroborate the results attained from the ACTA.

Fundamental and Flotation Techniques Assessing the Effect of Water Quality on Bubble-Particle Attachment of Chalcopyrite and Galena

L.L. October[1], K.C. Corin[1], M.S. Manono[1], N. Schreithofer[2] and J.G. Wiese[1]

[1]Centre for Minerals Research, Department of Chemical Engineering, University of Cape Town, Private Bag X3, Rondebosch 7701, South Africa

[2] Department of Bioproducts and Biosystems, Clean Technologies Research Group, Aalto University, Vuorimiehentie 1, 02150 Espoo, Finland

Abstract

Bubble-particle attachment has been studied in the most fundamental way from as early as 1934 by bringing a bubble into contact with a flat mineral surface and since then, techniques measuring this interaction have advanced. Water quality within flotation will impact the bubble particle attachment and as more operations recycle their water on site, an understanding of this process becomes vital. This study uses an Automated Contact Time Apparatus (ACTA) to assess the effect of water quality on bubble-particle attachment of selected sulfide minerals; galena and chalcopyrite, from a fundamental perspective. Classical microflotation tests are complemented with collector adsorption and mineral potential under degrading water quality to validate the ACTA and gain an understanding of the effect of water quality on bubble-particle attachment as well as subsequent flotation. This investigation showed that the results from the ACTA qualitatively showed similar trends as that of the classical microflotation technique for measuring floatability, however the quantitively these methods showed very different results. Due to the dynamic nature of the microflotation technique it may be assumed that plant recovery will resemble the results from this technique closer than that of the ACTA. Furthermore, this investigation showed an increase in zeta potential of both minerals as the concentration of inorganic electrolytes in the water increased. It can thus be speculated that the increase in bubble-particle attachment with increasing ionic strength of synthetic plant water may be attributed to electrical double layer compression and particle agglomeration.

Keywords: Bubble-Particle Attachment, Chalcopyrite, Froth Flotation, Galena, Ions, Water Quality

Graphical Abstract

Comparison of the Microflotation and ACTA outputs with changing water quality

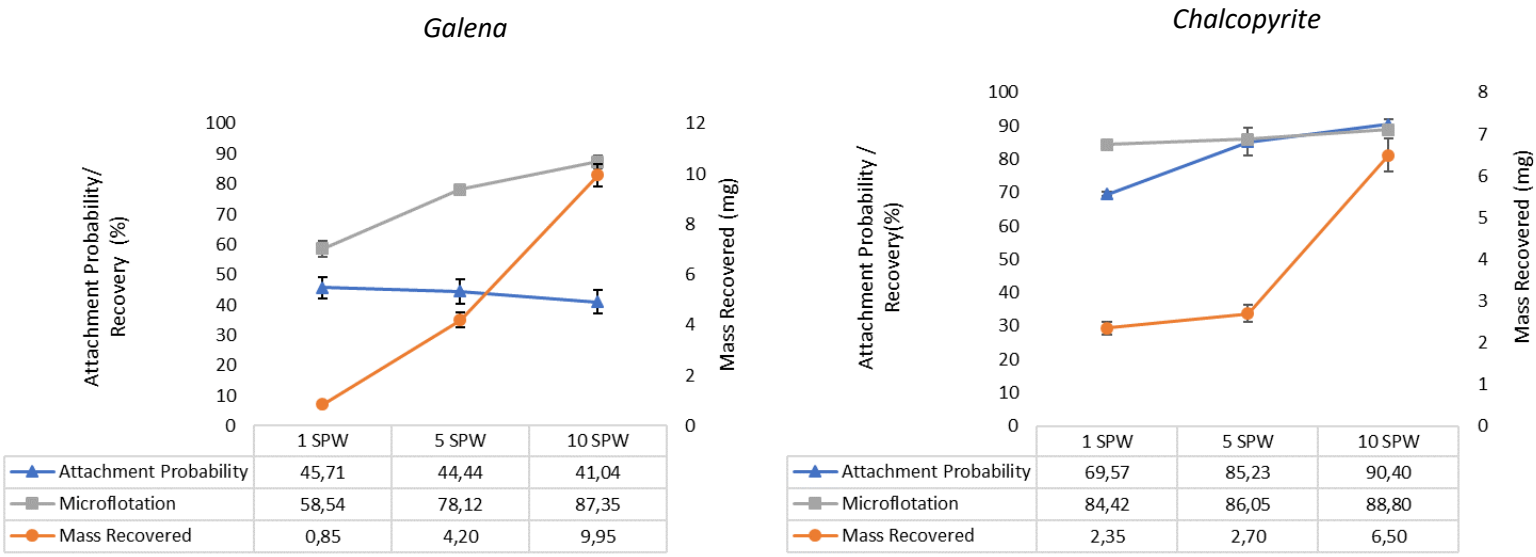

8.1 Introduction

Sven-Nilsson (1934) first presented the concept of induction time and described it as the minimum time that a bubble and particle are in contact such that the thinning of the hydration film to critical thickness and film rupture occurs. This author first measured the induction time by bringing a captive bubble towards a flat mineral surface and then moving it away from the mineral surface. Glembotsky (1953) used a similar technique to determine the induction time, however instead of a flat mineral surface, the single bubble was brought into contact with a bed of particles. The use of a bed of particles resembles an actual flotation system more than a flat mineral surface. Since then the concept of induction time and the equipment used to measure the induction time has advanced and commercialised (Yoon and Yordan, 1991; Ye *et al.,* 1989; Gu *et al.,* 2003; Albijanic *et al.,* 2011). The equipment was developed such that software is used to control bubble motion parameters as this does affect the nature in which the bubble interacts with the particle bed. Furthermore, the induction time apparatus is equipped with a camera to visualise the bubble-particle interaction and detect attachment.

Studies often use induction time and attachment time interchangeably, however Albijanic *et al.* (2010) clearly defined the difference between the two terms; the induction time being the time it takes for the thinning of the film at the air–water and solid–water interfaces to critical thickness. While the attachment time is the time it takes for the film to thin to critical thickness, rupture, and the attachment of particle to air bubble with contact angles in equilibrium.

The attachment timer described by Aspiala *et al.* (2018) and October *et al.* (2019) named the Automated Contact Time Apparatus (ACTA) generates six bubbles and tests the entire length of the particle bed.

Furthermore, the particles that have successfully attached to the bubbles are captured and can be further analysed for recovery, shape, size and composition. Thus, the ACTA allows for a more robust bubble-particle attachment probability measurement. These studies Aspiala *et al.* (2018) and October *et al.* (2019), have looked at the attachment probability of a mixture of hydrophilic and hydrophobic quartz and water quality effects on attachment probability of pyrrhotite respectively. Although in principle the ACTA is a more robust technique for measuring bubble-particle attachment, it is important to validate this instrument against a classical technique of measuring bubble-particle interactions before it can be used as a quick diagnostic testing tool on flotation plants (Aspiala *et al.,* 2018).

The efficiency of bubble-particle attachment is affected by various factors, chemical, hydrodynamic and operational. Water quality within flotation has been identified as an important parameter affecting the bubble-particle efficiency and has been gaining huge interest of late due to water scarcity in parts of the world (Bicak *et al.,* 2012; Manono *et al.,* 2012; Ikumapayi *et al.,* 2012; Slatter *et al.,* 2009). In studies with quartz it was found that increasing the ionic concentration, the induction time shortened; indicating that the particles' susceptibility to float increased (Yoon and Yordan, 1991; Laskowski and Iskra, 1970). These authors ascribed this effect to the compression of the electrical double layer with increases in ionic concentration; which was said to ultimately lead to the accelerated rupturing of the film at the air–water and solid water interfaces. Less fundamental batch flotation studies have shown that total solids recovery increased as the ionic concentration of plant water increased (Manono *et al.,* 2012; Corin and Wiese 2014). While studies by Ikumapayi *et al.* (2012) showed that as the water quality deteriorated, the mineral recovery decreased. Boujounoui *et al.* (2015) showed that the effect of ions on mineral recovery varies based on the mineral type.

Therefore, this investigation studies the effect of water quality on bubble-particle attachment in the most fundamental way by bringing bubbles into contact with a particle bed and uses classical microflotation as a validation technique for the ACTA. This study also aims to understand what happens at the mineral surface in terms of the change in particle potential and adsorption of collector with changes in water quality and how this may affect the way bubbles and particles interact.

8.2 Materials and Methods

8.2.1 Sample Preparation

Galena and Chalcopyrite were obtained from Ward's Science in 1 kg bulk packs. The respective samples were hammered into chunks passing 1000 µm. The respective chunks were placed into a pulveriser for about 10 seconds and subsequently dry screened using 125 µm, 106 µm, 75 µm and 38 µm screens for 30 minutes. The fraction above 125 µm was pulverised again and dry screened similarly. The fraction between 106 and 125 µm was used for the attachment time tests, as particles in this size fraction both allowed for the collection of particles and clear visibility of particles on the images (October *et al.,* 2020). The fraction below 38 µm was used for the zeta potential (i.e. electrokinetic potential) measurements as particles for this measurement must be fine enough such that some are still suspended in solution. The fraction between 38

and 75 µm was used for microflotation tests and adsorption studies (Mhlanga, 2011; Castelyn, 2012). The samples for each of the respective techniques, per mineral were split using a rotary splitter and placed into smaller plastic bags. Each bag was purged with nitrogen and stored below 30 °C. It is noted that the different particle size fractions used across the experimental techniques may be a limitation as particle properties may potentially be affected by particle size.

8.2.2 Water Quality

Synthetic Plant Water (1 SPW) used by Wiese *et al.* (2005) was prepared using salts of analytical grade and was used as the standard synthetic plant water in this investigation. In order to mimic recycled plant water, the baseline plant water (1 SPW) was increased by five and ten times the total dissolved solids. These waters were termed 5 SPW and 10 SPW respectively. The composition of each of the synthetic plant waters are shown in Table 8-1.

Table 8-1: Ionic composition of various water types

Plant Water Type	Ca^{2+} (mg/L)	Mg^{2+} (mg/L)	Na^{+} (mg/L)	Cl^{-} (mg/L)	SO_4^{2-} (mg/L)	NO_3^{-} (mg/L)	CO_3^{2-} (mg/L)	TDS (mg/L)	Ionic Strength (mol/L)
1 SPW	80	70	153	287	240	176	17	1023	0.0241
5 SPW	400	350	765	1435	1200	880	85	5115	0.1205
10 SPW	800	700	1530	2870	2400	1760	170	10230	0.241

8.2.3 Reagents

Sodium isobutyl xanthate (SIBX) of 97% purity, sourced from Senmin was used as a collector in this investigation. Collector solutions of 1% w/v were made fresh for each day of the experimental work, which is 0.06 mol/L SIBX xanthate solution. NaOH and HCl supplied by Merck were used for pH adjustment; 1% w/v solutions were made each day for both NaOH and HCl.

8.2.4 Automated Contact Time Apparatus

The automated contact time apparatus used in this work has previously been described in Aspiala *et al.* (2018) and October *et al.* (2019) and is illustrated in Figure 8-1 (B). Details of the functioning of the machine and operational details have comprehensively been documented in October *et al.* (2019). The particle bed was made with approximately 18 g of mineral sample in the fraction 106-125 microns. A slurry was made with the mineral particles and the water quality of interest, an equivalent of 50 g/t of SIBX was added (volume of 90 µL) and conditioned for 2 minutes. The pH of the slurry with 1 SPW prior to the addition of SIBX was 6.5, the subsequent mineral and water mixtures were then adjusted to 6.5 using the NaOH and HCl solutions. The particles in the slurry were allowed to settle for about 3 minutes and the liquid at the top was pipetted out, filtered and placed in the glass pool. The settled particles were used to build the

particle bed in the pool. Each of the water qualities were tested in this way and each condition was performed in duplicate to minimise experimental error.

8.2.5 Microflotation

In a beaker, 3 g of mineral was mixed with 50 mL of the water type under study. The pH of the slurry was then adjusted to 6.5 using the NaOH and HCl solutions. This was transferred into the microflotation cell (Figure 8-1 (A)) developed by Bradshaw and O'Connor (1996) with a funnel; the funnel was washed with the water type until the slurry reached just above the recycle point of the microflotation cell. The pump was switched on to 90 rpm and the pulp was circulated for 5 minutes. The volume equivalent to 50 g/t of SIBX was added to the slurry (volume of 15 µL). The water type under study was topped up to the 250 mL point of the cell and the cone was put in place. The microsyringe, providing an air supply of 7 mL/min was inserted at the base of the microflotation cell. Concentrates were collected after 2, 6, 12 and 20 minutes of flotation. The concentrates were oven dried and weighed. This procedure was followed for each of the water types and each condition was performed in duplicate to minimise error.

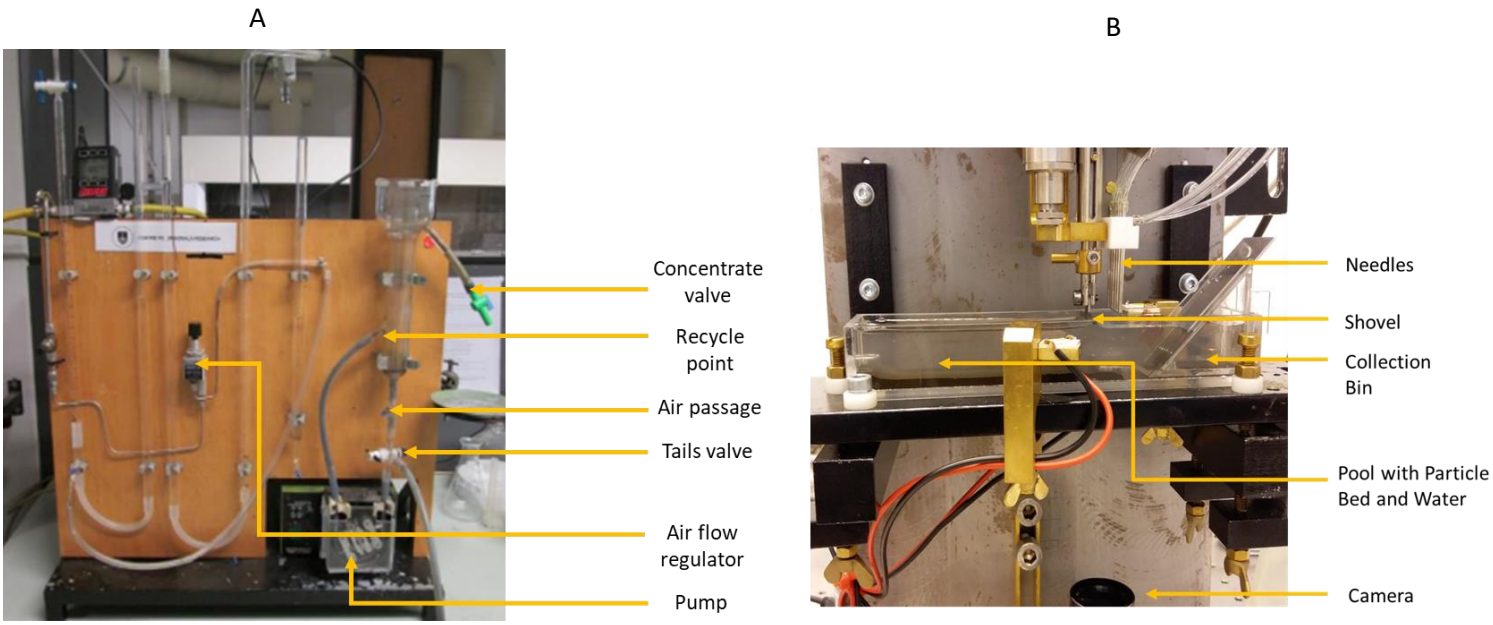

Figure 8-1: Bubble-particle attachment equipment (A) Microflotation Cell and (B) ACTA

8.2.6 Adsorption Tests

Five standard solutions ranging from 0.5 mg/L to 5 mg/L of SIBX were made up. The absorbance of each solution was measured in a quartz cuvette using the Ultrospec 2100 UV-vis spectrophotometer (Biochrom, USA) across the 200 to 500 nm range; step size was 1 nm and spectral bandwidth < 3 nm. The peak in absorbance was observed to be at 301 nm; the 5 absorbances at this wavelength were plotted against the concentration of SIBX to obtain a calibration curve.

In a conical flask, 3 g of mineral was mixed with 30 mL of the water quality under study. The pH of the slurry was then adjusted to 6.5 using the NaOH and HCl solutions. The equivalent of 50 g/t of SIBX (15 μL) was added to the mineral mixture; thus, the maximum xanthate concentration in the solution was 5 mg/L. The conical flasks containing the mineral mixture was covered with foil and inserted in the Ecobath shaker at 20 °C with shaking intensity of 141 rpm. After 15 minutes in the water bath a plastic syringe was used to draw out 10 mL of slurry. A 0.45 μm filter was attached to the end of the syringe and the solution was filtered. The filtrate was placed into a quartz cuvette, which was inserted into the UV-Vis spectrophotometer where the absorbance at 301 nm was measured. Measurements were corrected for the blanks for each of the solutions.

The equation of the calibration curve obtained and the absorbance at 301 nm was used to calculate the concentration of SIBX left in the solution and by mass balance the concentration adsorbed on the mineral surface. This technique was applied to each of the water types with each condition tested in duplicate to minimise experimental error.

8.2.7 Zeta potential Measurements

0.075 g of mineral sample was mixed in 100 mL of the water quality under study and placed on a magnetic stirrer for 5 minutes. The 100 mL suspension was evenly divided into 6 containers. The pH was adjusted to 6.5 using HCl and NaOH in order to match the pH at which the Microflotation and ACTA experiments were conducted. Each container was placed on the magnetic stirrer and the pH was measured again and readjusted if needed. The particles in each container were allowed to settle for 3 minutes and the particles suspended in the liquid were removed with a plastic pipette and inserted in the Malvern Dip Cell (Malvern Instruments Ltd., Malvern, UK). The dip cell was placed in the Zeta sizer Nano ZS90 (Malvern Instruments Ltd., Malvern, UK) and the zeta potential was measured. This procedure was followed for each water quality with each condition tested in triplicate in order to minimise experimental error.

8.3 Results

8.3.1 Effect of Water Quality on the Bubble-Particle Interactions

The automated contact time apparatus (ACTA) produced two outputs, the first is an attachment probability which is obtained from the images taken by the machine for each cycle (that is 66 cycles, with 396 possible bubble-particle attachment and thus the bubble-particle attachment probability for each run is the amount of bubbles that had particles attached to it over 396) and the mass of particles recovered in the collection bin. Figure 8-2 shows the attachment probability and the mass of galena and chalcopyrite particles recovered. The results presented in Figure 8-2 show that the attachment probability of galena was generally the same across the three water qualities, while the mass of galena particles recovered shows an increase with increasing ionic strength of the synthetic plant water. The attachment probability and mass recovered of chalcopyrite are seen to increase as the ionic strength of the synthetic plant water increases. The attachment probability of chalcopyrite in 1 SPW is observed to be 69.57% and increases to 90.40% in 10 SPW; the attachment probability of chalcopyrite is thus considerably higher compared to galena whose highest attachment probability was below 50%.

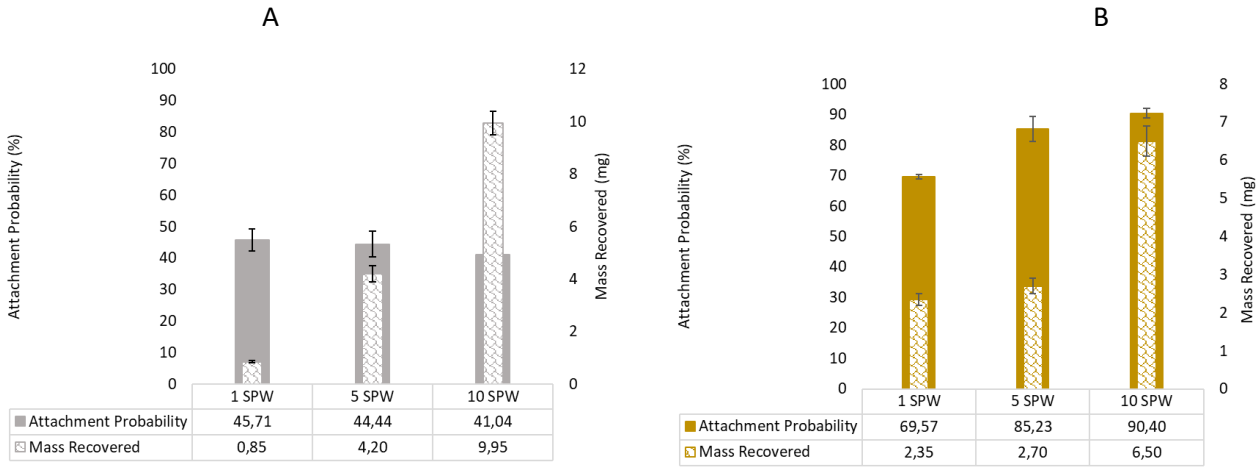

Figure 8-2: Attachment Probability and Mass Recovered under varying water quality for (A) galena and (B) chalcopyrite with ACTA (Error bars represent standard error of the mean)

Microflotation of galena and chalcopyrite results are displayed in Figure 8-3 and Figure 8-4 respectively. The solid curve represents a system with xanthate collector and the dotted curve in the absence of a collector. The tests conducted with the ACTA were in the presence of the collector and thus their trend can be compared to the microflotation testwork with collector. Figure 8-3 shows that in the first 4 minutes of flotation, the recovery of galena is generally the same across the various water qualities, however after 5 minutes of flotation it becomes clear that higher galena recoveries are achieved with synthetic plant water of increasing ionic strength. This trend of an increase in particles recovered with increasing ionic strength of plant water in the microflotation tests qualitatively match the trend observed in the ACTA in terms of mass recovered. However, it must be noted that quantitively the results from these two methods are vastly different when studying the percentage increase in recovery between the water types. The collector-chalcopyrite system in Figure 8-4 shows similarly high recoveries of chalcopyrite across the water types; ranging from 84.42% in 1 SPW to 88.80% in 10 SPW. A trend of increases in chalcopyrite recovery with

increasing ionic strength is however observed even for a system with no collector. These results complement the attachment probability and mass recovered data provided by the ACTA.

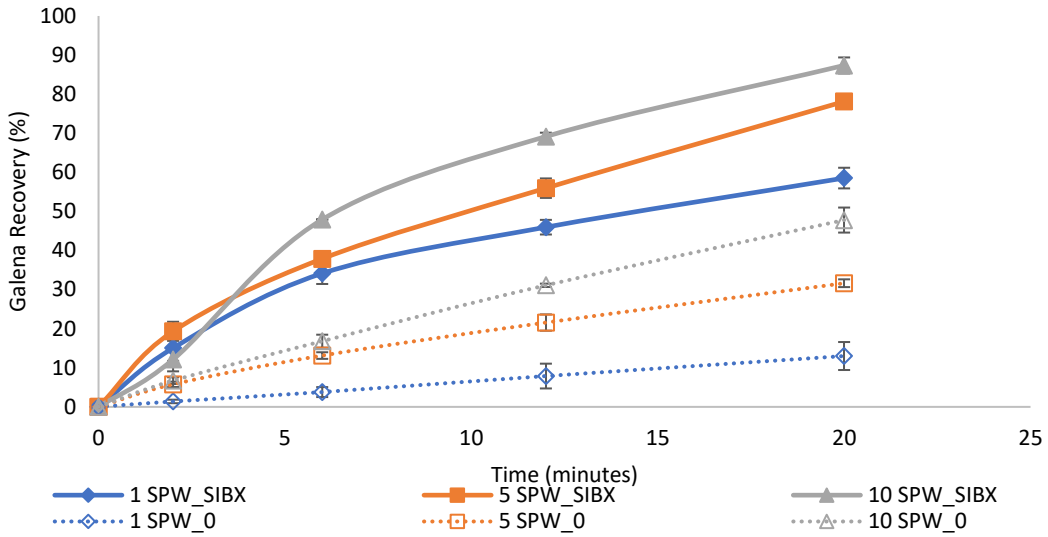

Figure 8-3: Recovery of galena under varying water quality with and without collector by microflotation

The microflotation results in Figure 8-3 and Figure 8-4 also allow for a comparison between collector and collectorless test results across the varying water qualities. In the system without collector the difference in recovery of both galena and chalcopyrite becomes clearly evident in that the recovery increases as the ionic strength of the synthetic plant water increases. Further, the expected result of collector flotation resulting in higher recoveries compared to collectorless flotation is observed; however, in both mineral systems recovery with 10 SPW in the absence of a collector is very close to the mineral recovery with 1 SPW and 50 g/t collector.

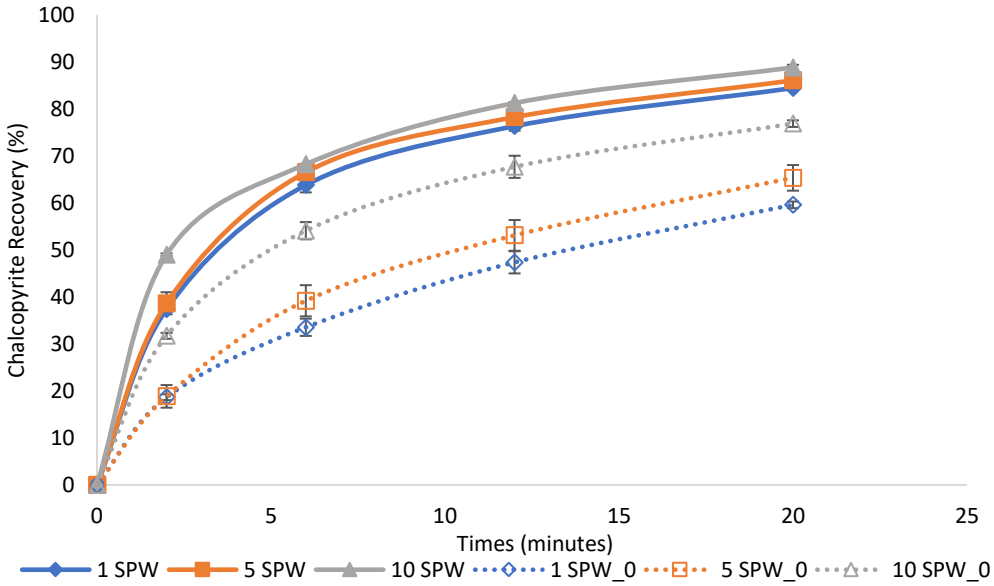

Figure 8-4:Recovery of chalcopyrite under varying water quality with and without collector by microflotation

8.3.2 Effect of Water Quality on Collector Adsorption

The effect of water quality on bubble-particle interactions was examined using a newer technique (the ACTA) as well as an established microflotation technique. The trends from these two techniques were generally similar. However, it is still not understood what happens at the mineral surface and why the differences in recoveries are observed under varying water quality. It therefore became important to understand the effect of ionic strength on collector (xanthate) adsorption. Figure 8-5 depicts the concentration of xanthate left in the solution and by mass balance xanthate adsorbed on the galena surface under the varying water qualities. It is evident that more xanthate is left in solution and less adsorbed on the mineral surface when the ionic strength of the synthetic plant water is increased. Under 1 SPW only 12% of xanthate was left in the solution while 67.8% of the xanthate stayed in solution at 10 SPW.

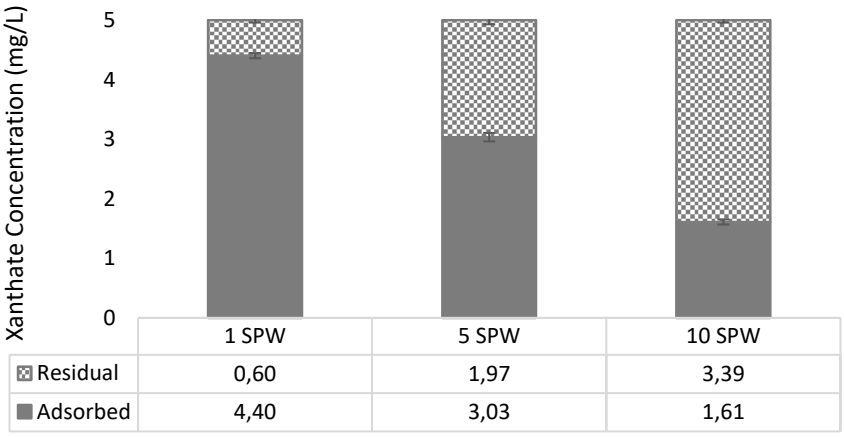

Figure 8-5: Collector concentration adsorbed on galena surface and remaining in solution

The residual and adsorbed xanthate concentration in the chalcopyrite system is depicted in Figure 8-6. It can be seen that the amount of xanthate adsorbed does not seem to differ greatly with increases in the ionic strength of the synthetic plant water.

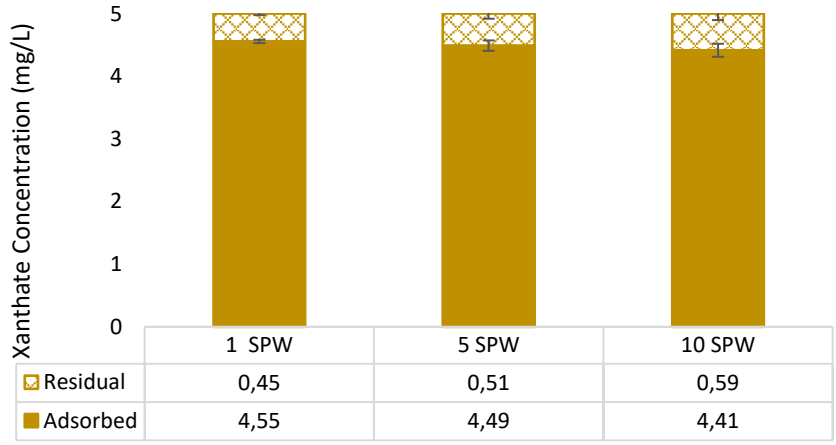

Figure 8-6: Collector concentration adsorbed on chalcopyrite surface and remaining in solution

8.3.3 Effect of Water Quality on Zeta potential

To further understand what happens at the mineral surface under the varying water qualities, it was deemed necessary to study the effect of ionic strength on the zeta potential of the minerals. Figure 8-7 gives an account of the zeta potential of galena with synthetic plant water of increasing ionic strength at pH 6.5. It is clearly evident that ultra-purified water yields the most negative potential of galena particles and that the potential of galena increases with increases in the ionic strength of the synthetic plant water. It should be noted that other studies by October *et al.* (2019) showed a negative zeta potential for both galena and chalcopyrite in ultra-purified water over the pH range 2 to 12. This study also showed that generally the zeta potential of these minerals increased with increasing ionic strength across the pH range.

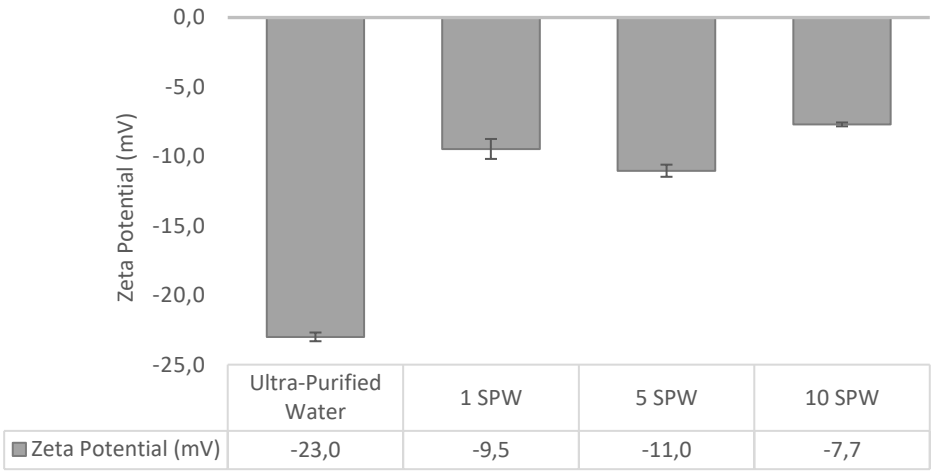

Figure 8-7: Zeta potential of galena under varying water quality at pH 6.5

The zeta potential results observed with galena are largely similar those of chalcopyrite shown in Figure 8-8, where the potential of the chalcopyrite increases with an increase in the ionic strength of synthetic plant water.

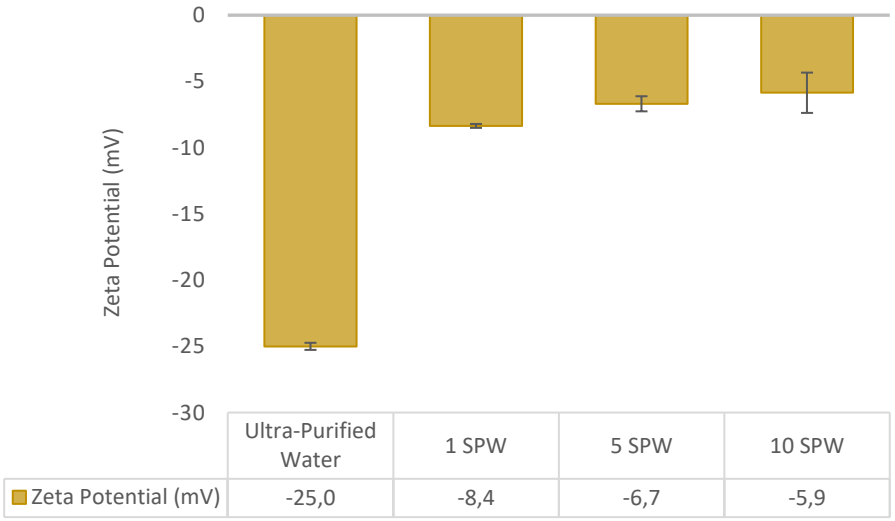

Figure 8-8: Zeta potential of chalcopyrite under varying water quality at pH 6.5

8.4 Discussion

8.4.1 Comparison between the outputs of the ACTA and Microflotation

Although the exact numbers and magnitude of the outputs of these instruments cannot be compared, the trend may be directly compared. Figure 8-9 provides a graphical representation with regard to the output trends of the two techniques under degrading water quality. The galena test work showed a general increase in the mass of particles recovered in the ACTA, while attachment probability did not change with increase in the ionic strength of the plant water. The microflotation tests however corroborated the mass recovered in the ACTA as seen in Figure 8-9 (A). The discrepancy between these two measures may be due to either multiple particles sitting on one bubble or heavy and agglomerated particles being collected when attachment does occur on few bubbles; which would lead to low attachment probability, but high mass recovered. Figure 8-9 (B) represents the chalcopyrite trends in bubble-particle interactions; the two ACTA outputs complement the microflotation trend. A clear trend of an increase in bubble-particle interactions with an increase in ionic strength of water is observed. Generally, the ACTA yielded both reproducible results and brought about results qualitatively comparable to the classical microflotation method. Quantitatively these two methods yield very different results, the ACTA recovery shows an increase of more than tenfold, whilst the increase in microflotation recovery is less than 50%. Due to the dynamic nature of the microflotation technique it may be assumed that plant recovery will resemble the results from this technique closer than that of the ACTA.

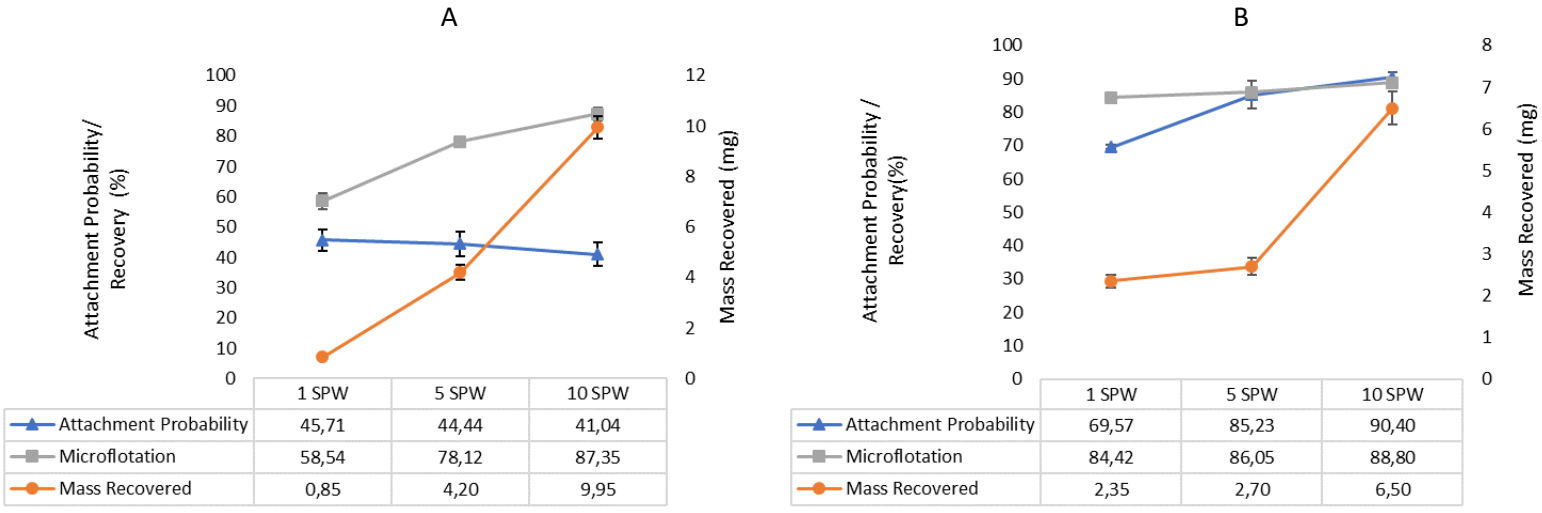

Figure 8-9: Trend comparison of the microflotation and ACTA output (A) galena and (B) chalcopyrite

8.4.2 Effect of Water Quality on Bubble-Particle Interactions

The ACTA and microflotation techniques respectively showed an increase in the bubble-particle attachment and recovery as the ionic strength of the plant water was increased. This result is in agreement with fundamental bubble-particle attachment tests where authors have shown that increases in ionic concentration lead to shorter induction times and ascribed this to the additional ions compressing the electrical double layer, resulting in the faster rupturing of the liquid film which makes bubble particle

attachment occur faster (Wang *et al.,* 2015; Yoon and Yordan, 1991; Laskowski and Iskra, 1970). These authors have also referred to certain ions in water having a "bridging" effect between negatively charged particles and negatively charged collector molecules, thus resulting in an increase in particle hydrophobicity. Other studies have however shown that in the presence of a collector, mineral hydrophobicity is reduced in saline waters due to the presence of oxyhydroxyl, carbonate and sulfoxy species (Ikumapayi *et al.,* 2012; Kirjavainen *et al.,* 2002; Hodgson and Agar, 1984).

8.4.3 Effect of Water Quality on Collector Adsorption

The adsorption of xanthate on the galena surface decreased as the ionic concentration of the plant water increased, this is in agreement with studies that have proposed that inorganic electrolytes compete with xanthate collector for adsorption on the mineral surface or that the amount of xanthate available for adsorption on the surface is reduced due to the formation of insoluble complexes between the collector and ions (Hodgson and Agar, 1984; Fuerstenau and Somasundaran, 2003; Ikumapayi *et al.,* 2012; Laskowski, 2013). Considering that the galena surface adsorbs less xanthate as the ionic strength of the water increases, it is expected that the galena particles will be less floatable; this was however not observed in this investigation as microflotation recovery, showed increases with deteriorating water quality. This suggests another mechanism having a greater effect on the galena bubble-particle attachment than xanthate adsorption; which may be related to the charge of the particles. Microflotation tests showed that in a chalcopyrite-SIBX system, high recoveries are achieved, regardless of the water quality, and may be due to the floatable nature of chalcopyrite. This result is further reinforced by the high xanthate adsorption on the chalcopyrite surface regardless of the water quality. Kinetics studies by Mustafa *et al.* (2004) showed that equilibrium of xanthate adsorption on chalcopyrite is established within ten minutes. It may thus be for this reason the effect of xanthate adsorption is more evident on the galena surface than with chalcopyrite.

A difference in the chalcopyrite recovery is however clearly evident in the absence of a collector. Thus, also suggesting that there is another mechanism having a significant impact on the bubble-particle attachment in solutions of high ionic strength.

8.4.4 Effect of Water Quality on Mineral Zeta Potential

The sulfide minerals in this study showed a very negative potential in ultra-purified water and became less negative as the ionic strength of the water was increased. This is indicative of the adsorption of metal cations on the mineral surface and the compression of the electrical double layer (Moignard *et al.,* 1977). As previously described, this may lead to a faster thinning of the water between the solid particle and the air bubble improving bubble-particle interactions. Due to increases in inorganic electrolytes in the bulk solution, counter-ions enter the Stern layer which in turn thicken the diffuse layer due to an increase in attraction force and decrease in repulsion force (Wang and Peng, 2014). Thus, the compression of the electrical double layer in high ionic strength solutions may promote particle aggregation; particle aggregation is common when the potential is close to 0 mV (Salopek *et al.,* 1992; Wang and Peng, 2014). This work was conducted at pH of 6.5, the potential of the minerals, particularly at 10 SPW is closer to 0 mV. In addition

to faster rupturing of the water film between the bubble and particle, particle agglomeration may also be responsible for the increase in bubble-particle attachment with increasing ionic strength of the plant water. It should also be noted that the zeta potential of the bubble is affected by the solution pH, concentration of electrolytes and type of metal ions present in the solution Yang *et al.* (2001) and thus this may be important to investigate in future studies.

8.5 Conclusions

This investigation showed that the results from the ACTA qualitatively showed similar trends as that of the classical microflotation technique for measuring floatability. Although the magnitude of the results from these two techniques are very different, the ACTA may be useful in showing the effect of changing a parameter on bubble-particle attachment when studying trends become important. From a practical perspective although microflotation tests are faster, the ACTA set-up is more compact and less labour intense due to its automation.

In terms of the effect of water quality on bubble-particle attachment, both microflotation and ACTA showed that the bubble-particle attachment increased with increases in the concentration of inorganic electrolytes in plant water. Both chalcopyrite and galena showed an increase in zeta potential as the concentration of inorganic electrolytes in the synthetic plant water increased. In terms of xanthate adsorption, an obvious decrease in xanthate adsorption on the galena surface was noted as the ionic strength of the plant water increased, while the xanthate adsorption on chalcopyrite seemed unaffected by the water quality.

The increase in zeta potential of the mineral particles as the ionic strength of water increases as seen in the experimental results may potentially be as a result of electrical double layer compression as shown in previous studies or charge neutralisation. EDL compression is known to ultimately lead to an increase in bubble-particle attachment; meaning that although less xanthate was adsorbed on the galena surface with deteriorating water quality, the effect of the increase in zeta potential of the mineral surface appeared to override this adsorption.

Furthermore, the galena-10 SPW system showed a large concentration of unabsorbed xanthate. Thus, a lower xanthate concentration should be considered in future studies to ascertain whether the same effect of increasing ionic strength of water results in lower collector adsorption on the mineral surface.

8.6 Acknowledgements

This work is financed by the National Research Foundation of South Africa (NRF) [Grant number 103641] and this project has received funding from the European Union H2020 programme under grant agreement No 730480. Any opinion, finding and conclusion or recommendation expressed in this material is that of the authors and the NRF does not accept any liability in this regard. Further the financial and technical contributions from the South African Minerals to Metals Research Institute (SAMMRI) is also acknowledged.

8.7 References

Albijanic, B., Ozdemir, O., Nguyen, A. & Bradshaw, D. (2010). A review of induction and attachment times of wetting thin films between air bubbles and particles and its relevance in the separation of particles by flotation. Advances in Colloid and Interface Science. 159: 1-21.

Albijanic, B., Amini, E., Wightman, E., Ozdemir, O., Nguyen, A. & Bradshaw, D. (2011). A relationship between bubble-particle attachment time and the mineralogy of a copper-sulphide ore. Minerals Engineering. 24: 1335-1339.

Aspiala, M., Schreithofer, N., Serna-Guerrero, R. (2018). Automated contact time apparatus and measurement procedure for bubble-particle interaction analysis. Minerals Engineering, 121(1):77-82.

Biçak, Ö.; Ekmekçi, Z.; Can, M.; Öztürk, Y (2012). The e_ect of water chemistry on froth stability and surface chemistry of the flotation of a Cu-Zn sulfide ore. International Journal of Minerals Processing. 102–103, 32–37.

Boujounoui, K., Abidi, A, Bacaoui, A., Amari, K.E.I. & Yaacoubi, A. (2015). The influence of water quality on the flotation performance of complex sulphide ores: case study at Hajar Mine, Morocco. Journal of the South African Institute of Mining and Metallurgy, 1243-1251.

Bradshaw, D. & O'Connor, C. (1996). Measurement of the sub-process of bubble loading in flotation. Minerals Engineering. 9: 443-448.

Castelyn, D. (2012). The effect of mixing thiol collectors in theflotation of pure sulphide ores. MSc.Eng Thesis, University of Cape Town, Faculty of Engineering and the Built Environment, Chemical Engineering Department, Cape Town, South Africa.

Corin, K.C. & Wiese, J.G. (2014). Investigating froth stability: a comparative study of ionic strength and frother dosage. Miner. Eng. 66–68, 130–134.

Fuerstenau, D. W. (1982). Mineral-water interfaces and the electrical double layer. In R. P. King, Principle of flotation. Johannesburg: SAIMM.

Fuerstenau, M.C., Somasundaran, P. (2003). Flotation. In: Fuerstenau, M.C., Han, K. (Eds.), Principles of Mineral Processing. Society for Mining, Metallurgy, and Exploration (SME), Littleton, Colorado, pp. 245–306.

Glembotsky, V.A. (1953). The time of attachment of bubbles to solid particles in flotation and its measurement. Lzv. Akad. Nauk SSSR, Otd. Tckhn. Nauk. 11, 1524–1531.

Gu, G., Xu, Z., Nandakumar, K. & Masliyah, J. (2003). Effects of physical environment on induction time of air-bitumen attachment. International Journal of Mineral Processing. 69: 235-250.

Hodgson, M. & Agar, G.E. (1989). Electrochemical investigations into the flotation chemistry of pentlandite and pyrrhotite: Process water & xanthate interactions. Canadian Metallurgical Quarterly 28 (3), 189 – 198.

Ikumapayi, F., Makitalo, M., Johansson, B. & Rao, K.H. (2012). Recycling of process water in sulphide flotation: Effect of calcium and sulphate ions on flotation of galena. Minerals Engineering. 39: 77-88.

Kirjavainen, V., Schreithofer, N. & Heiskanen, K. (2002). Effect of some process variables on flotability of sulfide nickel ores. International Journal of Mineral Processing. 65: 59-72.

Laskowski, J. & Iskra, J. (1970). Role of capillary effects in bubble-particle collision in flotation. Transactions of the Institution of Mining and Metallurgy. 79, C6.

Laskowski, J.S. (2013). From amine molecules adsorption to amine precipitate transport by bubbles: a potash ore flotation mechanism. Minerals Engineering. 45, 170–179.

Manono, M.S., Corin, K.C. & Wiese, J.G. (2012). An investigation into the effect of various ions and their ionic strength on the flotation performance of a platinum bearing ore from the Merensky reef. Minerals Engineering. 36-38, 231-236.

Mhlanga, S. (2011). Investigating the relative adsorption of polymeric depressants on pure minerals. MSc.Eng Thesis, University of Cape Town, Faculty of Engineering and the Built Environment, Chemical Engineering Department, Cape Town, South Africa.

Moignard, M.S., James, R.O., Healy, T.W. (1977). Adsorption of calcium at the zinc sulphide–water interface. Australian Journal of Chemistry 30, 733–740.

Mustafa, S., Hameed, A. & Naeem, A. (2004). Xanthate adsorption studies on chalcopyrite ore. International Journal of Mineral Processing. 74: 317-325.

October, L., Corin, K., Schreithofer, N., Manono, M. & Wiese, J. (2019). Water quality effects on bubble-particle attachment of pyrrhotite. Minerals Engineering, 131, 230-236.

October, L., Corin, K., Schreithofer, N., Manono, M. & Wiese, J. (2019). Considering the Ionic Strength and pH of Process Water on Bubble-Particle Attachment of Sulfide Minerals: Implications for Froth Flotation in Saline Water. In Mine Water-Technological and Ecological Challenges; Khayrulina, E., Wolkersdorfer, C.H., Polyakova, S., Bogush, A., Eds.; Perm State University: Perm, Russia, pp. 437–445.

Salopek, B., Krasic, D., Filipovic, S. (1992). Measurement and Application of Zeta-Potential. Rudarsko-Geolosko-Naftni Zbornik 4, 147–151.

Slatter, K.A., Plint, N.D., Cole, M., Dilsook, V., De Vaux, D., Palm, N., Oostendorp, B. (2009). Water Management in Anglo Platinum Process Operations: Effects of Water Quality on Process Operations. In: Abstracts of the International Mine Water Conference, Pretoria, South Africa, 19th – 23rd October 2009 Proceedings ISBN Number: 978-0-9802623-5-3. pp. 46–55.

Sven-Nilsson, I. (1934). Einfluß der Berührungszeit zwischen Mineral und Luftblase bei der Flotation. Kolloid-Zeitschrift 69, 230–232.

Yang, C., Dabros, T., Li, D., Czarnecki, J. & Masliyah, J.H. (2001). Measurement of the zeta potential of gas bubbles in aqueous solutions by microelectrophoresis method. Journal of Colloid and Interface Science. 243, 128–135. doi:10.1006/jcis.2001.7842.

Ye, Y. & Miller, J.D. (1989). Induction-time measurements at a particle bed. International Journal of Mineral Processing. 25 (3-4): 221-240.

Yoon, R. & Yordan, J.L. (1991). Induction-time measurements for the quartz-amine flotation system. Journal of Colloid and Interface Science. 141 (2): 374-383.

Wang, B. & Peng, Y. (2014). The effect of saline water on mineral flotation - A critical review. Minerals Engineering. 6, 13–24.

Wang, J., Xie, L., Lui, Q., Zeng, H. (2015). Effects of salinity on xanthate adsorption on sphalerite and bubble-sphalerite interactions. Minerals Engineering. 77, 34–41.

Wiese, J., Harris, P., Bradshaw, D. (2005) The influence of the reagent suite on the flotation of ores from the Merensky reef. Minerals Engineering. 18, 189–198.

Chapter 9 **Considering the Ionic Strength and pH of Process Water on Bubble-Particle Attachment of Sulfide Minerals: Implications for Froth Flotation in Saline Water**

Parts of this paper was presented and features in the published proceedings of the International Mine Water Association 2019 Conference (IMWA2019). Mine Water – Technological and Ecological Challenges. ISBN Number: 978-5-91252-145-4. p. 437 – 445 Perm, Russia

-It must be noted that the natural pH data (with collector) comes from Chapter 8.

Preceding chapters studied the effect of increasing ionic strength of plant water on the attachment of sulfide mineral particles to air bubbles in terms of fundamental bubble-particle attachment and microflotation experimental methods. Furthermore, the drivers responsible for changes in bubble-particle interactions under changes in water quality in terms of collector adsorption and sulfide mineral potential were largely investigated in Chapter 6 and Chapter 8.

Due to recycled process water consisting of varying streams of the process, the proportions of the dissolved solids will vary and may affect the pH of the system. This chapter considers the effect of increasing ionic strength of plant water at an elevated pH of 11; this was chosen as concentrators may very well operate at this pH upon the use of recycled plant water. Studies have been done assessing the effect of an elevated pH of 11 on mineral recoveries in batch flotation systems; however there seems to be a gap in understanding what happens fundamentally at the bubble-particle level under process water experiencing a combined effect of increasing ionic strength and pH. These parameters are important to study simultaneously because complex water systems at high pH values, may result in the formation of various oxyhydroxo complexes compromising the flotation efficiency.

Similar to work presented in Chapter 7 on a pyrrhotite system, this study explores how these complex water systems (of increasing ionic strength and pH) affect bubble-particle interaction of galena and chalcopyrite. This work also assesses the zeta potential of the sulfide mineral particles under these conditions.

Considering the Ionic Strength and pH of Process Water on Bubble-Particle Attachment of Sulfide Minerals: Implications for Froth Flotation in Saline Water

L.L. October[1], K.C. Corin[1], M.S. Manono[1], N. Schreithofer[2] and J.G. Wiese[1]

1Centre for Minerals Research, Department of Chemical Engineering, University of Cape Town, Private Bag X3, Rondebosch 7701, South Africa, Kirsten.Corin@uct.ac.za

2 Department of Bioproducts and Biosystems, Clean Technologies Research Group, Aalto University, Vuorimiehentie 1, 02150 Espoo, Finland

Abstract

Due to the current climate of water scarcity in mining areas and the fact that water treatment is costly; the recirculation of process water seems to be a viable option in mineral processing. A consequence of the recirculation of water is the build-up of ions such as Ca^{2+}, Mg^{2+}, Na^{+}, SO_4^{2-} and NO_3^{-} as well as increases in pH. This study thus considers the combined effect of increasing ionic strength and pH of process water on the froth flotation process. These parameters are important to study simultaneously because complex water systems at high pH values, may result in the formation of various hydroxo complexes compromising the flotation efficiency.

Both bubble-particle attachment tests and microflotation show decreases in attachment and sulfide recovery as the pH is increased to 11. However, at the elevated pH the recovery increases as the ionic strength (water recycles) is increased. This could be due to the compression of the electrical double layer by the indifferent ions as seen by the zeta potential measurements. Zeta potential measurements also show steep increases in the potential of the sulfide minerals at pH 11.

Although this work suggests that process water with a pH as high as 11 will result in decreased mineral recoveries, it has been shown that at increased levels of ionic strength (increased recirculation of process water) higher recoveries can be obtained. Thus, it can be concluded that if the pH of process water was to reach a pH of 11, the combined effect of recirculation of process water would not necessarily have detrimental effects on sulfides flotation performance.

Keywords: Bubble-particle Attachment, Ionic Strength, pH, Synthetic Plant Water

Graphical Abstract

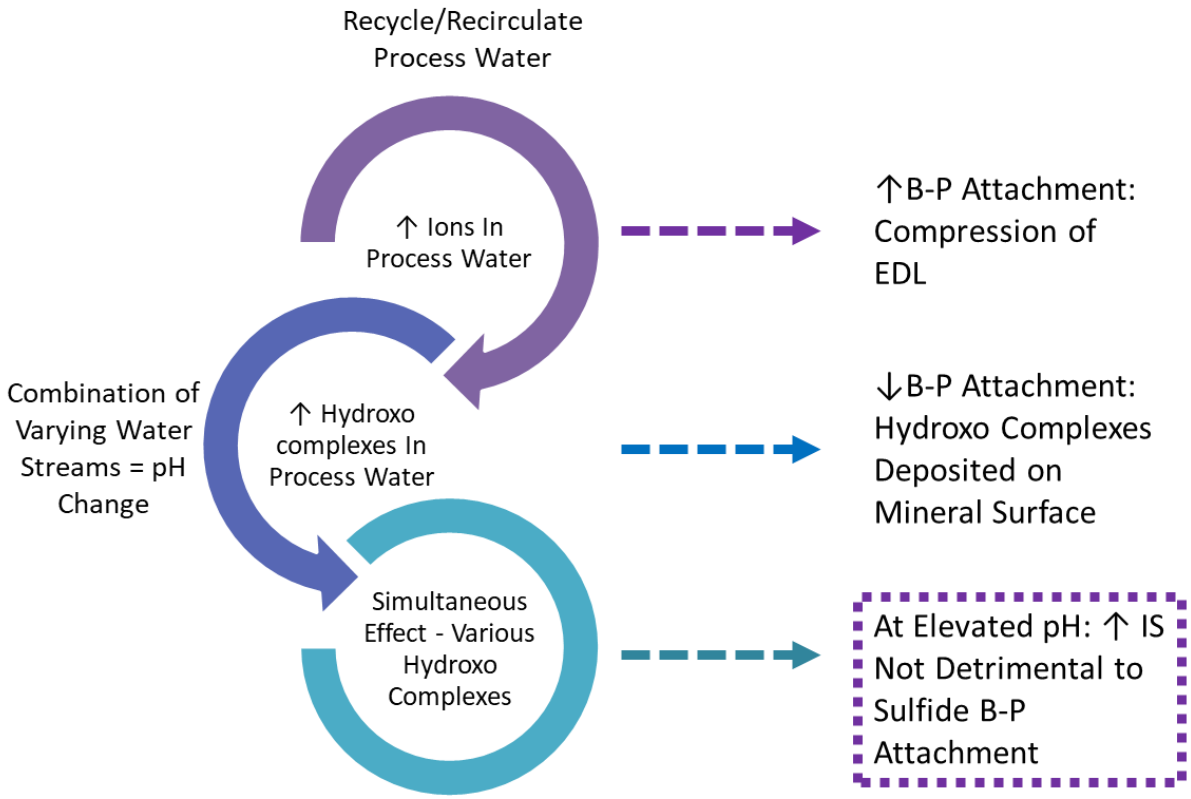

9.1 Introduction

Froth flotation takes advantage of a minerals surface properties as a means of separating valuable minerals from non-valuable gangue. When air is introduced into the mineral slurry, the hydrophobic particles (most often valuables) attach to the air bubbles and rise into the froth phase where they are eventually collected. Whereas the hydrophilic, (most often non-valuable) particles stay in the pulp zone (Wills and Finch, 2016).

This process thus depends on the attachment of particles to air bubbles; which makes the bubble-particle attachment sub-process critical in achieving the separation of valuables from non-valuables (Albijanic *et al.,* 2010).

Water scarcities in parts of the world with massive mining industries have led to recycled process water and sea water usage gaining huge interest in the mining industry. These water types are of high ionic strength and therefore their water chemistry is very different to that of fresh water and may negatively affect the froth flotation process (Rao and Finch, 1989). Recycled process water is a combination of varying water streams from the process thus the proportions of dissolved solids will vary and affect the pH of the system (Levay et al., 2001). It is therefore valuable to understand how a change in pH in recycled process water will affect the flotation process.

It has been proposed that upon the addition of electrolytes, the electrical double layer is compressed which lead to the accelerated rupturing of the wetting film at the air-water and solid-water interface and in turn assists in faster bubble-particle attachment (Laskowski and Iskra, 1970; Li and Somasundaran, 1993; Harvey *et al.*, 2002; Laskowski and Castro, 2015).

Manono *et al.* (2017) and Tadie *et al.* (2016) both reported a decrease in solids recovery with process water at elevated pH values in a flotation system and attributed this to the hydroxo complexes and its possible precipitation on the mineral surface, hence imparting hydrophilicty on the particles. This study thus looks at the simultaneous effect of increasing ionic strength and pH from both a flotation and fundamental bubble-particle attachment perspective in a chalcopyrite and galena system respectively.

9.2 Materials and Methods

9.2.1 Mineral Sample

1 kg of Galena and 1 kg of Chalcopyrite obtained from Ward's Science was crushed using a hammer to 100% passing 1000 microns. The respective sulfide mineral particles were then pulverized and sieved through 125, 106, 75 and 38 μm sieves to obtain size fractions of 38-75 μm and 106 -125 μm for the microflotation and attachment time tests respectively. The fraction below 38 microns was used for the zeta potential measurements. The two minerals in the 3 size fractions of interest (106-125 μm, 38-75 μm and <38 μm) were split, purged with nitrogen and refrigerated.

9.2.2 Water Quality

Standard synthetic plant water (1 SPW) as described by Wiese *et al.* (2005) was used as the baseline synthetic plant water for the test programme. In order to simulate the recycle, the amount of dissolved solids was increased five and ten times making up 5 SPW and 10 SPW respectively. The ionic concentrations of the three synthetic plant waters are depicted in Table 9-1.

Table 9-1: Concentrations of ions for the various water qualities

Water type	Ca^{2+} ppm	Mg^{2+} ppm	Na^{+} ppm	Cl^{-} ppm	SO_4^{2-} ppm	NO_3^{-} ppm	CO_3^{2-} ppm	TDS mg/L	Ionic Strength mol/L
1SPW	**80**	**70**	**153**	**287**	**240**	**176**	**17**	**1023**	**0.0241**
5 SPW	**400**	**350**	**765**	**1435**	**1200**	**880**	**85**	**5115**	**0.1205**
10 SPW	**800**	**700**	**1530**	**2870**	**2400**	**1760**	**170**	**10230**	**0.241**

9.2.3 Reagents

Sodium isobutyl xanthate (SIBX) - 97% purity, from Senmin was used as the collector in the microflotation and bubble-particle attachment tests. 1% w/v collector solutions were made fresh daily, this equates to 0.06

mol/L of xanthate solution. 1% w/v solutions of NaOH and HCl were made daily and used for pH adjustments. Both NaOH and HCl were supplied from Merck.

9.2.4 Attachment Time Tests

The attachment timer used in this investigation, the automated contact time apparatus (ACTA) was developed at Aalto University and has been described by Aspiala *et al.* (2018) and October *et al.* (2019). A detailed description of the experimental procedure in terms of particle bed building and running measurements is documented in October *et al.* (2019). Measurements were taken for each of the water qualities in Table 1. It is important to note that measurements were taken for each water quality and mineral mixture at the natural pH and at pH 11 in the presence of the collector SIBX (50 g/t). Further, these tests were performed in duplicate for each condition to minimise experimental error.

9.2.5 Microflotation Tests

The microflotation cell developed by Bradshaw and O'Connor (1996) was used to perform the microflotation tests in this work. 3 g of the respective sulfide minerals was mixed with 50 mL of the particular water quality under study and the pH was adjusted where applicable; the mixture was then ultra-sonicated for 5 minutes to allow for good dispersion of the mineral mixture. The suspension was then transferred to the microflotation cell and the pulp was circulated by a peristaltic pump at 90 rpm. 15 µL of the 1% SIBX solution was added to the slurry which is equivalent to 50 g/t SIBX. Air was then introduced at the base of the cell at a flow rate of 7 mL/min and concentrates were collected at 2, 6, 12 and 20 minutes of flotation. The tailings and four concentrates were then filtered, dried and weighed. The microflotation tests were performed in duplicate to minimise error.

9.2.6 Zeta Potential Measurements

Very dilute mixtures of the particular water type and particles were made up; the dilute mixtures were then equally divided in six containers and the pH was adjusted to 2, 4, 6, 8, 10 and 12 with dilute HCl or dilute NaOH. After 15 minutes on the magnetic stirrer the pH was measured again and adjusted where needed. 1 mL of the suspension was then transferred to the Malvern Dip Cell (Malvern Instruments Ltd., Malvern, UK) and inserted in the Malvern ZetaSizer (Malvern Instruments Ltd., Malvern, UK) where measurements were taken. All zeta potential measurements were performed in triplicate to reduce experimental error.

9.3 Results and Discussion

Figure 9-1 shows the recovery of galena in the microflotation cell for with the various synthetic plant waters at both the natural pH as well as at a pH 11. In terms of the galena recovery at the natural pH it is clear that the recovery increases as the ionic strength of the plant water increases, this can be attributed to the fact that an increase in ions result in the compression of the electrical double layer at the air-water and solid-water interface. This in turn will cause the accelerated rupturing of the film at the air-water and solid-water interface; increasing the attachment of particles to air bubbles (Laskowski and Iskra, 1970; Li and Somasundaran, 1993; Harvey *et al.*, 2002; Laskowski and Castro, 2015). The recovery of galena at the elevated pH reduced drastically compared to at the natural pH. With 1 SPW at a pH of 11 resulting in the

poorest galena recovery. Similar results were obtained by Tadie *et al.* (2016) and this was said to be as a result of the precipitation of hydroxide species on the mineral surface. The recovery does however increase as the ionic strength increases even at the high pH.

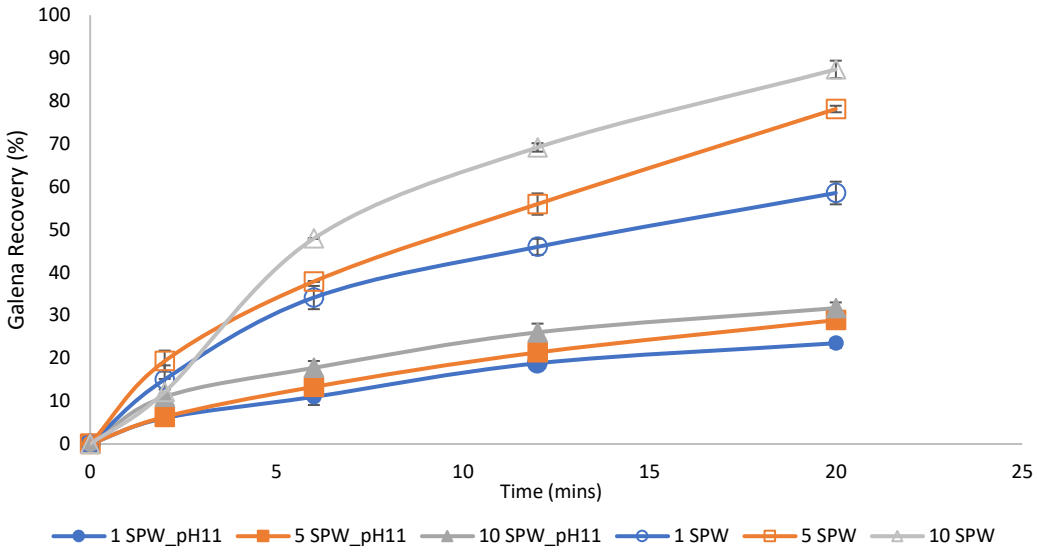

Figure 9-1: Microflotation of Galena with various water qualities

Attachment time tests were further done to understand the effect of increasing pH and ionic strength on the bubble-particle attachment from a fundamental perspective, examining both the probability of attachment and the mass recovered through particle-bubble contacts. It is important to note, that the attachment probability is calculated by dividing the amount of bubbles with one or more attached particles by the total number of bubbles, but does not take into consideration how many particles are actually attached to one particular bubble. In certain experimental conditions particles tend to attach to each other and get recovered as clusters. In these cases relatively large mass of particles can be recovered, even when the quantified attachment probability is low.

Figure 9-2 shows the attachment probability of galena particles to air bubbles with plant water of increasing ionic strength at both the natural pH and elevated pH so as to complement the microflotation results. The attachment contact time apparatus also collects the particles that have successfully attached to the bubbles, the mass recovered of these particles are also depicted in Figure 9-2. In terms of the attachment probability, it is clear that the probability of galena particles attaching to air bubbles are dramatically reduced at the high pH. However, the result of the combined effect of increasing ionic strength at pH 11 on the attachment probability is not clear. Therefore, the result showing the mass of particles that successfully attached to the bubbles prove to be useful. As with the microflotation tests, the mass of galena recovered in the ACTA increases with increasing ionic strength at the natural pH. In addition, at pH 11 the mass recovered is also significantly lower than at the natural pH but the mass recovered does increase with water of high ionic strength even at pH 11. Thus, matching the microflotation results.

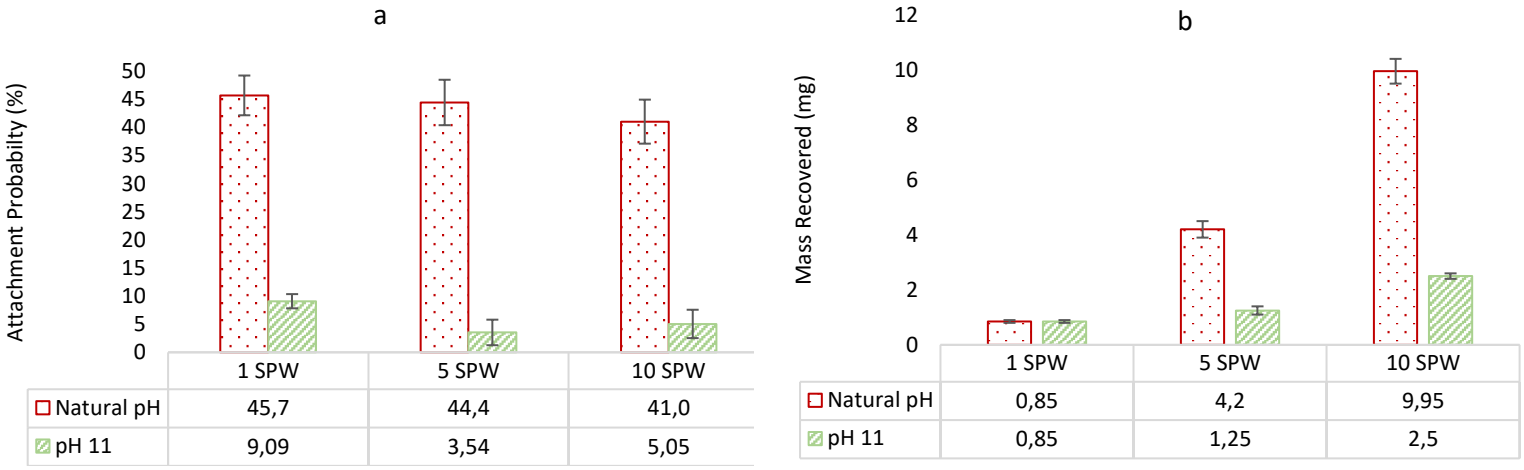

	1 SPW	5 SPW	10 SPW
Natural pH	45,7	44,4	41,0
pH 11	9,09	3,54	5,05

	1 SPW	5 SPW	10 SPW
Natural pH	0,85	4,2	9,95
pH 11	0,85	1,25	2,5

Figure 9-2: Attachment Probability (a) and Mass Recovered of Galena particles under various water qualities

Figure 9-3 shows the recovery of chalcopyrite in the microflotation cell for with the various synthetic plant waters at both the natural pH as well as at a pH of 11. The recovery of chalcopyrite at the natural pH is relatively similar with the three water qualities, this is possibly due to the floatable nature of chalcopyrite. However, the recovery of chalcopyrite with the highest ionic strength plant water does give a better recovery, as with galena this is attributed to the compression of the electrical double layer in waters of high ionic concentration. Similarly, as with galena the chalcopyrite recovery at the elevated pH is reduced drastically compared to at the natural pH. With 1 SPW at a pH of 11 resulting in the poorest chalcopyrite recovery. The recovery does however increase as the ionic strength increases even at the high pH.

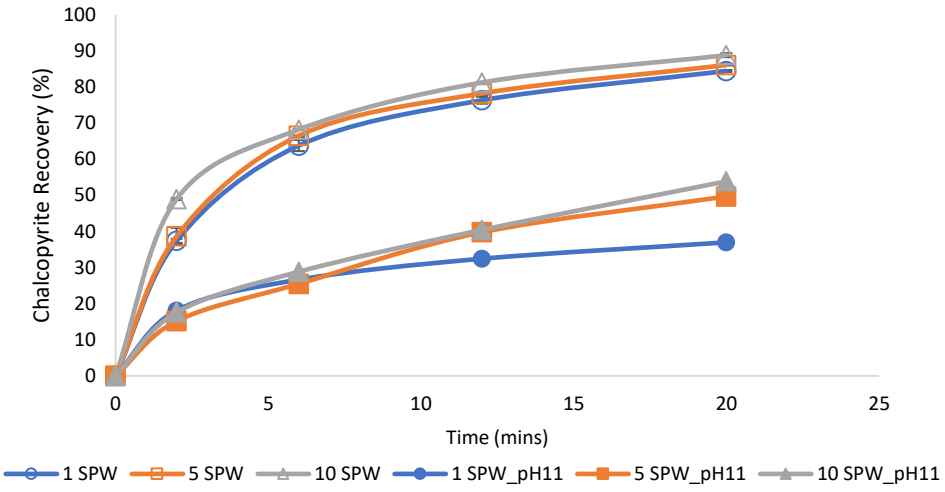

Figure 9-3: Microflotation of Chalcopyrite with various water qualities

Figure 9-4 shows the attachment probability of chalcopyrite particles to air bubbles with plant water of increasing ionic strength at both natural pH and elevated pH as well as the mass of particles recovered at the conditions under study. Both the attachment probability and mass recovered perfectly matches the results of the microflotation. Thus, reinforcing the trend of a decrease in bubble-particle attachment at an

increased pH but at a higher pH the bubble-particle attachment increases with waters of higher ionic strengths in both a flotation system as well as a fundamental bubble-particle attachment system.

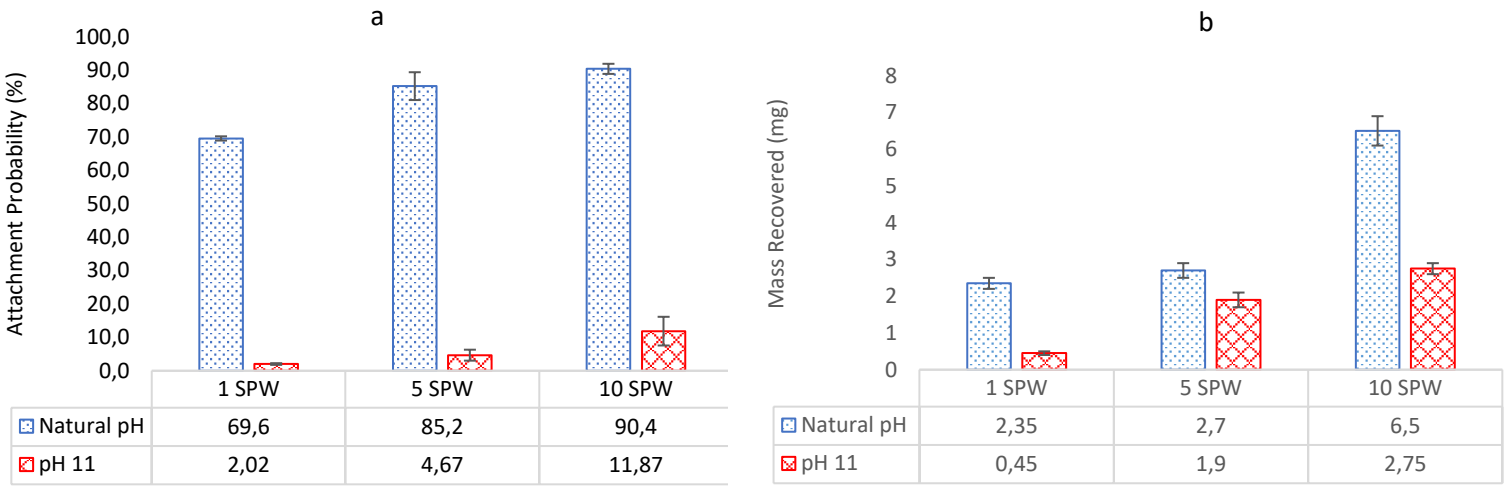

	1 SPW	5 SPW	10 SPW
Natural pH	69,6	85,2	90,4
pH 11	2,02	4,67	11,87

	1 SPW	5 SPW	10 SPW
Natural pH	2,35	2,7	6,5
pH 11	0,45	1,9	2,75

Figure 9-4: Attachment Probability (a) and Mass Recovered Chalcopyrite particles under various water qualities

Figure 9-5 show the zeta potential of galena (a) and chalcopyrite (b) under the various water qualities. Both sulfide minerals display a similar trend in terms of charge on the mineral; with the zeta potential becoming less negative with increase in ionic strength of the synthetic plant water. This phenomenon is indicative of the compression of the electrical double layer as the ionic concentration of the water increases (Moignard *et al.,* 1977). This result was also observed by October *et al.* (2019) in a pyrrhotite system as well as Ikumapayi *et al.* (2012) in a galena system. These authors attribute this to be due to the increased passivation of the mineral surface by the increasing cation concentration. Upon closer study of these zeta potential results, an increase in potential with all the synthetic plant water is observed between pH values of 10 and 12. Which is said to be because of metal hydroxide precipitation or oxidation at the mineral surface (Harvey *et al.,* 2002; Ikumapayi *et al.,* 2012; Hirajama *et al.,* 2016). Speciation diagrams as shown by Manono *et al.* (2018) show that at this pH range for these waters, the content of hydroxo species increases substantially with the highest concentration of these species occurring in the 10 SPW plant water at pH values of 11 and above.

A similar study by Manono *et al.* (2017) looking at the interactive effect of ionic strength and pH on a Merensky ore in a batch flotation system also showed a decrease in recovery at pH 11 and this was attributed to the increase in hydroxo complexes. While, Fuerstenau *et al.* (1999) proposed that in alkaline conditions metal ions hydrolyze and deposit hydrophilic metal hydroxides on the mineral surface. The decrease in sulfide mineral bubble-particle attachment at pH 11 from this more fundamental study considering pure minerals may also be attributed to the increase in hydroxo complexes deposited on the mineral surface as supported by the zeta potential measurements in Figure 9-5. This deposition of hydrophilic metal hydroxides on the mineral surface will also hinder the adsorption of the collector on the mineral surface, decreasing the bubble-particle attachment (Rao, 2004).

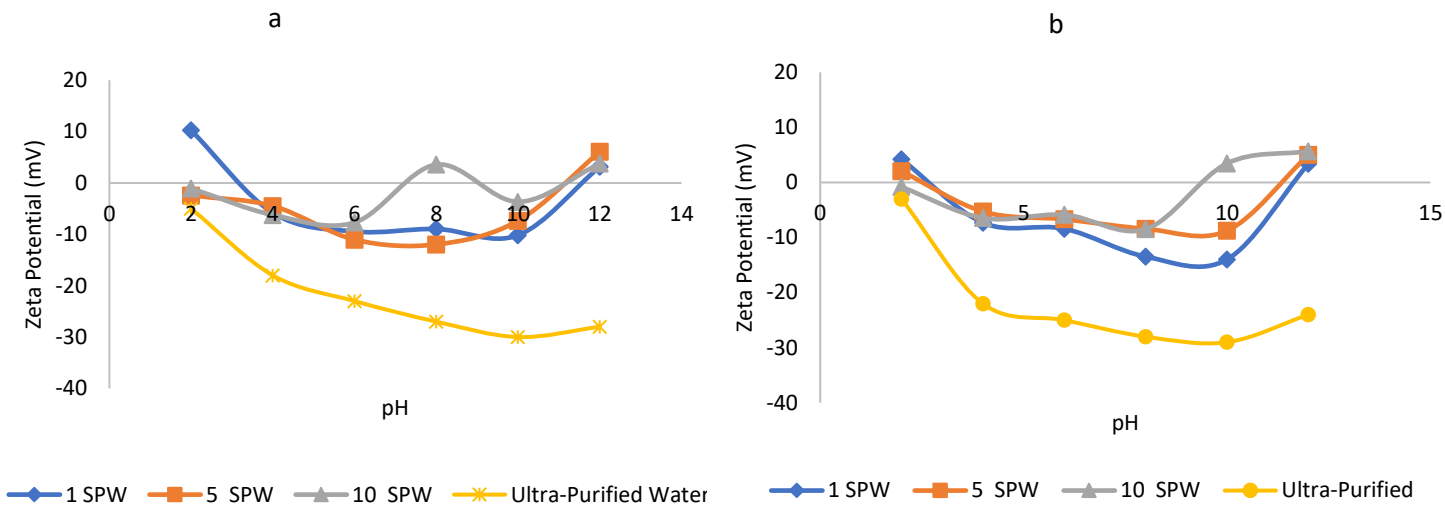

Figure 9-5: Zeta Potential of Galena (a) and Chalcopyrite (b) under various water qualities

The bubble-particle attachment results both fundamental and microflotation shows how the attachment of sulfide mineral particles to air bubbles increases with waters of higher ionic strength which is due to the compression of the electrical double layer as reinforced by Figure 9-5. At a high pH the bubble-particle attachment decreases significantly but however still increases with increasing ionic strength. It would be expected that a high pH and high ionic strength water would result in the poorest performance as the hydroxide concentration is even higher, but this is not the case demonstrating the effect of the compression of the electrical double layer even in alkaline solutions.

9.4 Conclusions

Fundamental bubble-particle attachment tests and microflotation tests show a significant decrease in the attachment of sulfide minerals to air bubbles with synthetic plant water at a pH of 11. This has been attributed to the increase in hydroxo complexes present at this pH, these species are known to induce hydrophilicity upon the particles or hinder the action of the collector. It is thus speculated that this may be reason for lower recoveries at the higher pH. This work does however show that increases in sulfide mineral recovery can be attained at a high pH with plant water of high ionic strengths.

9.5 Acknowledgements

This work is financed by the National Research Foundation of South Africa (NRF) [Grant number 103641] and this project has received funding from the European Union H2020 programme under grant agreement No 730480. Any opinion, finding and conclusion or recommendation expressed in this material is that of the authors and the NRF does not accept any liability in this regard. Further the financial and technical contributions from the South African Minerals to Metals Research Institute (SAMMRI) is also acknowledged.

9.6 References

Albijanic, B., Ozdemir, O., Nguyen, A. and Bradshaw, D. (2010). A Review of Induction and Attachment Times of Wetting Thin Films between Air Bubbles and Particles and Its Relevance in the Separation of Particles by Flotation. Advances in Colloid and Interface Science 159 (1). Elsevier B.V.: 1–21. https://doi.org/10.1016/j.cis.2010.04.003.

Aspiala, M., Schreithofer, N., Serna-Guerrero, R. (2018). Automated contact time apparatus and measurement procedure for bubble-particle interaction analysis, Minerals Engineering, 121(1):77-82.

Bradshaw, D. and O'Connor, C. (1996) Measurement of the sub-process of bubble loading in flotation. Minerals Engineering. 9: 443-448.

Fuerstenau, DW, Herrera-Urbina, R, McGlashan, DW (1999) Studies on the applicability of chelating agents as universal collectors for copper minerals. International Journal of Mineral Processing 58, pp 15-33.

Harvey, P.A., Nguyen, A.V. and Evans, G.M. (2002). Influence of Electrical Double-Layer Interaction on Coal Flotation. Journal of Colloid and Interface Science 250 (2): 337–43. https://doi.org/10.1006/jcis.2002.8367.

Hirajima, T., Pandhe, G., Suyantara, W., Ichikawa, O., Mohamed, A., Miki, H. and Sasaki, K. (2016). Effect of Mg^{2+} and Ca^{2+} as Divalent Seawater Cations on the Floatability of Molybdenite and Chalcopyrite. Minerals Engineering 96–97. Elsevier Ltd: 83–93. https://doi.org/10.1016/j.mineng.2016.06.023.

Ikumapayi, F., Makitalo, M., Johansson, B. and Hanumantha, K. (2012). Recycling of Process Water in Sulfide Flotation : Effect of Calcium and Sulphate Ions on Flotation of Galena. Minerals Engineering 39. Elsevier Ltd: 77–88. https://doi.org/10.1016/j.mineng.2012.07.016.

Laskowski, J., and Castro, S. (2015). Flotation in Concentrated Electrolyte Solutions. International Journal of Mineral Processing. 144, 50-55.

Laskowski, J. and Iskra, J. (1970). Role of capillary effects in bubble-particle collision in flotation. Transactions of the Institution of Mining and Metallurgy. 79, C6.

Levay, G., Smart, RStC, and Skinner, W. M. (2001). The impact of water quality on flotation performance. Journal of the South African Institute of Mining and Metallurgy, 101, 69-75.

Li, C. and Somasundaran, P. (1993). Role of Electrical Double Layer Forces and Hydrophobicity in Coal Flotation in NaCl Solutions. Energy and Fuels 7 (2): 244–48. https://doi.org/10.1021/ef00038a014.

Manono, M.S., Matibidi, K., Thubakgale, C.K., Corin, K.C., Wiese, J.G. (2017). Water Quality in PGM Ore Flotation: Depressing and Frothing Effects Of The Ionic Strength Of Plant Water And pH. In Proceedings of 13th International Mine Water Association Congress, Paper 1125, Finland, Lappeenranta, 25-30 June

Manono, M.S, Corin, K.C. and Wiese, J.G. (2018). Perspectives from Literature on the Influence of Inorganic Electrolytes Present in Plant Water on Flotation Performance. Physicochemical Problems of Mineral Processing 54 (4): 1191–1214. https://doi.org/10.5277/ppmp18157.

Moignard, M.S., James, R.O., Healy, T.W. (1977). Adsorption of calcium at the zinc sulfide–water interface. Australian Journal of Chemistry 30, 733–740.

October, L.L., Corin K.C., Schreithofer, N., Manono, M.S., Wiese, J.G. (2019). Water Quality Effects on Bubble-Particle Attachment of Pyrrhotite. Minerals Engineering 131. Elsevier Ltd: 230–236. https://doi.org/10.1016/j.mineng.2018.11.017.

Rao, S.R., Finch, J.A. (1989). A review of water re-use in flotation. Minerals Engineering 2 (1), 65–85.

Tadie, M, Corin, K, Wiese, J, O'Connor, C, (2016) Application of potential control to the flotation of galena by varying dissolved oxygen, pH and ionic strength levels. Presented at the XXVIII Mineral Processing Congress (IMPC2016), Quebec City, Canada.

Wiese, J., Harris, P., Bradshaw, D. (2005). The influence of the reagent suite on the flotation of ores from the Merensky reef. Minerals Engineering. 18, 189–198. doi:10.1016/j.mineng.2004.09.013.

Wills, B.A. and Finch, J.A. (2016). WILLS' Mineral Processing Technology, An introduction to the practical aspects of ore treatment and mineral recovery. Eighth Edition. Butterworth-Heinemann Elsevier.

Chapter 10 **A Fundamental Study Considering Specific Ion Effects on the Attachment of Sulfide Minerals to Air Bubbles**

Published in Minerals Engineering 151 pp: 106313. https://doi.org/10.1016/j.mineng.2020.106313

The results from "Fundamental and Flotation Techniques Assessing the Effect of Water Quality on Bubble-Particle Attachment of Chalcopyrite and Galena" presented in Chapter 8 showed that the results from the ACTA corroborated well with that of the classical microflotation technique for measuring floatability. This correlation was further reinforced by the mass of particles recovered in the collection bin which was possible due to the increase in particle size of -125+106 microns as opposed to the -75+38 microns used in the investigation "Water Quality Effects on Bubble-particle Attachment of Pyrrhotite" which did not collect any particles. Furthermore, reducing the contact time on the ACTA from 100 and 200 ms as per Water Quality Effects on Bubble-particle Attachment of Pyrrhotite" to 50 ms did show a difference attachment probability across varying water qualities even if a highly floatable mineral such as chalcopyrite.

This study "A Fundamental Study Considering Specific Ion Effects on the Attachment of Sulfide Minerals to Air Bubbles" published in Minerals Engineering and presented as Chapter 10 aims to determine if there are specific ions in plant water that are either beneficial, detrimental or have no effect on the bubble-particle attachment of galena and chalcopyrite. Phase one of the testwork assessing the effect of specific ions on bubble-particle attachment has been described in Chapter 7. Chapter 7 studied pyrrhotite and used the initial operational setting on the ACTA. Chapter 10 however aims to assess the impact of specific ions on bubble-particle interactions with chalcopyrite and galena under the ACTA operating conditions which were deemed comparable to microflotation for studying mineral floatability.

Chapter 10 further aims to explain the differences in the behaviour of bubble-particle interactions under various single salt solutions through studying the effect that these solutions have on the zeta potential of the mineral as well as their effect on collector adsorption.

A Fundamental Study Considering Specific Ion Effects on the Attachment of Sulfide Minerals to Air Bubbles

L.L. October[1], K.C. Corin[1], M.S. Manono[1], N. Schreithofer[2] and J.G. Wiese[1]

[1]*Centre for Minerals Research, Department of Chemical Engineering, University of Cape Town, Private Bag X3, Rondebosch 7701, South Africa*

[2] *Department of Bioproducts and Biosystems, Clean Technologies Research Group, Aalto University, Vuorimiehentie 1, 02150 Espoo, Finland*

Abstract

Bubble-particle attachment is one of the most fundamental sub-processes in froth flotation. It is of critical importance in achieving the separation of value from non-value. This sub-process is affected by many factors such as the chemistry of the pulp, action of the reagents, hydrodynamics and operational factors. Understanding the effects of these factors on bubble-particle attachment is thus crucial as they may in turn affect the mineral recoveries attained. With the current drive towards zero effluent discharge on mineral concentrators water quality is an important factor to understand as it can change the pulp chemistry and subsequently affect mineral recoveries. This study thus considers the effect of specific ions found in process water on the bubble-particle attachment of chalcopyrite and galena. Adsorption studies and zeta potential measurements were conducted to interpret the outcomes of the bubble-particle attachment tests. Pulps containing Ca^{2+} resulted in lower bubble-particle attachment probability and recovery of galena and chalcopyrite. Adsorption studies complemented the bubble-particle attachment findings well and showed that in Ca^{2+} containing waters, less xanthate was adsorbed on both the chalcopyrite and galena surfaces. The zeta potential measurements showed an increase in mineral potential with Ca^{2+} containing salts compared to the very negative mineral potential in $NaNO_3$. This work provides evidence of the passivation of the mineral surface with Ca^{2+}; which hindered the adsorption of xanthate on the mineral surface in Ca^{2+} containing solutions and subsequently resulted in poor bubble-particle attachment.

Keywords: Bubble-Particle Attachment, Chalcopyrite, Froth Flotation, Galena, Specific Ions, Water Quality

Graphical Abstract

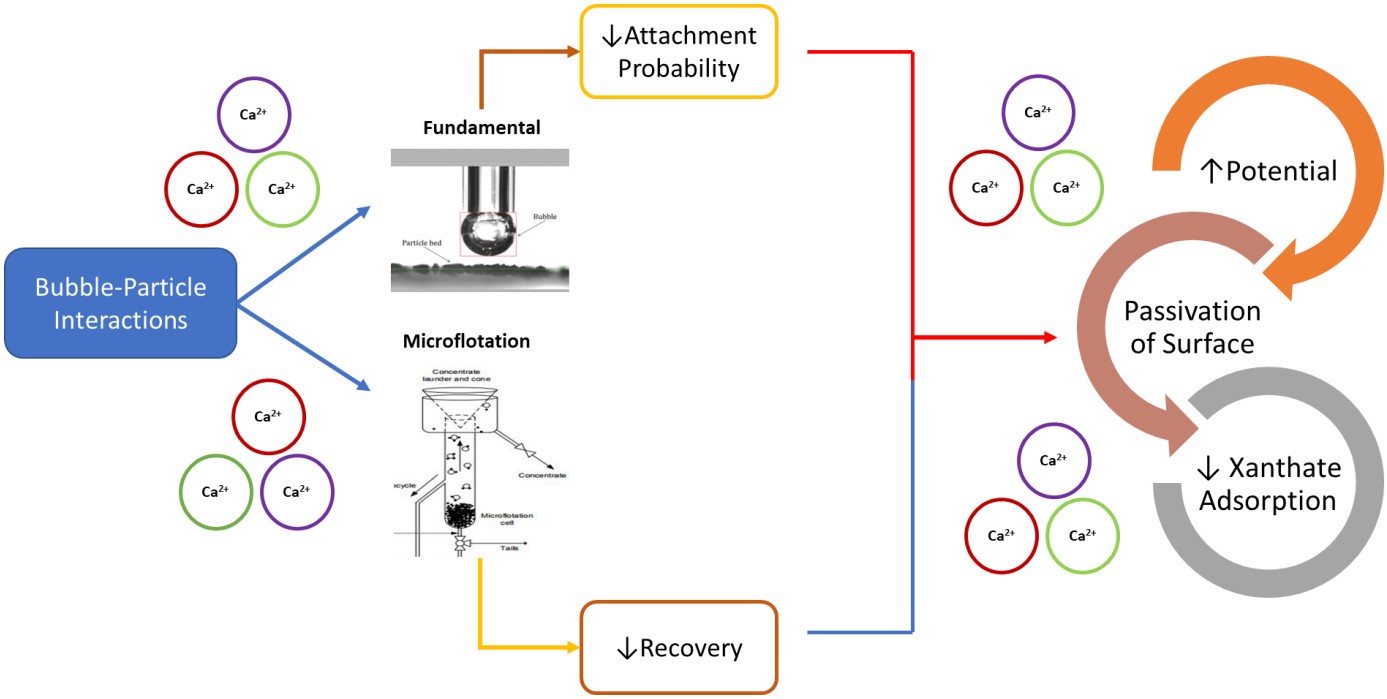

10.1 Introduction

Froth flotation is used as a method of separation in several industrial applications such as in the treatment of wastewater and domestic sewage by dissolved air flotation, de-inking of paper and in mineral processing. In mineral processing, the surface properties of the valuable particles are selectively altered such that they attach to air bubbles and are subsequently removed. The bubble-particle attachment sub-process is thus critical in achieving the desired separation of valuable particles (Albijanic *et al.,* 2010).

Chalcopyrite ($CuFeS_2$) is the most abundant and important cupriferous mineral on earth while galena (PbS) is the most important lead mineral. These respective minerals are often associated with other sulfide minerals and separated by means of froth flotation. Water scarcities challenging parts of the world have led to recycled process water and sea water usage gaining huge interest in the mining industry. These water types are of high ionic strength and thus their water chemistry is very different to that of fresh water and may negatively affect the efficiency of the separation in froth flotation (Rao and Finch, 1989).

Studies have shown that an increase in the ionic strength of process water results in higher solids and water recoveries (Corin *et al.,* 2011; Manono *et al.,* 2012; Corin and Wiese, 2014). Divalent and polyvalent ions are reported to be capable of adsorption on the mineral surface; while alkali metal cations adsorb on the mineral surface via electrostatic attraction without forming permanent chemical bonds with the mineral surface (Ma, 2005). Consequently, the zeta potential is not neutralised by these cations but rather passivated by these ions. The extent of passivation or screening affects the zeta potential of the mineral surface and can lead to the compression of the electrical double layer. It has been proposed that with an increase in the concentration of inorganic electrolytes, the electrical double layer compresses, leading to the accelerated rupturing of the film at the air-water and solid-water interface which leads to bubble-particle attachment

and in turn the recovery of mineral particles (Laskowski and Iskra, 1970; Li and Somasundaran, 1993; Harvey *et al.,* 2002; Laskowski and Castro, 2015).

Previous studies have considered complex synthetic water recipes to replicate conditions on a typical concentrator (October *et al.,* 2019). It is therefore of interest to determine if there are specific ions in plant water that are either beneficial, detrimental or have no effect on the flotation process. Batch flotation studies on a Merensky ore by Manono *et al.* (2016) showed that the Na^+ resulted in higher recoveries but lower mineral grades whereas the NO_3^- resulted in lower recoveries and higher mineral grades. It is however unclear whether there are specific ions in the plant water that have this type of influence on the fundamental bubble-particle attachment process. Both galena recovery and adsorption of xanthate collector on galena have been reported to decrease in the presence of Ca^{2+} (Ikumapayi *et al.,* 2012; Elizondo-Alvarez *et al.,* 2017). Elizondo-Alvarez *et al.* (2017) attributed the decrease of xanthate adsorption on the galena surface to be as a result of chemisorption of Ca^{2+} on active sites, hindering the action of the collector.

The effect that these inorganic electrolytes have on the final mineral recoveries may be due to many factors such as changes in the physicochemical properties of the solution, zeta potential, wetting characteristics and collector adsorption (Du *et al.,* 2014). It is widely known that the presence of ionic solutes affects the water structure. When the structure of water is very strongly hydrogen bonded even in the presence of cations and anions, these ions are termed structure making because they tend to retain the strong hydrogen bonds. Small, strongly hydrated inorganic ions such as Na^+, Li^+, Mg^{2+}, F^- and Cl^- are examples of structure makers. However, large inorganic ions, such as Cs^+ and I^- have the tendency to destroy the strongly hydrogen bonded water structure; these ions are termed structure breakers (Wang and Peng, 2014; Burdukova, 2007; Ma and Pawlik, 2005).

Hancer *et al.* (2001) in a study of KCl flotation proposed that if the collector adsorbs on the salt interface, the interfacial water will be displaced, and the collector will penetrate through the water structure. Therefore, if the water structure is strongly hydrogen bonded as a result of structure making ions, it will be difficult for the collector to adsorb on the mineral surface and in turn negatively affect the recovery. Conversely if the structure of water is destroyed due to structure breaking ions the collector can easily penetrate and adsorb at the mineral surface.

This study considers the effect of specific ions present in process water on bubble-particle interactions by means of fundamental bubble-particle attachment and flotation methods. The results of the bubble-particle interactions from both the fundamental and flotation perspective are then further investigated by studying the impact that these specific ions have on collector adsorption and on the mineral zeta potential. The aim of this study is therefore to determine if there are specific ions in plant water that are either beneficial, detrimental or have no effect on the bubble-particle attachment sub-process.

10.2 Materials and Methods

10.2.1 Materials

The chalcopyrite and galena, obtained from Ward's Science in 1 kg batches, were crushed using a hammer to 100% passing 1000 microns. The crushed minerals were pulverized and sieved through 75 and 38 micron sieves respectively. The fraction of particles greater than 75 microns was re-pulverized and re-sieved. The -75+38 microns sample was split using a rotary splitter and the split samples were individually purged with nitrogen and stored at -30°C. The -75+38 microns fraction was used for both the microflotation tests, attachment time tests and adsorption tests. The fraction below 38 microns was sieved through a 25 micron sieve and the particles below 25 microns were used for the zeta potential measurements. This fraction was similarly split, purged with nitrogen and stored at -30°C.

10.2.2 Water Quality

$CaSO_4$, $Ca(NO_3)_2$ and $NaNO_3$ solutions and synthetic plant water of 0.1205 M were used for the attachment timer measurements, microflotation tests, zeta potential measurements and adsorption studies. The ionic strength of 0.1205 M translates to five times the amount of dissolved solids of the standard synthetic plant water (1 SPW) as described by Wiese *et al.* (2005). Table 10-1 gives an account of the concentrations of the various ions in the solutions under investigation.

Table 10-1: Concentrations of ions for the various water qualities

Water Type	Ca^{2+} (mg/L)	Mg^{2+} (mg/L)	Na^{+} (mg/L)	Cl^{-} (mg/L)	SO_4^{2-} (mg/L)	NO_3^{-} (mg/L)	CO_3^{2-} (mg/L)	TDS (mg/L)	IS (mol/L)
SPW	**400**	**350**	**765**	**1435**	**1200**	**880**	**85**	**5115**	**0.1205**
$Ca(NO_3)_2$	**1610**	**-**	**-**	**-**	**-**	**4981**	**-**	**6591**	**0.1205**
$CaSO_4$	**1207**	**-**	**-**	**-**	**2894**	**-**	**-**	**4101**	**0.1205**
$NaNO_3$	**-**	**-**	**2770**	**-**	**-**	**7472**	**-**	**10242**	**0.1205**

10.2.3 Attachment Time Tests

The attachment contact time apparatus (ACTA) used in this investigation was developed at Aalto University and has previously been described by Aspiala *et al.* (2018) and October *et al.* (2019). A detailed description of the experimental procedure in terms of particle bed building and running measurements is documented in October *et al.* (2019). Measurements were taken for each of the water qualities in Table 10-1 with and without the addition of 50 g/t sodium isobutyl xanthate (SIBX) sourced from Senmin (97% purity). As described in October *et al.* (2019), a measurement is completed in 66 cycles across the particle bed and thus 66 images are obtained per measurement. Each image shows the six bubbles and where attachment of particles exists, thus the attachment probability is obtained by studying the images for attachment of particles out of the possible 396 bubbles per measurement. All tests were performed in duplicate to minimise error.

10.2.4 Microflotation Tests

The microflotation cell developed by Bradshaw and O'Connor (1996) was used. 3 g of pure mineral was mixed with 50 mL of the particular water quality under study; the pH of the mixture was adjusted to 6.5, the mixture was then ultra-sonicated for 5 minutes to allow for good dispersion of the mineral mixture and to remove oxidation products from the mineral surface. The suspension was transferred to the microflotation cell and the pulp was circulated by a peristaltic pump at 90 rpm. For collector runs, 50 g/t of SIBX was added to the slurry for each water type. Air was introduced at the base of the cell at a flow rate of 7 mL/min and concentrates were collected at 2, 6, 12 and 20 minutes of flotation. The tailings and four concentrates were filtered, dried and weighed. All tests were performed in duplicate to minimise error.

10.2.5 Zeta Potential Measurements

0.075 g of mineral particles was mixed with 60 mL of the particular water type; the dilute mixtures were equally divided in six containers and the pH was adjusted to 2, 4, 6, 8, 10 and 12 with dilute HCl or dilute NaOH. After 15 minutes on the magnetic stirrer the pH was measured again and adjusted where needed. 1 mL of the suspension was transferred to the Malvern Dip Cell and inserted in the Malvern ZetaSizer where measurements were taken. All measurements were performed in triplicate to reduce experimental error.

10.2.6 Adsorption Studies

3 g of pure mineral sample of fraction 75+38 μm was mixed with 30 mL of the particular water quality under study and the pH of the mixture was adjusted to 6.5. 50 g/t of SIBX (15 μL), was added to the flask containing the mineral slurry, this is equivalent to the collector concentration used in the microflotation and ACTA tests. The maximum amount of xanthate in the slurry was thus 5 g/t which is equivalent to 5 mg/L. The top of the flask was covered with tin foil and placed in an Ecobath shaker at a controlled temperature of 20 °C and speed of 141 rpm for 15 minutes. After 15 minutes in the water bath a plastic syringe was used to draw out about 15 mL of the suspension. A 0.45 μm filter was attached at the end of the syringe and the filtrate was collected in a sample container. The xanthate concentration was then measured by placing the filtrate in a quartz cuvette and reading the absorbance at wavelength 301 nm by means of a UV-Vis spectrophotometer. Prior to measuring the absorbance of the filtrate, calibration curves were constructed with solutions of known concentrations, as measured by the peak absorbance observed at 301 nm. The concentration of xanthate in solution for unknown samples could be calculated from the calibration curve. Adsorption tests were done in triplicate to minimise experimental error.

10.3 Results

10.3.1 Effect of specific ions on the recovery of chalcopyrite and galena

The chalcopyrite and galena recovery in microflotation tests in the three single salt solutions and plant water at equivalent ionic strength both in the absence (dashed line) and presence (solid line) of a collector is illustrated in Figure 10-1 and Figure 10-2 respectively. The $NaNO_3$ solution yields the highest recovery for the collector and collectorless systems for both the sulfide minerals. $CaSO_4$ and $Ca(NO_3)_2$ showed very similar recoveries with SIBX, however when the collector was absent from the system a cation and anion effect is observed between the three single salt solutions with both sulfide minerals; Na^+ performs better than its Ca^{2+} counterpart in the NO_3^- solution and NO_3^- outperforms SO_4^{2-} in the Ca^{2+} containing solutions in the chalcopyrite system. With galena, the Ca^{2+} again results in poorer recoveries both in the collector and collectorless systems. Interestingly, the synthetic plant water results in the highest chalcopyrite recovery with SIBX and without collector the recovery is only lower than the $NaNO_3$ solution. However, with the synthetic plant water, the lowest galena recovery is obtained both with and without SIBX.

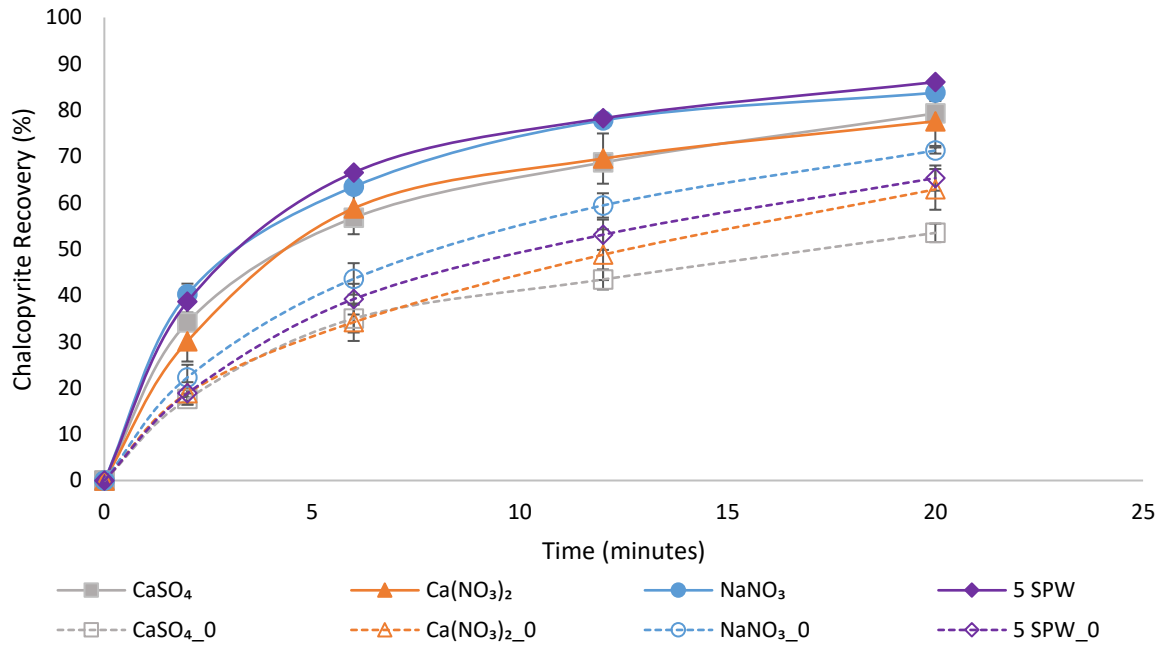

Figure 10-1: Chalcopyrite recovery in various ionic solutions with SIBX (solid line) and collectorless (dashed line)

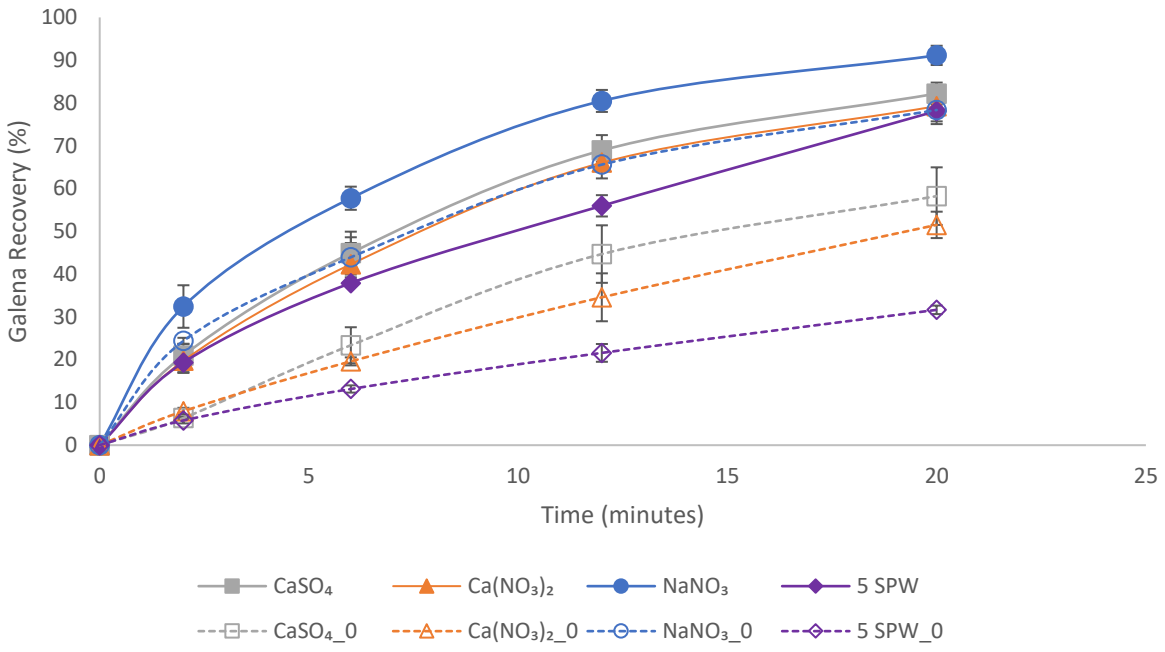

Figure 10-2: Galena recovery in various ionic solutions with SIBX (solid line) and collectorless (dashed line)

10.3.2 Effect of specific ions on the bubble-particle attachment of chalcopyrite and galena

The fundamental bubble-particle attachment tests are shown in Figure 10-3 for chalcopyrite and Figure 10-4 for galena. The attachment probability of chalcopyrite particles to air bubbles is observed to be higher in the $NaNO_3$ solution; the $NaNO_3$ solution also results in the highest chalcopyrite mass recovered. The attachment probability of chalcopyrite with the single salts solutions corroborates the microflotation tests; in that the Na^+ results in higher bubble-particle attachment compared to Ca^{2+} in NO_3^- solutions and the NO_3^- performs better than SO_4^{2-} in Ca^{2+} solutions. In the case of chalcopyrite, the mass recovered with $CaSO_4$ is slightly more than with $Ca(NO_3)_2$, this does not correspond with the attachment probability as it would be expected that a higher attachment probability will also result in a greater mass recovered. This discrepancy between the two measures can be expected due to the fact that attachment as measured by the attachment timer is deemed successful whether one or more particles are attached and the inability of the machine to detect the actual number of particles attached on each bubble. Furthermore, with the microflotation tests it was observed that in the presence of SIBX, the difference in chalcopyrite recovery was minimal in the $CaSO_4$ and $Ca(NO_3)_2$ solutions. For the synthetic plant water case at the same ionic strength as the single salt solutions with SIBX, an attachment probability of 85.2% is achieved and a total mass of 2.7 mg is recovered. This corresponds to the microflotation tests where the synthetic plant water resulted in the highest recovery of chalcopyrite in the SIBX system.

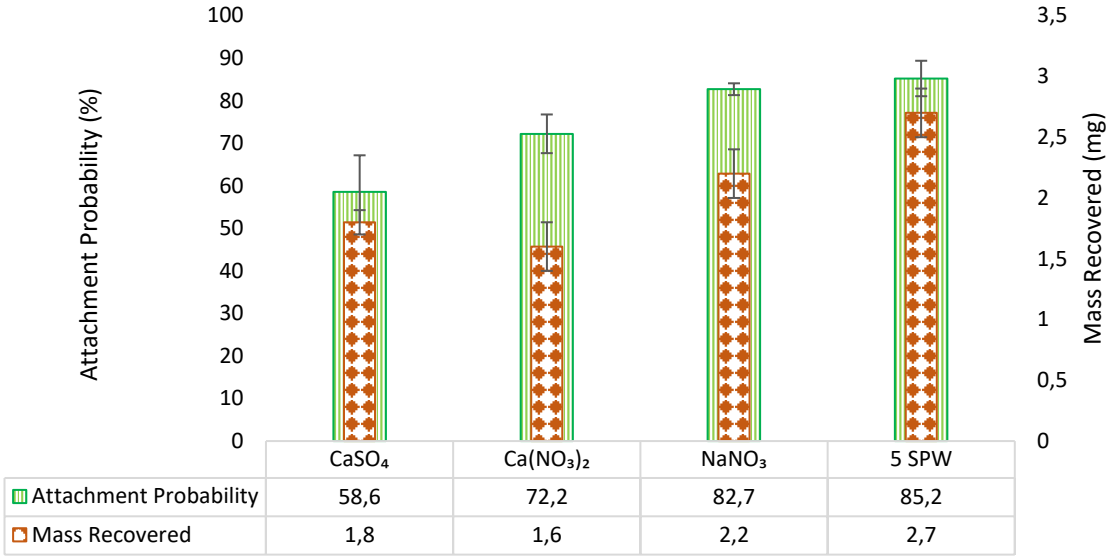

	$CaSO_4$	$Ca(NO_3)_2$	$NaNO_3$	5 SPW
Attachment Probability	58,6	72,2	82,7	85,2
Mass Recovered	1,8	1,6	2,2	2,7

Figure 10-3: Attachment probability and mass recovered of chalcopyrite in the various ionic solutions

In Figure 10-4 the attachment probability of galena particles to air bubbles and the mass of particles attached to air bubbles is highest in the $NaNO_3$ solution. This corresponds with what was observed in terms of galena recovery in the microflotation system. Again, suggesting that the Ca^{2+} has a negative effect on bubble-particle attachment as compared to Na^{+}, as with the microflotation tests.

In the case of the anions, it is the SO_4^{2-} that performs better than the NO_3^{-} with Ca^{2+} as the cation. The synthetic plant water results in the lower attachment probability of galena when compared to the $CaSO_4$ and $NaNO_3$ solutions, whereas the microflotation tests show that the complex water solution results in the poorest galena recovery compared to the three single salt solutions.

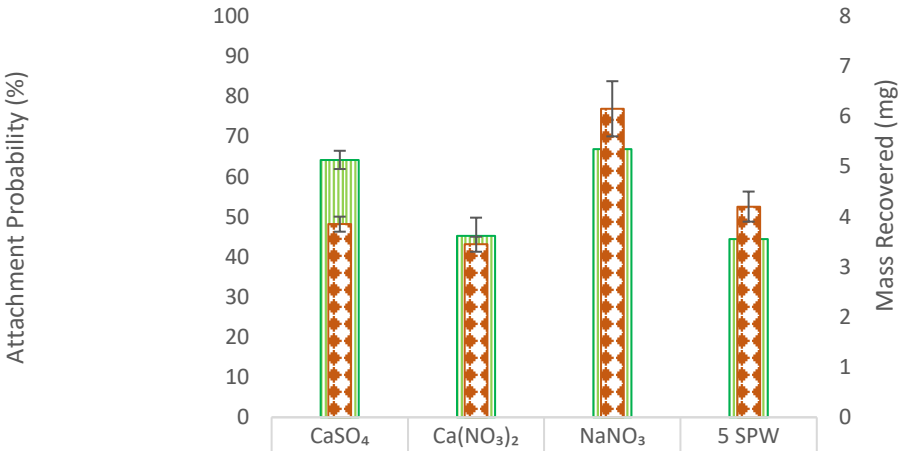

	$CaSO_4$	$Ca(NO_3)_2$	$NaNO_3$	5 SPW
Attachment Probability	64,14	45,20	66,79	44,44
Mass Recovered	3,85	3,45	6,15	4,2

Figure 10-4: Attachment probability and mass recovered of galena in the various ionic solutions

Both the microflotation and fundamental bubble-particle attachment techniques indicate that Ca^{2+} containing salts result in poorer performance compared to the Na^{+} containing salt. This therefore raises questions with regards to xanthate adsorption on the mineral surface as well as the charge of the mineral surface with Ca^{2+} containing solutions.

10.3.3 Effect of specific ions on the adsorption of xanthate on chalcopyrite and galena surfaces

Figure 10-5 and Figure 10-6 show the concentration of xanthate adsorbed on the mineral surface as well as the residual xanthate left in the solution for chalcopyrite and galena respectively. $CaSO_4$ and $Ca(NO_3)_2$ show a similar amount of xanthate adsorbed on the chalcopyrite surface in Figure 10-5, however a clear cation and anion effect can be observed in that Na^{+} results in a higher adsorption compared to Ca^{2+} for the NO_3^{-} salts. The NO_3^{-} results in a slightly better adsorption of xanthate onto chalcopyrite compared to the SO_4^{2-} for the Ca^{2+} salts. These adsorption results correspond relatively well with the microflotation and attachment timer results. The bubble-particle attachment techniques, both fundamental and flotation have indicated that Ca^{2+} containing salts result in lower attachment probability and recovery in a system with SIBX. The results in Figure 10-5 indicate that this is because less SIBX is actually adsorbed on the mineral surface in Ca^{2+} containing salts, indicating that the adsorption of xanthate on the chalcopyrite surface is hindered in the presence of Ca^{2+}.

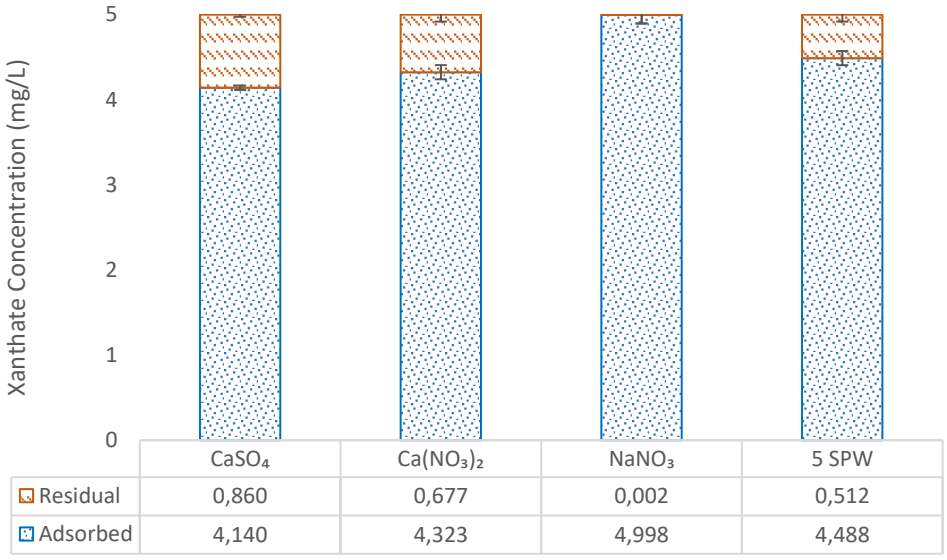

	$CaSO_4$	$Ca(NO_3)_2$	$NaNO_3$	5 SPW
Residual	0,860	0,677	0,002	0,512
Adsorbed	4,140	4,323	4,998	4,488

Figure 10-5: Xanthate adsorbed on chalcopyrite surface and residual xanthate in various ionic solutions

The adsorption of SIBX on the galena surface was predominantly high in the ionic solutions particularly in the single salt solutions, with only 0.01 mg/L of SIBX not adsorbed on the galena with the $NaNO_3$ solution, it is still however evident that Ca^{2+} containing salts result in lower adsorption of the collector on the mineral surface. The synthetic plant water however results in the lowest concentration of SIBX adsorbed on the galena; this corresponds well to the microflotation tests and bubble-particle attachment tests where the recovery and attachment probability of galena was lowest with synthetic plant water. This may be due to

the combined effect of the various ions in the solution or another ion that has not been investigated in this study hindering of xanthate adsorption on the galena, reducing its floatability.

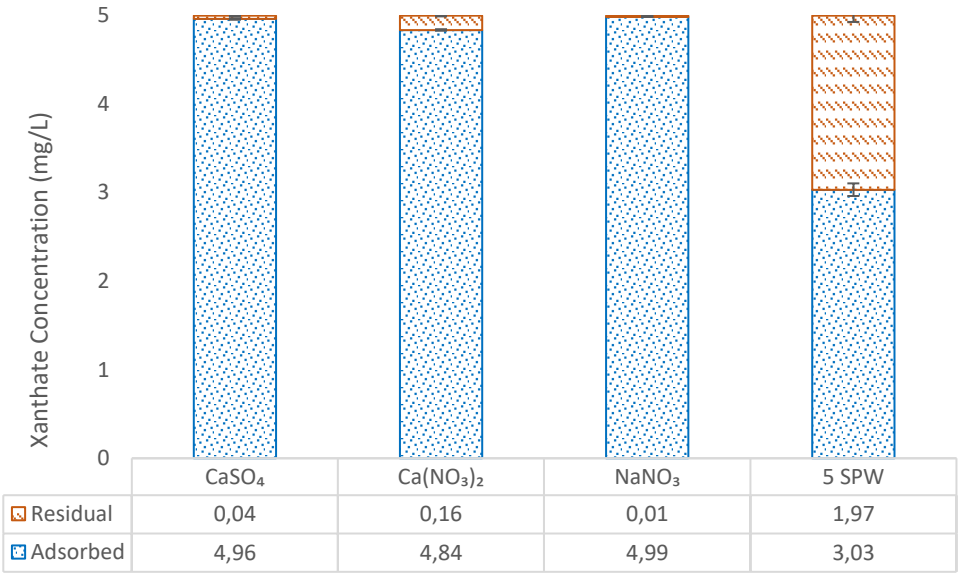

	$CaSO_4$	$Ca(NO_3)_2$	$NaNO_3$	5 SPW
Residual	0,04	0,16	0,01	1,97
Adsorbed	4,96	4,84	4,99	3,03

Figure 10-6: Xanthate adsorbed on galena surface and residual xanthate in various ionic solutions

10.3.4 Effect of specific ions on the zeta potential of chalcopyrite and galena

As illustrated in Figure 10-7 the zeta potential of both galena and chalcopyrite in the various ionic solutions display similar trends in that the ultra-purified water results in the most negative potential of the sulfide minerals. The isoelectric point of chalcopyrite is around pH 3 to 4 which is in agreement with studies by Ikumapayi *et al.* (2012) and Moignard and Healy (1972). Both minerals additionally show an increase in potential between pH 10 and 12 while the Ca^{2+} containing solutions result in a sign change from negative to positive mineral potential over this range. This may be due to metal hydroxide precipitation at the mineral surface (Harvey *et al.,* 2002; Ikumapayi *et al.,* 2012; Hirajama *et al.,* 2016). Work by Davila-Pulido *et al.* (2015) further attributed the reduction in hydrophobicity of sphalerite in the pH range of 7 to 11 to $Ca(OH)_2$ precipitation on the sphalerite surface. The monovalent salt and ultra-purified water however does not show this increase in potential between pH 10 and 12; thus this distinct increase in potential over pH 10 to 12 may be specific to Ca^{2+} or divalent ion containing solutions. Furthermore, the Ca^{2+} containing salt solutions result in a much less this negative or more positive potential of chalcopyrite and galena.

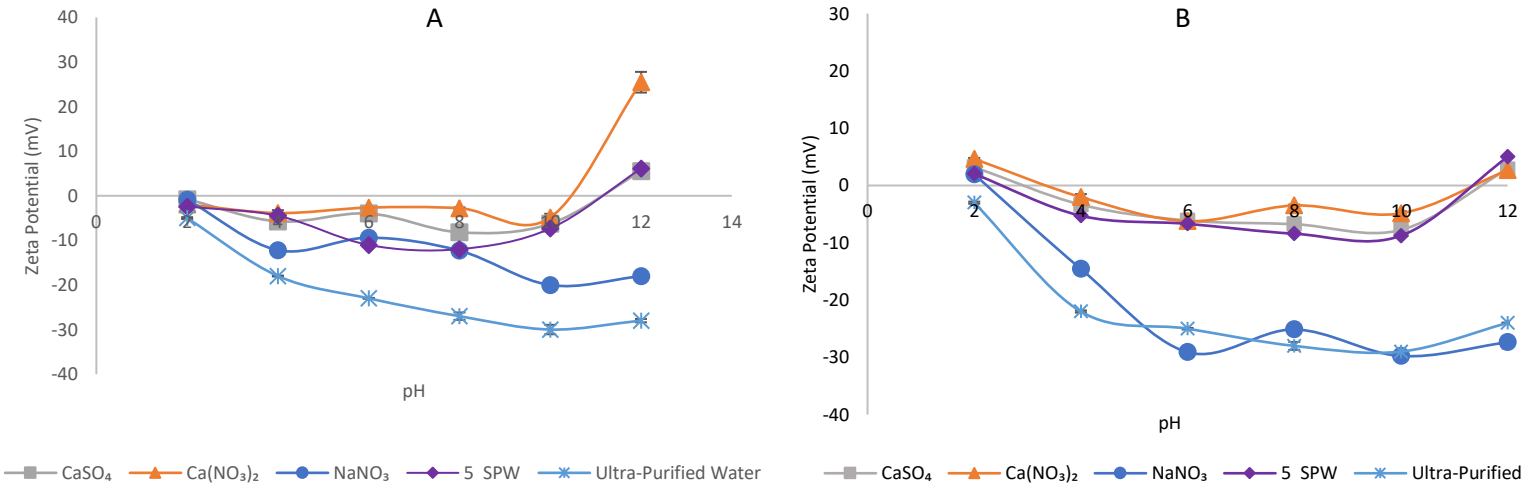

Figure 10-7: Zeta potential of galena (A) and chalcopyrite (B) in the various ionic solutions

10.4 Discussion

Synthetic plant water yielded the lowest galena recovery with and without SIBX, whilst this water quality resulted in the highest chalcopyrite recovery. The mechanism behind this result is not fully understood however, this may be due to the differences in mineral properties; as shown by Liu and Zhang (2000) the affinity of ions towards the mineral surface varies by mineral type. And given the complex nature of the synthetic plant water, the combination of the various ions such as Ca^{2+}, Mg^{2+}, Na^{+}, CO_3^{2-}, SO_4^{2-}, NO_3^{-} each having a different role and thus able to act simultaneously, some mineral dependent flotation response may be expected.

Microflotation tests of galena and chalcopyrite showed that Ca^{2+} containing solutions resulted in lower recovery of these mineral particles. And that the Na^{+} containing solution resulted in higher recoveries of these mineral particles; collectorless tests with the Na^{+} containing salts performed similarly to the system with the collector present. Bubble-particle attachment tests showed that even at this fundamental bubble-particle level, Ca^{2+} containing salts resulted in lower attachment probabilities and less particles recovered. Similarly, Na^{+} containing solutions outperformed the other salt solutions in terms of the probability of particle attachment to air bubbles.

Both techniques thus reinforced the negative effect of Ca^{2+} containing solutions on floatability. Studies have shown that solutions of increasing ionic strength lower the stability of the hydration layer (Wang and Peng, 2014) and that this is particularly evident in monovalent salt solutions (Blake and Kitchener, 1972; Li *et al.,* 2017). Hirajima *et al.* (2016) further ascribed longer induction times and thus decreased bubble-particle interactions to an increase in the hydration layer stability. Thus, a decrease in the stability of the hydration layer is expected to yield an increase in recovery. The results obtained in Figure 10-1 and Figure 10-2 show that the Na^{+} gave higher chalcopyrite and galena recoveries and this may be due to the reduced stability of the hydration layer in this monovalent salt solution (Li *et al.,* 2017).

In contact angle measurements Li *et al.* (2017) showed that the floatability of chalcopyrite was promoted with NaCl and KCl by increasing the xanthate adsorption on the mineral surface in a shorter time compared to divalent salts. This work confirms that in Ca^{2+} containing solutions less xanthate actually adsorbs onto the mineral surface. This is in alignment with the work of Ikumapayi *et al.* (2012) and Elizondo-Alvarez *et al.* (2017). Ikumapayi *et al.* (2012) showed that Ca^{2+} resulted in the formation of soluble complexes of calcium carbonate and sulfoxy species which resulted in a reduction of xanthate adsorption on the galena surface. While Elizondo-Alvarez *et al.* (2017), attributed this to the chemisorption of Ca^{2+} on active sites, hindering the action of the xanthate collector. Research by Fuerstenau (1982) detailed that above pH 6, Ca^{2+} adsorbs onto negatively charged pyrite via an electrostatic attraction; thus, hindering the oxidation of xanthate and ultimately its adsorption on the mineral surface. It should also be noted that the SPW also shows a significant concentration of sulfate (1200 mg/L) while it contains a lower concentration of calcium (400 mg/L), compared to the solutions of calcium nitrate (1610 mg Ca/L) and calcium sulfate (1207 mg Ca/L). This indicates the role of sulfate ions; probably playing in conjunction with calcium ions, since there is evidence that SO_4^{2-} passivates the galena surface and decreases the adsorption of xanthate, resulting in lower galena recoveries (Elizondo-Álvarez et al., 2017).

Across the pH 2 to 12 range, zeta potential measurements of both minerals showed a less negative potential on the surface in Ca^{2+} containing solutions. With the potential in $NaNO_3$ resembling that of ultra-purified water very closely. The potential of the mineral surface becoming less negative in Ca^{2+} containing solutions makes it clearly evident that Ca^{2+} passivates the mineral surface to a larger extent and indicates the compression of the electrical double layer (Ma, 2005; Li *et al.,* 2017; Ikumapayi *et al.*, 2012).

Collectorless microflotation results show that Na^+ achieves higher mineral recoveries, the potential of the mineral is also seen to be most negative with Na^+ compared to Ca^{2+}. Generally, $Ca(NO_3)_2$ resulted in the least negative potential of the mineral, followed by $CaSO_4$ and the synthetic plant water. A less negative zeta potential of the mineral surface is indicative of a decrease in the electrostatic repulsion between solid surfaces (Li *et al.,* 2017; Hirajima *et al.,* 2016).

It is thus expected that the $Ca(NO_3)_2$ solution would yield the highest mineral recoveries of the three salt solutions, however that was not the observation in the microflotation tests and bubble-particle attachment measurements with both galena and chalcopyrite. Fuerstenau (1982) proposed that the electrical double layer drives the adsorption of physically-adsorbing reagents by the magnitude and sign of the zeta potential and that a high zeta potential may hinder the adsorption of chemically-adsorbing collectors.

This work proved that less xanthate is adsorbed on chalcopyrite and galena surfaces in Ca^{2+} containing solutions hence the poorer bubble-particle attachment shown in the fundamental attachment timer and in a microflotation system observed in this work. Thus, the increased zeta potential and therefore high zeta potential on chalcopyrite and galena may either hinder the adsorption of xanthate; or the bubble-particle attachment of chalcopyrite and galena is affected more by the adsorption of collector on the mineral surface

regardless of the change in electrostatic repulsion that the ionic composition of the water brings to the system.

10.5 Conclusions

Two techniques assessing the bubble-particle attachment of chalcopyrite and galena were used, one fundamental and one simplifying what happens in the pulp phase in a flotation system. Both bubble-particle attachment techniques showed that Ca^{2+} containing solutions resulted in the lowest bubble-particle attachment, while the Na^{+} containing single salt solution consistently resulted in the highest bubble-particle attachment probability and recovery.

Adsorption test results further displayed that Ca^{2+} containing solutions resulted in less xanthate adsorbing on the mineral surface and hence reducing the attachment probability and subsequently mineral recovery as found in this investigation. Zeta potential measurements showed that the Ca^{2+} containing solutions result in the least negative mineral surface; which is indicative of the mineral surface being screened or passivated by these divalent cations. This investigation therefore provides evidence that the passivation of the mineral surface with Ca^{2+} inhibits the adsorption of xanthate and thus negatively affects the bubble-particle attachment.

10.6 Acknowledgements

This work is financed by the National Research Foundation of South Africa (NRF) [Grant number 103641] and this project has received funding from Academy of Finland Mineral Resources and Material Substitution MISU program and the the European Union H2020 programme under grant agreement No 730480. Any opinion, finding and conclusion or recommendation expressed in this material is that of the authors and the NRF does not accept any liability in this regard. Further the financial and technical contributions from the South African Minerals to Metals Research Institute (SAMMRI) is also acknowledged.

10.7 References

Albijanic, B., Ozdemir, O., Nguyen, A. and Bradshaw, D. (2010). A Review of Induction and Attachment Times of Wetting Thin Films between Air Bubbles and Particles and Its Relevance in the Separation of Particles by Flotation. Advances in Colloid and Interface Science 159 (1). Elsevier B.V.: 1–21. https://doi.org/10.1016/j.cis.2010.04.003.

Aspiala, M., Schreithofer, N., Serna-Guerrero, R. (2018). Automated contact time apparatus and measurement procedure for bubble-particle interaction analysis, Minerals Engineering, 121(1):77-82.

Blake, T.D., Kitchener, J.A. (1972) Stability of aqueous films on hydrophobic methylated silica. Journal of the Chemical Society. 68, 1435–1442.

Bradshaw, D. and O'Connor, C. (1996) Measurement of the sub-process of bubble loading in flotation. Minerals Engineering. 9: 443-448.

Burdukova, E. (2007) Surface properties of New York Talc as a function of pH, polymer adsorption and electrolyte concentration. PhD Thesis, University of Cape Town, Faculty of Engineering and the Built Environment, Department of Chemical Engineering, Cape Town, South Africa

Corin, K.C., Reddy, A., Miyen, L., Wiese, J.G. and Harris, P.J. (2011). The Effect of Ionic Strength of Plant Water on Valuable Mineral and Gangue Recovery in a Platinum Bearing Ore from the Merensky Reef. Minerals Engineering 24 (2): 131–37. https://doi.org/10.1016/j.mineng.2010.10.015.

Corin, K.C. and Wiese, J.G. (2014). Investigating Froth Stability : A Comparative Study of Ionic Strength and Frother Dosage. Minerals Engineering 66–68. Elsevier Ltd: 130–34. https://doi.org/10.1016/j.mineng.2014.03.001.

Du, H., Ozdemir, O., Wang, X., Cheng, F., Celik, M., Miller, J. (2014). Flotation chemistry of soluble salt minerals: from ion hydration to colloid adsorption. Mineral and Metallurgical Processing. 31 (1) Society for Mining, Metallurgy and Exploration Inc.: 1-20

Fuerstenau, D. W. (1982). Mineral-Water Interfaces and the Electrical Double Layer. In R. P. King, Principles of Flotation (pp. 17-30). Johannesburg: South African Institution of Mining and Metallurgy.

Harvey, P.A., Nguyen, A.V. and Evans, G.M. (2002). Influence of Electrical Double-Layer Interaction on Coal Flotation. Journal of Colloid and Interface Science 250 (2): 337–43. https://doi.org/10.1006/jcis.2002.8367.

Hencer, M., Celik, M. S. and Miller, J. D. (2001). The significance of interfacial water structure in soluble salt flotation systems. Journal of Colloid and Interface Science, 235. pp. 150–161.

Hirajima, T., Pandhe, G., Suyantara, W., Ichikawa, O., Mohamed, A., Miki, H. and Sasaki, K. (2016). Effect of Mg^{2+} and Ca^{2+} as Divalent Seawater Cations on the Floatability of Molybdenite and Chalcopyrite. *Minerals Engineering* 96–97. Elsevier Ltd: 83–93. https://doi.org/10.1016/j.mineng.2016.06.023.

Ikumapayi, F., Makitalo, M., Johansson, B. and Hanumantha, K. (2012). Recycling of Process Water in Sulfide Flotation : Effect of Calcium and Sulphate Ions on Flotation of Galena. Minerals Engineering 39. Elsevier Ltd: 77–88. https://doi.org/10.1016/j.mineng.2012.07.016.

Laskowski, J., and Castro, S. (2015). Flotation in Concentrated Electrolyte Solutions. International Journal of Mineral Processing. 144, 50-55.

Laskowski, J. and Iskra, J. (1970). Role of capillary effects in bubble-particle collision in flotation. Transactions of the Institution of Mining and Metallurgy. 79, C6.

Li, C. and Somasundaran, P. (1993). Role of Electrical Double Layer Forces and Hydrophobicity in Coal Flotation in NaCl Solutions. Energy and Fuels 7 (2): 244–48. https://doi.org/10.1021/ef00038a014.

Liu, Q. and Zhang, Y. (2000). Effect of calcium ions and citric acid on the flotation separation of chalcopyrite from galena using dextrin. Minerals Engineering 13 (13) Elsevier Ltd: 1405-1416.

Ma, X. and Pawlik, M. (2005). Effect of alkali metal cations on adsorption of guar gum onto quartz. Journal of Colloid and Interface Science 289: 48 - 55.

Ma, X. (2005). Effect of Alkali Metal Cations on Adsorption of Guar Gum onto Quartz. Master of Applied Sciences Thesis, University of British Columbia, Faculty of Graduate Studies Mining Engineering.

Manono, M.S., Corin K.C. and Wiese, J.G. (2012). An Investigation into the Effect of Various Ions and Their Ionic Strength on the Flotation Performance of a Platinum Bearing Ore from the Merensky Reef. Minerals Engineering 36–38. Elsevier Ltd: 231–36. https://doi.org/10.1016/j.mineng.2012.03.035.

Manono, M.S., Corin, K.C. and Wiese, J.G. (2016). The influence of electrolytes present in process water on the flotation behaviour of Cu-Ni containing ore. Minerals Engineering. 96-97, 99-107.

Moignard, M.S., James, R.O., Healy, T.W. (1977). Adsorption of calcium at the zinc sulfide–water interface. Australian Journal of Chemistry 30, 733–740.

October, L.L., Corin K.C., Schreithofer, N., Manono, M.S., Wiese, J.G. (2019). Water Quality Effects on Bubble-Particle Attachment of Pyrrhotite. Minerals Engineering 131. Elsevier Ltd: 230–236. https://doi.org/10.1016/j.mineng.2018.11.017.

Rao, S.R. and Finch, J.A. (1989). A review of water re-use in flotation. Minerals Engineering 2 (1), 65–85.

Wang, B. and Peng, Y. (2014). The effect of saline water on mineral flotation- A critical review Minerals Engineering. 66–68. Elsevier Ltd: 13–24. http://dx.doi.org/10.1016/j.mineng.2014.04.017.

Wiese, J.G., Harris, P.J. and Bradshaw, D.J. (2005). The influence of the reagent suite on the flotation of ores from the Merensky reef. Minerals Engineering 18 (2), 189–198.

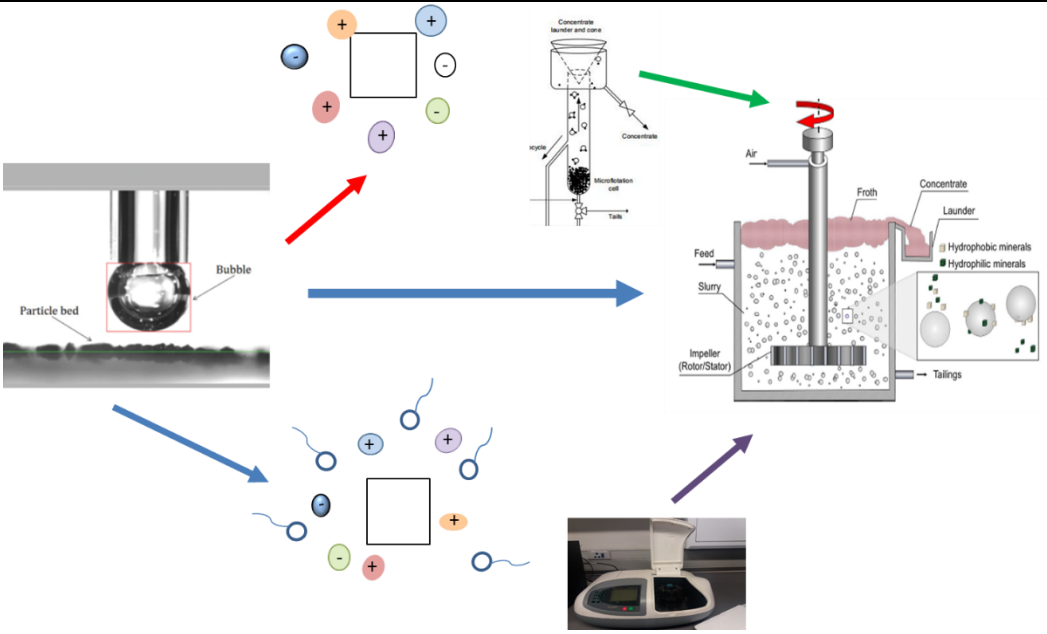

This chapter presents a consolidated discussion of the various publications and conference proceedings included in this dissertation. This chapter also aims to bring together and provide answers to the key questions as well as interrogate the results compared to what was hypothesised in Chapter 3. Four main themes are discussed in this chapter, namely the use of the ACTA as a means to measure floatability, the effect of synthetic plant water of increasing ionic strength on bubble-particle interactions, the effect of specific ions on bubble-particle interactions and the combined effect of ionic strength and pH of synthetic plant water on bubble-particle interactions.

11.1 The Use of the Automated Contact Time Apparatus as a Measure of Mineral Floatability

Phase one of this work studied the attachment probability of pyrrhotite; the pyrrhotite particle size was -75+38 microns, contact times of 100 ms and 200 ms and testwork in the presence of a collector considered a dosage of 100 g/t of SIBX. Under these conditions no particles were collected in the collection bin and the particles were visibly too fine as they moved into the camera and collection zones, the challenge was overcome through the use of a metal stopper at the end of the particle bed and start of the camera zone for phase one of the work. Although no particles were recovered in the ACTA for this phase, the single salt investigation in Chapter 7 showed a similar trend in attachment probability with the ACTA and classical microflotation testwork.

Phase 2 of the testwork used a larger particle size of -125+106 microns as well as a shorter contact time and collector dosage of 50 ms and 50 g/t respectively. The shorter contact time and lower collector dosages were used due to the floatable nature of chalcopyrite and galena; which were the minerals under study for phase 2. Under these conditions, particles that successfully attached to the bubbles were collected in the collection bin and could subsequently be weighed. Furthermore, both the attachment probability and mass

of particles recovered corroborated well with microflotation tests under the same conditions. Under synthetic plant water of increasing ionic strength, the attachment probability of galena did not change however a clear trend was observed with the mass of collected particles and further validated by microflotation testwork. As described in Chapter 8, this discrepancy between these two measures may be due to either multiple particles sitting on one bubble or heavy and agglomerated particles being collected when attachment does occur on few bubbles; which would lead to low attachment probability, but high mass recovered. Chalcopyrite did however show the same trend with all three outputs, microflotation recovery, attachment probability and mass of particles recovered with the ACTA. Figure 8-9, Figure 11-1 and Figure 11-2 provide a comparison of the outputs obtained from the ACTA and microflotation. Figure 11-1 shows the lowest attachment probability, recovery and particles recovered of galena in $Ca(NO_3)_2$ solution while the $NaNO_3$ solution resulted in the highest attachment probability, recovery and particles recovered. The outputs of the ACTA compared very well to what was observed with the classical microflotation technique; in that a nearly identical trend was displayed for the two methods of measuring particle floatability.

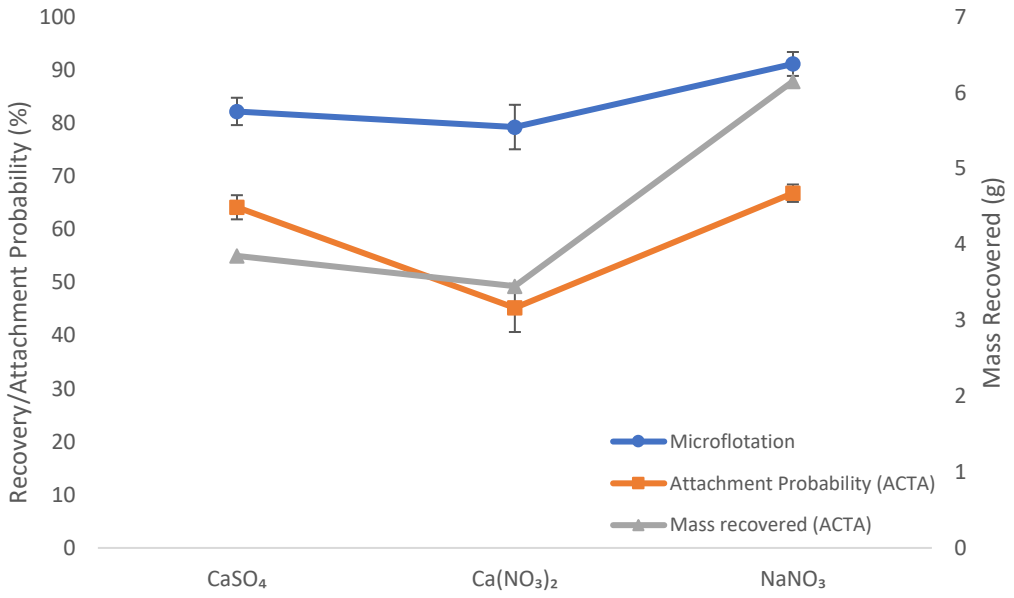

Figure 11-1: Trend comparison of the microflotation and ACTA output with galena

Figure 11-2 shows similar results in terms of the trends from these two techniques, this time with chalcopyrite. The $NaNO_3$ solution resulted in the highest attachment probability, recovery and mass recovered. However, in this case, the mass recovered from the ACTA and recovery from microflotation match very well. A difference is however seen in the $CaSO_4$ solution, where attachment probability of chalcopyrite is the lowest. The two other outputs (mass recovered and recovery) however show the $Ca(NO_3)_2$ solution to result in lowest bubble-particle attachment. Thus, reinforcing the importance of showcasing both the attachment probability and mass of particles collected when taking measurements with the ACTA.

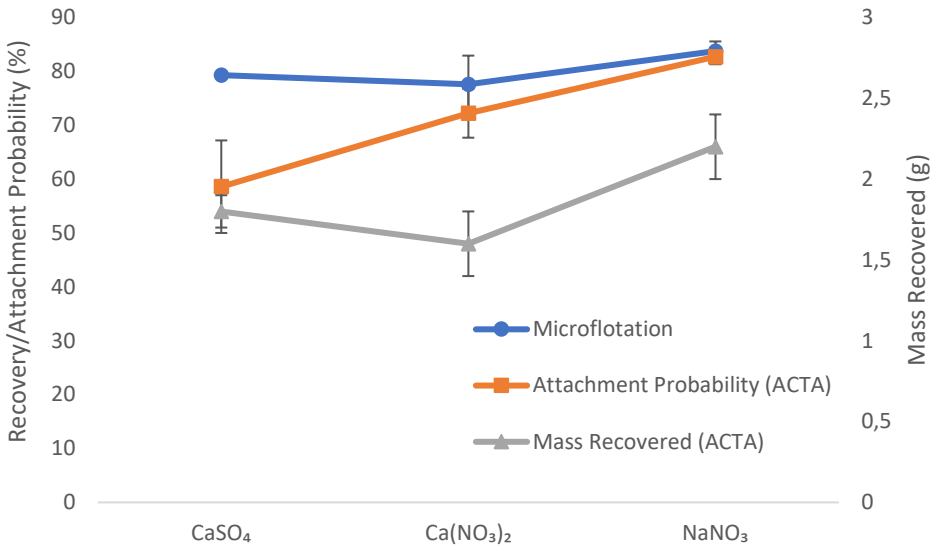

Figure 11-2: Trend comparison of the microflotation and ACTA output with chalcopyrite

The outcomes of this work thus proves that the results of the ACTA corroborated well with that of the classical microflotation technique for measuring floatability. Subsequently after the completion of these two phases, authors such as Pienaar *et al.* (2019) and Hartmann and Serna-Guerrero (2020) validated these findings as well under the specified conditions for the use of the ACTA as a measure for particle floatability. The study by Pienaar *et al.* (2019) was also done using a sulfide mineral, galena; the galena particles were of the same size as the galena particle in this investigation and a contact time of 20 ms was used. These authors showed a good correlation between microflotation test and the attachment probability from the ACTA; the mixture containing hexanol and SDEDTP showed the highest recovery and attachment probability while in the absence of reagents, low recoveries and attachment probabilities were achieved. The study by Hartmann and Serna-Guerrero (2020) used quartz particles of particle size -180+75 μm under various contact times; these authors also showed that the attachment probability coincided well with the flotation recovery.

11.2 The Effect of an Increase in Ionic Strength of Plant Water on Bubble-particle Interactions for Selected Sulfide Minerals

Chapter 3 hypothesised that the attachment of mineral particles to air bubbles will be improved in solutions of higher ionic strength. This is proposed to have been owing to the fact that upon the addition of ions to a three-phase system, the electrical double layer is compressed. When this compression occurs, the energy barrier for bubble-particle attachment to occur decreases leading to the faster rupturing of the film at the air-water and solid-water interface. By increasing the KCl concentration in a quartz system, Laskowski and Iskra (1970) and Yoon and Yordan (1991) showed an increase in bubble-particle attachment; the same result was seen by Wang *et al.* (2015) at lower NaCl concentrations with sphalerite The latter study did however show that NaCl concentrations greater than 0.1 M showed a decrease in bubble particle attachment as the NaCl concentration was increased.

Phase one of this investigation studied the bubble–particle attachment of pyrrhotite particles; the flotation behaviour of which is generally recognised to be complicated and largely affected by pH and oxidation potential (Miller, 2005). Generally, the work in Chapter 6 showed that with a complex water system such as synthetic plant water with various ions present, the attachment probability of pyrrhotite decreased with increasing ionic strength both in the absence and presence of a collector. The mass of particles recovered in the ACTA could not be determined due to the fineness of particles which limited the amount of particles moving into the collection bin; thus, this validation step could not be used to confirm the attachment probability.

Pyrrhotite oxidizes rapidly when exposed to air and results in the pyrrhotite surface being covered with ferric hydroxide (Miller *et al.,* 2005). This makes the mineral hydrophilic and may hinder any activation reaction from occurring on the surface of the mineral. 'The experimental work in Chapter 6 showed that with a higher concentration of inorganic electrolytes in the system, attachment to air bubbles decreases. It was however expected that attachment probability would increase with increasing ionic strength due to the effect of the electrical double layer and its eventual result of fastening the rupture of the film at the bubble-particle interface (Yoon and Yordan, 1991; Laskowski and Iskra, 1970). The experimental work from the ACTA would therefore suggest that in the pyrrhotite system the effect of the electrical double layer is not experienced. It may thus be that the hydrophilic coating on the pyrrhotite surface is obstructing the effect of the electrical double layer and is in fact causing pyrrhotite particles to become more hydrophilic as the inorganic electrolyte concentration is increased.

Studies using FTIR, XPS and voltammograms have however shown that collector treated mineral hydrophobicity is reduced in saline waters due to the presence of oxyhydroxo, carbonate and sulfoxy species (Ikumapayi *et al.,* 2012; Kirjavainen *et al.,* 2002; Hodgson and Agar, 1984). Adsorption studies and zeta potential determination tests are discussed later to further explore this idea of hydroxide coating on the mineral surface.

Contrary to the attachment probability results with pyrrhotite, the microflotation results presented in Chapter 7 with 1, 5 and 10 SPW at the natural pH of 6.5 in the absence and presence of SIBX showed an increase in pyrrhotite recovery with plant water of increasing ionic strength. This difference between the ACTA and microflotation tests is speculated to be due the fine particle size used in the ACTA during phase one of the test work. The importance of showcasing both the attachment probability and mass of particles collected when taking measurements with the ACTA has been demonstrated in this work and therefore with regards to pyrrhotite, it may be of more value to include the mass of particles recovered in the ACTA along with the attachment probability to conclusively determine the effect of plant water of increasing ionic strength on bubble-particle attachment.

Contrary to the findings presented in the phase one attachment probability test work. Phase two work showed an increase in attachment probability, mass of particles recovered in the ACTA and further validated by increases in microflotation recovery as the ionic strength of the plant water increases. This

trend was observed with both chalcopyrite and galena particles. Thus, the three techniques provided the same outcome; this result raises questions with regard to the findings of the phase one work which showed decreases in the bubble-particle attachment probability of pyrrhotite with increasing ionic strength of plant water. It became unclear as regards whether this was a mineral specific effect or that pyrrhotite behaves differently compared to galena and chalcopyrite under the same conditions, or that this effect resulted from the finer particle size used in phase one compared to phase two. As even the microflotation work under phase one conditions suggests an increase in bubble-particle attachment as the ionic strength of the water increases which follows an opposite trend compared to that observed with the ACTA.

One of the outcomes of this work was the importance of showcasing both the attachment probability and mass of particles collected when taking measurements with the ACTA. As it may be that multiple particles attach on one bubble or heavy and agglomerated particles are collected on one bubble which would lead to low attachment probability but high recovery; thus, creating a discrepancy between the attachment probability and recovery measures. This often happens in the froth flotation cell whereby particles are recovered from heavy/agglomerated particles that attach on a single bubble; unfortunately, attachment probability as a measure fails to take this into account. It is thus important to include the mass recovered from the ACTA as a measure when using this tool to measure floatability.

The results from the chalcopyrite and galena testwork may therefore be explained by the initial hypothesis regarding the compression of the electrical double layer and subsequent reduction in the energy barrier for bubble–particle attachment. As the concentration of inorganic electrolytes in solution increases more counterions enter the Stern layer and thicken the diffuse layer due to the increase in attraction force and decrease in repulsion force. Therefore, in solutions of high ionic strength, particle recovery may increase because of the reduction in repulsion between bubble and particle. This effect and the effect of zeta potential are discussed in Section 11.4 where the potential of the mineral surface is evaluated.

Another theory which is explored later is that the addition of certain ions to water with a "bridging" effect between negatively charged particles and negatively charged collector molecules results in an increase in particle hydrophobicity due to the ions altering the zeta potential of the particle (Wang *et al.,* 2015; Yoon and Yordan, 1991; Laskowski and Iskra, 1970).

11.3 The Effect of Increasing Ionic Strength of Plant Water on the Adsorption of Xanthate on the Mineral Surface of Selected Sulfide Minerals

Collector adsorption studies conducted on selected sulfide minerals showed that more xanthate was generally left in solution as the ionic strength of the synthetic plant water increased indicating that less xanthate adsorbs on the mineral surface as the ionic strength of the plant water increases. This result was generally observed with all three sulfide minerals under study. This is in alignment with the hypothesis proposed in Chapter 3 which stated that *the addition of ionic collector to an electrolyte solution could result in competition between the ions and collector for adsorption on the mineral surface, thus, resulting in less adsorption of xanthate on the mineral surface at high ionic strengths.*

Previous studies using XPS, FTIR, voltammograms and hydrophobicity tests proposed that inorganic electrolytes compete with xanthate collector for adsorption on the mineral surface or that the amount of xanthate available for adsorption on the surface is reduced due to the formation of insoluble complexes between the collector and ions (Hodgson and Agar, 1984; Fuerstenau and Somasundaran, 2003; Ikumapayi *et al.,* 2012; Laskowski, 2013). The results of this part of the study showed that as the concentration of ions in solution was increased, less xanthate adsorbed on the surface of the mineral. These results are in line with the findings of the aforementioned authors. With less xanthate adsorbing on the mineral surface in the presence of a higher concentration of inorganic electrolytes, this indicates that with more inorganic electrolytes possibly passivating the mineral surface to a greater extent, the xanthate collector will have more competition for adsorption on the mineral surface and as a result may not get the opportunity to adsorb on the mineral surface.

It is expected that the adsorption studies should explain the findings of the bubble-particle interactions testwork results. In the case of galena, less xanthate adsorbed onto the galena surface as the ionic strength of the water increased. However, in the presence of a collector, bubble-particle interactions within the galena system increased with increasing ionic strength of plant water at both a fundamental and microflotation level. This result implies that another mechanism, potentially relating to the zeta potential may be having a greater effect on the bubble-particle attachment of galena compared to the effect of xanthate adsorption.

Although the xanthate adsorption on chalcopyrite was incredibly high, less xanthate adsorbed on the mineral surface as the ionic strength of the plant water increased. The microflotation testwork with collector showed very high recoveries across all water qualities, possibly due to the high xanthate adsorption onto the chalcopyrite surface. Although chalcopyrite recoveries were high across the water types, 1 SPW showed a lower recovery compared to 10 SPW, further the attachment probability and mass recovered in the ACTA showed an increase in bubble-particle interactions with increasing ionic strength of plant water. Therefore, as with galena, the effect of the zeta potential may be having a greater effect on the bubble-particle attachment of chalcopyrite than the xanthate adsorption sub-process. Pyrrhotite however behaved slightly differently compared to galena and chalcopyrite in that bubble-particle attachment probability decreased with increasing ionic strength both in the absence and presence of collector. As mentioned in Section 11.2 this is attributed to the fine particle size used for the ACTA in phase one of this work. However, given the findings of the adsorption work, the aforementioned result could be because less xanthate adsorbs on the mineral surface as the water quality deteriorates.

11.4 The Effect of Increasing Ionic Strength of Plant Water on the Zeta potential of Selected Sulfide Minerals

The three sulfide minerals used in this study showed a very negative potential in ultra-purified water (ULP) and de-ionised water (DI) and became less negative as the ionic strength of the water was increased. In ULP and DI water between pH 4 and 12, the potential of galena, chalcopyrite and pyrrhotite ranged

between -20 mV and -28 mV whilst at the same pH range in synthetic plant water the potential of these sulfide minerals ranged between -5 mV and +10 mV. The fact that the charge on the mineral surface becomes less negative as the ionic strength of the plant water increases can be attributed to the adsorption of metal cation such as Ca^{2+}, $Mg^{2+,}$ Na^{+} on the surface of the mineral and at higher ionic concentrations, the ions cover the mineral surface to a greater extent and hence increase its zeta potential. Furthermore, this may be indicative of the compression of the electrical double layer (Moignard *et al.,* 1977). Another interesting observation from these measurements was that at the pH the bubble-particle testwork was conducted, around pH 7, the zeta potential is very close to 0 mV in 10 SPW and is in fact 0 mV with galena. As previously described in Chapter 2, the compression of the electrical double layer may lead to a faster thinning of the film at the air-water and solid-water interfaces improving bubble-particle interactions. This is said to be due to increases in inorganic electrolytes in the bulk solution, counterions enter the Stern layer which in turn thickens the diffuse layer as a result of the increase in attraction force and decrease in repulsion force (Wang and Peng, 2014). Therefore, the compression of the electrical double layer in high ionic strength solutions may promote particle recovery because of the reduction in repulsion between bubble and particle. Furthermore, particle aggregation is common when the potential is close to 0 mV (Salopek *et al.,* 1992; Wang and Peng, 2014). Upon deducing the zeta potential of the minerals via the operating pH, the results of this study show that in the case of galena and chalcopyrite the most successful bubble-particle interactions occur when the potential of the mineral surface is close to 0 mV. Subsequently, in addition to faster rupturing of the film between the bubble and particle, particle agglomeration may also be responsible for the increase in bubble-particle attachment with increasing ionic strength of the plant water.

In the case of pyrrhotite, particles with a more negative zeta potential resulted in a higher attachment probability, however the microflotation tests showed that an increase in ionic strength and hence increase in zeta potential resulted in higher recoveries.

Another factor to take into consideration is that the zeta potential of the bubble may also change in the presence of the various ionic solutions. Yang *et al.* (2001) showed that the zeta potential is not only dependent on the solution pH but also on the electrolyte concentration as well as ion type. The aforementioned study showed a decrease in the zeta potential towards more negative values with NaCl, while multivalent metal ions Ca^{2+} and Al^{3+} had a greater impact on the magnitude of the zeta potential and can even reverse the charge polarity.

11.5 The Effect of an Increase in Ionic Strength of Plant Water at pH 11 on the Bubble-Particle Interactions for Selected Sulfide Minerals

Chapter 7 and Chapter 9 assessed the effect of synthetic plant water of increasing ionic strength at pH 11 on bubble-particle attachment of pyrrhotite, galena and chalcopyrite. The trends were very similar across the three sulfide minerals under study. Firstly, the system at pH 11 yielded much lower recoveries, attachment probabilities and mass recovered compared to the minerals natural pH across all water types. Thus, with 1 SPW at pH of 6.5 the performance was much better compared to with 1 SPW at pH 11, this was the same for 5 SPW and 10 SPW. It must however be noted that although the bubble-particle

attachment performance was much lower at pH 11, the increase in ionic strength leading to increased mineral recoveries was still observed. Similar trends on mineral recoveries were obtained by Tadie *et al.* (2016) who studied galena recovery at high and low pH and ionic strength of synthetic plant water and Manono *et al.* (2017) who investigated the effect of ionic strength and pH on a Cu-Ni-PGM ore; they attributed their findings of lower mineral recoveries at pH 11 compared to pH 9 to the precipitation of hydroxide species on the mineral surface.

Speciation diagrams of 1 SPW, 5 SPW and 10 SPW shown by Manono *et al.* (2018) showed that at the pH range 10 to 12, the content of oxyhydroxo species increases substantially. Furthermore, the highest concentration of these species is present in the 10 SPW plant water at pH values of 11 and above.

The zeta potential between pH 10 and 12 across all water types show a distinct increase in the potential of the mineral surface; with the charge reversal taking place with 5 SPW and 10 SPW at around pH 11 across the three minerals. Given that oxyhydroxo complexes form at this pH range, this increase in zeta potential and charge reversal can be attributed to the deposition of these oxyhydroxo species on the mineral surface.

Furthermore, Fuerstenau *et al.* (1999) proposed that at alkaline pH, metal ions hydrolyze and deposit hydrophilic metal hydroxides onto the surface of the mineral. Thus, given the zeta potential and accompanying speciation diagrams from Manono *et al.* (2018), it is clear that these oxyhydroxo species are reducing the hydrophobicity of the mineral surface quite dramatically as compared to the tests conducted at the natural pH. of 6.5 Additionally, the deposition of these species on the mineral surface will hinder the adsorption of the collector on the mineral surface, thus also reducing the bubble-particle attachment as observed (Rao, 2004).

Interestingly however, the increasing recovery as the ionic strength of the water increases is still maintained even at pH 11 although the recoveries are low. This result shows that even in the presence of these oxyhydroxo species the effect of the compression of the electrical double layer in increased electrolyte concentration comes through. Intuitively it is expected that a higher concentration of ions in the water will result in greater amounts of the oxyhydroxo species at pH 11 which should in turn result in lower mineral recoveries. This logic seems to not be the case as the recoveries of 10 SPW at pH 11 are higher than the other water types; this result thus indicates that increases in sulfide mineral recovery can be attained at a high pH with plant water of high ionic strengths.

11.6 The Effect of Specific Ions in Plant Water on Bubble-particle Interactions of Selected Sulfide Minerals

Chapter 3 hypothesised that *"divalent ions such as Ca^{2+} and SO_4^{2-} will result in a greater attachment probability compared to monovalent ions. Divalent ions result in increased adsorption onto the mineral surface compared to monovalent ions; reducing the magnitude of the negative mineral charge and thus decreasing the energy barrier for bubble-particle attachment."*

The microflotation and ACTA studies conducted with galena, pyrrhotite and chalcopyrite however showed that Ca^{2+} containing solutions resulted in low recoveries and low attachment probabilities. While the $NaNO_3$ solution resulted in the highest recoveries and highest attachment probabilities across the three sulfide minerals. These results were observed both in the presence and absence of SIBX.

Studies by Wang and Peng (2014), Blake and Kitchener (1972) and Li *et al.* (2017) have shown that the stability of the hydration layer is decreased in solutions of higher ionic strength; particularly in monovalent salt solutions. When longer induction times were observed by Hirajima *et al.* (2016) these were ascribed to an increase in the hydration layer stability, subsequently resulting in decreased bubble-particle attachment. By this logic, a decrease in the stability of the hydration layer is expected to yield an increase in recovery and bubble-particle attachment in general. Therefore, the higher chalcopyrite, galena and pyrrhotite recoveries in the Na^+ solution as observed in this study may be due to the reduced stability of the hydration layer in this monovalent salt solution (Li *et al.,* 2017).

The fact that Ca^{2+} does result in decreased successful bubble-particle attachment, even lower than with plant water, raises questions with regards to how the xanthate adsorption on the mineral surface may be affected in Ca^{2+} containing solutions. Studies have shown that Ca^{2+} passivates the surface of the mineral and may as a result hinder the collector adsorption; these studies along with the adsorption studies are discussed in subsequent sections. However, this result of Ca^{2+} containing solutions yielding low mineral recoveries is also evident in the absence of SIBX indicating that collector – mineral adsorption is not the only process that may be affected by Ca^{2+}.

In terms of anions, Chapter 7 and Chapter 10 shows that generally NO_3^- resulted in lower recoveries and attachment probability as compared to SO_4^{2-} with Ca^{2+} as the cation in solution. The $NaNO_3$ solution yielded the highest mineral recoveries and attachment probability across the three sulfide minerals tested; therefore, it could be that the effect of the cation over-powers that of the anion. Furthermore, although $CaSO_4$ and $Ca(NO_3)_2$ solutions were of the same ionic strength; the $Ca(NO_3)_2$ solution has a higher concentration of Ca^{2+} at 1610 mg/L versus the 1207 mg/L of Ca^{2+} in the $CaSO_4$ solution. Thus, indicating that the Ca^{2+} in the $Ca(NO_3)_2$ solution may be deterring bubble-particle attachment more due to the increased amount of Ca^{2+} rather than the effect of the NO_3^-.

11.7 The Effect of Specific Ions in Plant Water on Xanthate Adsorption on the Surface of Selected Sulfide Minerals

Phase one exploratory work with pyrrhotite in single salt solutions was done in the absence of a collector hence the effect of specific ions on collector adsorption onto pyrrhotite cannot be reported on. Phase two work with galena and chalcopyrite did however make use of a collector when studying the effect of specific ions. Nonetheless, the three sulfide minerals used in this study generally behaved very similarly.

Chapter 10 showed strong correlations between bubble-particle attachment and collector adsorption. Both bubble-particle attachment techniques, ACTA and microflotation showed high bubble-particle attachment in the $NaNO_3$ solution; and the collector adsorption was highest with $NaNO_3$. Under $NaNO_3$ collector

adsorption was reported at 99.96% and 99.80% at the chalcopyrite and galena surface respectively. While both sulfide minerals reported lower collector adsorption in the $Ca(NO_3)_2$ solution; this single salt solution also yielded the lowest recoveries and attachment probabilities from the salt solutions under study. These results hence show a relationship does exist in that the salts yielding the lowest and highest recovery, also shows the lowest and highest collector adsorption respectively. It may therefore be deduced that Ca^{2+} containing solutions result in decreased xanthate adsorption on the mineral surface and as a result lower bubble-particle attachment. Studies have shown that Ca^{2+} increased the amount of xanthate necessary to create a hydrophobic surface (Hodgson and Agar, 1989; Ikumapayi *et al.*, 2012)

Li *et al.* (2017) also showed that the xanthate adsorption was increased and hence floatability increased in monovalent salt solutions while the opposite was shown with divalent salts; they attributed this to the precipitation of oxyhydroxo species on the mineral surface which in turn deterred the adsorption of the collector. This study by Li et al., (2017) was however conducted at pH 10; this work was conducted at pH 6.5 and the speciation diagrams in Chapter 7 do not show oxyhydroxo species present at this pH. Therefore, the reduction in xanthate adsorption in this work may not be due to the precipitation of oxyhydroxo species. A coal flotation study by Laskowski (1965) showed improved flotation in NaCl and KCl; he proposed that the electrical double layer around the coal particles was compressed in the salt solution and this resulted in the opening of hydrophobic surface sites on the particle which in turn attracted air bubbles by hydrophobic bonding. It may therefore be that the proposal by Laskowski (1965) only holds in monovalent salt solutions and that a three-phase mineral system reacts differently in the presence of divalent ions. Authors have studied the effect of Ca^{2+} and proposed that Ca^{2+} in solution passivates the negative mineral surface via electrostatic reactions and hinders the oxidation of xanthate resulting in lower xanthate adsorption on the surface (Fuerstenau, 1982; Elizondo-Alvarez *et al.,* 2017). Given the outcome of this study which shows lower collector adsorption in Ca^{2+} containing solutions and higher adsorption in Na^{+}, it is proposed that the valency of the ion determines whether the ion competes with collector molecules on the mineral surface or not.

From an anion perspective, the results of this study show that SO_4^{2-} results in slightly more xanthate adsorbed on chalcopyrite, while on the galena surface slightly more xanthate adsorption was observed with the NO_3^- solution. Barker (1983) showed that NO_3^- containing solution showed lower collector adsorption on pyrite however could not provide a reason for this result; while Elizondo-Álvarez *et al.* (2017) showed that mineral passivation by SO_4^{2-} was detrimental to xanthate adsorption. An important factor to consider in this study is that the accompanying Ca^{2+} cation concentration is different for $CaSO_4$ and $Ca(NO_3)_2$. The NO_3^- solution does have a higher Ca^{2+} concentration compared to the SO_4^{2-} solution, therefore it is expected that more Ca^{2+} could result in the mineral surface becoming more passivated with Ca^{2+} through chemisorption, in turn creating even more competition for the collector molecules to adsorb on the mineral surface.

Chapter 10 also studied the performance of synthetic plant water at the same ionic strength as the single salt solutions; the synthetic plant water generally showed lower xanthate adsorption compared to the single solutions. This was speculated to be due to the combined effect of the various ions in the water but could also be due to its significant SO_4^{2-} concentration at 1200 mg/L while it contains less Ca^{2+} compared to the single salt solutions. Studies by Elizondo-Álvarez *et al.* (2017) showed that SO_4^{2-} passivates the mineral surface hindering collector adsorption; in this investigation the SO_4^{2-} acting in conjunction with Ca^{2+}, results in the low xanthate adsorption under the synthetic plant water.

Although the effects of the xanthate adsorption under the varying water qualities are clearly evident in the bubble-particle attachment techniques; the bubble-particle tests show similar trends both in the presence and absence of a collector. Tests with the collector show increased bubble-particle interactions but the underlying trend remains fairly the same even in the absence of the collector. For example, the Na^+ containing salt yields the highest recoveries across the sulfide minerals under study both with and without a collector; while Ca^{2+} containing salts perform poorer both in the absence and presence of the collector. This result indicates that there may be another mechanism such as the effect on zeta potential at play; in addition to the effect that specific ions have on xanthate adsorption.

11.8 The Effect of Specific Ions in Plant Water on the Zeta potential of Selected Sulfide Minerals

The zeta potential of pyrrhotite, galena and chalcopyrite display similar trends with the single salt solutions under study. The potential of the three sulfide minerals is very negative under the $NaNO_3$ solution; in all cases the zeta potential is very similar to that of ULP and DI water under $NaNO_3$. $Ca(NO_3)_2$ on the other hand resulted in a more positive zeta potential of the three sulfide minerals. Although both are NO_3^- salts, it is clear the Ca^{2+} containing solution results in a more positive zeta potential of the sulfide mineral surface. Furthermore, particles in the $CaSO_4$ solution exhibited a zeta potential more positive than $NaNO_3$ but less than $Ca(NO_3)_2$; demonstrating a cation and anion effect in that Ca^{2+} and NO_3^- result in more positive zeta potential of the mineral. By considering the positive shift of the zeta potential in Ca^{2+}, it may be deduced that Ca^{2+} passivate the mineral surface to a greater degree than that of Na^+ (Ma, 2005; Li *et al.,* 2017). Work done by Ikumapayi *et al.* (2012), Li *et al.* (2017), and Hirajima *et al.* (2016) have also shown higher zeta potential with increased Ca^{2+} in solution.

Studies have further ascribed the increase in zeta potential in the presence of cations to the compression of the electrical double layer which in turn results in a decrease in the energy barrier for film rupture and the subsequent decrease in electrostatic repulsion between surfaces (Laskowski, 1965; Hirajima *et al.,* 2016; Li *et al.,* 2017).

The zeta potential therefore make it possible to infer a decrease in electrostatic repulsion between solid surfaces with Ca^{2+} containing salts; it would therefore be expected that more particles attach to the bubbles in Ca^{2+} containing solutions. Ca^{2+} is also known to result in particle aggregation (Li *et al.,* 2017) and the zeta potential being close to 0 mV in Ca^{2+} provides further evidence of particle aggregation (Salopek *et al.,* 1992; Wang and Peng, 2014) thus it would be expected to achieve more bubble-particle attachment in Ca^{2+}

solutions. Chapter 7 and Chapter 10 however report lower bubble-particle attachment in Ca^{2+} containing solutions. Adsorption studies on this work do however indicate that less xanthate is adsorbed on the mineral surface in Ca^{2+} solutions and hence lower bubble-particle attachment is reported. However as stated in Section 11.6, it has been shown that Ca^{2+} passivates the negative mineral surface via electrostatic reactions; this hinders the oxidation of xanthate, signifying that the electrical double layer drives the adsorption of physically-adsorbing reagents through the magnitude and sign of the mineral zeta potential (Fuerstenau, 1982; Elizondo-Alvarez *et al.,* 2017).

The NO_3-containing salt resulted in a more positive mineral potential compared to the SO_4^{2-} salt; although both contain a Ca^{2+} cation. As with the adsorption test results, this may not actually be due to an anion effect but possibly due to an over-powering effect of the Ca^{2+}; although these two salt solutions are of the same ionic strength (0.1205 M), $Ca(NO_3)_2$ has a significantly higher concentration of Ca^{2+} present compared to the $CaSO_4$ solution of 0.04 M and 0.03 M respectively (refer to Section 7.3.3)

It may therefore be that the more positive zeta potential and subsequent higher zeta potential on chalcopyrite and galena may hinder the adsorption of xanthate on the mineral surface. Furthermore, even in the absence of a collector, Ca^{2+} resulted in poorer mineral recoveries and attachment probabilities. The zeta potential showed close to 0 mV and often positive zeta potential with Ca^{2+} containing solutions. The synthetic plant water testwork showed that solutions which resulted in a surface chare close to 0 mV had a positive effect on the bubble-particle attachment due to the particle aggregation that occurs at this potential. This, however, is not seen with the single salt solutions; where particles in Ca^{2+} develop a more positive surface chare but the bubble-particle attachment is low. It should be noted that the Ca^{2+} concentration in the single salt solutions are almost double the concentration of Ca^{2+} in 10 SPW of 800 mg/L; this suggests that the concentration of specific inorganic electrolytes plays an important role in the bubble-particle attachment response. It may therefore be that the Ca^{2+} concentration in the single salt solutions (1610 mg/L in $Ca(NO_3)_2$ and 1207 mg/L in $CaSO_4$) is "relatively higher" which results in particle aggregation not occurring at the operating pH (6.5) and further also hindering collector adsorption in the presence of the collector.

11.9 References

Barker, L. M. (1983). The Effect of Electrolytes on the Flotation of Pyrite. MSc.Eng Thesis, University of Cape Town, Chemical Engineering.

Blake, T.D., Kitchener, J.A. (1972). Stability of aqueous films on hydrophobic methylated silica. Journal of the Chemical Society. 68, 1435–1442.

Elizondo-Alvarez, M.A., Flores-Alvarez, J.M., Davila-Pulido, G.I., Uribe-Salas, A. (2017). Interaction mechanism between galena and calcium and sulfate ions.Minerals Engineering. 111, 116–123.

Fuerstenau, D.W. (1982). Mineral-water interfaces and the electrical double layer. In: King, R.P. (Ed.), Principles of Flotation. South African Institution of Mining and Metallurgy, Johannesburg, pp. 17–30.

Fuerstenau, DW, Herrera-Urbina, R, McGlashan, D.W. (1999) Studies on the applicability of chelating agents as universal collectors for copper minerals. International Journal of Mineral Processing 58, pp 15-33.

Fuerstenau, M.C., Somasundaran, P. (2003). Flotation. In: Fuerstenau, M.C., Han, K. (Eds.), Principles of Mineral Processing. Society for Mining, Metallurgy, and Exploration (SME), Littleton, Colorado, pp. 245–306.

Hirajima, T., Suyantara, G.P.W., Ichikawa, O., Elmahdy, A.M., Miki, H., Sasaki, K. (2016). Effect of Mg^{2+} and Ca^{2+} as divalent seawater cations on the floatability of molybdenite and chalcopyrite.Minerals Engineering. 96, 83–93. https://doi.org/10.1016/j.mineng.2016.06.023.

Hartmann, R., and Serna-Guerrero, R. (2020). Towards a quantitative analysis of the wettability of microparticles using an automated contact timer apparatus. Minerals Engineering. 149:106240. doi: 10.1016/j.mineng.2020.106240

Hodgson, M., Agar, G.E. (1984). An electrochemical investigation into the natural flotability of pyrrhotite. In: Richardson, P.R., Srinivasan, S.S., Woods, R. (Eds.), Electrochemistry in Mineral and Metal Processing. ECS, Pennington, NJ, USA, pp. 185–201

Ikumapayi, F., Makitalo, M., Johansson, B. and Hanumantha, K. (2012). Recycling of Process Water in Sulfide Flotation : Effect of Calcium and Sulphate Ions on Flotation of Galena. Minerals Engineering 39. Elsevier Ltd: 77–88. https://doi.org/10.1016/j.mineng.2012.07.016

Kirjavainen, V., Schreithofer, N. and Heiskanen, K. (2002). Effect of calcium and thiosulfate ions on flotation selectivity of nickel-copper ores. Minerals Engineering , 59 (1-2), 1-5.

Laskowski J. (1965). Coal flotation in solutions with raised concentration of inorganic salts. Colliery Guardian, 361–365.

Laskowski, J.S. (2013). From amine molecules adsorption to amine precipitate transport by bubbles: A potash ore flotation mechanism. Minerals Engineering, Vol. 45, No. 1, pp. 170–179.

Laskowski, J. and Iskra, J. (1970). Role of capillary effects in bubble-particle collision in flotation. Transactions of the Institution of Mining and Metallurgy. 79, C6.

Li, Wanqing, Xiao, Qing, He, Nan, Ren, Zijie, Lartey, Clement, Gerson, Andrea (2017). The influence of common monovalent and divalent chlorides on chalcopyrite flotation. Minerals 7, 111. https://doi.org/10.3390/min7070111.'

Ma, X.. (2005). Effect of Alkali Metal Cations on Adsorption of Guar Gum onto Quartz. Master of Applied Sciences Thesis. University of British Columbia, Faculty of Graduate Studies Mining Engineering

Manono, M.S, Corin, K.C. and Wiese, J.G. (2018). Perspectives from Literature on the Influence of Inorganic Electrolytes Present in Plant Water on Flotation Performance. Physicochemical Problems of Mineral Processing 54 (4): 1191–1214. https://doi.org/10.5277/ppmp18157.

Miller, J.D. (2005). A review of pyrrhotite flotation chemistry in the processing of PGM ores. Minerals Engineering. 18 (18), 855–865. https://doi.org/10.1016/j.mineng.2005.02.011.

Moignard, M.S., James, R.O., Healy, T.W. (1977). Adsorption of calcium at the zinc sulphide– water interface. Australian Journal of Chemistry 30, 733–740.

Pienaar, D., Jordaan, T., McFadzean, B., O'Connor, C.T. (2019) The synergistic interaction between dithiophosphate collectors and frothers at the air-water and sulphide mineral interface. Minerals. Engineering 138, 125–132.

Rao, S.R. (2004). Surface Chemistry of Froth Flotation, 2nd edition, Kluwer Academic/Plenum Publishers, New York.

Salopek, B., Krasic, D., Filipovic, S. (1992). Measurement and Application of Zeta- Potential. Rudarsko-Geolosko-Naftni Zbornik 4, 147–151.

Wang, B., Peng, Y. (2014). The effect of saline water on mineral flotation – a critical review.Minerals Engineering. 66–68, 13–24. https://doi.org/10.1016/j.mineng.2014.04.017.

Wang, J.Y., Xie, L., Liu, Q.X., Zeng, H.B. (2015). Effects of salinity on xanthate adsorption on sphalerite and bubble-sphalerite interactions. Minerals Engineering. 77, 34–41.

Yang, C., Dabros, T., Li, D., Czarnecki, J., Masliyah, J.H. (2001). Measurement of the zeta potential of gas bubbles in aqueous solutions by microelectrophoresis method. Journal of Colloid and Interface Science. 243, 128–135. https://doi.org/10.1006/jcis.2001.7842

Yoon, R. and Yordan, J.L. (1991). Induction-time measurements for the quartz-amine flotation system. Journal of Colloid and Interface Science. 141 (2): 374-383.

Chapter 12 **Conclusions and Recommendations**

12.1 Conclusions

The main aim of this work was to investigate the effect of complex process waters and the recycling thereof on the bubble-particle attachment sub-process in a sulfide mineral system; as well as to identify specific ions within process water that control the bubble-particle attachment sub-process by either enhancing, hindering or having no effect on the bubble-particle attachment of sulfide minerals. This work also aimed to corroborate the use of the ACTA as a means to assess bubble-particle attachment at a fundamental level by comparison with the classical microflotation technique.

The overarching question which drove this work was stated as "*How do changes in water quality affect the bubble-particle attachment of sulfide minerals and subsequently collector adsorption and mineral potential*?" In an attempt to answer this overarching question, eight key questions were developed to meet each of the objectives (as outlined in Section 3.1) set out in this work.

Two underlying mechanisms are proposed for the impact seen on bubble-particle attachment. These two mechanisms which are detailed hereafter are drawn from the fundamental studies assessing the effects of water quality (ionic strength of SPW and specific ions) on collector adsorption and the zeta potential of the sulfide minerals.

The work assessing the effect of ionic strength on bubble-particle attachment, collector adsorption and zeta potentials showed that in increasing ionic strength of SPW, bubble-particle attachment increased, collector adsorption on the sulfide minerals decreased while the zeta potential of the minerals increased. The increase in bubble-particle attachment, which occurred despite the drop in collector adsorption, was attributed to the impact on the zeta potential of the minerals. Thus Mechanism I proposes that the effect of ions on the zeta potential of the minerals and the resulting impact on the electrical double layer, decreases the electrostatic repulsive forces that work against bubble-particle attachment, this in turn results in the thinning of the film at the air-water and solid-water interfaces and consequently bubble-particle attachment is promoted.

The work assessing the effect of specific ions on bubble-particle attachment, collector adsorption and zeta potentials showed that in the divalent Ca^{2+} containing single salts, bubble-particle attachment decreased, the adsorption of the collector on the sulfide minerals also decreased while an increase in the zeta potential of the minerals was seen compared to when a single salt solution containing the monovalent Na^{+} was used. The decrease in bubble-particle attachment in Ca^{2+} is attributed to the decrease in collector adsorption and the passivated sulfide mineral surface in Ca^{2+} salts as the concentration of Ca^{2+} in the selected single salt solutions was even greater than $[Ca^{2+}]$ in 10 SPW (which is the SPW with the highest total ionic strength). In other words compared to the surface passivation in the work considering increases in the ionic strength of SPW, it could be said that there is a level of surface passivation beyond which the induced zeta potential coupled with collector adsorption retardation is non-conducive for bubble-particle attachment. Thus,

Mechanism II proposes that the effect of ions on the collector and the resulting impact on mineral-collector interactions affecting the eventual bubble-particle attachment can be linked to the increased passivation of the mineral surface as this affects the mineral-collector reaction and subsequently negatively affects the bubble-particle attachment. Furthermore mineral surface passivating ionic species of the divalent Ca^{2+}, hydrophilic in nature, form in solution in increased [Ca^{2+}], hinder the adsorption of the collector causing a further increase in the hydrophilicity of the coated mineral surface and consequently retard the bubble-particle attachment of sulfide minerals.

The eight key questions attempting to answer the overarching question mentioned earlier are given in the bullet points hereafter.

1. How does an increase in ionic strength of plant water affect the bubble-particle attachment for selected sulfide minerals?

   Increasing the ionic strength of plant water resulted in an increase in bubble-particle attachment as indicated by the attachment probability and mass recovered from the ACTA as well microflotation tests; pyrrhotite however showed a decrease in attachment probability with increasing ionic strength, this difference in behaviour compared to galena and chalcopyrite was attributed to the finer particle size used in phase one of this work. Microflotation however showed increasing pyrrhotite recovery with increasing ionic strength. Zeta potential determination tests further confirmed the compression of the electrical double layer in solutions of high ionic strength; which indicates a decrease in electrostatic repulsion between solid surfaces (bubble-particle and particle-particle) under high ionic strength. This comes as a result of the mineral surface becoming more positively charged due to the passivation of cations on the mineral surface, considering that the bubble is assumed to be negatively charged this will result in a decrease in the energy barrier for bubble-particle attachment. The effect of this decrease in electrostatic repulsion is that the film at the air-water and solid-water interfaces will thin quicker, resulting in more bubble-particle attachment. Under the operating pH (6.5), the zeta potential is close to 0 mV in solutions of high ionic strength; particle agglomeration can therefore be inferred at this zeta potential, meaning that particles will aggregate and cluster together resulting in more particles attaching to the air bubbles upon bubble-particle contact in solutions of high ionic strength.

2. How does an increase in the ionic strength of plant water affect the adsorption of xanthate on the mineral surface of selected sulfide minerals?

   Increasing the ionic strength of plant water resulted in a decrease in the amount of xanthate adsorbed at the sulfide mineral surface. Adsorption studies showed that

with water of high ionic strength, more xanthate is left in solution; indicating that less xanthate is actually being adsorbed on the mineral surface when there are more inorganic electrolytes in the system. This action was attributed to the fact that with a higher ionic strength, more inorganic electrolytes passivate the mineral surface; resulting in greater competition for the xanthate molecules to adsorb on the mineral surface.

3. How does an increase in ionic strength of plant water affect the zeta potential of selected sulfide minerals?

   The zeta potential of pyrrhotite, galena and chalcopyrite became more positive as the ionic strength of the water was increased. ULP and DI water resulted in the most negative zeta potential while 10 SPW resulted in a more positive mineral charge. This is indicative of an adsorption of cations on the mineral surface and the compression of the electrical double layer; which further results in a decrease in repulsion between solid surfaces (bubble and particle as well as particle and particle). This decrease in repulsion between bubble and particle as well as particle and particle come as a result of the increasingly positive mineral surface due to the passivation of cations on the mineral surface and negative surface of the bubble; which decreases the energy barrier for bubble-particle attachment to occur. This decrease in repulsion between solid surfaces thus results in higher bubble-particle attachment and particle aggregation (Mechanism I).

4. Are there specific ions in plant water that control bubble-particle interactions on selected sulfide minerals?

   Pyrrhotite, galena and chalcopyrite showed lower bubble-particle attachment in Ca^{2+} containing solutions as indicated by the attachment probability and mass recovered from the ACTA as well microflotation tests. The $NaNO_3$ solution generally resulted in the highest bubble-particle attachment for all three sulfide minerals. The effect of the valency of the cation was clearly evident in that the divalent Ca^{2+} passivated the mineral surface more than the monovalent Na^{+}; as shown by the zeta potential; this increased passivation of the mineral surface proved to be detrimental to bubble-particle attachment unlike with synthetic plant water where the increased mineral passivation by cations enhanced bubble-particle attachment. This difference is speculated to be due to the fact that the Ca^{2+} concentration is about double that of 10 SPW; which alludes to the fact that there may be a maximum concentration of cations' passivation of the mineral surface which enhances bubble-particle attachment and above this concentration bubble-particle attachment is negatively impacted. The adsorption of Ca^{2+} on the sulfide

mineral surface further proved to have negative effects on the adsorption of the collector; which will in turn affect its bubble-particle attachment efficiency.

5. Are there specific ions in plant water that either deter/improve the adsorption of xanthate on the mineral surface of selected sulfide minerals?

   Adsorption studies have shown that Ca^{2+} containing solutions were more effective at deterring the adsorption of xanthate on the sulfide mineral surface. More xanthate was left in solution under Ca^{2+} containing solutions meaning less xanthate actually adsorbed on the mineral surface. The $NaNO_3$ solution resulted in greater xanthate adsorption; even more xanthate was adsorbed in $NaNO_3$ than with synthetic plant water of the same ionic strength.

6. How do specific ions present in plant water affect the zeta potential on selected sulfide minerals?

   Zeta potential determination tests have shown that Ca^{2+} containing solutions result in a more positive zeta potential of pyrrhotite, galena and chalcopyrite; and solutions of higher Ca^{2+} concentration resulted in an even more positive zeta potential of the sulfide minerals. Given the effect of Ca^{2+} on the zeta potential, adsorption of xanthate and the responding bubble-particle attachment, this work suggests that the increased passivation of the mineral surface by Ca^{2+} (under much higher Ca^{2+} concentrations than in SPW) hinders the action of the collector. This relates to mechanism II in terms of the effect of the ions on the collector which results in the mineral-collector interactions hindered, negatively affecting bubble-particle attachment.

7. How does an increase in ionic strength of plant water at high pH affect the bubble-particle interactions for selected sulfide minerals?

   Synthetic plant water solutions at pH 11, resulted in significantly lower bubble-particle attachment compared to at the natural pH of 6.5. The presence of oxyhydroxo species has proven to be detrimental in bubble-particle attachment as shown by attachment probability and mass recovered in the ACTA as well as recovery from microflotation. It is believed that the deposition of these species induce hydrophilicity and hinder the action of the collector. Although bubble-particle attachment was low at pH 11; pH 11 solutions showed an increase in bubble-particle attachment as the ionic strength of the plant water was increased which indicates the effect of the compression of the electrical double layer due to the increase in ionic concentration (as discussed in key question 1).

8. Can the ACTA be used to determine the floatability of mineral particles?

   This work has shown that the outputs of the ACTA coincide well with that of the classical microflotation technique. This study also presented the importance of showcasing both the attachment probability and mass of particles collected when taking measurements with the ACTA. It is however important to note that the recommended particle size for sulfide minerals in the ACTA is -125+106 μm; such that it is able to collect the particles that successfully attached to the air bubbles.

The ACTA was constructed with the intent of it being a quick diagnostic tool on flotation plants to assess the bubble-particle efficiency under varying conditions; the outcome of this work showed that this instrument is a viable option as a measure for particle floatability. The findings of this work will provide flotation operations with an understanding of how specific ions within plant water affect bubble-particle attachment; which will allow for the water quality to be tailored towards achieving high bubble-particle attachment of value and subsequently high mineral recoveries.

12.2 Recommendations

Recommendations for future work are presented below from ideas and unanswered questions emerging from the findings of this study.

- Flotation pulps with ionic solutions may not only result in a change in the zeta potential of the particle, but upon the introduction of air bubbles the zeta potential of the air bubbles may be altered as well. It may therefore be of interest to understand how the charge on the bubble changes under the various ionic solutions; the charge of the bubble and particle as well as the resulting bubble-particle attachment can then be used to determine a relationship between the zeta potential of the two surfaces and the resulting bubble-particle attachment under various ionic solutions.
- When studying whether a specific ion within the plant water controls the bubble-particle attachment and underlying factors such as zeta potential and xanthate adsorption, this study used single salt solutions of the same ionic strength of the plant water. This however results in very high concentrations of the cation and anion; much higher than that of the same cation and anion in the plant water of the same ionic strength. It would however be interesting to see how the bubble-particle attachment, zeta potential and collector adsorption will be affected if the cations and anions in the various single salt solutions are of the same concentration of the respective cations and anions in the plant water.
- The exact effect of NO_3^- was not determined in this study, due to the over-powering effect of the Na^+ and Ca^{2+} cations. Barker (1983) showed that NO_3^- reduced xanthate adsorption but could not provide the mechanism by which this occurred. The previous recommendation of using the same ion concentration as in the plant water would therefore enable the effect of NO_3^- to be understood.

- Include the use of molecular dynamics simulation (MD) or density function theory (DFT) to explore the interactions between specific ions and the minerals, collector-ion-minerals as well as between the bubbles and mineral particles.
- Further investigate cases where the mass recovered increases with synthetic plant water of increasing ionic strength, but the attachment probability is almost constant. Rate of sedimentation measurements may be used to first investigate this mechanism.
- The decrease in collector adsorption with synthetic plant water of increasing ionic strength can be additional evidence that the electrostatic mechanism is the main driving force of the liquid film rupture under the specified conditions. Therefore, further analysis of the results supported by contact angle measurements must be considered.

12.3 References

Barker, L. M. (1983). The Effect of Electrolytes on the Flotation of Pyrite. MSc.Eng Thesis, University of Cape Town, Chemical Engineering.

Appendices

Appendix A: Raw Data Galena

ACTA

	Attachments out of 396	
	1	2
1 SPW	147	178
5 SPW	195	167
10 SPW	192	160

	Attachment out of 396	
	1	2
$CaSO_4$	245	263
$NaNO_3$	258	271
$Ca(NO_3)_2$	161	197
5 SPW	195	167

Microflotation

1 SPW

Conditions	Time		sample + fp	fp	mass	Cum mass	%		Conditions		sample + fp	fp	mass	Cum mass	%
Galena:	2	C1	0,32	0,29	0,03	0,03	0,943396		Galena:	C1	0,34	0,3	0,04	0,04	2
1 SPW	6	C2	0,35	0,3	0,05	0,08	2,515723		1 SPW	C2	0,38	0,31	0,07	0,11	5
No collector	12	C3	0,36	0,29	0,07	0,15	4,716981			C3	0,44	0,31	0,13	0,24	11
	20	C4	0,46	0,31	0,15	0,3	9,433962			C4	0,45	0,33	0,12	0,36	17
		Tails	7,8	4,92	2,88					Tails	6,83	5,02	1,81		
					3,18								2,17		

5 SPW

Conditions	Time		sample + fp	fp	mass	Cum mass	%		Conditions		sample + fp	fp	mass	Cum mass	%
Galena:	2	C1	0,43	0,31	0,12	0,12	5,084746		Galena:	C1	0,39	0,27	0,12	0,12	6
5 SPW	6	C2	0,47	0,3	0,17	0,29	12,28814		5 SPW	C2	0,44	0,3	0,14	0,26	14
No collector	12	C3	0,48	0,31	0,17	0,46	19,49153			C3	0,47	0,29	0,18	0,44	24
	20	C4	0,62	0,31	0,31	0,77	32,62712			C4	0,43	0,3	0,13	0,57	31
		Tails	6,61	5,02	1,59					Tails	6,29	5	1,29		
					2,36								1,86		

10 SPW

Conditions	Time		sample + fp	fp	mass	Cum mass	%		Conditions		sample + fp	fp	mass	Cum mass	%
Galena:	2	C1	0,53	0,34	0,19	0,19	7,569721		Galena:	C1	0,42	0,29	0,13	0,13	6
10 SPW	6	C2	0,51	0,32	0,19	0,38	15,13944		10SPW	C2	0,59	0,31	0,28	0,41	18
No collector	12	C3	0,72	0,33	0,39	0,77	30,67729			C3	0,61	0,32	0,29	0,7	32
	20	C4	0,82	0,31	0,51	1,28	50,99602			C4	0,87	0,58	0,29	0,99	45
		Tails	6,15	4,92	1,23					Tails	6,52	5,29	1,23		
					2,51								2,22		

1 SPW

Conditions	Time		sample + fp	fp	mass	Cum mass	%		Conditions		sample + fp	fp	mass	Cum mass	%
Galena:	2	C1	0,71	0,29	0,42	0,42	18,34061		Galena:	C1	0,6	0,3	0,3	0,3	12
1 SPW	6	C2	0,61	0,31	0,3	0,72	31,44105		1 SPW	C2	0,93	0,29	0,64	0,94	37
SIBX	12	C3	0,6	0,31	0,29	1,01	44,1048			C3	0,59	0,31	0,28	1,22	48
	20	C4	0,55	0,28	0,27	1,28	55,8952			C4	0,66	0,32	0,34	1,56	61
		Tails	5,91	4,9	1,01					Tails	5,75	4,76	0,99		
					2,29								2,55		

5 SPW

Conditions	Time		sample + fp	fp	mass	Cum mass	%		Conditions		sample + fp	fp	mass	Cum mass	%
Galena:	2	C1	0,78	0,33	0,66	0,66	21,78218		Galena:	C1	0,81	0,31	0,5	0,5	17
5 SPW	6	C2	0,78	0,29	0,49	1,15	37,9538		5 SPW	C2	0,95	0,33	0,62	1,12	38
SIBX	12	C3	0,99	0,31	0,47	1,62	53,46535			C3	0,92	0,31	0,61	1,73	58
	20	C4	1,07	0,3	0,77	2,39	78,87789			C4	0,85	0,29	0,56	2,29	77
		Tails	4,71	4,07	0,64					Tails	4,65	3,98	0,67		
					3,03								2,96		

10 SPW

Conditions	Time		sample + fp	fp	mass	Cum mass	%		Conditions		sample + fp	fp	mass	Cum mass	%
Galena:	2	C1	0,64	0,32	0,32	0,32	15,16588		Galena:	C1	0,47	0,29	0,18	0,18	9
10 SPW	6	C2	0,95	0,26	0,69	1,01	47,8673		10SPW	C2	0,97	0,2	0,77	0,95	48
SIBX	12	C3	0,78	0,31	0,47	1,48	70,14218			C3	0,71	0,31	0,4	1,35	68
	20	C4	0,62	0,3	0,32	1,8	85,30806			C4	0,72	0,3	0,42	1,77	89
		Tails	4,22	3,91	0,31					Tails	5,12	4,91	0,21		
					2,11								1,98		

DI

Conditions	Time		sample + fp	fp	mass	Cum mass	%		Conditions		sample + fp	fp	mass	Cum mass	%
Galena:	2	C1	0,7156	0,3022	0,4134	0,4134	27,4338		Galena:	C1	0,6904	0,3088	0,3816	0,3816	25
1 SPW	6	C2	0,764	0,319	0,445	0,8584	56,96463		1 SPW	C2	0,7729	0,312	0,4609	0,8425	54
	12	C3	0,5658	0,3273	0,2385	1,0969	72,79182			C3	0,6902	0,32	0,3702	1,2127	78
	20	C4	0,512	0,3012	0,2108	1,3077	86,78081			C4	0,4614	0,3116	0,1498	1,3625	88
		Tails	5,5277	5,3285	0,1992					Tails	5,5586	5,3703	0,1883		
					1,5069								1,5508		

CaSO4

Conditions	Time		sample + fp	fp	mass	Cum mass	0		Conditions		sample + fp	fp	mass	Cum mass	%
Galena:	2	C1	0,46	0,33	0,13	0,13	6,074766		Galena:	C1	0,52	0,32	0,2	0,2	7
1 SPW	6	C2	0,73	0,27	0,46	0,59	27,57009		1 SPW	C2	0,68	0,3	0,38	0,58	19
	12	C3	0,82	0,31	0,51	1,1	51,40187			C3	0,87	0,3	0,57	1,15	38
	20	C4	0,61	0,32	0,29	1,39	64,95327			C4	0,7	0,29	0,41	1,56	51
		Tails	5,78	5,03	0,75					Tails	5,43	3,96	1,47		
					2,14								3,03		

Ca(NO3)2

Conditions	Time		sample + fp	fp	mass	Cum mass	%		Conditions		sample + fp	fp	mass	Cum mass	%
Galena:	2	C1	0,51	0,31	0,2	0,2	8,733624		Galena:	C1	0,48	0,3	0,18	0,18	7
5 SPW	6	C2	0,62	0,35	0,27	0,47	20,52402		5 SPW	C2	0,59	0,3	0,29	0,47	19
	12	C3	0,76	0,31	0,45	0,92	40,17467			C3	0,57	0,31	0,26	0,73	29
	20	C4	0,66	0,33	0,33	1,25	54,58515			C4	0,78	0,29	0,49	1,22	48
		Tails	4,98	3,94	1,04					Tails	4,97	3,67	1,3		
					2,29								2,52		

NaNO3

Conditions	Time		sample + fp	fp	mass	Cum mass	%		Conditions		sample + fp	fp	mass	Cum mass	%
Galena:	2	C1	0,95	0,32	0,63	0,63	25,0996		Galena:	C1	0,86	0,3	0,56	0,56	24
10 SPW	6	C2	0,85	0,26	0,59	1,22	48,60558		10SPW	C2	0,73	0,36	0,37	0,93	39
	12	C3	0,72	0,31	0,41	1,63	64,94024			C3	0,96	0,32	0,64	1,57	66
	20	C4	0,57	0,3	0,27	1,9	75,69721			C4	0,66	0,31	0,35	1,92	81
		Tails	4,51	3,9	0,61					Tails	5,45	5	0,45		
					2,51								2,37		

1 SPW

Conditions	Time		sample + fp	fp	mass	Cum mass	0		Conditions		sample + fp	fp	mass	Cum mass	%
Galena:	2	C1	0,4266	0,3158	0,1108	0,1108	6,227168		Galena:	C1	0,4158	0,3216	0,0942	0,0942	6
1 SPW	6	C2	0,4289	0,3101	0,1188	0,2296	12,90395		1 SPW	C2	0,3633	0,3114	0,0519	0,1461	9
pH 11	12	C3	0,447	0,3163	0,1307	0,3603	20,24954			C3	0,4369	0,3032	0,1337	0,2798	17
	20	C4	0,3869	0,3102	0,0767	0,437	24,56022			C4	0,4029	0,322	0,0809	0,3607	22
		Tails	6,6441	5,3018	1,3423					Tails	5,9366	4,69	1,2466		
					1,7793								1,6073		

5 SPW

Conditions	Time		sample + fp	fp	mass	Cum mass	%		Conditions		sample + fp	fp	mass	Cum mass	%
Galena:	2	C1	0,4448	0,3189	0,1259	0,1259	5,533093		Galena:	C1	0,4712	0,3058	0,1654	0,1654	7
5 SPW	6	C2	0,4724	0,3028	0,1696	0,2955	12,98673		5 SPW	C2	0,4629	0,3104	0,1525	0,3179	14
pH 11	12	C3	0,5023	0,3172	0,1851	0,4806	21,12156			C3	0,5102	0,3261	0,1841	0,502	22
	20	C4	0,4818	0,323	0,1588	0,6394	28,10055			C4	0,4999	0,3115	0,1884	0,6904	30
		Tails	6,1486	4,5126	1,636					Tails	6,5092	4,8721	1,6371		
					2,2754								2,3275		

10 SPW															
Conditions	Time		sample + fp	fp	mass	Cum mass	0		Conditions		sample + fp	fp	mass	Cum mass	%
Galena:	2	C1	0,5344	0,3256	0,2088	0,2088	9,222615		Galena:	C1	0,6008	0,3133	0,2875	0,2875	13
10 SPW	6	C2	0,4742	0,3171	0,1571	0,3659	16,16166		10SPW	C2	0,467	0,3178	0,1492	0,4367	19
pH 11	12	C3	0,4911	0,3139	0,1772	0,5431	23,98852			C3	0,5129	0,316	0,1969	0,6336	28
	20	C4	0,4635	0,3194	0,1441	0,6872	30,35336			C4	0,4222	0,3107	0,1115	0,7451	33
		Tails	6,4857	4,9089	1,5768					Tails	6,2542	4,7424	1,5118		
					2,264								2,2569		

Zeta Potential

1 SPW					
pH	1	2	3		Average Zeta Pot
2	11,2	9,7	9,8		10,24333333
4	-6,2	-6,5	-4,9		-5,823333333
6	-10,9	-8,7	-8,8		-9,463333333
8	-9,5	-8,5			-8,955
10	-11,4	-11,1	-8,0		-10,17
12	3,2	3,4	2,9		3,178333333
5 SPW					
pH	1	2	3		Average Zeta Pot
2	-2,4				-2,42
4	-2,8	-4,6	-6,1		-4,486666667
6	-10,7	-10,5	-11,9		-11,03333333
8	-10,6	-11,6	-13,7		-11,96666667
10	-7,5	-7,6	-6,9		-7,346666667
12	6,6	6,4	5,2		6,083333333

10 SPW					
pH	1	2	3		Average Zeta Pot
2	-2,5	0,39			-1,0625
4	-6,6	-5,9	-6,2		-6,226666667
6	-7,5	-8,0	-7,6		-7,696666667
8	3,9	3,5	3,3		3,58
10	-3,2	-4,1			-3,66
12	3,9	4,1	3,4		3,77

$CaSO_4$					
pH	1	2	3		Average Zeta Pot
2	-0,6	-0,6	-1,2		-0,79
4	-5,7	-6,0	-5,7		-5,753333333
6	-4,0	-4,1	-3,8		-3,97
8	-7,5	-7,5	-9,6		-8,196666667
10	-6,1	-6,1	-6,7		-6,283333333
12	5,13	6,3	5,1		5,5
$Ca(NO_3)_2$					
pH	1	2	3		Average Zeta Pot
2	-2,6	-2,1	-1,3		-1,963333333
4	-2,7	-3,9	-5		-3,873333333
6	-2,0	-2,9	-3,0		-2,65
8	-3,0	-2,4	-3,0		-2,783333333
10	-3,4	-4,9	-6,3		-4,873333333
12	21,7	25,0	29,7		25,46666667

$NaNO_3$					
pH	1	2	3		Average Zeta Pot
2	-1,1	-1,2	-0,4		-0,886666667
4	-11,8	-12,3	-12,5		-12,2
6	-8,02	-9,3	-10,9		-9,396666667
8	-12,3	-12,5	-12,1		-12,3
10	-20,8	-19,6	-19,7		-20,03333333
12	-20,0	-17,7	-16,4		-18,03333333

Adsorption Calibration Curve: Absorbance vs Wavelength

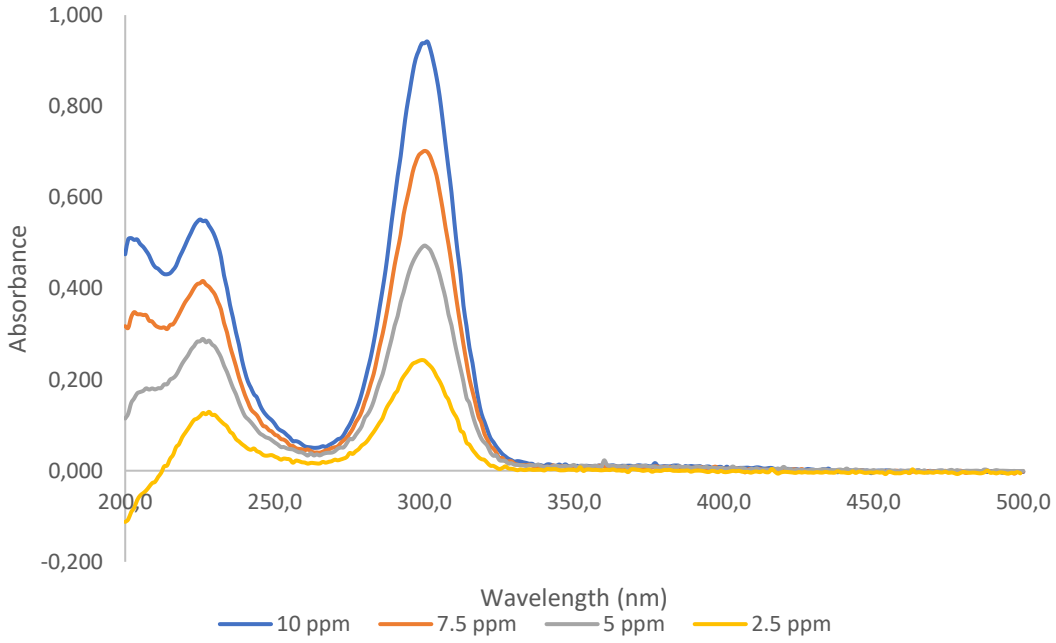

Calibration Data

Concentration (mg/l)	Absorbance
0	0
1,25	0,0925
2,5	0,135
5	0,368
7,5	0,525
8,75	0,596
10	0,721

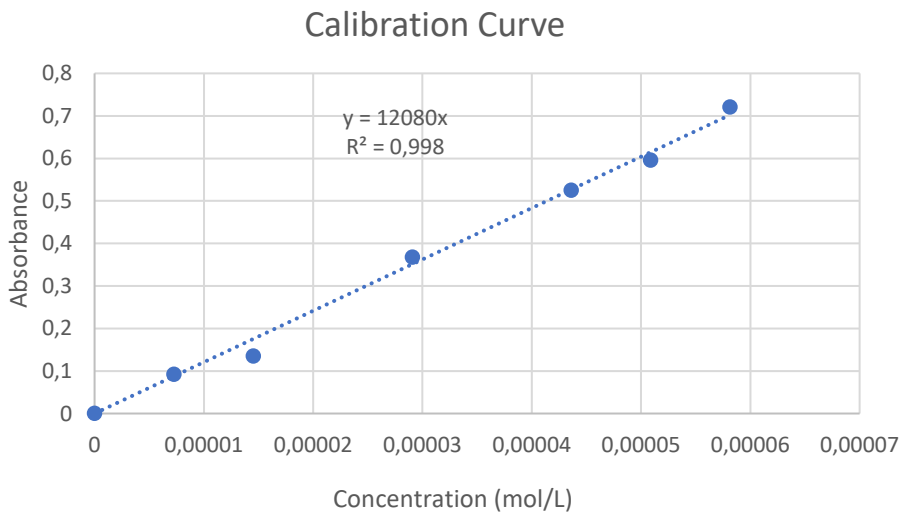

Adsorption Studies

	Absorbance at 300 nm		
	1	2	3
1 SPW	0,039	0,045	0,044
5 SPW	0,133	0,143	0,134
10 SPW	0,235	0,241	0,238

	Absorbance at 300 nm		
	1	2	3
$CaSO_4$	0,003	0,002	0,003
$Ca(NO_3)_2$	0,012	0,011	0,011
$NaNO_3$	0,001	0,001	0,001
5 SPW	0,133	0,143	

Appendix B: Raw Data Chalcopyrite

ACTA

	Attachments out of 396	
	1	2
1 SPW	273	278
5 SPW	354	321
10 SPW	352	364

	Chalcopyrite_pH 11		
	1	2	Ave
1 SPW	2,27	1,77	2,02
5 SPW	3,03	6,31	4,67
10 SPW	16,16	7,58	11,87

	Attachments out of 396	
	1	2
$CaSO_4$	198	266
$NaNO_3$	322	333
$Ca(NO_3)_2$	268	304

Microflotation

1 SPW															
Conditions	Time		sample + fp	fp	mass	Cum mass	%		Conditions		sample + fp	fp	mass	Cum mass	%
Ccp	2	C1	0,6189	0,3164	0,3025	0,3025	18,03171		Galena:	C1	0,6574	0,3133	0,3441	0,3441	19
1 SPW	6	C2	0,5458	0,3166	0,2292	0,5317	31,69409		1 SPW	C2	0,6047	0,3178	0,2869	0,631	35
No Collector	12	C3	0,5388	0,3158	0,223	0,7547	44,98689			C3	0,5719	0,316	0,2559	0,8869	50
	20	C4	0,5409	0,308	0,2329	0,9876	58,86981			C4	0,4995	0,3107	0,1888	1,0757	60
		Tails	4,68	3,99	0,69					Tails	5,2274	4,5187	0,7087		
					1,6776								1,7844		

5 SPW															
Conditions	Time		sample + fp	fp	mass	Cum mass	0		Conditions		sample + fp	fp	mass	Cum mass	%
Ccp	2	C1	0,7735	0,3193	0,4542	0,4542	21,2372		Galena:	C1	0,5706	0,3179	0,2527	0,2527	16
5 SPW	6	C2	0,6247	0,3122	0,3125	0,7667	35,84888		5 SPW	C2	0,698	0,2969	0,4011	0,6538	42
No Collector	12	C3	0,6026	0,304	0,2986	1,0653	49,81063			C3	0,5263	0,313	0,2133	0,8671	56
	20	C4	0,593	0,3196	0,2734	1,3387	62,5941			C4	0,4926	0,3127	0,1799	1,047	68
		Tails	4,75	3,95	0,8					Tails	4,2217	3,73	0,4917		
					2,1387								1,5387		

10 SPW															
Conditions	Time		sample + fp	fp	mass	Cum mass	0		Conditions		sample + fp	fp	mass	Cum mass	%
Ccp	2	C1	0,9804	0,3131	0,6673	0,6673	30,76391		Galena:	C1	1,0264	0,3147	0,7117	0,7117	33
10 SPW	6	C2	0,7725	0,3093	0,4632	1,1305	52,11839		10SPW	C2	0,8143	0,3054	0,5089	1,2206	56
No Collector	12	C3	0,6173	0,312	0,3053	1,4358	66,19335			C3	0,6014	0,3157	0,2857	1,5063	69
	20	C4	0,5049	0,324	0,1809	1,6167	74,53322			C4	0,5217	0,3029	0,2188	1,7251	79
		Tails	5,0247	4,4723	0,5524					Tails	5,2447	4,7912	0,4535		
					2,1691								2,1786		

1 SPW

Conditions	Time		sample + fp	fp	mass	Cum mass	%		Conditions		sample + fp	fp	mass	Cum mass	%
Ccp	2	C1	0,89	0,3093	0,5807	0,5807	36,81841		Galena:	C1	1,02	0,3257	0,6943	0,6943	38
1 SPW	6	C2	0,72	0,3192	0,4008	0,9815	62,23054		1 SPW	C2	0,81	0,3097	0,5003	1,1946	65
SIBX	12	C3	0,52	0,3129	0,2071	1,1886	75,3614			C3	0,53	0,3116	0,2184	1,413	77
	20	C4	0,45	0,3114	0,1386	1,3272	84,14913			C4	0,45	0,3141	0,1359	1,5489	85
		Tails	4,33	4,08	0,25					Tails	4,25	3,97	0,28		
					1,5772								1,8289		

5 SPW

Conditions	Time		sample + fp	fp	mass	Cum mass	0		Conditions		sample + fp	fp	mass	Cum mass	%
Ccp	2	C1	0,91	0,3071	0,6029	0,6029	36,27557		Galena:	C1	0,93	0,318	0,612	0,612	41
5 SPW	6	C2	0,82	0,3166	0,5034	1,1063	66,56438		5 SPW	C2	0,7	0,32	0,38	0,992	66
SIBX	12	C3	0,52	0,3189	0,2011	1,3074	78,66426			C3	0,48	0,3107	0,1693	1,1613	78
	20	C4	0,44	0,3154	0,1246	1,432	86,16125			C4	0,44	0,3183	0,1217	1,283	86
		Tails	4,46	4,23	0,23					Tails	4,58	4,37	0,21		
					1,662								1,493		

10 SPW

Conditions	Time		sample + fp	fp	mass	Cum mass	0		Conditions		sample + fp	fp	mass	Cum mass	%
Ccp	2	C1	1,23	0,3092	0,9208	0,9208	49,24591		Galena:	C1	1,05	0,3172	0,7328	0,7328	49
10 SPW	6	C2	0,67	0,3137	0,3563	1,2771	68,30142		10SPW	C2	0,61	0,3176	0,2924	1,0252	68
SIBX	12	C3	0,55	0,312	0,238	1,5151	81,03006			C3	0,52	0,3198	0,2002	1,2254	81
	20	C4	0,45	0,3153	0,1347	1,6498	88,23404			C4	0,43	0,3105	0,1195	1,3449	89
		Tails	4,31	4,09	0,22					Tails	4,61	4,45	0,16		
					1,8698								1,5049		

1 SPW

Conditions	Time		sample + fp	fp	mass	Cum mass	0		Conditions		sample + fp	fp	mass	Cum mass	%
Galena:	2	C1	0,6604	0,3296	0,3308	0,3308	18,12305		Galena:	C1	0,6604	0,3296	0,3308	0,3308	18
1 SPW	6	C2	0,4631	0,3075	0,1556	0,4864	26,64767		1 SPW	C2	0,4631	0,3075	0,1556	0,4864	27
pH 11	12	C3	0,4072	0,3014	0,1058	0,5922	32,44398			C3	0,4072	0,3014	0,1058	0,5922	32
	20	C4	0,4019	0,3192	0,0827	0,6749	36,97474			C4	0,4019	0,3192	0,0827	0,6749	37
		Tails	6,0255	4,8751	1,1504					Tails	6,0255	4,8751	1,1504		
					1,8253								1,8253		

5 SPW

Conditions	Time		sample + fp	fp	mass	Cum mass	0		Conditions		sample + fp	fp	mass	Cum mass	%
Galena:	2	C1	0,6095	0,3086	0,3009	0,3009	15,17781		Galena:	C1	0,6095	0,3086	0,3009	0,3009	15
5 SPW	6	C2	0,5124	0,308	0,2044	0,5053	25,48802		5 SPW	C2	0,5124	0,308	0,2044	0,5053	25
pH 11	12	C3	0,5914	0,3081	0,2833	0,7886	39,77806			C3	0,5914	0,3081	0,2833	0,7886	40
	20	C4	0,5132	0,3168	0,1964	0,985	49,68474			C4	0,5132	0,3168	0,1964	0,985	50
		Tails	5,9078	4,9103	0,9975					Tails	5,9078	4,9103	0,9975		
					1,9825								1,9825		

10 SPW

Conditions	Time		sample + fp	fp	mass	Cum mass	0		Conditions		sample + fp	fp	mass	Cum mass	%
Galena:	2	C1	0,6714	0,3105	0,3609	0,3609	17,60745		Galena:	C1	0,6714	0,3105	0,3609	0,3609	18
10 SPW	6	C2	0,5516	0,3214	0,2302	0,5911	28,83837		10SPW	C2	0,5516	0,3214	0,2302	0,5911	29
pH 11	12	C3	0,5471	0,3098	0,2373	0,8284	40,41567			C3	0,5471	0,3098	0,2373	0,8284	40
	20	C4	0,5873	0,3117	0,2756	1,104	53,86154			C4	0,5873	0,3117	0,2756	1,104	54
		Tails	5,9169	4,9712	0,9457					Tails	5,9169	4,9712	0,9457		
					2,0497								2,0497		

CaSO4

Conditions	Time		sample + fp	fp	mass	Cum mass	0		Conditions		sample + fp	fp	mass	Cum mass	%
Ccp	2	C1	0,5866	0,33	0,2566	0,2566	16,38151		Galena:	C1	0,6198	0,3159	0,3039	0,3039	19
1 SPW	6	C2	0,5541	0,31	0,2441	0,5007	31,96502		1 SPW	C2	0,6302	0,3201	0,3101	0,614	38
No collector	12	C3	0,4556	0,31	0,1456	0,6463	41,26021			C3	0,4412	0,3178	0,1234	0,7374	46
	20	C4	0,4701	0,31	0,1601	0,8064	51,4811			C4	0,4658	0,3057	0,1601	0,8975	55
		Tails	6,54	5,78	0,76					Tails	5,552	4,832	0,72		
					1,5664								1,6175		

Ca(NO3)2

Conditions	Time		sample + fp	fp	mass	Cum mass	0		Conditions		sample + fp	fp	mass	Cum mass	%
Ccp	2	C1	0,6952	0,3163	0,3789	0,3789	19,66677		Galena:	C1	0,6204	0,3161	0,3043	0,3043	18
5 SPW	6	C2	0,5151	0,3133	0,2018	0,5807	30,14118		5 SPW	C2	0,6508	0,3103	0,3405	0,6448	38
No collector	12	C3	0,5688	0,3155	0,2533	0,834	43,2887			C3	0,5838	0,3138	0,27	0,9148	54
	20	C4	0,613	0,3204	0,2926	1,1266	58,47607			C4	0,546	0,3262	0,2198	1,1346	67
		Tails	6,6	5,8	0,8					Tails	4,9976	4,4457	0,5519		
					1,9266								1,6865		

NaNO3

Conditions	Time		sample + fp	fp	mass	Cum mass	0		Conditions		sample + fp	fp	mass	Cum mass	%
Ccp	2	C1	0,5575	0,3116	0,2459	0,2459	19,53293		Galena:	C1	0,6614	0,3256	0,3358	0,3358	25
10 SPW	6	C2	0,5796	0,3202	0,2594	0,5053	40,13822		10SPW	C2	0,5963	0,3014	0,2949	0,6307	47
No collector	12	C3	0,5328	0,3233	0,2095	0,7148	56,77973			C3	0,5217	0,3189	0,2028	0,8335	62
	20	C4	0,4856	0,3115	0,1741	0,8889	70,60926			C4	0,4536	0,3208	0,1328	0,9663	72
		Tails	6,28	5,91	0,37					Tails	5,0753	4,6981	0,3772		
					1,2589								1,3435		

CaSO4

Conditions	Time		sample + fp	fp	mass	Cum mass	0		Conditions		sample + fp	fp	mass	Cum mass	%
Ccp	2	C1	1,1061	0,32	0,7861	0,7861	35,35894		Galena:	C1	1,0954	0,3148	0,7806	0,7806	33
1 SPW	6	C2	0,8254	0,31	0,5154	1,3015	58,54174		1 SPW	C2	0,8412	0,3204	0,5208	1,3014	55
SIBX	12	C3	0,5446	0,31	0,2346	1,5361	69,0941			C3	0,6219	0,3057	0,3162	1,6176	68
	20	C4	0,5371	0,32	0,2171	1,7532	78,8593			C4	0,5853	0,3145	0,2708	1,8884	80
		Tails	6,3	5,83	0,47					Tails	5,3523	4,8712	0,4811		
					2,2232								2,3695		

Ca(NO3)2

Conditions	Time		sample + fp	fp	mass	Cum mass	0		Conditions		sample + fp	fp	mass	Cum mass	%
Ccp	2	C1	1,0665	0,3	0,7665	0,7665	34,47268		Galena:	C1	0,7355	0,3	0,4355	0,4355	26
5 SPW	6	C2	0,9748	0,31	0,6648	1,4313	64,37149		5 SPW	C2	0,7859	0,32	0,4659	0,9014	53
SIBX	12	C3	0,5553	0,32	0,2353	1,6666	74,9539			C3	0,48493	0,3	0,18493	1,08633	64
	20	C4	0,4969	0,32	0,1769	1,8435	82,90983			C4	0,4383	0,3	0,1383	1,22463	72
		Tails	4	3,62	0,38					Tails	6,3	5,83	0,47		
					2,2235								1,69463		

NaNO3

Conditions	Time		sample + fp	fp	mass	Cum mass	0		Conditions		sample + fp	fp	mass	Cum mass	%
Ccp	2	C1	1,0943	0,34	0,7543	0,7543	37,92167		Galena:	C1	1,1347	0,31	0,8247	0,8247	43
10 SPW	6	C2	0,8188	0,3	0,5188	1,2731	64,00382		10SPW	C2	0,7153	0,32	0,3953	1,22	63
SIBX	12	C3	0,5943	0,31	0,2843	1,5574	78,29672			C3	0,5786	0,3	0,2786	1,4986	77
	20	C4	0,4542	0,31	0,1442	1,7016	85,54623			C4	0,4112	0,32	0,0912	1,5898	82
		Tails	4,3975	4,11	0,2875					Tails	6,26	5,91	0,35		
					1,9891								1,9398		

Zeta Potential

1 SPW					
pH	1	2	3		Average Zeta Pot
2	4,1	4,6	4,0		4,216666667
4	-7,0	-7,3	-7,6		-7,306666667
6	-8,5	-8,3			-8,4
8	-12,1	-14,0	-14,3		-13,46666667
10	-13,8	-14,3	-13,8		-13,96666667
12	3,3	3,5	3,5		3,406666667
5 SPW					
pH	1	2	3		Average Zeta Pot
2	2,4	2,1	1,6		2,033333333
4	-4,6	-5,8	-5,5		-5,286666667
6	-6,8	-6,1	-7,2		-6,69
8	-8,3	-8,4	-8,6		-8,41
10	-8,9	-8,7	-8,7		-8,763333333
12	5,2	5,8	4,0		5,01
10 SPW					
pH	1	2	3		Average Zeta Pot
2	-0,8	-0,3	-1,5		-0,823666667
4	-6,4	-6,5	-6,5		-6,453333333
6	-4,9	-7,6	-5,1		-5,856666667
8	-8,8	-7,6	-9,0		-8,473333333
10	3,5				3,46
12	5,2	5,8	6,0		5,67
Ultra-Purified Water					
pH	1	2	3		Average Zeta Pot
2	4,1	4,6	4,0		-3
4	-7,0	-7,3	-7,6		-22
6	-8,5	-8,3			-25
8	-12,1	-14,0	-14,3		-28
10	-13,8	-14,3	-13,8		-29
12	3,3	3,5	3,5		-24

$Ca(NO_3)_2$					
pH	1	2	3		Average Zeta Pot
2	4,4	5,0	4,6		4,65
4	-1,5	-2,6			-2,03
6	-5,8	-6,3	-6,6		-6,23
8	-3,3	-3,3	-3,8		-3,486666667
10	-4,3	-4,8	-5,5		-4,853333333
12	3,0	2,8	2,2		2,696666667

$NaNO_3$					
pH	1	2	3		Average Zeta Pot
2	2,9	1,5	1,5		1,963333333
4	-12,7	-15,1	-15,9		-14,56666667
6	-28,1	-28,6	-30,6		-29,1
8	-24,7	-24,5	-26,2		-25,13333333
10	-30,0	-28,7	-30,6		-29,76666667
12	-25,6	-27,2	-29,3		-27,36666667
$CaSO_4$					
pH	1	2	3		Average Zeta Pot
2	-2,4				-2,42
4	-2,8	-4,6	-6,1		-4,486666667
6	-10,7	-10,5	-11,9		-11,03333333
8	-10,6	-11,6	-13,7		-11,96666667
10	-7,5	-7,6	-6,9		-7,346666667
12	6,6	6,4	5,2		6,083333333

Absorbance Calibration Data

Concentration (mg/L)	Absorbance
0	0
2,5	0,2086792
5	0,303
6,25	0,410
7,5	0,599
10	0,830

Calibration curve

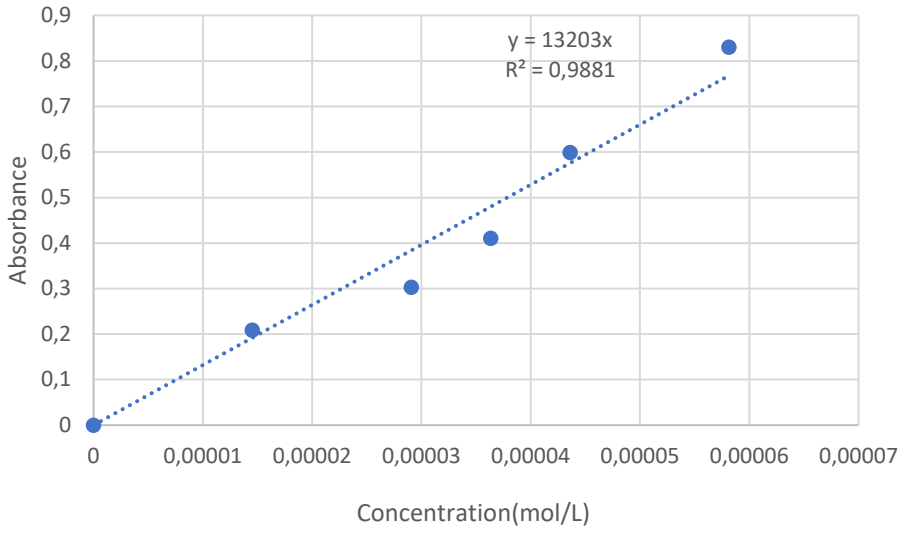

Adsorption Studies

	Absorbance at 300 nm			
	1	2	3	Average
1 SPW	0,032	0,036		0,034
5 SPW	0,038	0,1	0,029	0,039
10 SPW	0,053	0,037		0,045

	Abs @ 300 nm		
Ca(NO3)2	0,052002	0,0579	0,0632
CaSO4	0,066	0,0634	0,0575
NaNO3	0,000168	0,000179	0,000206

Appendix C: Raw Data Pyrrhotite

Microflotation

1 SPW

Conditions	Time		sample + fp	fp	mass	Cum mass	%		Conditions		sample + fp	fp	mass	Cum mass	%
pyrrhotite:	2	C1	0,47	0,34	0,13	0,13	4,36		pyrrhotite:	C1	0,31	0,26	0,05	0,05	1,77
No Collector	6	C2	0,58	0,29	0,29	0,42	14,09		CMC	C2	0,45	0,27	0,18	0,23	8,13
	12	C3	0,72	0,3	0,42	0,84	28,19			C3	0,65	0,25	0,4	0,63	22,26
	20	C4	0,51	0,26	0,25	1,09	36,58			C4	0,49	0,29	0,2	0,83	29,33
		Tails	20,04	18,15	1,89					Tails	11,84	9,84	2		
					2,98								2,83		

5 SPW

Conditions	Time		sample + fp	fp	mass	Cum mass	%		Conditions		sample + fp	fp	mass	Cum mass	%
pyrrhotite:	2	C1	0,48	0,34	0,14	0,14	6,76		pyrrhotite:	C1	0,49	0,34	0,15	0,15	7,77
No Collector	6	C2	0,52	0,31	0,21	0,35	16,91		CMC	C2	0,6	0,34	0,26	0,41	21,24
	12	C3	0,59	0,32	0,27	0,62	29,95			C3	0,59	0,38	0,21	0,62	32,12
	20	C4	0,5	0,33	0,17	0,79	38,16			C4	0,46	0,34	0,12	0,74	38,34
		Tails	12,05	10,77	1,28					Tails	11,92	10,73	1,19		
					2,07								1,93		

10 SPW

Conditions	Time		sample + fp	fp	mass	Cum mass	%		Conditions		sample + fp	fp	mass	Cum mass	%
pyrrhotite:	2	C1	0,73	0,46	0,27	0,27	10,27		pyrrhotite:	C1	0,75	0,6	0,15	0,15	5,32
No Collector	6	C2	0,84	0,48	0,36	0,63	23,95		CMC	C2	0,98	0,65	0,33	0,48	17,02
	12	C3	0,83	0,31	0,52	1,15	43,73			C3	1,09	0,54	0,55	1,03	36,52
	20	C4	0,69	0,51	0,18	1,33	50,57			C4	0,84	0,54	0,3	1,33	47,16
		Tails	16,83	15,53	1,3					Tails	9,9	8,41	1,49		
					2,63								2,82		

1 SPW

Conditions	Time		sample + fp	fp	mass	Cum mass	%		Conditions		sample + fp	fp	mass	Cum mass	%
pyrrhotite:	2	C1					0,00		pyrrhotite:	C1					0,00
SIBX	6	C2	0,2	0,07	0,13	0,13	8,67		CMC	C2	0,25	0,09	0,16	0,16	10,53
	12	C3	0,28	0,09	0,19	0,32	21,33			C3	0,24	0,12	0,12	0,28	18,42
	20	C4	0,17	0,1	0,07	0,39	26,00			C4	0,22	0,08	0,14	0,42	27,63
		Tails	0,3	0,15	0,15	0,54	36			Tails	0,24	0,14	0,1	0,52	34,21053
			5,65	4,69	0,96						5,66	4,66	1		
					1,5								1,52		

5 SPW

Conditions	Time		sample + fp	fp	mass	Cum mass	%		Conditions		sample + fp	fp	mass	Cum mass	%
pyrrhotite:	2	C1	0,44	0,3	0,14	0,14	14,58		pyrrhotite:	C1	0,48	0,3	0,18	0,18	13,74
SIBX	6	C2	0,52	0,31	0,21	0,35	36,46		CMC	C2	0,49	0,31	0,18	0,36	27,48
	12	C3	0,4	0,3	0,1	0,45	46,88			C3	0,54	0,3	0,24	0,6	45,80
	20	C4	0,51	0,31	0,2	0,65	67,71			C4	0,51	0,31	0,2	0,8	61,07
		Tails	4,92	4,61	0,31					Tails	5,12	4,61	0,51		
					0,96								1,31		

10 SPW

Conditions	Time		sample + fp	fp	mass	Cum mass	%		Conditions		sample + fp	fp	mass	Cum mass	%
pyrrhotite:	2	C1	0,88	0,31	0,57	0,57	22,09		pyrrhotite:	C1	0,65	0,31	0,34	0,34	15,60
SIBX	6	C2	0,73	0,3	0,43	1	38,76		CMC	C2	0,76	0,3	0,46	0,8	36,70
	12	C3	1,2	0,31	0,89	1,89	73,26			C3	0,86	0,31	0,55	1,35	61,93
	20	C4	0,7	0,3	0,4	2,29	88,76			C4	0,78	0,3	0,48	1,83	83,94
		Tails	4,97	4,68	0,29					Tails	5,03	4,68	0,35		
					2,58								2,18		

1 SPW

Conditions	Time		sample + fp	fp	mass	Cum mass	%		Conditions		sample + fp	fp	mass	Cum mass	%
Galena:	2	C1	0,32	0,3	0,02	0,02	0,833333		Galena:	C1	2,66	2,65	0,01	0,01	0
1 SPW	6	C2	0,39	0,32	0,07	0,09	3,75		1 SPW	C2	3,34	3,27	0,07	0,08	2
pH 11	12	C3	0,37	0,34	0,03	0,12	5			C3	3,11	3,03	0,08	0,16	5
	20	C4	0,35	0,3	0,05	0,17	7,083333			C4	2,98	2,9	0,08	0,24	7
		Tails	6,07	3,84	2,23					Tails	7,45	4,42	3,03		
					2,4								3,27		

5 SPW

Conditions	Time		sample + fp	fp	mass	Cum mass	%		Conditions		sample + fp	fp	mass	Cum mass	%
Galena:	2	C1	0,38	0,3	0,08	0,08	2,564103		Galena:	C1	0,35	0,32	0,03	0,03	1
5 SPW	6	C2	0,39	0,31	0,08	0,16	5,128205		5 SPW	C2	0,4	0,29	0,11	0,14	5
pH 11	12	C3	2,45	2,42	0,03	0,19	6,089744			C3	0,39	0,33	0,06	0,2	7
	20	C4	2,55	2,47	0,08	0,27	8,653846			C4	0,44	0,35	0,09	0,29	10
		Tails	7,03	4,18	2,85					Tails	6,75	4,02	2,73		
					3,12								3,02		

10 SPW

Conditions	Time		sample + fp	fp	mass	Cum mass	%		Conditions		sample + fp	fp	mass	Cum mass	%
Galena:	2	C1	0,43	0,32	0,11	0,11	3,525641		Galena:	C1	0,39	0,32	0,07	0,07	2
10 SPW	6	C2	0,3	0,28	0,02	0,13	4,166667		10SPW	C2	0,35	0,32	0,03	0,1	3
pH 11	12	C3	0,45	0,31	0,14	0,27	8,653846			C3	0,44	0,33	0,11	0,21	6
	20	C4	0,39	0,33	0,06	0,33	10,57692			C4	0,49	0,3	0,19	0,4	12
		Tails	6,62	3,83	2,79					Tails	6,78	3,92	2,86		
					3,12								3,26		

Zeta Potential

1 SPW					
pH	1	2	3		Average Zeta Pot
2	-10,1	-9,4	-10,3		-9,946666667
4	-4,9	-7,9	-10,5		-7,736666667
6	-6,7	-7,9	-8,6		-7,73
8	-7,9	-7,4	-9,4		-8,236666667
10	-10	-10	-9,1		-9,706666667
12	-4,2	-4,5	-3,8		-4,173333333
5 SPW					
pH	1	2	3		Average Zeta Pot
2	-2,4	-4,4	-6,2		-4,323333333
4	-2,9	-3,2	-4,1		-3,416666667
6	-2,7	-4,1	-3,8		-3,503333333
8	-5,8	-11,1	-8,8		-8,533333333
10	-6,4	-2,4			-4,375
12	2,1	3,6			2,825
10 SPW					
pH	1	2	3		Average Zeta Pot
2	-4,0	-3,0	-4,4		-3,816666667
4	-4,3				-4,34
6	-4,1	-4,2	-7,6		-5,28
8	-7,6	-7,6	-7,1		-7,42
10	4,8	3,6	3,3		3,926666667
12	8,8	8,2	9,8		8,913333333
Ultra Purified Water					
pH	1	2	3		Average Zeta Pot
2	-19,5	-20,2	-19,1		-19,6
4	-21,5	-21,4	-22,1		-21,67
6	-25,5	-23,2	-23,3		-24
8	-26,2	-25,7	-26,1		-26
10	-28,9	-28,5	-28,1		-28,5
12	-19,1	-19	-19,4		-19,17

	Average Potential					
pH	2	4	6	8	10	12
NaNO3	-10,5	-15,733	-15,7	-19,4	-19,33	-26,7
Ca(NO3)2	8,09	-1,233	-2,624	3,51	-6,29	31,567
CaSO4	-2,163	-8,0387	-5,187	-3,33	-5,1	1,36

Calibration Curve: Absorbance vs Wavelength

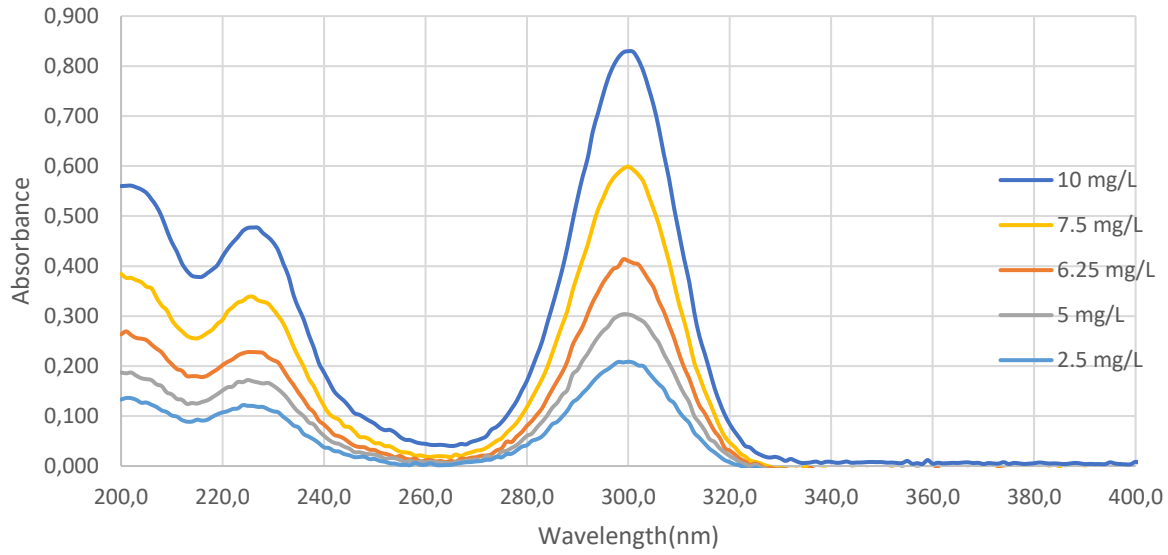

Calibration Data

Concentration (g/l)	Absorbance			
0	0	0	0	0
0,01	0,787	0,792	0,792	0,790333333
0,00625	0,537	0,537	0,538	0,537333333
0,00375	0,307	0,312	0,312	0,310333333
0,0025	0,199	0,199	0,2	0,199333333
0,00125	0,076	0,076	0,077	0,076333333

Calibration curve: Absorbance vs concentration

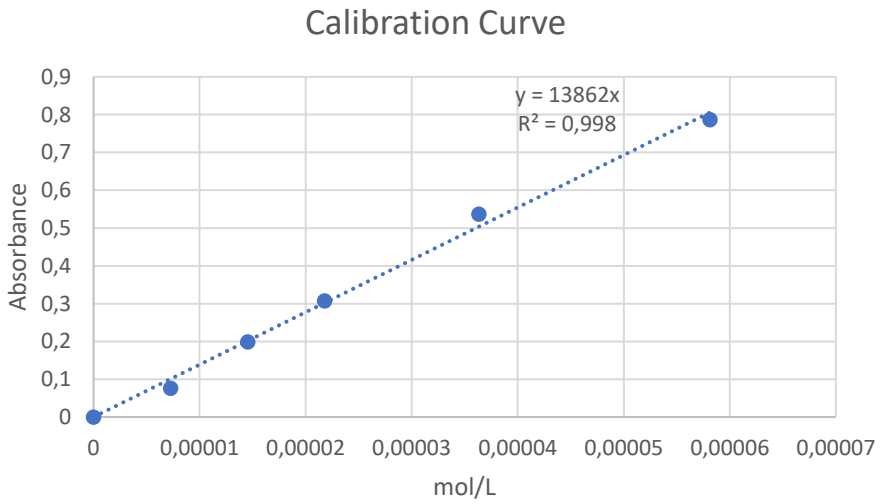

Adsorption Studies Measurements

	Absorbance		
1 SPW	0,246	0,235	0,25
5 SPW	0,271	0,272	0,271
10 SPW	0,332	0,332	0,331